Bacterial nanocellulose as drug delivery system for lipophilic drugs

Dissertation

To Fulfill the

Requirements for the Degree of

„doctor rerum naturalium“ (Dr. rer. nat.)

Submitted to the Council of the Faculty of

Biological Sciences

of the Friedrich Schiller University Jena

by Dipl.-Pharm. Yaser Alkhatib

born on the 3rd of January 1990 in Anabek
Damas Suburb - Syria

Reviewer:

1st reviewer: Prof. Dr. Dagmar Fischer (Erlangen)

2nd reviewer: Prof. Dr. Anna Kipp (Jena)

3rd reviewer: Prof. Dr. Matthias G. Wacker (Singapore)

Date of defense: 22. July.2021

-To my family-

Acknowledgment

First of all, I would like to express my sincere gratitude to my supervisor **Prof. Dr. Dagmar Fischer** for giving me the opportunity to be part of her research group and for providing the interesting topic. I appreciate her continuous support through the valuable scientific input and suggestions. I would also like to thank her for the motivational words and the sponsorship to attend different conferences.

I must also thank **Dr. Gabriele Blume** for the huge amount of support and patience in sharing her expertise through my time in Jena. The interesting discussions with her, and her expertise in nanocarrier systems and preparation methods were essential in bringing this thesis to fruition.

My gratitude to **Dr. Dana Kralisch** and her working group for providing the bacterial nanocellulose and for her support through informative discussions.

I gratefully acknowledge the opportunities offered by **Prof. Dr. Alfred Fahr** and **Prof. Dr. Paola Luciani** to use their laboratories and instruments during my time in Jena.

Furthermore, I would like to thank **Dr. Jana Thamm** for her support in the electron microscope investigations, and **Alexander Mohn**, **Angela Herre** and **Ramona Brabetz** for their technical support.

I would like show my gratitude to all my former colleagues in Jena during my PhD for the great memories and constructive exchange of ideas. Especially the "Männerbüro" members: **Sven Kattner**, **Paul Warncke** and **Martin Rabel** for the extraordinary discussions. And certainly, to **Lisa, Matthias, Uwe, Berit, Yvette, Julia, Stephan**, and **Markus** for their support and time.

Finally, I would like to thank **my family,** and my cousins **Adnan** and **Husam** who supported me through my journey and were always by my side with encouragement and support.

Thank you all!

Table of Contents

List of abbreviations

3D	Three dimensional
5-LO	5-lipoxygenase
ADMET	Absorption, distribution, metabolism, excretion, and toxicity
AKBA	3-*O*-acetyl-11-keto-β-boswellic acid
API	Active pharmaceutical ingredients
ATP	Adenosine triphosphate
BNC	Bacterial nanocellulose
CMC	Critical micelle concentration
CoQ10	Coenzyme Q10
DSMZ	German Collection of Microorganisms and Cell Cultures
FDA	Food and Drug Administration
GRAS	Generally recognized as safe
HET-CAM	Hen's egg test at the chorion allantois membrane
HET-CAV	Hen's egg test at the chick area vasculosa
ICCVAM	Interagency Coordinating Committee on the Validation of Alternative Methods
k. xylinus	*Komagataeibacter xylinus*
KBA	11-keto-β-boswellic acid
log P	*n*-octanol-water partition coefficient
LTs	Leukotrienes
MTT	(3-[4,5-dimethylthiazol-2-yl]-2,5-diphenyl-tetrazolium bromide)
NADPH	Nicotinamide adenine dinucleotide phosphate
NSAIDs	Non-steroidal anti-inflammatory drugs
O/W nanoemulsions	Oil in water nanoemulsions
OECD	Organization for Economic Co-operation and Development
PCS	Photon correlation spectroscopy
PEO-*b*-PCL	Poly(ethylene oxide)-*b*-poly(caprolactone)
PEO	Poly(ethylene oxide)

Ph. Eur.	European pharmacopoeia
PHMB	Polyhexanide
PPO	Poly(propylene oxide)
SEM	Scanning electron microscopy
TC	Terminal complexes
TEMPO	(2,2,6,6-Tetramethylpiperidin-1-yl)oxyl
USP	United States pharmacopoeia
UV	Ultraviolet
W/O/W nanoemulsions	Water in oil in water nanoemulsions

1. Introduction

1.1. Cellulose

Cellulose is the most common organic polymer in nature. It is a high molecular weight homopolymer composed of (1→4) –D- anhydroglucopyranose chains linked by ß-glycosidic linkages. The geometry of cellulose parallel chains is determined by the intra-and inter-molecular hydrogen bonding (1-4). Cellulose has a wide range of sources such as marine animals, plants (e.g., cotton, wood) and bacterial sources (5). Bacterial nanocellulose is referred to in literature by different names, including bacterial cellulose (6, 7), microbial cellulose (8-10) and even biocellulose (11, 12).

1.1.1. Biosynthesis of bacterial nanocellulose

BNC has been extensively studied in the medical and pharmaceutical fields over the last three decades. In 1886 Adrian J. Brown described BNC for the first time as the formation of a white, mechanically stable, gelatinous material formed during the fermentation of vinegar (13). Several bacterial genera have been identified as BNC producers such as *Agrobacterium*, *Alcaligenes, Pseudomonas* and *Rhizobium* (14, 15). However, the most intensively investigated bacterial nanocellulose producer is the rod shaped, aerobic, non-pathogenic Gram-negative bacterium *Komagataeibacter xylinus* (*K. xylinus*), previously categorized as *Actetobacter* or *Gluconacetobacter*, which belong to the genera *Acetobacteraceae* (16, 17).

The biosynthesis of cellulose by *K. xylinus* consumes a variety of sugars and carbohydrate sources. The most laboratory investigated sugar is glucose, which is provided in the fermentation medium (18, 19). For cultivation of bacteria during the biosynthesis of BNC, the well-established Hestrin-Schramm medium is the most frequently used medium in lab-scale and commercial production (20, 21). Its main components are: 2% glucose as a carbon source, 0.5% peptone and 0.5% yeast

extract as nitrogen and vitamin source, and sodium phosphate and citric acid to maintain a stable pH of 6 (20). Glucose as a carbon source has proven to provide a high cellulose yield, as have other carbon sources, such as maltose, fructose, and sucrose (22, 23). A bacterium can convert up to 108 glucose molecules per hour into cellulose (24). This bioprocess includes several enzymatic reactions, among which is the phosphorylation of glucose into glucose-6-phosphate, which is then isomerized into glucose-1-phosphate. This intermediary will yield a uridine phosphate glucose, which is considered the building block of nanocellulose (18, 25, 26). The biosynthesis process takes place between the outer cell membrane and the cytoplasm membrane of the bacterial cell in a synthesizing complex or terminal complexes (TC), which have pores at the surface of the bacterium arranged in a lineal form (Figure 1) (24, 25). These linear chains are extracellularly secreted into the surrounding medium through the cell pores of the outer cell membrane. Those chains will subsequently assemble to form ribbon-shaped fibrils of twisted strands. This process is strongly influenced by the pores longitudinal positioning on the *K. xylinus* cell membrane (18, 27). The cellulose fibers then aggregate to form a three dimensional (3D) network at the liquid air interphase of the culture medium. The formation of the 3D network pellicle is associated with the rotation and division of the bacterial cell (28). *K. xylinus* bacteria produce the cellulose pellicle as a survival and protection strategy, as BNC protects the bacteria from predators, UV radiation and drying. BNC also helps the bacteria to stay near the surface of the medium, where it can maintain a higher oxygen level (29).

One of the earliest reported commercial products containing BNC is Nata de Coco, a traditional South-East Asian dish prepared under static cultivation conditions in coconut water (30, 31). Several cultivation types have been developed for scale-up production of BNC, such as agitated, static conditions, static conditions featured with fed-bed technology, and a combination of static and agitated conditions (32, 33). Moreover, the type of cultivation and the cultivation conditions

play a major role in defining the form and size of the produced BNC (15).

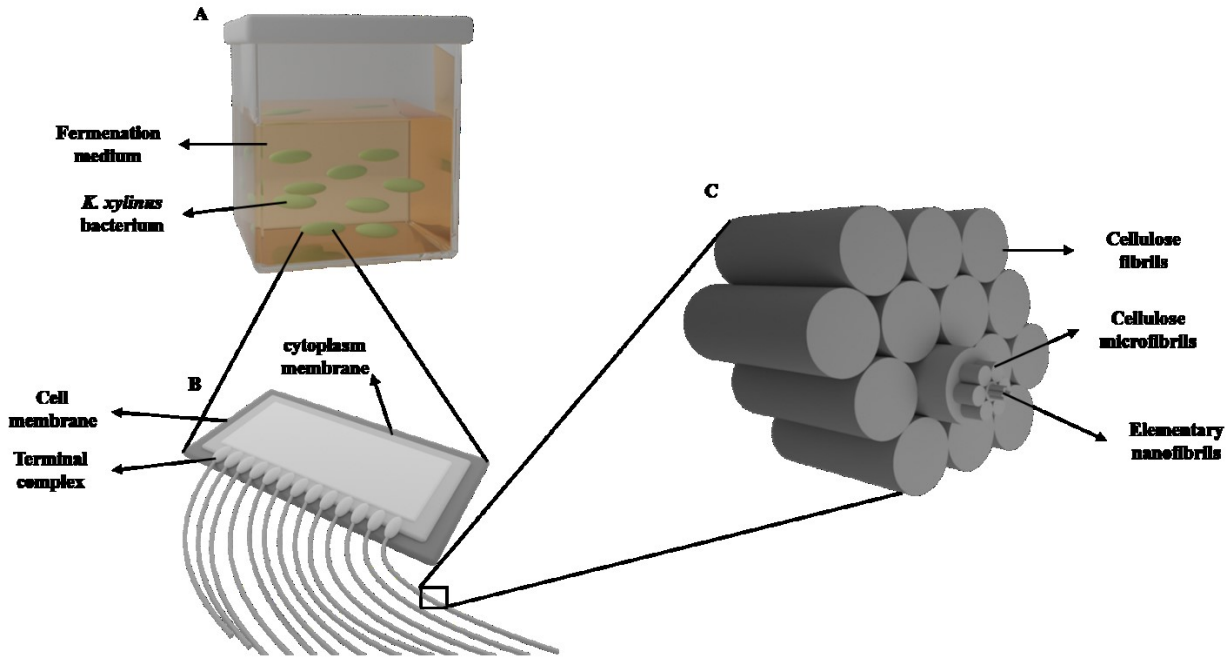

Figure 1. A simplified schematic diagram of: A) biosynthesis of BNC by the cultivation of *K. xylinus* in a Hestrin-Schramm medium. B) biosynthesis of cellulose fibrils in the terminal complexes located between the cytoplasm membrane and outer cell membrane. C) each cellulose fibril consists of multiple cellulose microfibrils which also consist of elementary nanofibrils (modified according to (34-36))

1.1.2. Properties of bacterial nanocellulose

The disposition of cellulose synthesizing complexes and the nanometer dimensional fibers (20-100 nm) form a 3D-network with an enormous surface area held together by hydrogen bonds (34, 37). The enormous surface area (>150 m^2/g) and the free hydroxyl groups will allow the binding of large amounts of water up to 99% in addition to high water absorption and water retention values. This gives the BNC a hydrophilic character where water is bound in and on the fibril network. (38, 39). Although BNC has the same chemical structure of ß-1,4-glucans as plant cellulose, BNC surpasses other cellulose sources in various aspects such as higher purity and macromolecular properties. The superiority of BNC is highlighted by its high purity, the absence

of lignin, hemicelluloses and pectin, a high degree of polymerization of up to 2000-8000, and a crystallinity between 73-95%. In contrast, plant cellulose has a polymerization degree of 300-1700 and a purity <80% (40, 41). The highly crystalline structure combined with the nanometer network structure result in the high mechanical stability of BNC, highlighted by a Young's modulus of 15 GPa and a tensile strength of 200-300 MPa. This tensile strength is comparable to the strong synthesized fibers and heat resistant aramid fibers (Kevlar®) (26, 42). Moreover, BNC has a high thermal stability up to 300 °C which allows sterilization by autoclaving (25, 43). BNC can be purified from bacterial and medium residues with a simple purification step by boiling with sodium hydroxide followed by washing with purified water until reaching a neutral pH (23, 44).

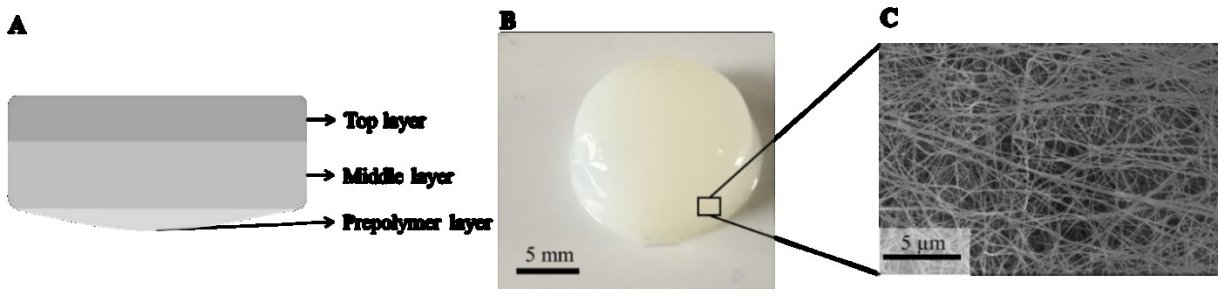

Figure 2. A) Schematic presentation of the typical multilayered BNC biosynthesized in static cultivation conditions. B) photography of a turned over native BNC. C) SEM image of the nanocellulose network

The typical static cultivation conditions yield BNC fleeces produced on the liquid/air interphase and with a typical multilayered structure (Figure 2). Through scanning electron microscopy (SEM) investigations, the top BNC surface in direct contact with air is characterized as a compacted cellulose network structure, followed by a porous middle layer and an adjacent gelatinous loose prepolymer layer as a bottom layer. This 3-layer structure occurs due to the gradual synthesis of cellulose into the medium (25, 45). The properties of BNC are dependent not only on the cultivation conditions and the type of cellulose-producing bacteria, but also on the other cultivation

conditions such as pH, temperature, and the composition of the cultivation medium (46-52).

BNC shows high biocompatibility along with other outstanding properties, which facilitates the utilization of BNC in the medical and pharmaceutical fields (26, 53), due to BNC's biocompatibility and its 3D-nanostructure which supports cell proliferation (10). The biocompatibility of BNC has been proven by *ex ovo* test, where no irritative reaction has been reported (54). In addition, this has been proven by several *in vitro* cytotoxicity studies such as the cell viability assay using MTT (3-[4,5-dimethylthiazol-2-yl]-2,5-diphenyl-tetrazolium bromide) assay using several cell lines like the mouse embryo fibroblasts and Chinese hamster ovary cells (55-58). Moreover, *in vivo* studies have shown the absence of fibrotic capsules and giant cells as well as other macroscopic indications of inflammation after an implantation over one year in different host species such as mice, rats, Syrian golden hamsters, rabbits, sheep, pigs and humans (59-62). According to the American Society for Testing and Material standards (63), BNC can be classified as a highly hemocompatible and nonhemolytic material (64, 65).

1.1.3. Application fields of bacterial nanocellulose

According to the forecast of Decision Databases (66) the global market of BNC is expecting a growth in the period of 2020 until 2025 to reach a value of 539.3 million US dollar reflected in several application fields starting from a market value in 2019 of 333.9 million US dollar. This expectation is due to the previously mentioned diverse properties of the natural biopolymer BNC and the rising number of studies made about this material in several application fields (67). BNC has been used widely in the food industry as a desert, dietary supplement, and rheology modification agent, where it is also used in low cholesterol diets (30, 68-70). In the food packaging industry BNC is used in combination with sorbic acid to increase the safety and shelf-life of food products (71). BNC has been registered since 1992 by the FDA as generally recognized as safe (GRAS) (72). BNC is used in several other industries and industrial processes such as: filter

membrane synthesis (73, 74), the paper industry (75, 76), energy storage, fuel cell membranes and other technical applications (77-79). Furthermore, BNC is also used in ocular materials and in the cosmetics field in facial masks (80-83). Several cosmetics brands have entered the market with their products such as Bio Enzymes™ from the company Talika® (84), Leaders™ from the company Leaders Cosmetics® (85) and others such as Biocellulose mask from the American company Bel Mondo Beauty, Celmat from BOWIL Biotech in Poland. In Germany various companies have brought products to market such as: JeNaCell with Epi Nouvelle+ Basic, and MDM Cosmetics with the product Nanodermin. BNC was also introduced in several biomedical applications (Figure 3).

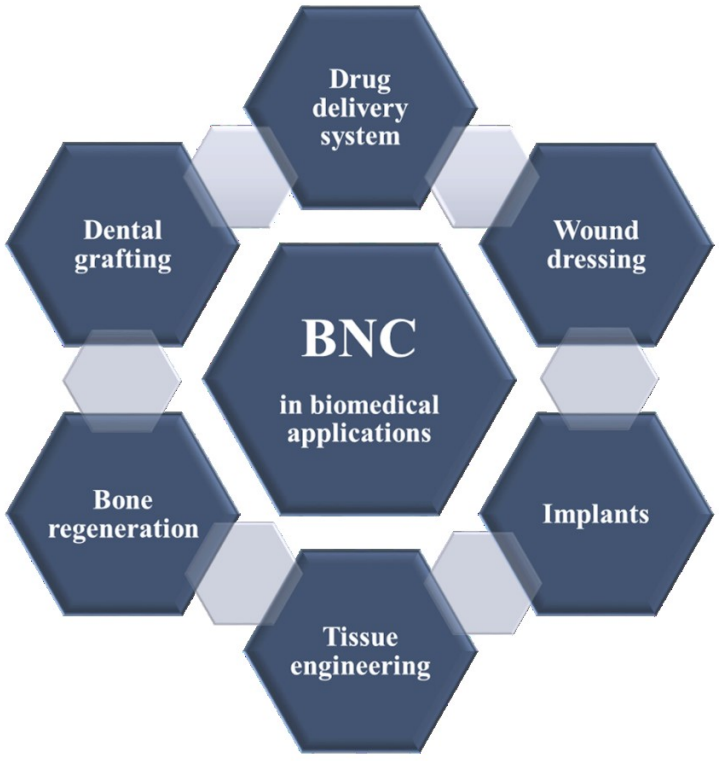

Figure 3. Biomedical application fields of BNC

1.1.3.1. BNC application in the wound dressing and regenerative medicine

One of the more widely investigated applications is the utilization of BNC as a wet wound dressing for chronic wounds, wounds after burn injury, and diabetic foot (26, 86-89). Wound healing is a

complex process, which involves different type of cells and products such as collagen and growth factors to facilitate the cell proliferation process (90, 91). The warm and humid environment of a wound may motivate normal skin flora to enter the wound (92). When skin healing is delayed, more aggressive microbes could proliferate and colonize an open wound. The most common bacteria in wounds are the Gram-positive *Staphylococcus aureus* and the Gram-negative *Escherichia coli* and *Pseudomonas aeruginosa* (93, 94). Therefore, the isolation of wounds with a wound dressing to shield an open wound from external contamination is a recommended strategy (95). There is demand in the medical field for further development of traditional wound dressings. Sulaeva and colleagues (53) concluded that the properties of a modern wound dressing are as follows: a wound dressing which provides a moist wound environment, able to absorb exudate excess, has appropriate gas diffusion, is antimicrobially active, biocompatible, non-toxic, thermally and mechanically stable and painless in removal (53, 96). BNC with its high water content, flexibility, simple modification techniques, and other properties can fulfill these requirements (26, 97). BNC can build a mechanically stable protective layer between damaged skin and the outer atmosphere, which prevents contamination with bacterial and mechanical influences while still providing good permeability to gases and liquids (98, 99). Several BNC-based products have been introduced to the market by various companies, summarized in Table 1. BNC-based wound dressings have demonstrated superior wound healing processes in comparison to conventional gauze and other traditional wound dressings as shown by Solway and colleagues (100, 101), where BNC samples were used in treating diabetic foot and skin tears in a population of frail elderly. Solway and colleagues reported painless removal, reduced infection, fast epithelialization and faster tissue regeneration rates in comparison to traditional wound dressings. Similar findings were also demonstrated in different *in vitro* and clinical studies (99, 102-105). The frequency of changing the wound dressing over the healing period is an important aspect

which plays a role in accelerating the wound healing process. In a study by Schmitz and colleagues (106), BNC-based wound dressings showed a lower exchange rate and costs savings of up to 70% in comparison with traditional wound dressings over an application period of three months (106). Several BNC modifications have been also initiated to improve BNC as wound dressing, such as the addition of antimicrobial drugs (87) and improving the transparency of BNC which could be achieved either by including additives or by the co-cultivation of two cellulose-productive bacteria (97, 107). These modifications would facilitate the long-term application of BNC as a wound dressing and potentially improve patient compliance.

Table 1. Examples of BNC-based wound dressing marketed products

Product name	**Company**
BioFill® BioProcess® NexFill® Gengiflex®	Fibrocel Productos Biotecnologicos LTDA (Brazil)
Membracel®	Vuelo Pharma (Brazil)
BioNext®	BioNext (Brazil)
Suprasorb®X	Lohmann & Rauscher GmbH (Germany)
Cuticell Epigraft®	BSN Medical GmbH (Germany)
Epicite Hydro	JeNaCell GmbH (Germany)
Celmat® Wound	Bowil Biotech (Poland)
DermaFill™	Cellulose Solutions LLC (USA)

Native or modified BNC has been used in several biomedical applications (5, 83, 108-111). For example as a replacement membrane for the Dura mater (112, 113), in artificial cornea (114-116), cartilage (117, 118), and eardrum (119) and as scaffold for bone regeneration (120-123). Furthermore, BNC-based products (BASYC®, BActerial SYnthesized Cellulose) developed by Klemm and colleagues (25) demonstrated good suitability as a blood vessel replacement material

as shown by other works (65, 124-128). All these application areas rely on the fact that the human body does not produce ß-glucosidase enzymes which are responsible for hydrolyzing glycosidic bonds in BNC, thus making BNC in general not biodegradable in the human body (129). However, several studies have modified the degradability of BNC either by loading the BNC with the enzyme cellulase (130), or by chemical modifications such as oxidation by (2,2,6,6-Tetramethylpiperidin-1-yl)oxyl (TEMPO) or sodium periodate (131, 132).

1.1.3.2. BNC as drug delivery system

The unique 3D-nanostructure along with the enormous available surface area and hydrogen bonds offer the prospect of using BNC as a drug delivery system (35, 133). This is also enabled by several modification approaches on two different levels, during biosynthesis which is called *in situ* modifications and after biosynthesis which is called *post*-modifications (83, 134, 135). The *in situ* modifications by the addition of additives into the cultivation medium yield modified BNC with new properties such as porosity, crystallinity, and density of the inner-structure (136, 137). These types of modifications facilitate novel BNC applications as a drug delivery system. For example the addition of carboxymethylcellulose lead to denser nanostructure and less elastic BNC with a prolonged release behavior of loaded methotrexate (138). The addition of poly(ethylene glycol) resulted in a denser structure but with higher transparency of the BNC, which could be useful in wound dressing applications (97, 139). Furthermore, Abdelraof and colleagues (140) demonstrated in their research an increase in biocompatibility and antimicrobial activity by the addition of glass nanocomposites (140). However, the *in situ* modifications are limited to additives and drugs which show compatibility with the cultivation medium and do not impact the viability of the cellulose-producing bacteria. Furthermore, modifying BNC by the *in situ* modifications limits the use of simple standard purification method (alkaline treatment at high temperature) due to the possible heat-sensitivity of the incorporated drug and loading efficiency. (133, 141). Therefore, several

post-modifications techniques were developed to modify properties of BNC or to facilitate BNC with a bioactivity (83, 133). For example, the addition of ß-cyclodextrin, chitosan, polyvinyl alcohol, and sodium alginate improved the mechanical stability of BNC (142-144). These *post*-modification techniques could be categorized depending on the type of BNC (wet native, semi dried, or dried BNC). Wet native BNC could be loaded with active ingredients by the standard sorption method under submerse condition (145, 146), vortexing of native BNC with loading medium (147), injection of drug into the core of native BNC (54), perforation of the BNC using a laser (118), boiling (148), vacuuming, and spraying of the drug solution (97, 133). Furthermore, the drying of BNC promoted the use of other loading techniques like re-swelling of air-dried, semi-dried, freeze-dried, and critical point dried BNC (54, 149, 150) with respect to the effect of drying process on the BNC structure (151, 152).

The combination of BNC with an active pharmaceutical ingredient via the different modification techniques facilitates the usage of BNC as drug delivery system for different therapeutic fields, summarized in Table 2. This started with the combination of antimicrobial drugs into BNC to act as a modern wound dressing. This type of combination is currently available on the market. The German company Lohmann & Rauscher GmbH combined the antimicrobial Polyhexanide (polyhexamethylene biguanide, PHMB) with BNC in the product Suprasorb® X + PHMB (153). Moreover, the activation of BNC by loading it with plasmid facilitates a systemic application as implants (54, 154), and for oral and dental applications by loading berberin (148, 155), doxycyclin (132), and paracetamol (156). The packaging industry uses BNC as a packaging material. The addition of an active ingredient like antiseptics or natural materials to BNC facilitates longer food conservation periods as shown by the addition of nisin (157, 158) and vanillin (159).

Table 2. An overview of research utilized BNC as drug delivery system for wound management and various other applications (modified according to (87, 110))

Therapeutic group	Active pharmaceutical ingredient
Antibiotics	amoxicillin (160), ampicillin (161), ceftriaxone (162), ciprofloxacin (163), doxycyclin (132), fusidic acid (164), gentamycin (161, 165), nisin (157, 158), tetracycline (166, 167)
Anticoagulants	heparin (168)
Anti-inflammatories and analgesics	ibuprofen (149, 169-171), diclofenac (97, 149, 169, 172, 173), beclomethasone dipropionate (174), paracetamol (156)
Antiseptics	benzalkonium chloride (150, 175), PHMB (57, 176, 177), povidone-iodine (177, 178), octenidine (146, 178), silver sulfadiazine (179)
Cardiovascular	propranolol (180)
Cytostatic	doxorubicin (181, 182)
Enzymes	lipase (183)
Histamine antagonist	famotidine (184)
Local anesthetic	lidocaine (149, 169, 185)
Metallic particles	copper (143, 186), silver (145, 187-191), titanium dioxide (192, 193), zinc oxide (96)
Natural substances	Brazilian propolis (194), berberin (148, 155), caffeine (169, 195), *scrophularia striata*-extract (142), vanillin (159)
Protein	bovine serum albumin (147, 152, 196), insulin (197), laccase (198), sericin (57, 199)
Relaxants	tizanidine (184)
Vitamins	retinol (200), vitamin B (201)

Drugs loaded into BNC with an *n*-octanol-water partition coefficient (log P) value below 4 represent more than 80% of the portfolio of drugs used in combination with BNC (110). This is because the hydrophilic nature of BNC presents a major challenge for the incorporation of lipophilic drugs. However, the number of the lipophilic preclinical drugs under development has

significantly increased over the last 30 years, driven by the relationship between potency and ADMET (absorption, distribution, metabolism, excretion, and toxicity) of a drug and its lipophilicity (202, 203). Interest in lipophilic drug applications has driven several trials which attempt mitigate the hydrophilicity of BNC. These approaches can be categorized into three main groups: i) by chemical modifications of the BNC fibers, ii) by enhancing drug solubility, and iii) by incorporation of disperse multiphase systems into BNC (110). Several approaches to chemical modifications aiming to substitute the hydroxyl groups with reactive functional groups were reported in the literature. Examples include: acetylation, amidation, carbamation, esterification, etherification, and oxidation (52). Hu and colleagues (204) reported a successful, economical and environmentally friendly, solvent-free acetylation trial for BNC using acetic anhydride in the presence of iodine as a catalyst. However, hydrophobic characteristics were limited to the BNC surface and showed a decrease in the wettability of the BNC. Surface modification yields inhomogeneous drug distribution across the BNC structure and will limit it only to the surface. Another study by Avila Ramirez and colleagues (205) reported hydrophobization of BNC by acetylation with citric acid in a solvent-free medium under fixed reaction conditions. This method showed a successful hydrophobization of the BNC surface but caused a decrease in the crystallinity and thermal stability of BNC. However, these types of modifications were also limited to hydrophobization of the surface of BNC, which led to uncontrolled loading efficiency due to the high density of the hydrophobized surface and changes in the BNC structure, such as decrease in the BNC pore sizes (184). Another strategy described in the literature is oxidation of BNC with TEMPO followed by coupling BNC with lipophilic primary amines or amino acids (tryptophan or phenylalanine) (86). However, the modified BNC showed a decrease in the water binding capacity and fast release of the loaded lipophilic drugs (indomethacin and diclofenac) within 24 hours. This is because the drugs are not homogenously distributed in the BNC and are instead concentrated on

the surface of the BNC. Lee and colleagues (206) reported an esterification of the BNC with acetic acid, hexanoic acid or dodecanoic acid. This modification reduced the thermal stability of BNC, which can potentially limit the use of heat-reliant purification process of the modified BNC. Thus, several essential properties of BNC as a drug delivery system are impacted by chemical modifications. This results in issues such as low biocompatibility with the tissues of target organ as well as uncontrolled drug release due to inhomogeneous loading and drug distribution.

The second alternative strategy to overcome the hydrophilicity of BNC is by enhancing the drug solubility, which is described by several reports in the literature. For example, Xiao and colleagues (155) presented an oral application of BNC incorporating the lipophilic berberine hydrochloride. They enhanced the solubility of berberine hydrochloride by forming an inclusion complex of berberine hydrochloride and cyclodextrin. This method was also demonstrated for other drugs like curcumin (207). Cyclodextrin formed nano-sized macrocycles, which are characterized by a hydrophilic outer surface surrounded by hydroxyl groups and an internal lipophilic cavity covered with glycosidic oxygens and hydrogen bonds (208). Although this method would facilitate the use of BNC as drug delivery system for lipophilic drugs, it is limited to the size of the lipophilic cavity of cyclodextrin. Thus making the cavity size of cyclodextrin the determinant factor when choosing drugs to be incorporated within BNC. Moreover, the formation of cholinium-based ionic liquids with lipophilic drugs demonstrated an effective method to incorporate lipophilic drugs as shown by Chantereau and colleagues in two different studies (201, 209), where they demonstrated a successful incorporation of vitamin B, ibuprofen, ketoprofen and naproxen to the hydrophilic BNC. Alternatively, the modification of the drug itself by forming highly-water soluble salts was presented as an efficient method by Huang and colleagues (148), where they used the higher-solubility berberine sulfate and compared it with the low-solubility berberine hydrochloride form. The modification of the drugs to form better soluble salts is an effective method, but it is limited

to a handful of drugs which have active charged moieties. Moreover, a recent study by Silva and colleagues (169) demonstrated the use of ethanolic drug solutions such as by dissolving ibuprofen in ethanol or the addition of a cosolvent such as glycerol to enhance the solubility of the lipophilic drugs ibuprofen and diclofenac (149, 173). The addition of a cosolvent demonstrates an effective alternative method to incorporate lipophilic drugs, although the presence of cosolvents could negatively influence some of the properties of BNC such as its moisturizing properties and high biocompatibility (210, 211).

Recently, the BNC scientific community explored an alternative strategy to incorporate lipophilic drugs into BNC by formulating drugs into a disperse multiphase systems. In 2015, Numata and colleagues (200) reported the incorporation of retinol into BNC by the utilization of poly(ethylene oxide)-*b*-poly(caprolactone) PEO-*b*-PCL solid nanoparticles. However, the triblock copolymer PEO-*b*-PCL nanoparticles showed a high affinity to BNC (212). Additionally, an incomplete release of retinol from the BNC was reported due to the lack of stability of the solid nanoparticles and an early release of the retinol within the BNC structure. This led to a low total release of retinol from the BNC and the maximum release occurred after only 4 hours (200). In another study, an incorporation of the flavonoid natural product silymarin in BNC, which has a poor bioavailability due to its low water solubility, has been reported. Tsai and colleagues (213), formulated silymarin and zein to form spherical nanoparticles which were able to adsorb on the BNC nanofibers. This addition of silymarin/zein nanoparticles enabled BNC to have an antioxidant and antibacterial effect, which could facilitate the use of BNC in the packaging industry. However, the addition of the silymarin/zein nanoparticles decreased the water binding capacity of BNC (213). In addition, Marquele-Oliveira and colleagues (6) incorporated the lipophilic Brazilian propolis into BNC by employing a liquid self-microemulsifying formulation. This method required an isotropic mixture of oil, surfactant, and cosurfactant to yield a microemulsion upon mixing with water. The loading

process into BNC was performed after a solvent exchange of BNC, where the water was removed by pressure and replaced with 96% alcohol. The BNC/propolis film showed a sustained release and a high level of antimicrobial activity against both Gram-negative and Gram-positive bacteria.

1.2. Dermal applications

While the topical application of a drug can target conventional dermal diseases, wound injuries, and cosmetics, dermal application could be an alternative application route to the oral route when treating acute and chronic diseases by so called “transdermal applications” (214). Both dermal and transdermal application routes offer many advantages such direct targeting of injured areas of the skin, increased bioavailability by avoiding gastrointestinal absorption, bypassing the first-pass metabolism, reducing the frequency of dosing, avoiding drug-drug interactions by combined therapy, and reducing side effects (215). However, the efficiency of topical and transdermal route is dependent on properties of the chemical compounds, where compounds with a molecular weight below 500 Dalton and a log P value between 1 and 3 best can penetrate the stratum corneum and are generally accepted candidates for transdermal applications (216, 217).

A number of approaches has been developed to increase the penetration and permeation of drugs. Physical methods such as microneedles and magnetophoresis (218-220), chemical methods such as alcohols, fatty alcohols, and glycols (221, 222) and carrier and vehicle methods like micelles, liposomes, nanoemulsions and gels (Figure 4) (223-227).

1.2.1. Liposomes

In 1965, Alec Bangham described liposomes as spherical vesicles composed of a phospholipid bilayer containing an aqueous core with the ability to encapsulate hydrophilic and lipophilic drugs (228). In general, liposomes provide a suitable platform for lipophilic drugs to increase their solubility, stability and half-life to achieve higher bioavailability as well as reduced toxicity and widen the therapeutic index for different application routes including the oral, dermal and

parenteral routes (229, 230). Liposomes provide a drug delivery system to transport drugs into deeper layers of the skin. In 1980 Mezei and colleagues (231) reported the transdermal delivery of triamcinolone acetonide five times higher than that of conventional ointment into the skin. Liposomes can be formulated from a single phospholipid or from a combination of different types of phospholipids. Phosphatidylcholine is one of the most common used phospholipids (232). The first liposomal product was introduced into the US market in 1995 with the name Doxil® for the treatment of ovarian cancer and AIDS-related Kaposi's sarcoma (233). Several other liposomal formulations are undergoing clinical trials, and over 20 products have entered the US and European markets from different therapeutic groups such as cytostatics, antimicrobials, opioids, local anesthetics, photosensitizers, immunostimulants, or vaccines (225, 234).

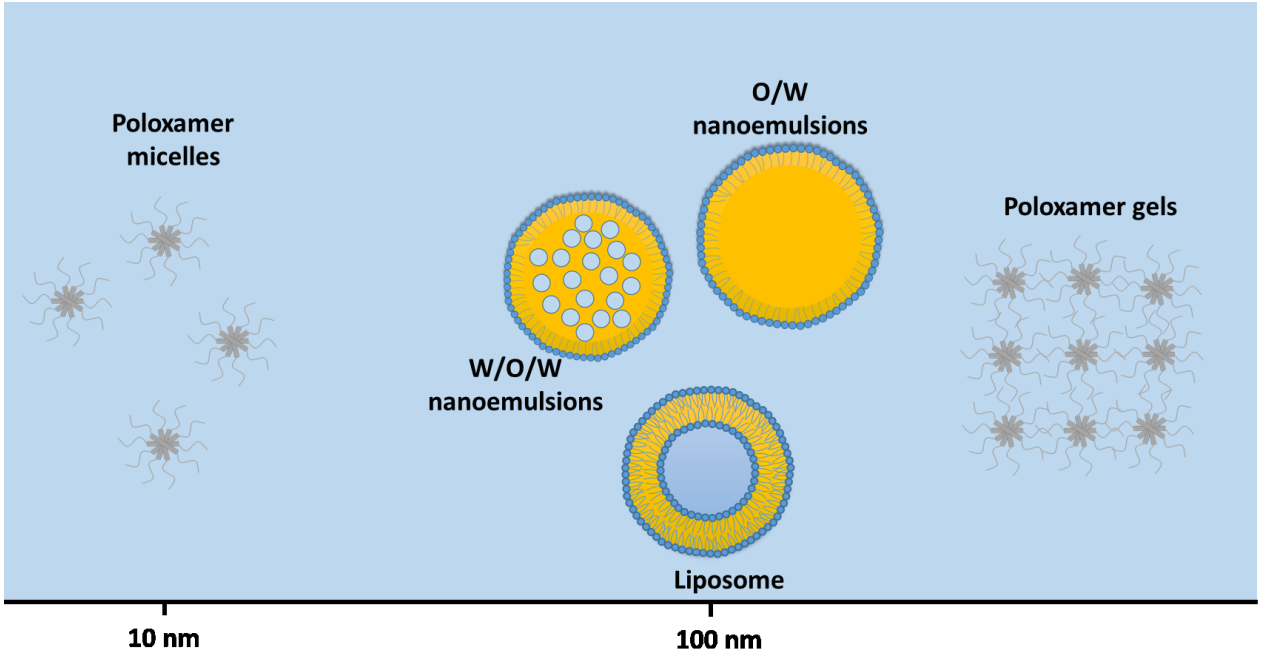

Figure 4. Schematic overview of different carrier systems including Poloxamer micelles (6 – 10 nm), liposome, O/W and W/O/W nanoemulsions (90 - 150 nm) and Poloxamer gels.

1.2.2. Nanoemulsions

Nanoemulsions are described as a heterogeneous system where two immiscible liquids are

dispersed, the dispersed phase (droplets) and the outer continuous phase (the liquid surrounding the droplets). The system is stabilized by an interfacial layer of emulsifiers and co-emulsifiers (235, 236). Generally, nanoemulsions have a droplet size range between 20 and 500 nm. Due to the small droplet size they can be optically transparent to opalescent (237). Nanoemulsions have a higher solubilization capacity in comparison to simple micellar dispersions and a high kinetic stability (238). Based on the components and the type of emulsifiers, nanoemulsions could be categorized into three types: water in oil (W/O) where water is the dispersed liquid in the continuous oil phase, oil in water (O/W), and water in oil in water (W/O/W) multiple nanoemulsions (239). Nanoemulsions formulations have been used in different application routes such as oral, ocular, pulmonary, parenteral, and dermal routes (238). Shakeel and colleagues (240), described the ability of nanoemulsions formulations to improve the permeation of the drugs ketoprofen and celecoxib in comparison to other conventional gel formations. Several nanoemulsions formulations have reached the market (238, 241) such as Liple® which contains prostaglandin E1 for intravenous vasodilation, diazepam nanoemulsions with the name Diazemuls®, and propofol nanoemulsions under the name Diprivan® (238). Nanoemulsions need to be formulated into secondary structure to realize dermal long-term applications due to their low viscosity.

1.2.3. Poloxamer micelles and gels

In 1950, BASF Corporation launched Poloxamer products in various markets. Poloxamers have several trade names, such as Pluronic®, Synperonic®, and Tetronic® (242). The non-ionic Poloxamers are composed of the hydrophilic poly(ethylene oxide) (PEO) and hydrophobic poly(propylene oxide) (PPO) blocks in the form of a triblock copolymer (PEO/PPO/PEO) (243). Several grades of Poloxamers could be obtained by changing the ratio of the hydrophilic PEO to the lipophilic PPO (244). Poloxamers show a temperature and concentration dependency in their

self-assembling and gel formation behaviors. Poloxamers can self-assemble above certain concentration, known as “critical micelle concentration” (CMC), in which the hydrophobic PPO blocks dehydrate in higher temperatures and become less soluble. These phenomena will lead to the formation of micelles with a dehydrated PPO core and hydrated PEO shell form. By further increasing the concentration and temperature above a certain temperature, known as the “sol-gel temperature”, micelles will get packed and form gels (245, 246). Poloxamers are listed in both United States pharmacopoeia (USP) and European pharmacopoeia (Ph. Eur.) as non-toxic and non-irritant excipients where they are used as a solubilizer, emulsifier, or stabilizer (247). Poloxamers have been used in diverse fields of pharmaceutical applications such as tissue engineering, wound healing, and drug delivery systems (248-251).

1.2.4. Therapeutic groups for dermal applications

By employing different penetration enhancement approaches, dermal and transdermal application routes could present alternative administration routes for a broader group of drugs, such as antimicrobials, antiseptics, antiviral, anti-inflammatory, antioxidants, hormones, and corticosteroids (252, 253). In the following sections, the drugs applied within this thesis are introduced and described. The lipophilicity of a drug is an important parameter for its skin penetration capability. The three chosen drugs were selected due to their high lipophilic properties, low penetration ability, and as proof-of-concept for the use of BNC as a drug delivery system for dermal applications.

1.2.4.1. Coenzyme Q10

Coenzyme Q10 (CoQ10), which is also called ubiquinone, consists of a *p*-benzoquinone ring with a polyisoprenoid side chain (254). It is a fat-soluble vitamin-like molecule. CoQ10 can be found occurring naturally in cellular membranes (255). In 1957, CoQ10 was first isolated from beef heart mitochondria by Frederick Crane (256). CoQ10 has an important role in the energy producing

metabolic pathways, where it acts in the synthesis of adenosine triphosphate (ATP) as an electron transporter from the reduced nicotinamide adenine dinucleotide phosphate (NADPH) and succinate dehydrogenase to the cytochrome system (255). As well as the role of CoQ10 as an antioxidant by reduction of pro-oxidative compounds which leads to a reduced level of lipid peroxidation (257). CoQ10 became one of the most used dietary supplement, due to its contribution in treating different diseases (254). Several companies introduced CoQ10 preparations into the market such as Dr. Loges + Co. GmbH with their product Q10-Loges® Concept as capsules. Moreover, most of the CoQ10 medical products were for the oral route in which CoQ10 has a poor gastrointestinal tract absorption profile, where 2-10 hours are required to reach the T_{max} due to its high molecular weight (863 Da) and poor water solubility (254). Therefore, other routes of administration have been studied, especially dermal routes (258-261).

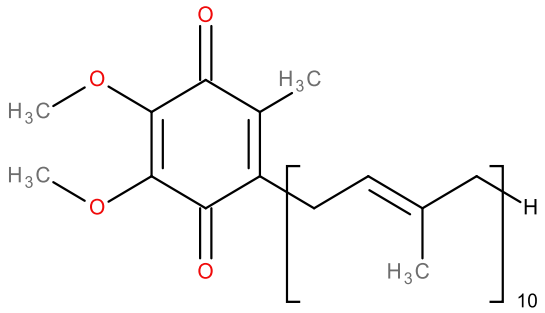

Figure 5. Chemical structure of the coenzyme Q10 (modified according to (254))

1.2.4.2. Boswellia serrata-extract

The natural gum resin *Boswellia serrata* can be obtained by the incision of the stem or branches of *Boswellia serrata*. The main components of this extract are volatile oils, pure resin, and mucus. The resin contains around 30% of its weight in boswellic acids (262). This plant is native to India, and its extract is widely used in traditional ayurvedic medicine (263). The boswellic acids are pentacyclic triterpenoids, which can exist in two configurations (α or β) (Figure 5). However,

different pharmacological studies indicated that β-configured acids have stronger bioactivities than the α-configured ones (264). Boswellic acids present a promising natural alternative to non-steroidal anti-inflammatory drugs (NSAIDs). The two main boswellic acids are the 3-*O*-acetyl-11-keto-β-boswellic acid (AKBA) and 11-keto-β-boswellic acid (KBA) which are recognized as highly effective anti-inflammatories (263, 265).

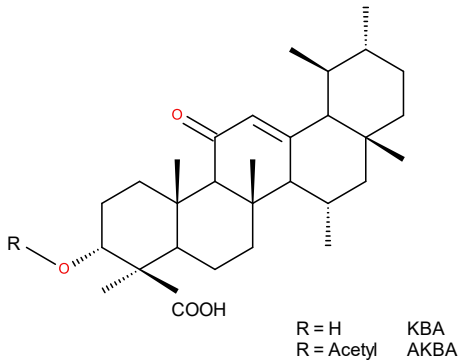

Figure 6. Chemical structure of the two boswellic acids AKBA and KBA (modified according to (263))

Chronic inflammatory diseases could be promoted by an excess over-production of leukotrienes (LTs), where LTs are a potent mediator which start the inflammatory response. One anti-inflammatory strategies is to inhibit the biosynthesis of LTs by inhibition of the enzyme 5-lipoxygenase (5-LO), as 5-LO initiate biosynthesis of LTs by oxygenation of the arachidonic acid which yields at the end LTs (266). In a recent study Gilbert and colleagues (267) indicated that boswellic acids could inhibit the biosynthesis of LTs not only by inhibiting the 5-LO but also by provoking a change in the region-specificity towards a 12-lipoxygenating enzyme (267). Furthermore, the usage of boswellic acids in wounds has demonstrated a beneficial effect on fibroplasia and collagen synthesis (268).

However, the two main boswellic acids have a high lipophilicity of a log P of 8 for AKBA and 7 for KBA. This characteristic causes low solubility and bioavailability of the boswellic acids.

Therefore, research to improve the bioavailability for oral or dermal applications has been performed (269). However, a repeated long-term application is needed for the boswellic acids, due to their short half-life which is about 6 hours for KBA.

1.2.4.3. Octenidine

Octenidine hydrochloride is a bispyridine antimicrobial compound. It is composed of two cationic pyridine residues which are separated by ten methylene groups (270). Octenidine is stable in a wide pH range between 1.6 to 12.2 (271). The two non-interacting cation-active centers give octenidine the ability to bind readily onto negatively charged bacterial cell membranes. Octenidine demonstrates a broad-spectrum of antimicrobial effect, covering Gram-negative and Gram-positive bacteria and fungi as well as several viral species (272). It has low toxicity in comparison to other ammonium compounds such as benzalkonium chloride due to the lack of an amide and ester structure (270). Moreover, octenidine does not develop resistance with loss of effectivity, in contrast to other antiseptics (273). Several studies showed that octenidine is effective at low concentration of 0.1% (274, 275). Besides the use of octenidine in dental applications, it is widely used to treat open wounds and skin burns (276). Although octenidine shows a high level of antimicrobial activity, no adverse effects on the epithelial or wound tissues have been registered (277-279).

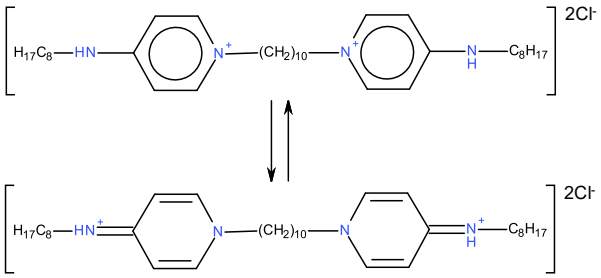

Figure 7. Chemical structure of octenidine dihydrochloride (modified according to (271))

2. Objectives

The natural biopolymer BNC has been widely investigated in the medical and pharmaceutical fields as a drug delivery system and wound dressing for acute wounds. However, these applications are still limited to hydrophilic drugs due to the strong hydrophilicity of BNC. The incorporation of lipophilic drugs is still a challenge for further exploitation of BNC as a drug delivery system for dermal applications and wound dressings for acute and chronical wounds.

For the realization of a BNC-based drug delivery system for dermal applications, three different lipophilic drugs to treat acute and chronic infected skin were selected. These are the anti-inflammatory *Boswellia serrata* extract, antioxidant Coenzyme Q10, and the antiseptic octenidine. The selected drugs would be incorporated into BNC by the formulation with nanoscale colloidal carrier systems including micelles and O/W and W/O/W nanoemulsions as well as hydrogels and liposomes as a reference system. The preparation and characterization of the carrier system should be optimized to obtain stable nanocarrier systems with regard to hydrodynamic diameter and zeta potential in the relevant storage, handling, and body temperature. Additionally, this thesis focuses on the selection of a suitable loading technique to achieve a homogeneous drug distribution within the BNC network and a high drug loading efficiency of the lipophilic drugs into BNC. Therefore, the loading of drug loaded carrier systems into BNC was investigated via several *post*-modification loading techniques. In view of the intended application as dermal drug delivery system and wound dressing, the mechanical stability of BNC is an essential property during handling and application. Therefore, the impact of the incorporation of the carrier systems on the mechanical stability of BNC have to evaluated. Regarding the ability of BNC to absorb wound exudates, the water binding capacity of BNC loaded with the carrier system have to determined. In addition, the biocompatibility of the newly developed BNC with and without carrier systems must be investigated to avoid unexpected skin or tissues irritation effects.

For treating acute and chronical skin infections, the drug release has to be optimized for a short-term application within 24-48 hours to treat acute infections and a long-term drug over a period of one week for treatment of chronical infections. Therefore, this investigation has to be performed by studying the effect of the physiochemical characterization of the different carrier systems on the release behavior, and by determining of the effect of using different loading techniques and types of BNC (native or freeze-dried BNC) on the release behavior of the lipophilic drug.

Although native BNC *per se* does not show antimicrobial activity, the incorporation of lipophilic drugs into BNC would fulfill this gap. Hence, the impact of loading and release on the antimicrobial activity of octenidine has to be tested. In addition, the ability of the BNC-based drug delivery systems to deliver the lipophilic drug into the skin has to be investigated by skin penetration studies.

3. List of publications

Publication 1

Overcoming the hydrophilicity of bacterial nanocellulose: Incorporation of the lipophilic coenzyme Q10 using lipid nanocarriers for dermal applications

Alkhatib, Y., Blume, G., Thamm, J., Steiniger, F., Kralisch, D., Fischer, D.

Published in: European Journal of Pharmaceutics and Biopharmaceutics, 2021, 158, p. 106-112

In this presented study, loading of lipophilic drugs into the hydrophilic BNC was investigated. Lipophilic CoQ10 was formulated with three different types of colloidal carrier systems: liposomes, O/W and W/O/W nanoemulsions. The physiochemical characterizations of the loaded carrier system demonstrated stable hydrodynamic diameters and zeta-potential over a period of 30 days. The carrier systems were in the range of about 90-120 nm and a negative zeta-potential. BNC was loaded with the drug loaded carrier systems by different loading techniques which yielded high loading efficiencies as well as homogenous distribution of CoQ10 in the 3D-structure of BNC. The loading of the carrier systems did not have an impact on the high mechanical stability of BNC. The type of carrier system and the loading technique were used the two major factors influencing the release behavior of CoQ10, which were investigated by using Franz diffusion cells test. Both O/W and W/O/W nanoemulsions with and without BNC delivered CoQ10 into the skin. However, the CoQ10 distribution in the skin layers was reliant upon the type of carrier system used.

The incorporation of the drug loaded carrier systems facilitates the use of BNC as drug delivery system for lipophilic drugs with high loading efficiency, this opens up new possibilities for the use of BNC.

Alkhatib, Y.	Conception of the study, characterization of bacterial nanocellulose and nanocarriers, loading and release data and analysis of the mechanical tests, penetration studies, drafting and revision of the manuscript
Blume, G.	Conception of the study, preparation of nanocarriers, drafting and revision of the manuscript
Thamm, J.	Microscopy, revision of the manuscript
Steiniger, F.	Microscopy, revision of the manuscript
Kralisch, D.	Preparation of the nanocellulose fleeces, revision of the manuscript
Fischer, D.	Conception of the study, interpretation of data, drafting and revision of the manuscript, corresponding author, supervision

Publication 2

Development and characterization of bacterial nanocellulose loaded with *Boswellia serrata* extract containing nanoemulsions as natural dressing for skin diseases

Karl, B., Alkhatib, Y., Beekmann, U., Bellmann, T., Blume, G., Steiniger, F., Thamm, J., Werz, O., Kralisch, D., Fischer, D.

Published in: International Journal of Pharmaceutics, 2020, 587, Article 119635

In this presented study, the utilization of BNC in combination with the lipophilic *Boswellia serrata* extract was investigated for anti-inflammatory skin treatment. Hence, the *Boswellia serrata* extract was formulated into O/W and W/O/W nanoemulsions formulations. These nanoemulsions demonstrated stability with regard to the hydrodynamic diameters and potentials in the three relevant temperatures over a 30 day period. The loading of the drug loaded nanoemulsions via the post-modification submerse absorption loading technique revealed a

loading efficiency of about 10%. Native BNC maintained its unique properties, such as softness and mechanical stability, after the incorporation of the drug loaded nanoemulsions. Biphasic release profiles were obtained via Franz cell diffusion test for both AKBA and KBA incorporated in the two nanoemulsions. Through the shell-less hen's egg test, it was shown that the loading of BNC with the two nanoemulsions did not influence the unique biocompatibility of native BNC. Both AKBA and KBA were detected in the different layers of skin via HPLC after skin penetration studies using porcine skin. The penetration of the boswellic acids was influenced by the type of the nanoemulsions, application time and frequency of application.

In summary, the incorporation of the lipophilic *Boswellia serrata* extract into BNC is facilitated by utilizing nanoemulsions to deal with the hydrophilicity of BNC.

Karl, B.	Conception of the study, preparation and physicochemical characterization of bacterial nanocellulose and nanocarriers, mathematical analysis of release profiles, penetration studies, transfer and aseptic preparation, drafting and revision of the manuscript
Alkhatib, Y.	Characterization of bacterial nanocellulose and nanocarriers, loading and release data and analysis of the mechanical tests, penetration studies, drafting and revision of the manuscript
Beekmann, U.	Synthesis and purification of bacterial nanocellulose, revision of the manuscript
Bellmann, T.	Biocompatibility testing, revision of the manuscript
Blume, G.	Preparation of nanocarriers, revision of the manuscript
Steiniger, F.	Microscopy, revision of the manuscript
Thamm, J.	Microscopy, revision of the manuscript

Werz, O.	Revision of the manuscript, supervision
Kralisch, D.	Revision of the manuscript, supervision
Fischer, D.	Conception of the study, interpretation of data, drafting and revision of the manuscript, corresponding author, supervision

Publication 3

Controlled extended octenidine release from a bacterial nanocellulose/Poloxamer hybrid system

Alkhatib, Y., Dewaldt, M., Moritz, S., Nitzsche, R., Kralisch, D., Fischer, D.

Published in: European Journal of Pharmaceutics and Biopharmaceutics, 2017, 112, p. 164-176

Several studies reported the use of BNC as drug delivery system. However, the controlled release of a drug was limited to short and moderate-terms, and no study has reported a long-term application. In this presented work, incorporation of the antiseptic octenidine in combination with Poloxamers 338 and 407 at micellar and gel concentrations was investigated. The utilized systems were characterized for their hydrodynamic size, surface charge, and dynamic viscosity. The critical micellar concentration and the gelation temperature was determined for both Poloxamer 338 and 407. The obtained release profiles of octenidine by Franz cell diffusion system revealed that the release behavior is impacted by the type and concentration of Poloxamers. For the first time a controlled release up to seven days was achieved by using Poloxamer 408 at the gel concentration. The incorporation of Poloxamers at the gel concentrations improved the mechanical stability of BNC. In addition, the newly developed system showed no impact on the high antimicrobial activity of octenidine against *Staphylococcus aureus* and *Pseudomonas aeruginosa* via agar diffusion test and the quantitative Live/Dead® BacLight™ kit. Moreover, the incorporation of Poloxamers into

BNC did not impact the outstanding biocompatibility of native BNC after local application in a shell-less hen's egg test.

To sum up, the loading of octenidine in combination with Poloxamers into BNC resulted in a wound dressing system for long-term applications.

Alkhatib, Y.	Fermentation and physiochemical characterization of bacterial nanocellulose and Poloxamer micelles and gels, determination of CMC and gelation temperature of Poloxamers, loading and release of Poloxamer, biocompatibility testing, analysis of mechanical tests, water retention and water absorption measurements, antimicrobial effectivity, drafting and revision of the manuscript
Dewaldt, M. (maiden name: Neumann, M.)	Characterization of bacterial nanocellulose, establishment of loading and release of octenidine, mechanical tests, rheology measurements, establishment of agar diffusion test, mathematical analysis of release profiles, revision of the manuscript
Nitzsche, R.	Particle size and zeta potential measurements, revision of the manuscript
Moritz, S.	Conception of the study, drafting and revision of the manuscript, laboratory supervision for Marie Dewaldt
Kralisch, D.	Preparation of the nanocellulose fleeces, revision of the manuscript
Fischer, D.	Conception of the study, interpretation of data, drafting and revision of the manuscript, corresponding author, supervision

4. Publications

4.1. Publication 1

Overcoming the hydrophilicity of bacterial nanocellulose: Incorporation of the lipophilic coenzyme Q10 using lipid nanocarriers for dermal applications

Y. Alkhatib, G. Blume, J. Thamm, F. Steiniger, D. Kralisch, D. Fischer

European Journal of Pharmaceutics and Biopharmaceutics, 2021, 158, p. 106-112

DOI 10.1016/j.ejpb.2020.10.021

European Journal of Pharmaceutics and Biopharmaceutics 158 (2021) 106–112

Contents lists available at ScienceDirect

European Journal of Pharmaceutics and Biopharmaceutics

journal homepage: www.elsevier.com/locate/ejpb

Overcoming the hydrophilicity of bacterial nanocellulose: Incorporation of the lipophilic coenzyme Q10 using lipid nanocarriers for dermal applications

Yaser Alkhatib [a], Gabriele Blume [b], Jana Thamm [a], Frank Steiniger [c], Dana Kralisch [a,d], Dagmar Fischer [a,d,*]

[a] Pharmaceutical Technology and Biopharmacy, Institute of Pharmacy, Friedrich-Schiller-University Jena, Lessingstraße 8, 07743 Jena, Germany
[b] Sopharcos Dr. Gabriele Blume, Im Schloss 7, 36396 Steinau an der Strasse, Germany
[c] Electron Microscopy Center, University Hospital Jena, Friedrich-Schiller-University Jena, Ziegelmühlenweg 1, 07743 Jena, Germany
[d] Jena Center for Soft Matter (JCSM), Friedrich-Schiller-University Jena, Philosophenweg 7, 07743 Jena, Germany

ARTICLE INFO

Keywords:
Bacterial nanocellulose
Drug delivery
Nanoemulsion
Coenzyme Q10
Skin
Liposome

ABSTRACT

Although used in a wide range of medical and pharmaceutical applications, the potential of the natural biopolymer bacterial nanocellulose (BNC) as drug delivery system is by far not fully exploited. Particularly, the incorporation of lipophilic drugs is still considered as an unsolved task. In the present study, the homogeneous incorporation of the lipophilic coenzyme Q10 (CoQ10) into BNC was accomplished by several post-synthesis techniques utilizing different nanoemulsions and liposomes. All colloidal carriers were in the range of about 90–120 nm with negative zeta potentials and storage stabilities up to 30 days. The biphasic drug release profiles of loaded BNC were found to be dependent on the type of colloidal carrier and the loading technique. Favorable characteristics such as high mechanical stability and high loading capacity were retained after the incorporation of the lipophilic components. Penetration studies using excised porcine skin revealed CoQ10 distributions also in deeper skin layers dependent on the type of the colloidal carrier system. In conclusion, hydrophilic BNC could be loaded with water-insoluble drugs as shown for the model drug CoQ10 by the use of lipidic colloidal carriers which offers new possibilities of application in pharmacy and medicine.

1. Introduction

Bacterial nanocellulose (BNC) belongs to the natural and sustainable hydropolymers and is typically used in dermal and transdermal applications, preferentially wound dressings, implants and tissue engineering. It is characterized by a three-dimensional cross-linked structure of ultrafine cellulose fibres which is responsible for outstanding physicochemical and biological properties [1]. BNC has attracted wide interest in biomedical applications due to its excellent biocompatibility, unique mechanical and thermal properties, high water binding capacity, and the impregnation with large amounts of drugs due to the enormous surface-area-to-volume ratio [1]. However, its high water content of > 90% limits the application as drug delivery system for water-insoluble drugs although they are a major trend and still unmet need of the pharmaceutical industry.

Up to now only a limited number of papers discussed the incorporation of hydrophobic molecules in BNC by using two strategies. On the one hand, lipophilic compounds can be integrated into BNC after chemical fibre modification such as oxidation using periodate or acetylation with acetic anhydride [2]. Although fibre hydrophobization allowed an effective decrease of the surface energy of BNC and thus a high selectivity to absorb oils, nonpolar liquids and drugs, often the unique properties of the BNC were changed. Alternatively, hydrophobic drugs were directly covalently linked to the fibres or incorporated in cyclodextrins, nanoparticles, microemulsions or ionic liquids [2,3].

The aim of the present study focussed on the development of a loading technique for the water-insoluble drug coenzyme Q10 (CoQ10) into BNC using lipid nanosystems like nanoemulsions and liposomes,

* Corresponding author at: Pharmaceutical Technology and Biopharmacy, Institute of Pharmacy, Friedrich-Schiller-University, Lessingstraße 8, 07743 Jena, Germany.
E-mail addresses: yaser.alkhatib@uni-jena.de (Y. Alkhatib), info@sopharcos.de (G. Blume), dana.kralisch@uni-jena.de (J. Thamm), frank.steiniger@med.uni-jena.de (F. Steiniger), dana.kralisch@uni-jena.de (D. Kralisch), dagmar.fischer@uni-jena.de (D. Fischer).

https://doi.org/10.1016/j.ejpb.2020.10.021
Received 20 April 2020; Received in revised form 2 October 2020; Accepted 27 October 2020
Available online 12 November 2020

without the need of chemical modification of the native BNC. CoQ10 was selected as model drug due to its high lipophilicity (log P > 10) and role in skin applications as antioxidant [4]. The uptake and release of the CoQ10 containing colloidal carriers in and from BNC as well as the influence of the exchange of water by lipid components on the physicochemical characteristics of BNC were determined. Furthermore, drug transport from BNC into excised porcine skin was quantified by tape stripping experiments.

2. Materials and methods

2.1. Preparation and characterization of colloidal carriers containing CoQ10

All CoQ10 (GfN & Selco GmbH) containing nanocarriers were produced utilizing a top-down high-pressure homogenisation (Microfluidizer® M 110 S, Microfluidics Corporation, Westwood, USA) under cooling at 550 bar (O/W, liposome) and 350 bar (W/O/W) for 3 min [5]. The O/W nanoemulsion consisted of a lipophilic phase containing 3.5% Imwitor 375 (IOI Oleo GmbH, Hamburg, Germany), 1.5% co-emulsifier diglycerol monooleate (Nikko Chemicals Co., Japan), 15% soybean oil (Henry Lamotte, Bremen, Germany), and 10% ethanol. The W/O/W nanoemulsion was formulated using a lipophilic phase consisting of 10.5% Imwitor 375, 4.5% ethyl oleate (Crodamol™ EO, Croda GmbH, Nettetal, Germany), and 10% ethanol. For both O/W and W/O/W nanoemulsions 69.5% and 74.5% purified water was used, respectively, as hydrophilic phase. The liposomal reference system was composed of 10% Lipoid S75® (Lipoid, Ludwigshafen, Germany), 15% ethanol and 74.5% phosphate buffered saline (PBS) pH 6.5. For all nanocarriers CoQ10 was dissolved in ethanol at 50 °C followed by addition of the emulsifying agent and the oil and stirring until a homogeneous mixture was obtained. Afterwards, the hydrophilic phase was added and homogenized using the Ultra-Turrax® T25B (Janke & Kunkel GmbH, Staufen, Germany) at 9,500 rpm for 1 min before treatment with the Microfluidizer.

Nanocarriers were characterized regarding hydrodynamic diameter (HD) and polydispersity index (PDI) by dynamic light scattering using the Zetasizer Nano ZS (Malvern Instrument, Germany; Software: Zetasizer V7.2) equipped with a 4 mW He-Ne laser (633 nm) in Milli-Q water (1:100) in a minimal volume cuvette ZEN 0040 at a 173° and 25 °C. Zeta potential (ZP) was measured in a Zetasizer cuvette DTS1060 using laser Doppler anemometry at 25 °C.

For the testing of the storage stability undiluted nanocarrier preparations were investigated as synthesized at 4 °C (temperature-controlled refrigerator), room temperature and 37 °C (drying cabinet) in airtight brown glass bottles in the dark. Macroscopic changes, particle sizes and zeta potentials were determined at different time points by laser light scattering techniques as described before. Results were statistically evaluated by one-way ANOVA (significance level $p = 0.05$) using Microsoft Excel 2016 software.

Cryogenic transmission electron microscopy (cryo-TEM) was performed by applying 5 µL of each CoQ10 nanocarrier to copper grids coated with a perforated carbon film (Quantifoil Micro Tools GmbH, Germany). After plunging into liquid ethane at −180 °C, specimen were transferred with a Gatan 626 cryo-transferholder to the Philips CM120 cryo-TEM (LaB_6 cathode source operated at 120 kV accelerating voltage and stage maintained at −178 °C). Recording of the images was done with a 2 k CMOS camera F216 (TVIPS GmbH, Germany). In order to minimize the noise, four sequential images were taken and averaged to one.

2.2. Preparation of CoQ10 containing BNC

BNC (24-well) was biosynthesized by *Komagataeibacter xylinus* DSM 14,666 (culture collection of the Friedrich-Schiller-University Jena, German Collection of Microorganisms and Cell Cultures, Braunschweig, Germany) in Hestrin-Schramm medium at 28 °C followed by purification as described previously [6]. Never-dried (nd) and freeze-dried (fd, 37 mbar, −85 °C condenser temperature, 72 h) fleeces were used for loading experiments. Three different post-synthesis loading techniques for CoQ10 were applied: (i) "re-swelling": fd-fleeces were loaded by re-swelling with 750 µL CoQ10 nanocarrier dispersion for 15 min; (ii) "injection": 125 µL CoQ10 nanocarrier dispersion were injected into the core of the nd-BNC fleeces using a disposable syringe; (iii) "submerse absorption": nd-BNC was incubated under submerse conditions in 10 mL CoQ10 nanocarrier dispersion on a temperature-controlled orbital shaker at 70 rpm and 20 °C for 48 h. The amount of loaded CoQ10 into BNC was calculated by the difference of the CoQ10 concentration of the loading solution before and after the loading process [7].

2.3. Physicochemical characterization of loaded BNC

Loaded BNC samples were investigated using cryo-scanning electron microscopy (cryo-SEM). Pieces of 2 mm were cut and frozen in a liquid propane/ethane mixture (1:1) (Linde Gas, Pullach, Germany) cooled by liquid nitrogen. Using a BALTEC VCT 100 Cryo-Transfer-Unit (BAL-TEC, Balzers, Liechtenstein), frozen specimen were transferred in a BALTEC Med 020 Coating System where specimen were cut at −140 °C, etched for 5 min at −95 °C and sputtered with 7 nm gold/palladium. Frozen specimen were investigated with the SEM LEO 1530 Gemini (Carl Zeiss AG, Oberkochen, Germany) using the InLens detector at 6 kV acceleration voltage.

The mechanical stability of BNC was measured as described previously by applying a test weight of 400 g perpendicular for 10 min [7].

Release the CoQ10 from loaded BNC was performed using the Franz cell diffusion system (SES-Analysensysteme, Bechenheim, Germany) under stirring with 12 mL Milli-Q water at 32 °C as receiver compartment. The BNC fleeces were placed directly on top of the diffusion cells without the use of a membrane. Aliquots were withdrawn at defined time points up to 48 h and replaced by fresh, pre-heated medium. The CoQ10 concentration was quantified using high-performance liquid chromatography (HPLC) (Shimadzu Corporation, USA) with a Hypersil™ BDS C18 column (250 mm, 3 mm × 5 µm, Macherey-Nagel, USA, injection volume 40 µL). The mobile phase consisted of methanol and hexane (80:20, 1 mL/min) with a gradient elution program. The chromatograms were recorded at 275 nm and processed using the Chromeleon™ 6.8 software from Dionex™. The linearity ranged between 0.66 and 66 µg/mL with $R^2 = 0.999$, a limit of detection of 0.07 µg/mL and a limit of quantification of 0.17 µg/mL. The retention time of CoQ10 was 9.97 ± 0.02 min. All experiments were run in triplicate and repeated once.

2.4. Ex vivo penetration studies of CoQ10

Skin penetration experiments were carried out using the tape stripping technique with porcine ear skin obtained from local supplier. Skin discs (2.19 cm^2) were fixed on PBS 7.4 saturated filter paper with a self-adhesive aluminium foil (Alu930 SE, Coroplast, Germany). After 6 h of nanocarrier application (10 µL/cm^2) or the loaded BNC, skin was tape stripped 15times with an adhesive tape (tesafilm® kristall-klar, tesa SE, Norderstedt, Germany). One drop of cyanoacrylate-based glue (UHU GmbH & Co. KG, Bühl/Baden, Germany) was added for strip number 15. Each strip was extracted in methanol/hexane (80:20) and measured by HPLC. Untreated skin was used as control. All experiments were performed in triplicates and repeated once. The results of the skin penetration studies were evaluated statistically by one-way ANOVA followed by a Tukey post-hoc test (significance level $p = 0.05$) using Microsoft Excel 2016 software.

3. Results and discussion

CoQ10 was used as a lipophilic model drug for skin applications,

with a low water solubility of about 0.193 μg/mL, and a molar mass of 863 g/mol which all result in low skin penetration. Since its direct incorporation into BNC resulted in recrystallization and inhomogeneous distribution (data not shown), three different lipid nanocarriers were used to exchange the water in the 3D-network of the BNC. The skin-friendly single (O/W) and double (W/O/W) nanoemulsions due to the natural origin of the main emulsifier and the low ratio of surfactants, were formulated using a top-down high-pressure homogenization procedure and contained a final concentration of 3.32 ± 0.05 CoQ10 in O/W and 3.21 ± 0.09 mg/mL CoQ10 in W/O/W nanoemulsions. For comparison, standard liposomes (3.20 ± 0.06 mg/mL CoQ10) made of phosphatidylcholine were used. PCS measurements revealed mean hydrodynamic diameters of about 115 nm (O/W), 94 nm (W/O/W), and 98 nm (liposomes) with a monodisperse distribution as represented by a PDI below 0.17 for all preparations, with a trend to higher poyldispersities and variability for the W/O/W nanoemulsions (Table 1). A negative zeta potential below −60 mV for all nanocarriers was determined indicating high repulsive electrical forces among the droplets to avoid coalescence. All data were comparable to empty nanocarriers indicating that the drug had no influence on these parameters (data not shown). Size data, a spherical morphology and the typical internal structures were confirmed by cryo-TEM (Table 1). Moreover, the three types of nanocarriers showed a high stability with no significant change ($p > 0.05$) regarding to HD and ZP over up to 30 days storage at three different temperatures: (i) 4 °C for storage, (ii) room temperature for handling, (iii) 37 °C as body temperature (Table 1).

Nd-BNC fleeces cultivated at the air–liquid interface were characterized by a diameter of about 1.60 ± 0.01 cm, height of 0.56 ± 0.02 cm, average mass of 1.09 ± 0.03 g, a calculated volume of 1.13 ± 0.04 cm^3 and total surface area as 6.87 ± 0.11 cm^2. The dimensions of fd-BNC samples were comparable to nd-BNC with reduction of the mass to about 1.3% of the initial weight due to complete water loss. Three different post-synthesis loading techniques were compared for the incorporation of the different nanocarriers at room temperature [8] : (i) "re-swelling" of fd-BNC with CoQ10 nanocarrier dispersion within 15 min, (ii) "injection" of the dispersion into the core of nd-BNC to form a core–shell system, and (iii) "submerse absorption" under orbital shaking for 48 h. The macroscopic inspection of all loaded BNCs after cross-sectioning revealed a homogeneous distribution of CoQ10 in case of submerse absorption (Fig. 1A) and re-swelling (data not shown), and the formation of a yellow CoQ10 core after injection (data not shown). Both techniques, re-swelling and injection, showed a complete uptake of the dispersions and were considered as fast and efficient methods enabling 100% loading efficacy without drug loss. A comparison of the calculated amount of loaded CoQ10 per BNC fleece revealed differences depending on the type of loading, and ranged from 0.38 ± 0.03 mg for injection, to 2.43 ± 0.05 mg for re-swelling, and 3.03 ± 0.18 mg for the absorption loaded BNC. In contrast, under the chosen conditions the submerse absorption technique accomplished an uptake of 9–10% of the drug from the supernatant (Fig. 1A) which is related to the ratio of 1 mL BNC fleece to 10 mL loading solution and comparable to reports for small molecules and micelles [7]. In contrast to ethanolic CoQ10 solutions incorporated in BNC which were characterized by the formation of large, macroscopically visible CoQ10 crystals due to the evaporation of the ethanol (data not shown), none of the loaded BNCs showed macroscopically detectable recrystallization events. Using cryo-SEM, both types of BNC fleeces, native (nd, Fig. 1B) and freeze-dried (fd, data not shown), loaded via the submerse absorption technique with nanoemulsions or liposomes demonstrated 3D-nanofiber structures comparable to the unloaded nd- and fd-BNC indicating that the network was not influenced by the loading process or the presence of the nanocarriers. The incorporated nanoparticles were clearly detectable in the BNC network associated with the nanofibers (Fig. 1B). The loading of nanocarriers did not have an impact on the mechanical stability of BNC as determined by perpendicular loading of BNC with a 400 g weight for 10 min. No changes of the compressive strain, no weight reduction or water loss could be detected (Fig. 2).

The release behavior of loaded BNC was investigated using a Franz cell diffusion system at 32 °C. Samples were collected at defined time points over up to 48 h and quantified by HPLC. Release profiles were presented as the release of the cumulative amount of CoQ10 in dependency of time (Fig. 3). All formulations demonstrated a biphasic release profile with an initial burst up to 8–10 h followed by a slower release rate and a plateau reaching equilibrium conditions. The total cumulative release and the height of the plateau were found to be dependent on the type of nanocarrier and the loading technique. Independent of the loading technique, the CoQ10 release from BNC decreased with W/O/W > O/W nanoemulsions > liposomes. For the

Table 1
Physicochemical characterization of CoQ10 containing nanocarriers regarding morphology, particle size, polydispersity and zeta potential after preparation, storage for 30 days as synthesized at different temperatures, and release. All experiments were performed in triplicates and repeated once.

		O/W	W/O/W	Liposome
Cryo-TEM		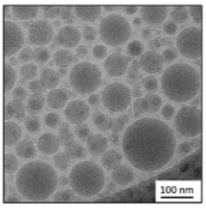	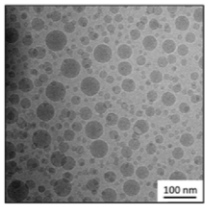	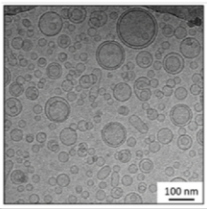
Day 1	HD (nm)	114.5 ± 6.8	94.1 ± 1.6	98.0 ± 1.8
	PDI	0.11 ± 0.00	0.11 ± 0.03	0.16 ± 0.01
	ZP (mV)	−68 ± 1	−72 ± 3	−62 ± 6
30 days at 4 °C	HD (nm)	119.4 ± 8.9.	92.6 ± 12.7	100.8 ± 0.6
	PDI	0.11 ± 0.00	0.15 ± 0.04	0.13 ± 0.30
	ZP (mV)	−77 ± 4	−79 ± 6	−66 ± 7
30 days at RT °C	HD (nm)	119.3 ± 7.5	78.9 ± 13.7	101.3 ± 8.2
	PDI	0.09 ± 0.00	0.13 ± 0.02	0.17 ± 0.03
	ZP (mV)	−70 ± 2	−79 ± 9	−69 ± 5
30 days at 37 °C	HD (nm)	116.2 ± 6.9	82.3 ± 12.4	98.6 ± 5.9
	PDI	0.09 ± 0.02	0.15 ± 0.04	0.17 ± 0.06
	ZP (mV)	−68 ± 1	−80 ± 8	−73 ± 4
After release	HD (nm)	111.3 ± 1.9	101.7 ± 21.6	117.2 ± 2.9
	PDI	0.11 ± 0.01	0.17 ± 0.04	0.14 ± 0.02
	ZP (mV)	−65 ± 1	−73 ± 2	−63 ± 5

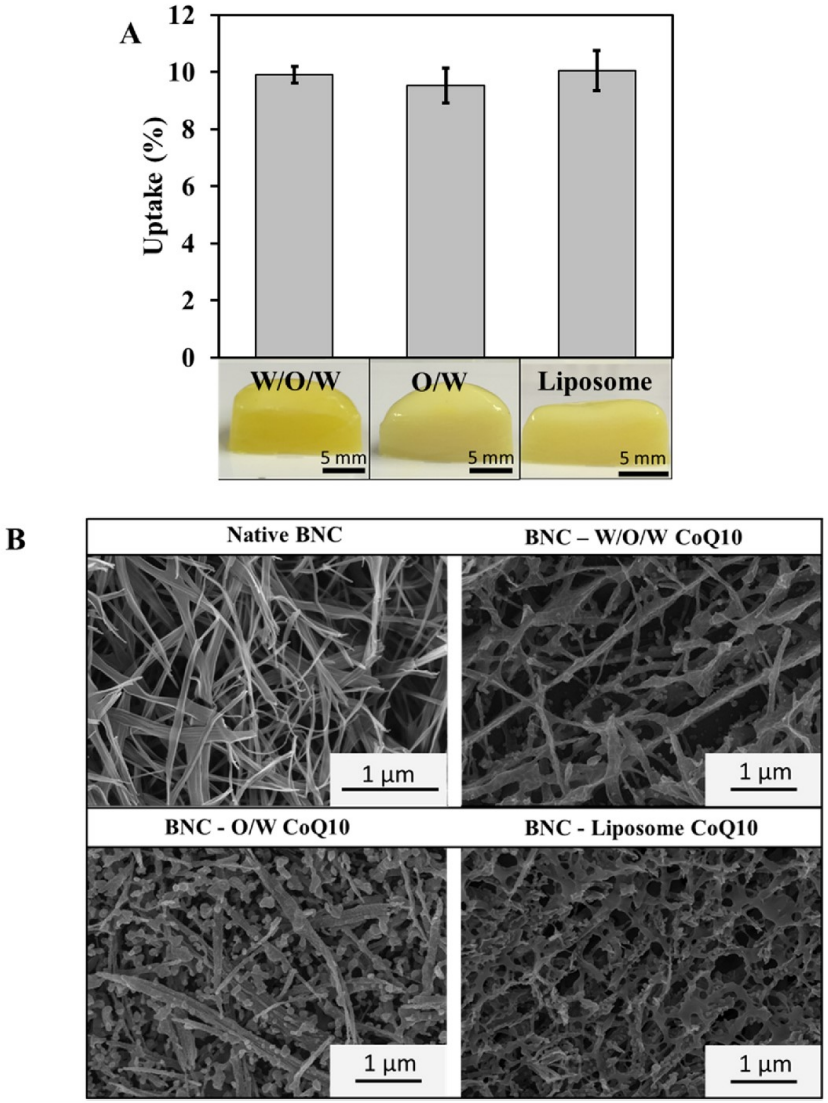

Fig. 1. Percentage of CoQ10 loading in nd-BNC by the submerse absorption technique using different nanocarriers with representative photographs after cross-sectioning (mean ± SD, $n = 3$) **(A)**. Cryo-SEM images of absorption loaded native BNC with and without CoQ10 **(B)**.

different behaviour of the nanoemulsions the smaller particle size and the higher hydrophilic content of the W/O/W nanoemulsion were suggested to be responsible for this effect. In contrast, BNC containing CoQ10 liposomes showed a very slow, incomplete release, which might be related to their less flexible structure.

Changing the type of loading from absorption to re-swelling and injection reduced the cumulative drug release per time. As previously shown by Müller et al. [9], fd-BNC is characterized by some structural changes of the 3D-nanofiber network such as partial aggregation of the free polymer strands due to the lyophilization process. These effects could retard drug diffusion and consequently, drug release and explain the lower release performance of the BNC produced by re-swelling *vs.* submerse absorption. The lowest drug release rate obtained for the core–shell systems after injection reflects the longer diffusional pathway of the drug from the core to the acceptor medium. The understand more about the release mechanism of the nanoemulsions, the withdrawn samples of the release experiments were investigated regarding HD and PDI using photon correlation spectroscopy. As shown in Table 1, HD and PDI remained unchanged before and after release suggesting that particles were released from the BNC which might be advantageous to support penetration into the skin.

Mathematical modelling of the release curves for the nanoemulsions followed the Ritger-Peppas equation [10]. All samples showed a linear equation with regression coefficients (r^2) of 0.936–0.989 and diffusional exponents of n = 0.45–0.52 which represented a diffusional process overlayed by swelling controlled mechanisms (Table 2).

For the implementation of the newly developed system in the field of dermal applications, a proof-of-concept skin penetration study was performed. In the first step, the nanoemulsions without BNC were applied for 6 h on excised porcine skin and demonstrated penetration profiles as shown in Fig. 4A. For W/O/W nanoemulsions higher amounts of CoQ10 could be detected in the middle and deeper skin layers whereas for the O/W nanoemulsions more CoQ10 accumulated on the skin surface. This effect might be related to the higher hydrophilicity

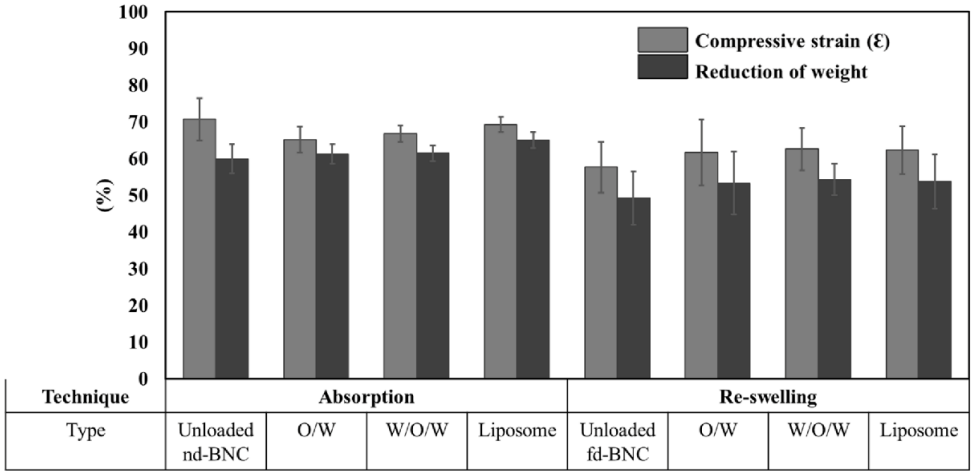

Fig. 2. Mechanical stability represented by the reduction of weight and compressive strain (ε) of unloaded BNC in comparison to BNC with nanocarriers loaded with CoQ10 presented as mean ± SD, measured in quintuplicates and repeated twice.

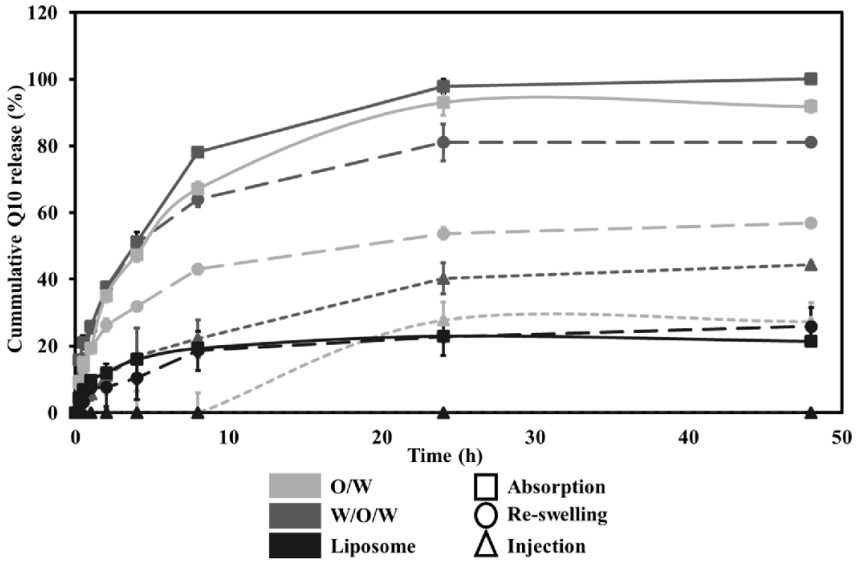

Fig. 3. Time dependent cumulative release profile of CoQ10 from the BNC loaded with nanocarriers using the absorption, re-swelling and injection techniques, measured in Franz diffusion cell at 32 °C over 48 h (mean of 3 BNC fleeces ± SD).

Table 2
Mathematical modelling of cumulative release profile using the Ritger and Peppas equation.

Loading Technique		Power law equation	Diffusion exponent n	Linear regression R^2
O/W	Absorption	y = 0.5026x + 1.3568	0.52	0.985
	Re-swelling	y = 0.4878x + 1.1972	0.49	0.936
W/O/W	Absorption	y = 0.4502x + 1.4843	0.45	0.989
	Re-swelling	y = 0.5223x + 1.4515	0.52	0.983

and smaller particle size of the W/O/W nanoemulsions. Based on the *in vitro* release data only adsorption loaded BNC with CoQ10 containing nanoemulsions (2.83 ± 0.04 mg for W/O and 3.17 ± 0.13 mg for W/O/W) were tested under the same conditions (Fig. 4 B). A comparable trend as for the pure nanoemulsions could be observed. Both types of BNC with O/W and W/O/W nanoemulsions delivered CoQ10 into the skin. BNC loaded with the W/O/W nanoemulsion showed a significant ($p < 0.05$), about three times higher amount of CoQ10 even in the deeper layers, whereas BNC with O/W nanoemulsion formed a depot in the upper layers. Due to the depot effect of the BNC matrix and the additional liberation step of the nanocarriers from the nanocellulose network before penetration into the skin, drug release was retarded compared to the pure nanoemulsions and resulted in lower CoQ10 concentrations especially in the upper layers. Conclusively, the tested delivery systems provided a controlled release system which could be custom designed to the aimed application.

The applied CoQ10 amount was about 15fold to 200fold higher than described in other reports where antioxidative properties of sera in women were confirmed or *in vitro* in keratinocyte cell cultures the

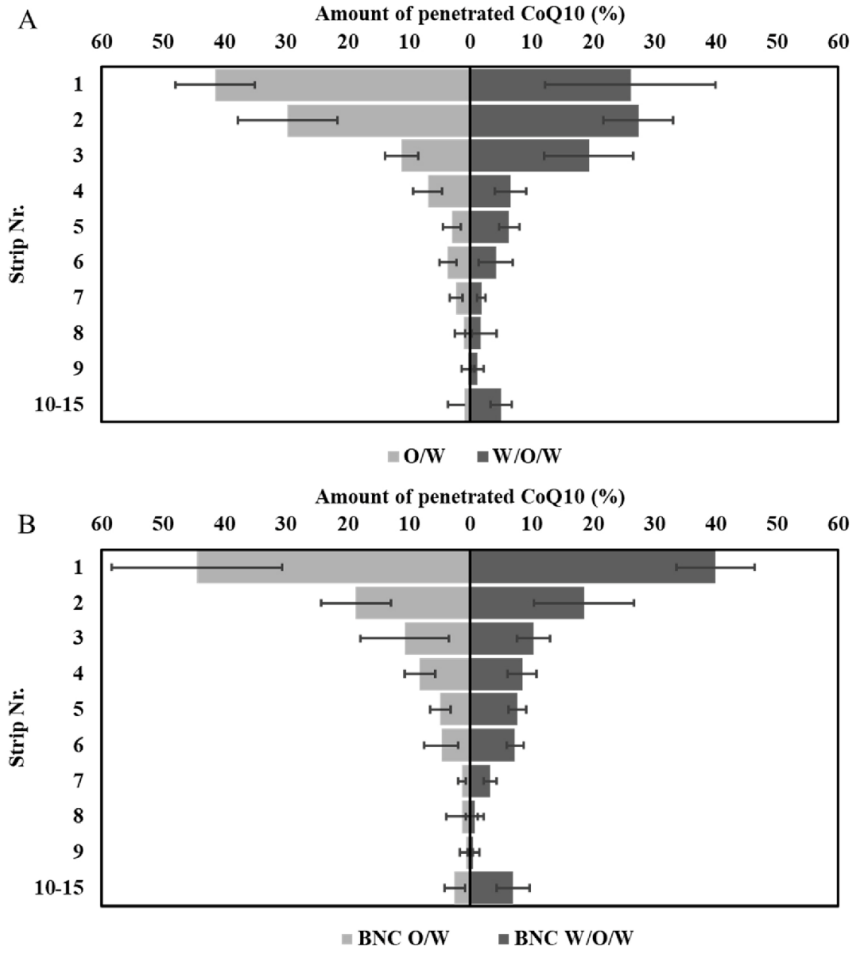

Fig. 4. Skin penetration studies using tape stripping experiments on porcine skin of CoQ10 nanoemulsions (O/W and W/O/W) without BNC after an application time of 6 h (n = 3) **(A)** in comparison to BNC loaded with nanoemulsions **(B)**.

radical production after UV-radiation was decreased, respectively. The total amount of CoQ10 that penetrated into the skin was determined to be 22.17 ± 9.26 μg/cm^2 and 25.09 ± 7.18 μg/cm^2 for O/W and W/O/W nanoemulsions after 6 h of application, respectively. Although difficult to compare due to different test settings, these amounts of CoQ10 were found to be comparable to that reported in the literature for other dermal delivery systems. For example, Korkmaz et al. [11] described that the use of solid lipid nanoparticles incorporated in a hydrogel improved the CoQ10 delivery into deeper skin layers up to 38 μg/cm^2. Teeranchaideekul et al. [12] reported a transport of a total of 4 μg CoQ10 over 24 h into deeper skin layers by nanoemulsions. The bioactive CoQ10 concentration reported in the literature varied depending on the type of experiment. Whereas Zhang et al.[13] claimed a concentration of 2 μM CoQ10 (corresponding to 1.73 μg) effective against skin aging, Yue et al. [14] reported that the optimal concentration of CoQ10 to protect cells form UV radiation is 11.6 μM (corresponding to 10.01 μg/mL).

4. Conclusion

The present study demonstrates the potential of BNC as drug delivery system for lipophilic drugs realized by the exchange of water in the nanofiber network by differently structured lipid carriers. Variations of the lipid nanocarriers and the loading technique revealed the possibility to adapt and control the release profile. Especially the nanoemulsions accomplished the successful release and penetration of the model drug CoQ10 into the skin, whereas the potential of the liposomes should be further investigated e.g. by variation of the lipid composition. The preferential characteristics of the nd BNC remained mostly unchanged and judges the potential application as hydropolymer in skin applications. Therefore, in future studies biological applications and biocompatibility will be investigated.

Acknowledgements

The authors would like to thank Angela Herre and Ramona Brabetz for their excellent technical support as well as the JeNaCell GmbH for providing the *Komagataeibacter xylinus* culture.

References

[1] T. Carvalho, et al., Latest advances on bacterial cellulose-based materials for wound healing, delivery systems, and tissue engineering, Biotechnol. J. 14 (2019) 1900059.
[2] D. Klemm, et al., Nanocellulose as a natural source for groundbreaking applications in materials science: Today's state, Mater. Today 21 (2018) 720–748.
[3] M. Badshah, et al., Surface modification and evaluation of bacterial cellulose for drug delivery, Int. J. Biol. Macromol. 113 (2018) 526–533.
[4] S. Kumar, et al., Novel carriers for coenzyme Q10 delivery, Curr. Drug Deliv. 13 (2016) 1184–1204.

[5] Blume, G., Colloidal carrier system with penetration properties for encapsulating lipophilic active agents and oils for topical use. 2015, WO0002012089184A3.
[6] D. Kralisch, et al., White biotechnology for cellulose manufacturing—The HoLiR concept, Biotechnol. Bioeng. 105 (2010) 740–747.
[7] Y. Alkhatib, et al., Controlled extended octenidine release from a bacterial nanocellulose/Poloxamer hybrid system, Eur. J. Pharm. Biopharm. 112 (2017) 164–176.
[8] Y. Pötzinger, et al., Immobilization of plasmids in bacterial nanocellulose as gene activated matrix, Carbohydr. Polym. 209 (2019) 62–73.
[9] A. Muller, et al., The biopolymer bacterial nanocellulose as drug delivery system: investigation of drug loading and release using the model protein albumin, J. Pharm. Sci. 102 (2013) 579–592.
[10] P.L. Ritger, N.A. Peppas, A simple equation for description of solute release II. Fickian and anomalous release from swellable devices, J. Control. Release 5 (1987) 37–42.
[11] E. Korkmaz, E.H. Gokce, O. Ozer, Development and evaluation of coenzyme Q10 loaded solid lipid nanoparticle hydrogel for enhanced dermal delivery, Acta Pharmaceutica 63 (4) (2013) 517.
[12] V. Teeranachaideekul, et al., Cetyl palmitate-based NLC for topical delivery of Coenzyme Q10 – Development, physicochemical characterization and in vitro release studies, Eur. J. Pharm. Biopharm. 67 (1) (2007) 141–148.
[13] M. Zhang, et al., Coenzyme Q10 enhances dermal elastin expression, inhibits IL-1α production and melanin synthesis in vitro, Int. J. Cosmet. Sci. 34 (3) (2012) 273–279.
[14] Y. Yue, et al., The advantages of a novel CoQ10 delivery system in skin photoprotection, Int. J. Pharm. 392 (1) (2010) 57–63.

4.2. Publication 2

Development and characterization of bacterial nanocellulose loaded with Boswellia serrata extract containing nanoemulsions as natural dressing for skin diseases

B. Karl, Y. Alkhatib, U. Beekmann, T. Bellmann, G. Blume, F. Steiniger, J. Thamm, O. Werz, D. Kralisch, D. Fischer

International Journal of Pharmaceutics, 2020, 587, Article 119635

DOI 10.1016/j.ijpharm.2020.119635

International Journal of Pharmaceutics 587 (2020) 119635

Contents lists available at ScienceDirect

International Journal of Pharmaceutics

journal homepage: www.elsevier.com/locate/ijpharm

Development and characterization of bacterial nanocellulose loaded with *Boswellia serrata* extract containing nanoemulsions as natural dressing for skin diseases

Berit Karl[a], Yaser Alkhatib[a], Uwe Beekmann[a], Tom Bellmann[a], Gabriele Blume[b], Frank Steiniger[c], Jana Thamm[a], Oliver Werz[d,e], Dana Kralisch[a,e], Dagmar Fischer[a,e,*]

[a] *Pharmaceutical Technology and Biopharmacy, Friedrich Schiller University Jena, Lessingstraße 8, 07743 Jena, Germany*
[b] *Sopharcos Dr. Gabriele Blume, Im Schloss 7, Steinau an der Straße, Germany*
[c] *Electron Microscopy Center, University Hospital Jena, Friedrich Schiller University Jena, Ziegelmuehlenweg 1, 07743 Jena, Germany*
[d] *Pharmaceutical and Medicinal Chemistry, Philosophenweg 14, 07743 Jena, Germany*
[e] *Jena Center for Soft Matter (JCSM), Friedrich Schiller University Jena, Philosophenweg 7, 07743 Jena, Germany*

ARTICLE INFO

Keywords:
Bacterial nanocellulose
Nanoemulsion
Boswellia serrata
Inflammation
Skin
Drug delivery

ABSTRACT

The combination of the anti-inflammatory lipophilic *Boswellia serrata* extract with the natural hydropolymer bacterial nanocellulose (BNC) for the treatment of skin diseases is counteracted by their different hydro/lipophilicity. To overcome the hydrophilicity of the BNC, the water in its network was exchanged by single and double nanoemulsions. Incorporation of the *Boswellia serrata* extract in the nanoemulsions formed particles of about 115 to 150 nm with negative zeta potential and storage stability over 30 days at temperatures between 4 and 32 °C. Their loading into the BNC did not change the preferential characteristics of the nanocellulose like water absorption and retention, softness, and pressure stability in a relevant way. Loaded BNC could be sterilized by an electron-beam procedure. A biphasic drug release profile of lead compounds was observed by Franz cell diffusion test. The biocompatibility of the loaded BNC was confirmed *ex ovo* by a shell-less hen's egg test. Tape stripping experiments using porcine skin determined a dependency of the drug penetration into skin on the type of nanoemulsion, single *vs.* repeated applications and the incubation time. In conclusion, the hydrophilicity of BNC could be overcome using nanoemulsions which offers the possibility for the anti-inflammatory skin treatment with *Boswellia serrata* extract.

1. Introduction

Cutaneous wound healing is a complex physiological mechanism involving many cell types in the three highly programmed, consecutive steps: inflammation, proliferation and remodeling (Gonzalez et al., 2016). The deregulation of one step, which results in a failure to orderly progress through these phases, may cause impaired wound healing and the development of chronic wound conditions. Impaired tissue repair can be favored by advanced age, comorbidities like diabetes or hypertension, adiposity or a weakened immune system (Khalil et al., 2015). In the case of insufficient self-healing capacities of wounds, therapeutic invention becomes inevitable, which results in enormous health care expenditures every year (Olsson et al., 2019).

The gum resin of *Boswellia serrata*, a natural product that is widely used in traditional ayurvedic medicine, contains several pentacyclic triterpenoids, e.g. boswellic acids, with a potent anti-inflammatory, immunomodulatory, antitumor and hypolipidemic activity. Lipophilic extracts of the gum resin derived from *Boswellia serrata* (*B. serrata* extracts, BSE), were discussed as natural substitutes for non-steroidal anti-inflammatory drugs (NSAID) such as ibuprofen or naproxen for the treatment of inflammatory, arthritic and analgesic events (Abdel-Tawab et al., 2011). The anti-inflammatory effects have been mainly attributed to the inhibition of 5-lipoxygenase, an enzyme which initializes the conversion of arachidonic acid to leukotrienes, promoting chronic inflammatory diseases (Rådmark et al., 2015). 3-*O*-acetyl-11-keto-β-boswellic acid (AKBA) and 11-keto-β-boswellic acid (KBA) were identified as the most effective anti-inflammatory compounds of BSE. The therapeutic potential of standardized BSE for treating skin diseases was

* Corresponding author at: Pharmaceutical Technology and Biopharmacy, Friedrich Schiller University Jena, Lessingstraße 8, 07743 Jena, Germany.
E-mail addresses: berit.karl@uni-jena.de (B. Karl), yaser.alkhatib@uni-jena.de (Y. Alkhatib), uwe.beekmann@uni-jena.de (U. Beekmann), tom.bellmann@uni-jena.de (T. Bellmann), info@sopharcos.de (G. Blume), frank.steiniger@med.uni-jena.de (F. Steiniger), jana.thamm@uni-jena.de (J. Thamm), oliver.werz@uni-jena.de (O. Werz), dana.kralisch@uni-jena.de (D. Kralisch), dagmar.fischer@uni-jena.de (D. Fischer).

https://doi.org/10.1016/j.ijpharm.2020.119635
Received 27 March 2020; Received in revised form 6 July 2020; Accepted 7 July 2020
Available online 18 July 2020

recently shown by Pengzong et al. in diabetic foot ulcer by the inhibition of oxido-inflammatory markers, increased collagen synthesis and angiogenesis, promotion of growth factors and inhibition of apoptosis (Pengzong et al., 2019). A significantly higher new blood vessel formation and epithelization of wounds could be shown after treatment with the BSE.

However, BSE is highly lipophilic suffering from a low aqueous solubility and poor bioavailability even after topical administration. Due to an elimination half-life of KBA of about 6 h, BSE formulations have to be repeatedly applied several times a day for long-term applications (Abdel-Tawab et al., 2011; Sharma et al., 2004; Skarke et al., 2012). To overcome these limitations, BSE has been formulated in lipid-based drug delivery systems for dermal and oral applications (Mehta, 2014) such as solid lipid nanoparticles (Shi et al., 2012), nanomicelles (Goel et al., 2010), niosomes, phytosomes, and liposomes (Sharma et al., 2010).

Bacterial nanocellulose (BNC) is a renewable, ultrapure and 3D-nano-structured hydropolymer consisting of nanocellulose and > 90% water, with outstanding physicochemical and biological properties (Pötzinger et al., 2017). Its extraordinary fitness for dermal applications can be explained by its high biocompatibility, impermeability to bacteria, painless removal, gas permeability and non-allergenicity as well as high absorptivity for wound exudate (Portela et al., 2019). It has been drawn tremendous attention during the last ten years as drug delivery system due to its large nano-sized network facilitating a high drug load for hydrophilic small and high molar mass drugs (Pötzinger et al., 2017). However, due to its high water content a direct incorporation of lipophilic drugs is not possible and requires more sophisticated drug delivery strategies. For this purpose the encapsulation of lipophilic drugs in cyclodextrins (Gupta et al., 2019), disperse multiphase systems like nanoparticles (Numata et al., 2015a) or microemulsions (Marquele-Oliveira et al., 2019) before incorporation into BNC, the formation of ionic liquids inside BNC (Chantereau et al., 2019) or the covalent binding of drugs directly to the nanofibers (Ye et al., 2018) were reported. A second option is based on surface modification of the BNC to enhance the lipophilicity of the fibers, e.g. by acetylation (Ávila Ramírez et al., 2017; Badshah et al., 2018).

In the present study, a strategy to incorporate a lipophilic BSE into the hydrophilic BNC for the application as anti-inflammatory active dressing to treat skin diseases was investigated by replacing the water in the three-dimensional BNC fiber network with single and double nanoemulsions. Loading techniques were developed and optimized to accomplish controllable release profiles and storage stability without impairment of the favorable material properties. The delivery systems were intensively characterized regarding their physicochemical characteristics, biocompatibility as well as efficient release and skin penetration. In particular, different application scenarios for the optimized drug delivery systems were investigated *ex vivo* on porcine skin.

2. Materials and methods

2.1. Preparation of materials

2.1.1. Preparation of nanoemulsions

Two different types of nanoemulsions, O/W (Blume, 2011a) and W/O/W (Blume, 2011b) (both Sopharcos Dermal Drug Delivery, Steinau an der Straße, Germany), were prepared according to Blume (Blume, 2015), consisting of an emulsifier, a hydrophilic aqueous and a lipophilic oil phase. Quantities of ingredients are mentioned according to the Food and Drug Administration code (Food and Drug Administration (FDA), 2014). The lipophilic phase of the O/W nanoemulsions contained 1–5% Imwitor® 375 (glyceryl citrate/lactate/linoleate/oleate) (IOI Oleo GmbH, Hamburg, Germany), 1–5% glyceryl monooleate (Gattefossé SAS, Saint-Priest, France), 10–25% *Helianthus annuus* seed oil (Henry Lamotte Oils GmbH, Bremen, Germany), and 10–25% propylene glycol (Henry Lamotte Oils GmbH). Preparation of loaded O/W nanoemulsions was performed with 1% BSE (Boswellin® Super, kindly provided by Sabinsa Europe GmbH, Langen, Germany). The outer hydrophilic phase was composed of ultrapure water. The lipophilic phase of the W/O/W nanoemulsions consisted of 5–10% emulsifying agent, in particular Imwitor® 375 (glyceryl citrate/lactate/linoleate/oleate), 1–5% ethyl oleate (Croda Health Care, Goole, United Kingdom), and 10–25% propylene glycol, which functioned as preserving agent. For drug-loaded W/O/W nanoemulsions 1% BSE was added to the lipophilic phase. Ultrapure water was used to build up the inner and outer hydrophilic phase. The preparation of both types of nanoemulsions was conducted with the same procedure. The BSE was mixed with the preserving agent until complete dissolution. Afterwards, the solution was heated to 50 °C. The emulsifying agent and the oil were added to the solution and stirred until a homogenous mixture was obtained. By adding water during dispersion of the phases, pre-emulsions were formed. The Ultra-Turrax® T25B (Janke & Kunkel GmbH, Staufen, Germany) was utilized at 9500 rpm for 1 min to disperse the phases. Finally, particle size was reduced by utilizing a Microfluidizer® M 110 S (Microfluidics Corporation, Westwood, USA) under cooling at 550 bar (O/W nanoemulsion) or 350 bar (W/O/W nanoemulsion).

2.1.2. Preparation and purification of BNC fleeces from Komagataeibacter xylinus

BNC fleeces were produced under static conditions by the bacteria strain *Komagataeibacter xylinus* DSM 14666 (culture collection of the Friedrich Schiller University Jena, deposited at the DSMZ, German Collection of Microorganisms and Cell Cultures, Braunschweig, Germany) in Hestrin-Schramm medium in 24-well plates as described before at 28 °C for 7 days (Kralisch et al., 2010). After alkaline purification with 0.1 N aqueous sodium hydroxide solution (Carl Roth GmbH + Co. KG, Karlsruhe, Germany), washing with deionized water was performed until neutral pH was reached followed by autoclaving (121 °C, 15 min, 2 bar). BNC fleeces were characterized regarding dimensions and weight to calculate surface area and volume as reported earlier (Müller et al., 2013).

2.2. Methods

2.2.1. High performance liquid chromatography (HPLC)

The lead compounds of the BSE, i.e., AKBA and KBA, were quantified by an isocratic HPLC according to a modified method published by Shah et al. (Shah et al., 2008) for marketed formulations. A Dionex™ HPLC system (Dionex Softron GmbH, Germering, Germany) equipped with the UV detector UVD 340U, ASI-100 T automated sample injector, P 680A LPG-4 HPLC pump, the thermostated column compartment TCC-100 and a Zorbax Eclipse 5 XDB-C18 (150 × 4.6 mm) column (Agilent Technologies Inc., Santa Clara, CA, USA) was used for quantification at 260 nm. Control of the measurement parameters and analysis of the chromatograms were realized with the Chromeleon™ 6.8 software from Dionex™. The HPLC was operated with an isocratic flow of 1 mL/min. The mobile phase was composed of acetonitrile (Rotisolv® HPLC Gradient, Carl Roth GmbH + Co. KG) and 0.1% formic acid (AnalaR NORMAPUR®, VWR International S.A.S, Radnor, PA, USA) at a ratio of 90:10 and degassed by the Degasys DG-2410 (Dionex Softron GmbH). Each run was conducted with an injection volume of 20 µL. Calibration curves with linear correlation were established with isolated AKBA and KBA (both Carl Roth GmbH & Co. KG) as reference compounds in a concentration range from 0.5 to 150 µg/mL and 0.25 to 75 µg/mL, respectively. Under optimized conditions retention times of 4.82 ± 0.04 min and 8.17 ± 0.14 min for AKBA (Fig. A.1a) and KBA (Fig. A.1b), respectively, could be realized. Correlation coefficients displayed linearity with values of 0.99981 (AKBA) and 0.99999 (KBA). The limit of detection (LOD) for AKBA was 0.02 µg/mL and the limit of quantification (LOQ) was 0.08 µg/mL. For KBA 0.07 µg/mL was calculated as LOD and 0.11 µg/mL as LOQ.

2.2.2. Physicochemical characterization of nanoemulsions

Hydrodynamic diameter (D_H), polydispersity index (PDI) and zeta potential (ZP) of the nanoemulsions were measured by laser light scattering techniques. D_H and PDI were investigated using the Zetasizer Nano ZS (Malvern Instrument, Germany) equipped with a 4 mW He-Ne laser (633 nm) in Milli-Q® water in a minimal volume cuvette ZEN 0040 (Brand, Wertheim, Germany) at a 173° scattering angle at 25 °C. Mean of Z-average of 5 measurements ± SD was calculated. For determination of the ZP, laser Doppler anemometry was performed by measuring the electrophoretic mobility at 25 °C in a Zetasizer cuvette DTS1060 (Malvern Instruments). Calculation was performed using the Malvern software 7.2 and displayed as mean ± SD (n = 3).

Viscometry was conducted by using a Bohlin CVO rheometer (Malvern Instruments Ltd., Malvern, UK) equipped with a cone (radius 20 mm), having an angle of 4°, and a plate (radius 40 mm), forming a cone plate apparatus. Gap size between cone and plate was set to 0.15 mm. The nanoemulsion (1.3 mL) was dropped on the tempered plate. A constant shear rate of 100/s was used and measuring temperature was set to 20 °C. Calculation of dynamic viscosity was performed by the Bohlin Rotational Software as a function of time from the shear stress every 10 s.

To investigate storage stability of nanoemulsions loaded with BSE, samples were stored at 4 °C, room temperature and skin temperature (32 °C). After preparation of loaded nanoemulsions equal amounts were filled into brown glass bottles for protection against light and closed airtight. Samples stored at 4 °C were kept in a refrigerator while samples at 32 °C were stored in a drying cabinet (WTC Binder, Tuttlingen, Germany). External changes like discolorations or deformations, particle sizes, PDIs, ZPs and amount of AKBA and KBA were determined at different time points *via* laser light scattering technique, Doppler anemometry and HPLC as described in previous sections. Results were expressed as mean ± SD (n = 3).

2.2.3. BSE loading and in vitro release experiments

For loading of BSE in the BNC, fleeces were incubated under submerse conditions and light exclusion in 10.0 mL loading dispersion (nanoemulsions with and without BSE) at 70 rpm and room temperature for 48 h on a temperature-controlled orbital shaker (IKA® KS 400 ic control, IKA®-Werke GmbH & Co. KG, Staufen im Breisgau, Germany). The amount of loaded AKBA and KBA into the BNC was measured by HPLC and calculated by the difference of their concentration of the loading solution before and after the loading process as described before (Moritz et al., 2014). To investigate the release behavior of the loaded BNC fleeces vertical diffusion cells (Franz cell, Gauer Glas, Püttlingen, Germany) were used. Milli-Q® water was applied as release medium in the acceptor compartment with a volume of 12.0 mL, tempered at 32 °C and stirred with 110 rpm. The donor compartment was filled with the loaded BNC fleece. For the diffusion area a size of 1.77 cm^2 was set. Aliquots (400 µL) were taken from release medium after 0, 0.25, 0.5, 1, 2, 4, 8, 24, 48, 72 h, and replaced with freshly tempered release medium. The lead compounds AKBA and KBA were quantified *via* HPLC. All experiments were performed in triplicates and independently repeated once. Results were mathematically modelled according to the Ritger and Peppas equation (semi-empirical power law) (Ritger and Peppas, 1987) (Eq. (1)):

$$M_t/M_\infty = kt^n \quad (1)$$

where M_t represents the cumulative release of AKBA and KBA at the time t and M_∞ the cumulative release at infinite time. The predominant mechanism of release (swelling or diffusion) was investigated by plotting the logarithmic release (%) between 5 and 60% against the logarithmic time. A linear regression and its gradient could be determined which represent the value of the diffusional exponent *n*.

2.2.4. Water binding characteristics

For determination of the water absorption value (WAV) fleeces were sliced into 4 pieces, hydrated in loading solution for 2 h, and dried until mass constancy at 50 °C in a drying cabinet. Weight and dimensions of the fleeces were determined before and after the procedure as described in section 2.1.3. Calculation of the WAV was carried out by Eq. (2):

$$WAV = Wi/Wd * 100\% \quad (2)$$

where Wi represents the weight of BNC fleece before drying while Wd represents weight of BNC fleece after the drying step. An additional centrifugation step for 15 min at 1073 g (Eppendorf MiniSpin®, Eppendorf, Hamburg, Germany) after cutting fleeces into two pieces and incubating them for 2 h in loading solution, was performed to determine the water retention value (WRV). Characterizing the dimensions and drying until mass constancy was performed as described for WAV. Values were calculated by Eq. (3):

$$WRV = (Wi - Wd/Wd) * 100\% \quad (3)$$

where Wi represents the dry weight of the BNC fleece whereas Wd shows the weight after the centrifugation step. Mean ± SD was shown for measurements. Experiments were performed in quadruplicate and repeated once. For statistical evaluation, a one-way ANOVA followed by a Tukey post-hoc test (significance level p = 0.05) was performed by using Microsoft Excel 2016 software.

2.2.5. Characterization of BNC fleeces by morphology, transparency, and mechanical performance

Morphology of the BNC samples was investigated by cryo-scanning electron microscopy (cryo-SEM). Samples with a size of 2 mm were positioned on gold carriers BU012 129-T (BAL-TEC AG), and rapidly frozen by liquid nitrogen-cooled ethane/propane 50:50 (Linde Gas, Pullach, Germany). Specimen were transferred with a BAL-TEC VCT 100 (Bal-TEC, Balzers, Liechtenstein) into an EM ACE 900 freeze fracture device (Leica-Mikrosysteme GmbH, Vienna, Austria), fractured at −150 °C, etched at −95 °C for 7 min and coated at −150 °C with 3 nm platinum/carbon and 5 nm carbon. For visualization, samples were transferred to a scanning electron microscope (LEO 1530 Gemini, Carl Zeiss AG, Oberkochen, Germany) with the VCT 100 cryo transfer system to a cooled stage (−150 °C). Images were recorded digitally with an InLens SE detector at 6 kV. For measurement of transparency samples were placed into 24-well plates (Greiner bio-one GmbH, Frickenhausen, Germany) followed by spectrophotometric measurements at 600 nm (Tecan Spark 10 M, Tecan Group Ag, Männedorf, Switzerland). Experiments were performed in triplicates. The mechanical stability was determined by compressing BNC fleeces with a weight of 400 g for 10 min at room temperature. Unloaded BNC fleeces were analyzed as negative control. Dimensions and weight were investigated before and after compression as described above. Experiments were performed in quadruplets and repeated once. Compressive strain ε was calculated by utilizing Eq. (4):

$$\varepsilon = \Delta h/h_0 * 100\% \quad (4)$$

The height change is shown by Δh, whereas h_0 (mm) shows the height of the BNC fleece before compression. Mass reduction was determined by Eq. (5):

$$m_{loss} = \Delta m/m_0 * 100\% \quad (5)$$

Δm represents the difference between mass of BNC before and after compression while m_0 represents initial mass of BNC. Statistical analysis for transparency measurements and compression stability studies was performed by one-way ANOVA followed by a Tukey post-hoc test (significance level p = 0.05). Microsoft Excel 2016 software was used for statistical investigation.

2.2.6. In vitro penetration experiments in porcine skin

In vitro penetration studies were performed on skin dissected from porcine ears received from a local supplier. Porcine ears were washed and shaved followed by dissection of full-thickness skin. Skin was

punched into homogenous circles with an area of 10.18 cm^2 and stored at −20 °C until use. After thawing, pieces were fixed with self-adhesive aluminum foil (Alu930 SE, Coroplast, Germany) on PBS pH 7.4 moistened filter paper. In the center of the aluminum foil piece, a round cavity was punched with an area of 4.91 cm^2 to apply the test materials after fixation of the skin. Three different studies with unloaded and loaded BNC were performed on the skin: 1) Nanoemulsions (10 µL/cm^2) or loaded BNC samples were applied on the skin for 6 and 24 h, respectively. 2) In a repeated dose set up, BSE-containing BNC was applied onto skin followed by addition of BSE-containing nanoemulsions on top of the BNC sample every 2 h. The process was repeated over 10 h. 3) An experimental set-up over 3 days was conducted by administration of BSE-containing BNC samples onto skin and replacement of the skin samples after 24 and 48 h (total incubation time 72 h). After the defined incubation time BNC was removed, and tape stripping was performed 16 times. Adhesive strips (tesafilm® kristall-klar, tesa SE, Norderstedt, Germany) were applied onto the skin and weighted with 845 g for 10 s to ensure complete contact between porcine skin and adhesive strip. Afterwards, strips were removed and transferred to a reaction tube. Strip number 15 und 16 were performed utilizing additionally one drop of cyanoacrylate-based glue (UHU GmbH & Co. KG, Bühl/Baden, Germany) for 5 min before placing the adhesive strip to the skin to reach deeper skin layers. Tape strips were processed using acetonitrile, ultrasonication (Merck ultrasonic bath, Merck KGaA, Darmstadt, Germany) and centrifugation (Beckman Coulter™ Allegra, Beckman Coulter, Brea, CA, USA) at 10 °C and 20000 g for 10 min. The supernatants of the samples were analyzed *via* HPLC as described above. Experiments were performed on at least 3 porcine skin samples compared to untreated porcine skin as control.

2.2.7. Ex ovo shell-less hen's egg test on the chick area vasculosa (CAV)

To determine the biocompatibility of nanoemulsions, BSE and BNC experiments on shell-less hen's eggs, called HET-CAV (hen's egg test on chick area vasculosa) were performed (Luepke, 1985). Fertilized eggs from a local supplier were incubated at 37 °C and 80% relative humidity for 72 h before transfer into petri dishes containing Ringer's solution pH 7.0. Only eggs in the development stages between 14 and 17 according to Hamburger and Hamilton (Hamburger and Hamilton, 1951) were selected. After an incubation time of 1 h, liquid samples were locally administered on the CAV using an O-ring (Kremer GmbH, Wächtersbach, Germany), whereas BNC fleeces (4 mm diameter) with and without BSE were directly placed on the CAV surface. 1% (m/v) sodium dodecyl sulfate (SDS) solution and 0.9% (m/v) aqueous sodium chloride (NaCl) solution (both Carl Roth GmbH & Co. KG) were used as positive and negative control, respectively. After 0, 1, 2, 4 and 8 h, eggs were inspected regarding hemorrhage, vascular lysis, blood component aggregation and stop of the heartbeat. All experiments were performed in quintuplicate and repeated once.

2.2.8. Transfer aspects and sterilization of BNC

Commercially available BNC (JeNaCell GmbH, Jena, Germany) was loaded with optimized BSE-containing nanoemulsions. Unloaded and loaded BNC samples were packed into primary packaging material and sealed. E-beam sterilization was performed by irradiation according to company internal procedures. Fleeces were investigated macroscopically before and after sterilization and by HPLC analysis of an extract for stability testing. Extracts were obtained by immersing fleeces in 20 mL Milli-Q® water and shaking at 200 rpm for 72 h on an orbital shaker. D_H and PDI of single and double nanoemulsions before and after sterilization were verified in the extracts. Control BNC was examined regarding the presence and amount of aerobic mesophilic bacteria, *Escherichia coli, Pseudomonas aeruginosa, Staphylococcus aureus* and *Candida albicans* according to DIN EN ISO 17516 (DIN EN ISO 17516:2013-08, 2013).

3. Results and discussion

3.1. Formulation of the BSE in nanoemulsions

The BSE Boswellin® Super was used for the incorporation into BNC due to its high content of the two lead compounds AKBA and KBA. Both substances represent small molecules with molar masses of 512.7 g/mol (AKBA) and 470.7 g/mol (KBA). They can be selectively identified and quantified in the region of their UV maximum at 260 nm, which has been determined by a wavelength screen in preliminary experiments (data not shown). A survey of the literature revealed that titration (Singh et al., 2008), reversed phase high performance liquid chromatographic (RP-HPLC) (Ganzera and Khan, 2001), high performance thin layer chromatographic (HPTLC) (Pozharitskaya et al., 2006), and capillary electrochromatographic (Ganzera et al., 2003) methods were reported for determination of boswellic acids. An overview about the characteristics of AKBA and KBA is provided in Table A.1.

AKBA and KBA have log P values of 8 and 7, respectively, indicating their high lipophilicity (Karlina et al., 2007). They can be categorized according to the Biopharmaceutical Classification System in class IV, representing drugs with a low water solubility and low permeation capability (Miller et al., 2016). Consequently, a direct incorporation of the BSE into the hydrophilic BNC, e.g. after dissolution in alcohols, was not possible due to recrystallization phenomenon (data not shown). Therefore, the BSE was formulated first into nanoemulsions before loading into the BNC. Nanoemulsions were selected since they favor the advantages of a high solubilization capacity for lipophilic drugs, thermodynamic stability, low particles sizes and a favorable penetration into the skin (Singh et al., 2017).

Two different types of nanoemulsions, a single O/W and a double W/O/W nanoemulsion were selected for the encapsulation of the BSE. Natural or vegetal components such as plant oils and surfactants derived from plants were used for the formulations. All oils were unsaturated and biodegradable. The amount of surfactants and co-surfactants was about 3-fold lower than in typical micro- and nanoemulsions for topical delivery (Abd et al., 2018), which could be a parameter for better tolerability and skin friendliness. The preparation of the nanoemulsions occurred in three steps: (i) mixing of the components, (ii) homogenization by Ultra-Turrax followed by (iii) high pressure homogenization. This preparation process is a broadly used high energy method to manufacture nanoemulsions (Chevalier and Bolzinger, 2019). The physicochemical characteristics of all preparations are summarized in Table A.2.

The procedure was found to be easy to handle, fast to conduct and highly reproducible. After high pressure homogenization, homogeneous and opaque preparations could be obtained. Under optimized conditions, both types of nanoemulsions offered similar loading capacities. The incorporated AKBA was determined at 3.87 ± 0.06 mg/mL and 3.66 ± 0.03 mg/mL for O/W and W/O/W nanoemulsions, respectively, as measured by HPLC. Incorporated KBA reached concentrations of 0.43 ± 0.06 mg/mL and 0.40 ± 0.01 mg/mL for O/W and W/O/W nanoemulsions, respectively. The mean particle size of the empty O/W and W/O/W nanoemulsions was found to be about 149 nm and 113 nm, respectively. The incorporation of 1% BSE did not influence the mean D_H of the nanoemulsions with an increase of only 1–4 nm. The polydispersity of all preparations was below 0.16 indicating monodisperse particle size distributions. The zeta potentials of the empty nanoemulsions revealed negative values with –72 mV and –80 mV for O/W and W/O/W nanoemulsions, respectively, which were related to the surfactants and the fatty acids and are favorable to prevent aggregation (Singh et al., 2017). The presence of BSE did not change the surface charge. The dynamic viscosity measured by a rheometer at a shear rate of 100/s and a temperature of 20 °C was found to be 6.67 ± 0.17 mPa*s for BSE-loaded O/W nanoemulsions and 3.92 ± 0.17 mPa*s for BSE-loaded W/O/W nanoemulsions under the chosen conditions. The higher dynamic viscosity of the BSE-loaded O/

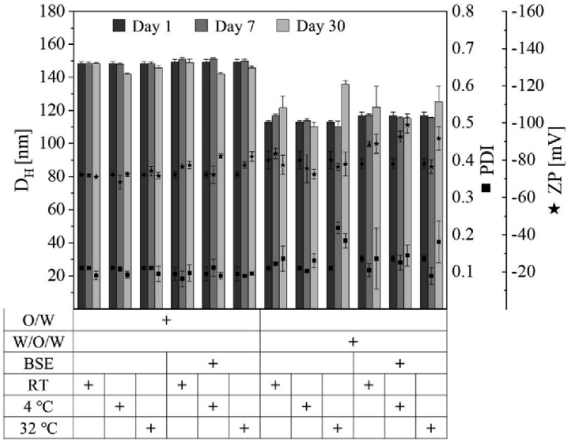

Fig. 1. Time-dependent storage stability testing by comparison of D_H, PDI and ZP of O/W and W/O/W nanoemulsion with and without BSE after 1, 7, and 30 days at room temperature (RT), 4 °C and 32 °C (mean ± SD, n = 3).

W nanoemulsions could be explained by the utilization of 4-times higher concentration of natural oil (*Helianthus annuus* seed oil) for the preparation. Comparable pH values of 5.68 (O/W) and 5.56 (W/O/W) could be measured which are in the range of the natural pH value of the skin of about 5.5.

3.2. Storage stability of BSE-loaded nanoemulsions

Concerning the storage stability of the BSE-loaded nanoemulsions three different set ups were investigated over up to 1, 7 and 30 days which represent relevant storage conditions: (i) 4 °C in the refrigerator, (ii) 20 °C at room temperature, and (iii) 32 °C as standard skin temperature as well as regional specific standard storage temperature. D_H, PDI, ZP (Fig. 1) and the AKBA and KBA content (Fig. 2) were determined to conduct storage stability.

The D_H of all empty and BSE-loaded nanoemulsions was found to be unchanged over 30 days with values between 150 nm (O/W) and 115 nm (W/O/W) for all formulations independent of the storage temperature (Fig. 1). Only for the W/O/W nanoemulsion stored at 32 °C a slight increase of size and polydispersity could be measured after 30 days. For all other preparations, the PDIs remained comparable up to 30 days even at the highest temperature of 32 °C indicating the homogenous distribution and good physical stability of the colloidal nanoemulsions without agglomeration or aggregation. The high stability might be attributed to the highly negative ZPs below −72 mV triggering the electrostatic repulsion between the particles thus showing a lower tendency to agglomerate or aggregate (Silva et al., 2012). Moreover, the amount of AKBA (Fig. 2a) and KBA (Fig. 2b) determined by HPLC over up to 30 days, remained unchanged in all preparations. The HPLC chromatograms displayed clearly separated peaks at characteristic retention times which could be unambiguously assigned to stable AKBA and KBA indicating that no decomposition has been occurred. Stability data have been extended to 150 days without any kind of change (data not shown).

Although nanoemulsions offer many advantages as delivery vehicle for skin application, their low viscosity restricts a convenient application, particularly with respect to long-term administration. Therefore, in the following the combination with BNC was investigated which also favors the advantage of a skin-friendly and wound-healing promoting environment.

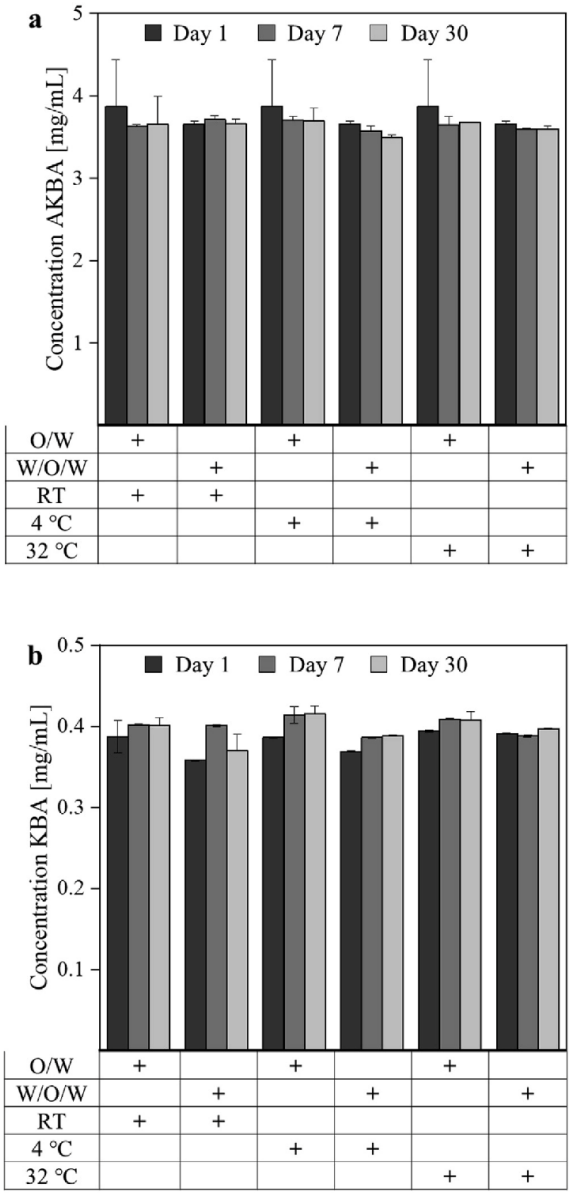

Fig. 2. Concentration of AKBA (a) and KBA (b) in O/W and W/O/W nanoemulsion quantified by HPLC after storage at 4 °C, room temperature (RT) and 32 °C over 30 days (mean ± SD, n = 3).

3.3. Formulation of the BSE-loaded BNC

The biotechnologically derived BNC samples produced by *K. xylinus* under static cultivation conditions in Hestrin-Schramm medium as pellicles at the air–liquid interface in 24-well plates, were homogeneous, cylindrical in shape, with an opaque visual appearance, and a gelatinous solid texture. A standard material was used that has been widely described in previous publications with well-controlled and reproducible synthesis (Alkhatib et al., 2016; Kralisch et al., 2010; Müller et al., 2013; Pötzinger et al., 2019). Extensive characterization of the material properties was reported before (Alkhatib et al., 2016; Moritz et al., 2014). According to previous reports (Alkhatib et al., 2016; Moritz et al., 2014), the samples used for the following experiments

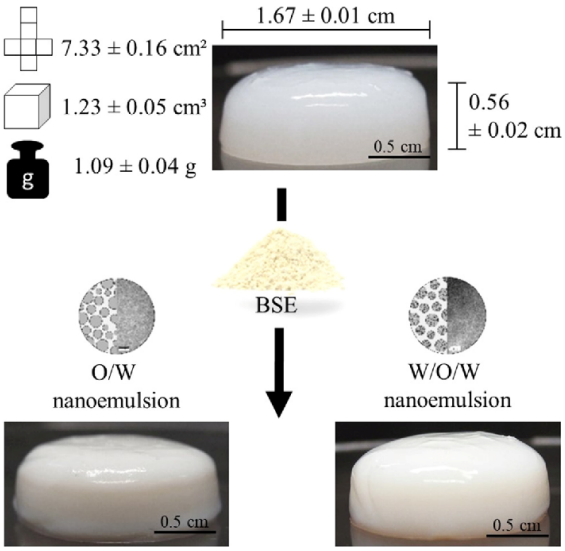

Fig. 3. Dimensions, surface, volume and weight of unloaded BNC sample and outer appearance of BNC before and after loading with O/W or W/O/W nanoemulsion and BSE.

were comparable regarding their dimensions with low standard deviations. The average height was 0.56 ± 0.02 cm, the average diameter 1.67 ± 0.01 cm, and the average mass 1.09 ± 0.04 g. As a result of these measurements the average volume could be calculated as 1.23 ± 0.05 cm^3, and the total surface as 7.33 ± 0.16 cm^2 (Fig. 3).

Different methods to load drugs or additives into the three-dimensional BNC fiber network were described that could be distinguished in terms of efficiency, mechanical stress, and duration. Preferentially, post-loading techniques are selected since they are less stressful for drugs and additives and easy to perform. Additionally, the reproducibility is higher than for *in situ* loading since the growth of the cellulose-producing bacteria can be affected by drugs (Pötzinger et al., 2017). The nanoformulated BSE was incorporated into the BNC by a submerse immersion technique at ambient temperature under gentle shaking (70 rpm) on an orbital shaker for 48 h. During this process, the water inside the BNC was replaced by the different types of nanoemulsions with and without BSE. Although this loading technique is typically used for the incorporation of smaller components like drugs, additives and micelles of about 6 to 10 nm (Alkhatib et al., 2016), presumably due to the flexibility of the nanoemulsion droplets an integration into the BNC network with up to 5 µm pores and spaces (Anton-Sales et al., 2019) seemed to be possible by diffusion and capillary forces in a comparable way. Numata et al. reported the deposition of retinol containing polymer nanoparticles composed of poly(ethylene oxide)-*b*-poly(caprolactone) with particles sizes of *ca.* 40–80 nm, but less flexibility, into BNC by immersion over one day based on diffusional processes (Numata et al., 2015a). Even larger silymarin-zein nanoparticles of about 200 nm could be incorporated into the BNC network (Tsai et al., 2018).

The loaded BNC was investigated by macroscopic inspection, which revealed a homogeneous appearance with a smooth surface without visible drug aggregates. The presence of the BSE resulted in a light yellowish coloration of the BNC. Fig. 4a shows the surface and a cross-section of the BNC fleeces with and without BSE after loading. Compared to unloaded BNC, loaded fleeces appeared to be significantly ($p < 0.05$) less transparent and less shiny due to the presence of the nanoemulsions. Transparency measurements at 600 nm revealed a transmittance of about 82% for unloaded BNC, while BNC loaded with BSE-containing nanoemulsions showed only a transmittance of about

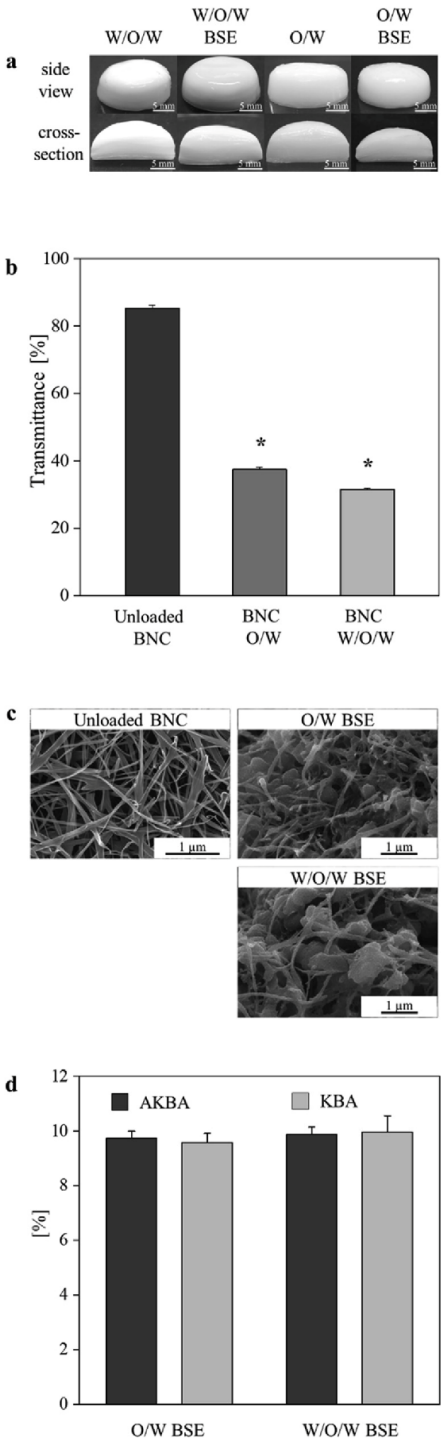

Fig. 4. Physicochemical characterization of the loaded BNC: Representative photographs of BNC samples and their cross-sections loaded with nanoemulsion with and without BSE (a). Transmission of unloaded BNC in comparison to BNC loaded with BSE-containing nanoemulsions measured by spectrophotometry at 600 nm. *$p < 0.5$ BSE-loaded BNC *vs.* unloaded BNC as determined by one-way ANOVA with Tukey post-hoc test (b). Cryo-SEM images of unloaded BNC and BNC loaded with BSE-containing nanoemulsion (c). Percentage loading efficiencies of BSE-loaded BNC determined by HPLC (mean ± SD, n = 3) (d).

31–37% (Fig. 4b). Due to the incorporation of BSE-containing nanoemulsions the weight of BNC increased about 3.6 to 4.4% according to the higher density of the nanoemulsions in comparison to water (data not shown). Cryo-SEM images revealed droplets on the surface of the BNC fibers indicating the presence of the nanoemulsions (Fig. 4c), whereas unloaded BNC showed a smooth fiber surface.

The calculation of the percentage loading efficiency was performed by quantitative HPLC measurements of AKBA and KBA in the loading solution before and after the formulation process. Comparable values for AKBA and KBA between 9 and 10% could be determined both for O/W and W/O/W nanoemulsions (Fig. 4d), which is related to the ratio of 1 mL BNC fleece to 10 mL loading solution. The values are in line with reports for small molecules (Wiegand et al., 2015) and micelles (Alkhatib et al., 2016) under comparable loading conditions. Silica nanoparticles incorporated into BNC by immersion revealed an uptake up to 10% after immersion in 400 mL of 0.05 to 1% silica sol for 2 to 3 weeks (Yano et al., 2008). Compared to the standard BSE, the ratio of the AKBA to KBA uptake into BNC was found to be in the same region for both types of nanoemulsions indicating that comparable relative amounts of AKBA and KBA were incorporated into the BNC. The total amount of loaded AKBA was determined to be 2.38 ± 0.33 mg (O/W) and 2.24 ± 0.46 mg (W/O/W), whereas 0.27 ± 0.03 mg (O/W) and 0.25 ± 0.03 mg (W/O/W) KBA were taken up into the fleeces. Since the average capacity of a BNC fleece used in these experiments was about 1 mL a concentration of 2.24 to 2.38 mg/mL AKBA could be suggested in every BNC sample. It has been shown that 5-lipoxygenase (5-LO), which plays a major role in inflammatory processes, could be inhibited by AKBA and KBA. Studies revealed IC_{50} values for AKBA in cell-free assays from 16 to 50 µM, dependent on the experimental settings (Poeckel and Werz, 2006) which refers to a concentration of 0.008 to 0.025 mg/mL AKBA. Consequently, the BNC fleeces were loaded with a 100-fold higher AKBA concentration, which is possibly necessary to reach a sufficient AKBA concentration for 5-LO inhibition in the skin after dermal application.

3.4. Dimensional stability of loaded BNC

The integrity of dressing materials is essential during the application by patients or health care personal on the skin as well as after the fixation by second dressing materials. Furthermore, packing and unpacking of the product could lead to a loss of loaded drug or deformation of the dressing. This has to be taken into consideration, although an exceptional mechanical pressure stability has been demonstrated for native BNC (Czaja et al., 2007). To confirm that the incorporation of nanoemulsions and BSE does not impair this advantageous characteristic of the BNC, fleeces were loaded and submitted to a mass force of 400 g at room temperature for 10 min (Alkhatib et al., 2016). Height and weight of the fleeces were measured before and after the treatment as representative parameters for the dimensional stability.

The compressive strain determined by height reduction, of unloaded BNC containing > 90% water in the three-dimensional network, was about 66% which is in line with results of other reports (Fig. 5a) (Alkhatib et al., 2016). BNC typically shows mechanical anisotropy with a high tensile modulus along the fiber layer direction, but a low compressive modulus perpendicular to the stratified direction (Abeer et al., 2014). The findings corresponded to a weight reduction of 55% related to a partial squeezing out of water followed by a reduction of weight and height of the BNC and the formation of flat disks caused by the mechanical stress (Fig. 5b). Incorporation of additional substances can decrease or improve mechanical stability due to interactions with the fiber network of the BNC, crosslinking or higher viscosity of the substances consolidating the BNC network (Numata et al., 2015b). The replacement of the internal water of the BNC by O/W and W/O/W nanoemulsions did not change the compressive strain and the weight loss significantly ($p > 0.05$) compared to unloaded native BNC.

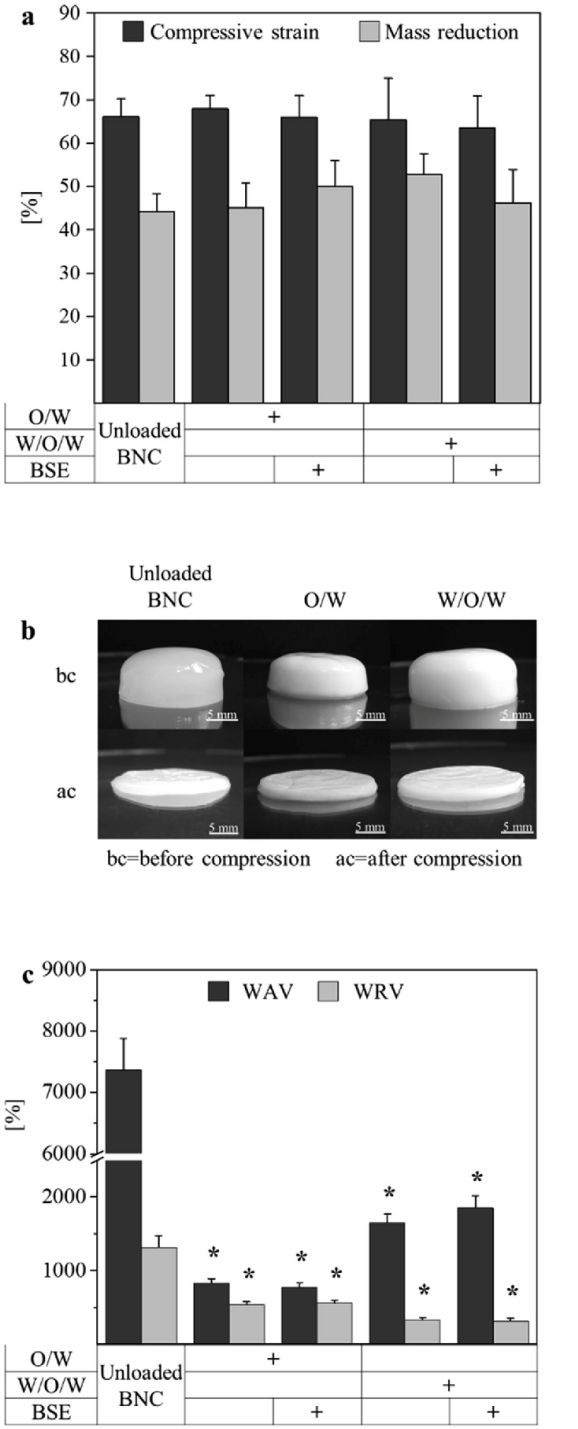

Fig. 5. Comparison of compressive strain and mass reduction of unloaded BNC, BNC loaded with nanoemulsion (O/W and W/O/W) and BNC loaded with BSE-containing nanoemulsion (O/W and W/O/W) (mean ± SD, n = 4, repeated once) (a). Photographs of unloaded BNC and BNC loaded with BSE-containing nanoemulsion (O/W and W/O/W) before and after compression with 400 g for 10 min (b). WAV and WRV of unloaded BNC in comparison to O/W and W/O/W nanoemulsion unloaded or loaded with BSE (mean ± SD, n = 3, repeated once) (c). *p < 0.5 loaded BNC *vs.* unloaded BNC as determined by one-way ANOVA followed by Tukey post-hoc test.

Compressive strains of about 68% (O/W) and 65% (W/O/W) correlated with weight reductions of about 53% (O/W) and 45% (W/O/W) as shown in Fig. 5a. The addition of the BSE neither induced further relevant changes of the compressive strain nor of the weight reduction.

Conclusively, although the water in the BNC network was replaced by the more lipophilic nanoemulsions and the BSE, the mechanical characteristics of the BNC fleeces were not changed in a relevant manner under the chosen conditions.

3.5. Water absorption and retention studies

Two major conditions are decisive for the healing of wounds. On the one hand, the maintenance of a moist environment within the wound is known to be highly relevant for the progress of tissue repair (Powers et al., 2016). On the other hand, a balanced wound exudate is important for an improved healing since an increased volume of exudate as seen in chronic wounds, or a changing composition could impair an ordered progress of wound healing (White and Cutting, 2006). Clinically, native wet BNC is typically used for the treatment of slight or moderate exudating wounds and was reported to have an exceptional high absorptivity and retention for liquids and wound exudates in many studies (Muangman et al., 2011).

For determination of the WAV and the WRV all samples were incubated in a loading medium for 2 h at room temperature followed by air drying up to a constant weight (WAV) or centrifugation before complete drying (WRV). The WAV of unloaded native BNC which represents the amount of water included in the network structure, showed the highest values of 7370% (Fig. 5c), which is in the same range as described before (Alkhatib et al., 2016). The presence of both types of nanoemulsions reduced the WAV significantly ($p < 0.05$) in comparison to unloaded BNC where the more lipophilic O/W nanoemulsion revealed lower WAV (831%) than the W/O/W counterpart (1652%) with a larger fraction of aqueous components. No significant changes ($p > 0.05$) were observed after addition of the BSE indicating that the characteristics of the nanoemulsions were more important for the interaction with water.

A comparable behavior could be observed for the WRV that characterizes the behavior of BNC under the influence of mechanical pressure simulated by centrifugation before the drying step (Fig. 5c). The WRV of unloaded BNC of about 1300%, which is in line with former reports (Udhardt et al., 2005), decreased by the incorporation of nanoemulsions to values between 300% and 550%. Again, the presence of the BSE had no additional significant influence ($p > 0.05$) on the WRV.

Taking these data together, the impregnation of the BNC fiber network with the more lipophilic nanoemulsions, diminished the capability to absorb and retain water as a hydrophilic component. The available space and the amount of trapping sites for penetrating water molecules was reduced by the lipophilic additives. This effect was found to be more pronounced with a higher amount of lipophilic components as shown by the comparison of O/W and W/O/W nanoemulsions. The BSE had no further influence on the water binding characteristics, which might be related to its incorporation into the vesicular structures of the nanoemulsion and therefore, a masking of its characteristics. Wound dressings for a moist wound management should provide a balance between absorption and retention of wound exudate correlating with the moisturizing of the wound. The optimal balance between these two requirements need to be investigated and adjusted in further studies.

3.6. In vitro release profiles of BSE-loaded BNC

Drug release experiments were performed in vertical Franz type diffusion cells over up to 72 h. Fleeces were positioned airtight in the donor compartment, so that only one site of the BNC fleeces stayed in contact with the release medium comparable to skin application. The temperature of the release medium water was set to 32 °C as physiological temperature of human skin. The cumulative drug release was quantified by HPLC for the two lead compounds AKBA and KBA in dependency of the release time as shown in Fig. 6a.

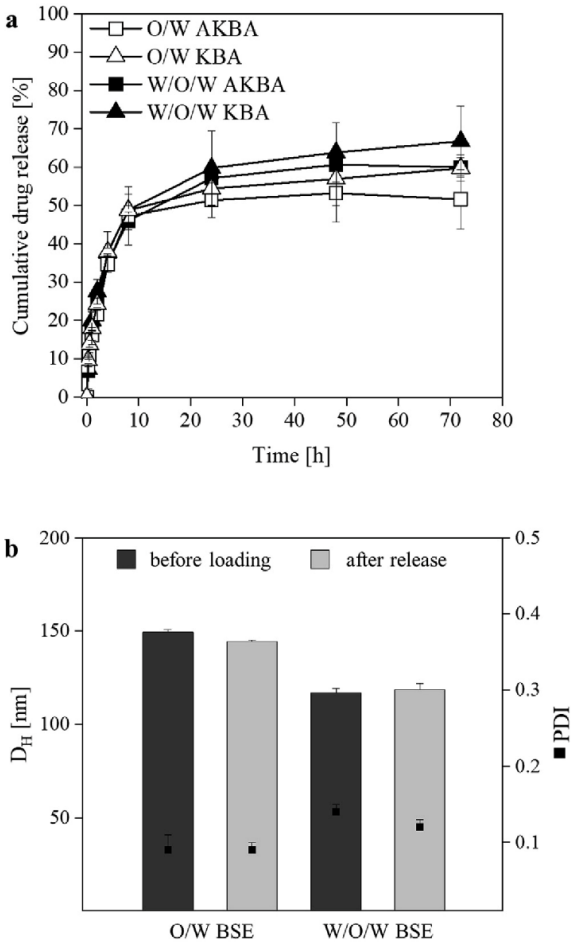

Fig. 6. Cumulative release profiles of the lead compounds AKBA and KBA from the BNC, measured in Franz diffusion cells at 32 °C over up to 72 h (a). D_H and PDI of BSE loaded nanoemulsions before incorporation into the BNC and after release were determined by laser light scattering (b). All experiments were performed in triplicates and repeated once.

For all samples, over 72 h a biphasic release profile could be observed. During the first 8 to 10 h more than two thirds (73–81%) of the maximum cumulative release of AKBA and KBA could be detected as initial fast release followed by a slower release and equilibrium conditions at ≥ 24 h. The less lipophilic KBA (Karlina et al., 2007) exhibited an about 10 to 14% higher release rate after 72 h than AKBA for both types of nanoemulsions which was suggested to be related to its better compatibility with the release medium. The amount of AKBA and KBA that could be quantified in the surrounding medium was lower for the O/W nanoemulsions than for the W/O/W nanoemulsions resulting from the higher hydrophilic content of the double nanoemulsions although their slightly larger size. Moreover, the viscosity of O/W nanoemulsions, which is to a small degree higher than the viscosity of W/O/W nanoemulsions has to be taken into consideration, since it may decrease the mobility of AKBA and KBA in the nanoemulsion and finally, the diffusion from BNC to the release medium.

Since the solubility of the lead compounds in water is very low, it

had to be investigated in which form they were released from the BNC. Furthermore, to support the penetration of AKBA and KBA into the skin, the release of intact nanoemulsion droplets would be preferred. Based on the loading experiments which showed an efficient uptake of the nanoemulsions into the BNC only by diffusional and capillary processes, also *vice versa* a comparable release behavior was suggested. Therefore, photon correlation spectroscopy (PCS) was performed with the release media before and after all release experiments (Fig. 6b) which showed that for all preparations the particle sizes as well as the polydispersity remained unchanged before and after release indicating that particles were released from the BNC.

To receive more insight into the release mechanism, the Ritger-Peppas model was applied to mathematically describe the cumulative release curves (Ritger and Peppas, 1987) taking a non-biodegradable material and a cylindric geometric dimension of the BNC into consideration. Drug release of BNC for hydrophilic small molecules was described to be mainly driven by swelling and diffusion (Alkhatib et al., 2016). In the present study, for all release profiles regression coefficients of 0.954 to 0.989 were obtained, indicating applicability of the model. Values for *n*, the diffusional exponent, between 0.45 and 0.89 point to an anomalous release behavior, while values above 0.89 indicate a Case-II transport and below 0.45 a Fickian diffusion (Ritger and Peppas, 1987). All samples exhibited comparable diffusional exponents *n* (0.52–0.60) indicating a Fickian diffusion overlayed by swelling controlled (anomalous, non-Fickian transport) mechanisms which confirmed that the different formulations revealed comparable transport mechanisms for AKBA and KBA independent of the type of nanoemulsion.

Conclusively, it is of major importance that by the use of nanoemulsions for the incorporation of lipophilic drugs into the BNC obviously release patterns could be reached that are comparable to that of hydrophilic small molecules such as octenidine (Moritz et al., 2014), ibuprofen, lidocaine (Trovatti et al., 2012) and polihexanide (Wiegand et al., 2015). Even the delivery mechanisms are comparable as shown by the Ritger-Peppas calculation. However, compared to the hydrophilic drugs, in the present setting the maximum cumulative release of the lead compounds is lower. An explanation for this could be an incomplete release of the nanoemulsions from the BNC. A partial dissolution of the nanoemulsions could also lead to a lower maximum release since the solubility of AKBA and KBA *per se* in the release medium is negligible. Since the skin consists of hydrophilic and lipophilic components a higher maximum release *in vivo* is likely. With a view to the intended application, a fast initial release of AKBA and KBA would be advantageous to reach effective therapeutic concentrations of anti-inflammatory lead compounds very fast followed by a subsequent release of the BSE to maintain a constant concentration at the application area (Saghazadeh et al., 2018).

3.7. Ex ovo biocompatibility studies in a shell-less hen's egg model

Biocompatibility testing as a prerequisite for the safe and non-irritative application to the skin, is usually conducted in *in vitro* cell culture experiments using keratinocytes (Wiegand and Hipler, 2009) or even more complex systems such as three-dimensional co-cultures of keratinocytes and fibroblasts (Ravi et al., 2015), or *in vivo* skin irritancy tests (Organisation for Economic Cooperation and Development (OECD), 2010). In order to avoid animal tests but to work in complex systems as close as possible to the physiological situation without the need of an ethical permission, in the present study the biocompatibility was tested in a shell-less hen's egg model applying test materials on the CAV as a suitable alternative to predict the skin irritation of test samples as described before (Alkhatib et al., 2016).

Pre-incubated (72 h) eggs were opened and transferred to petri dishes. The test items were locally applied directly to the CAV to determine adverse effects according to the recommendations of ICCVAM (ICCVAM, 2010) by visual inspection regarding vascular lysis, aggregation, hemorrhage, and stop of the heartbeat after 1, 2, 4 and 8 h. For the liquid test samples, the uncontrolled spreading over the surface of the egg was avoided by pipetting the samples in an O-ring placed directly on the blood vessel system. All materials were tested in the same concentrations as in loaded BNC. Fig. 7 summarizes the observations of the application of loaded BNC as well as all single components in comparison to the controls as a clustergram. The validity of the assay was proven by several controls. Physiological saline (negative

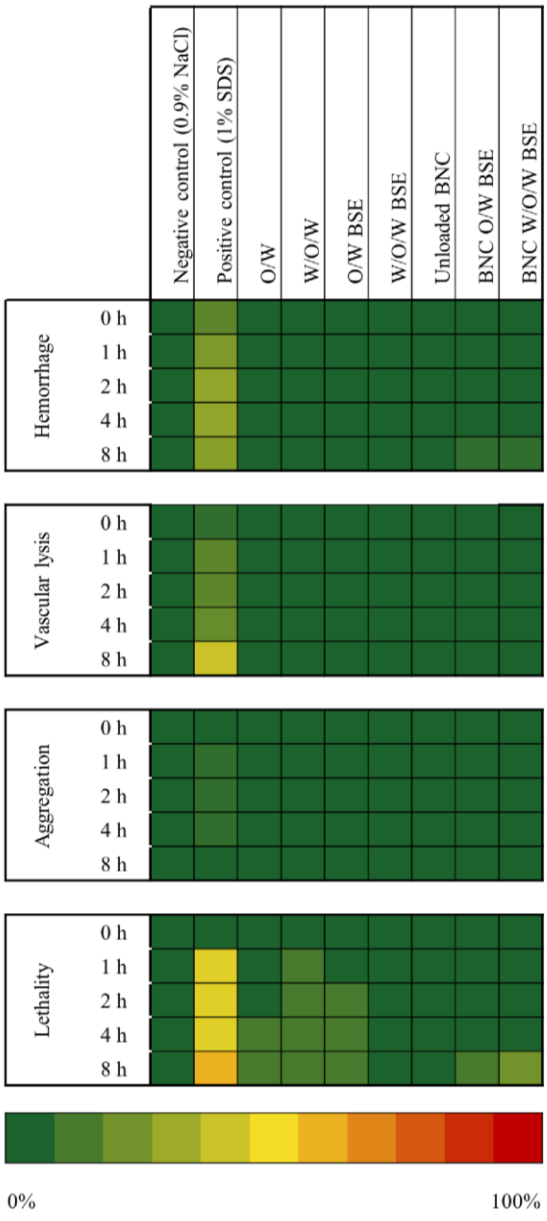

Fig. 7. Clustergram showing time-dependent adverse effects of the locally applied materials in the shell-less hen's egg test up to 8 h. The columns show the type of applied material, whereas the rows represent the time-dependent adverse effects. Intensity of color scale represents the percentage of affected eggs. Negative control (0.9% NaCl), positive control (1% SDS), O/W and W/O/W nanoemulsion without and with BSE (15 µg/mL related to AKBA amount), unloaded BNC and BNC with BSE-containing nanoemulsions are shown. Experiments were performed in quintuplicates and repeated once.

control) did not induce any changes whereas the positive control 1% (m/v) SDS developed in the first 2 h hemorrhagic effects followed by vascular lysis and stopping of the heartbeat. Acceptable concurrent negative control ranges based on historical lab data ranged between 0 and 1/10 eggs.

The blood vessel systems of the eggs treated with the two types of empty nanoemulsions or with the BSE-loaded nanoemulsions did not show relevant changes at concentrations of 15 µg/mL (related to AKBA amount). 0–2/10 eggs were lost by stopping of the heartbeat which represents a range comparable to the historical control values. The high tissue compatibility of unloaded BNC has already been proven in this model by Alkhatib et al. under comparable conditions (Alkhatib et al., 2016). Correspondingly, in the present study no tissue alterations or irritations could be observed up to 8 h. In accordance to the literature, BNC alone can be generally considered as highly compatible with biological tissues invoking nor or only moderate body response in vitro and *in vivo*, even in skin applications (Gisela et al., 2006; Jeong et al., 1997). After the application of BNC loaded with BSE-containing nanoemulsions, the surface of the blood vessel systems and the surrounding tissues did not show any toxic sign.

Burlando et al. showed a low to moderate toxicity on skin for AKBA over 48 h in *in vitro* studies with fetal dermal fibroblasts (HFFF2), differentiated and undifferentiated keratinocytes (HaCaTs and NTCT 2544) by using NRU and MTT assays and AKBA concentrations of 0.23 to 230 µg/mL (Burlando et al., 2008). Concentrations used in the HET-CAV experiment were lower indicating a high biocompatibility of BNC loaded with BSE and nanoemulsions. *Ex ovo* findings need to be proven by *in vivo* skin experiments in further studies.

3.8. Ex vivo skin penetration of AKBA and KBA

For the treatment of skin diseases, penetration into the deep layers of the skin is necessary to reduce inflammation and to enable the regeneration of the skin. The lipophilicity of drugs is a prominent parameter for their skin penetration capability where drugs with a log P value ≤ 2 were reported to have a high potential for skin penetration (Guy and Hadgraft, 1989). AKBA and KBA with log P values of 8 and 7, respectively, are apparently not able to penetrate the intact skin and may require a formulation approach to enhance penetration (Karlina et al., 2007). Nanoemulsions interact with skin cells due to their small droplet sizes and flexible, fluidic character (Shaker et al., 2019), which makes them potent candidates for formulating drugs with a poor penetration ability like AKBA and KBA. Therefore, in *ex vivo* skin penetration studies the liberation of BSE-loaded nanoemulsions from the BNC and their ability to transport AKBA and KBA into the skin was investigated. Tape stripping experiments on porcine skin (Saarbrücken model) are widely used as a model to simulate the skin penetration of substances (Klang et al., 2012). After incubation of the skin with test substances, adhesive strips were utilized to perform tape stripping followed by a quantification of AKBA and KBA in the tapes by HPLC.

In the present study, different therapeutically relevant application scenarios were simulated: (i) single application of nanoemulsions containing BSE followed by incubation over 6 h (ii) single application of BNC containing BSE-loaded nanoemulsions followed by incubation over 24 h, and (iii) repeated application of BSE-loaded nanoemulsions onto BNC every 2 h over 10 h with a total incubation time of 24 h. Fig. 8 shows the skin penetration profiles of AKBA and KBA in correlation to the depth of skin penetration. Adhesive strips, which were used for tape stripping were divided into three groups (1–3; 4–14; 15–16) and categorized as upper skin layers, middle skin layers and deeper skin layers.

As standard application setting, nanoemulsions containing BSE were applied onto porcine skin for 6 h followed by quantification of AKBA and KBA in the tape strips by HPLC. The W/O/W nanoemulsion revealed higher amounts of AKBA and KBA in the middle and deeper layers of the skin than the O/W nanoemulsion whereas for the O/W nanoemulsion more drug accumulated on the surface of the skin and in the first few strips (1–3). The reason for this could be related to the smaller droplet sizes and lower viscosity of the W/O/W compared to the O/W nanoemulsion facilitating the deeper transport. Higher lipophilicity of O/W in comparison to the W/O/W nanoemulsion could also be an explanation for minor penetration into the skin. Since a moderate lipophilicity is preferable for transdermal penetration (Guy and Hadgraft, 1989), more O/W nanoemulsion droplets might stuck in the upper layers of the skin in contrast to less lipophilic W/O/W nanoemulsion. The knowledge about the different penetration behavior could be utilized to control penetration in dependency of administration.

When utilizing BNC as a carrier for the nanoemulsions less amount of AKBA and KBA in comparison to the pure nanoemulsions accumulated in the upper layers whereas a higher amount of boswellic acids could be quantified in the middle layers. Deeper skin layers comprised nearly unchanged amounts for the lead compounds in the W/O/W nanoemulsion while for the O/W nanoemulsion they revealed an increased concentration due to utilization of BNC. Transport of active substances across the skin is dependent on the concentration gradient as reported in the literature (Alkilani et al., 2015). The increased concentration gradient due to the use of BNC as depot might force the released nanoemulsions to penetrate deeper into the skin. Additionally, the enhanced transport of the lead compounds in the O/W nanoemulsion into deeper layers might be related to less hydrogen bonds between the more lipophilic O/W nanoemulsion and the BNC fleece. A higher release of AKBA and KBA for W/O/W nanoemulsions had also been shown in *in vitro* release experiments supporting this finding.

As a second scenario, the effect of repeated dosing was investigated. Therefore, BSE-loaded BNC fleeces were administrated, and the incubation time extended to 24 h. For a time period of 10 h every 2 h the BSE-containing nanoemulsion was added onto the BNC surface. The amount of added nanoemulsion represented the weight loss of the BNC fleece within 2 h that had been determined in previous experiments (data not shown). Consequently, we expected higher concentration of AKBA and KBA in the deeper layers due to the higher concentration gradient. Interestingly, in the upper skin layers less boswellic acids were evident but contrary to the former assumptions amounts in middle and deeper skin layers revealed to be similar or only slightly higher in comparison to experiment set up without repeated dosing. A possible explanation for these findings might be a saturation of the skin layers due to the high amount of nanoemulsions.

Third penetration set up examined the impact of a skin change after 24 h, aiming to simulate removal of substances inside the skin due to transportation mechanisms. BNC loaded with nanoemulsions and BSE was applied onto a new intact skin after 24 h incubation on the first skin. This procedure was repeated after 48 h. Results demonstrated the highest amounts of boswellic acid in the skin within the first 24 h for both, O/W and W/O/W nanoemulsions. Increasing the concentration gradient by renewing the porcine skin generated less additional occurrence of AKBA and KBA (5 to 20%). These findings correlate well with the results of the release studies, which showed a burst release within the first 8 h followed by a constant, but slower release afterwards.

3.9. Transfer aspects and development of a sterilization method

Suitable dressings are usually low in germs and ideally sterile. The most common methods to sterilize such products are heat sterilization or autoclaving (Rutala and Weber, 2013) given that the products and drugs are stable. BNC is well-known to be resistant against the harsh conditions of autoclaving. Thermal stability without any thermal decomposition has been shown up to 300 °C (Surma-Ślusarska et al., 2008). To test the stability of BSE during autoclaving, it was sterilized at 121 °C and 2 bar for 15 min according to the Ph. Eur. 9.7 (European Pharmacopoeia 9.7, 5.1.1, 2019) followed by quantification of AKBA and KBA by HPLC. A decreased amount of 73% of initially loaded AKBA emerged after autoclaving. The HPLC peak of KBA split up into two not

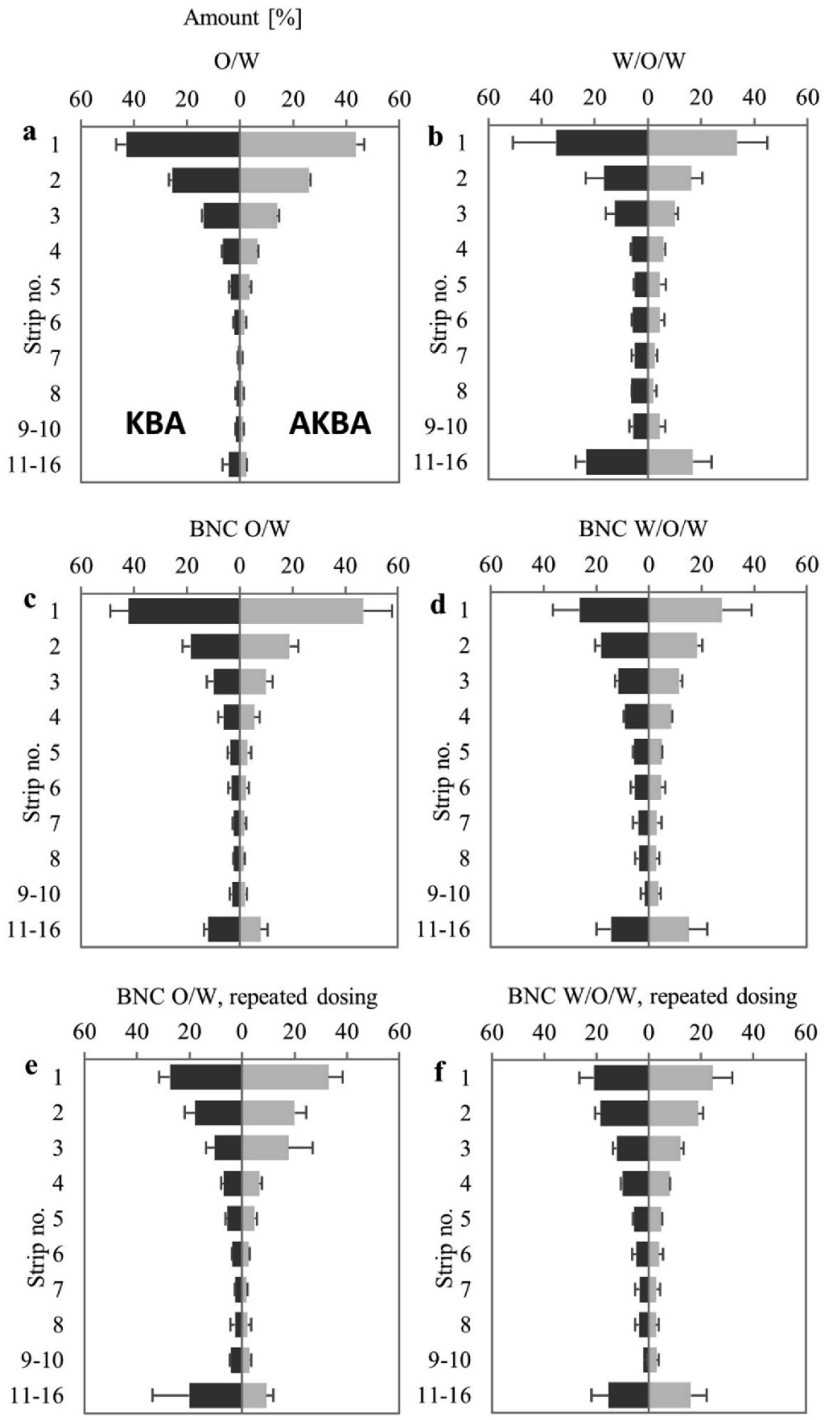

Fig. 8. Penetration studies *via* tape stripping experiments on porcine skin of BSE-loaded O/W (a) and W/O/W (b) nanoemulsion after an incubation time of 6 h, BNC with BSE-loaded O/W (c) and W/O/W (d) nanoemulsion after an incubation time of 24 h and BNC with BSE-loaded O/W (e) and W/O/W (f) nanoemulsion after a repeated dose application (n = 3).

clearly separated peaks, which made a quantification impossible (Fig. A.2a, b). Consequently, an alternative, more gently and often utilized technique for sensitive products, the e-beam sterilization, was applied. The artificially made radiation consisting of accelerated electrons was applied to the products in their primary package to inactivate micro-organisms and DNA fragments. This process only lasts several seconds and only slightly heats up the products by about 20 °C. Additionally, cooling of the product is possible. To evaluate the applicability for BNC

loaded with BSE and nanoemulsions, fleeces were sterilized by irradiation.

The sterilized products were investigated regarding morphology, particle size, and sterility. The surface of the loaded BNC fleeces appeared homogenous, aggregates and discolorations did not emerge. The D_H of the O/W and W/O/W nanoemulsions was determined as described above by PCS and was found not to be affected by the sterilization process with only 1 to 4% variation (Fig. A.2c). A homogenous particle size distribution before and after sterilization could be confirmed by a PDI below 0.16. The HPLC chromatograms displayed separated peaks at the same retention times before and after sterilization showing the stability of AKBA and KBA without the formation of side products. The microbial load of an unloaded control BNC was inspected. Examined parameters incorporated the aerobic mesophilic bacteria *Escherichia coli, Pseudomonas aeruginosa, Staphylococcus aureus* and *Candida albicans*. Results for all bacteria fell below specification limits according to DIN EN ISO 17516 (DIN EN ISO 17516:2013-08, 2013). Conclusively, e-beam sterilization of BNC, nanoemulsions and BSE is a feasible technique to sterilize the BSE-loaded BNC before application.

4. Conclusion

In the present study, the hydrophilicity of BNC for the loading with the lipophilic BSE has been overcome by the exchange of the water in the BNC network by different types of nanoemulsions. Small sized, negatively charged BSE containing single and double nanoemulsions were found to be stable over 30 days under varying storage conditions. Their loading into BNC produced homogeneous, mechanically stable and e-beam sterilizable matrices with preferential water holding capacities highly suitable for dermal applications. The compatibility of the loaded BNC with biological tissues could be demonstrated in a shell-less hen's egg model. The release profiles of the lead drugs could be controlled by the type of nanoemulsion and revealed a biphasic release profile comparable to the typical profiles of hydrophilic molecules. Advantageously, intact nanoemulsions were released favoring the penetration of the lead compounds into skin. Tape stripping experiments using porcine skin determined a dependency of the drug penetration into skin on the type of nanoemulsion, single *vs.* repeated applications and the incubation time.

If formulations have to be selected based on the available physicochemical and biological data, for the treatment of superficial skin diseases AKBA and KBA formulated in the O/W nanoemulsion are preferable since penetration studies demonstrated the transport in the upper skin layers. In contrast, the W/O/W nanoemulsion facilitated drug transport into deeper skin layers that can be used to support the healing of more chronic skin diseases. Taking all these results together, the development of this natural dressing based on BNC incorporating a lipophilic natural anti-inflammatory substance with enhanced penetration capabilities due to the utilization of nanoemulsions forms the basis for combinations with further lipophilic drugs and materials. In further studies scale-up experiments, *in vivo* biocompatibility and effectiveness studies will follow.

CRediT authorship contribution statement

Berit Karl: Conceptualization, Methodology, Validation, Formal analysis, Investigation, Data curation, Writing - original draft, Writing - review & editing, Visualization. **Yaser Alkhatib:** Methodology, Validation, Formal analysis, Investigation, Writing - review & editing. **Uwe Beekmann:** Methodology, Validation, Investigation, Writing - review & editing. **Tom Bellmann:** Validation, Investigation, Writing - review & editing. **Gabriele Blume:** Methodology, Formal analysis, Investigation, Resources, Writing - original draft, Writing - review & editing. **Frank Steiniger:** Methodology, Validation, Formal analysis, Investigation, Writing - review & editing. **Jana Thamm:** Methodology, Formal analysis, Investigation, Writing - review & editing, Visualization. **Oliver Werz:** Resources, Data curation, Writing - original draft, Writing - review & editing, Supervision, Funding acquisition. **Dana Kralisch:** Resources, Data curation, Writing - review & editing, Supervision, Funding acquisition. **Dagmar Fischer:** Conceptualization, Resources, Data curation, Writing - original draft, Writing - review & editing, Supervision, Project administration, Funding acquisition.

Declaration of Competing Interest

The authors declare that they have no known competing financial interests or personal relationships that could have appeared to influence the work reported in this paper.

Acknowledgement

This work was supported by the Free State of Thuringia and the European Social Fund (2016 FGR 0045). Additionally, the authors would like to thank JeNaCell GmbH for providing BNC as well as their assistance in e-beam sterilization experiments and Laboratorien Dr. Freitag GmbH for the microbiological testing.

Appendix A. Supplementary data

Supplementary data to this article can be found online at https://doi.org/10.1016/j.ijpharm.2020.119635.

References

Abd, E., Benson, H., Roberts, M., Grice, J., 2018. Minoxidil skin delivery from nanoemulsion formulations containing eucalyptol or oleic acid: Enhanced diffusivity and follicular targeting. Pharmaceutics 10, 19.

Abdel-Tawab, M., Werz, O., Schubert-Zsilavecz, M., 2011. Boswellia serrata - an overall assessment of in vitro. preclinical, pharmacokinetic and clinical data. Clin. Pharmacokinet. 50, 349–369.

Abeer, M.M., Mohd Amin, M.C., Martin, C., 2014. A review of bacterial cellulose-based drug delivery systems: their biochemistry, current approaches and future prospects. J. Pharm. Pharmacol. 66, 1047–1061.

Alkhatib, Y., Dewaldt, M., Moritz, S., Nitzsche, R., Kralisch, D., Fischer, D., 2016. Controlled extended octenidine release from a bacterial nanocellulose/Poloxamer hybrid system. Eur. J. Pharm. Biopharm. 112, 164–176.

Alkilani, A.Z., McCrudden, M.T.C., Donnelly, R.F., 2015. Transdermal drug delivery: Innovative pharmaceutical developments based on disruption of the barrier properties of the stratum corneum. Pharmaceutics 7, 438–470.

Anton-Sales, I., Beekmann, U., Laromaine, A., Roig, A., Kralisch, D., 2019. Opportunities of bacterial cellulose to treat epithelial tissues. Curr. Drug Targets 20, 808–822.

Ávila Ramírez, J.A., Fortunati, E., Kenny, J.M., Torre, L., Foresti, M.L., 2017. Simple citric acid-catalyzed surface esterification of cellulose nanocrystals. Carbohydr. Polym. 157, 1358–1364.

Badshah, M., Ullah, H., Khan, A.R., Khan, S., Park, J.K., Khan, T., 2018. Surface modification and evaluation of bacterial cellulose for drug delivery. Int. J. Biol. Macromol. 113, 526–533.

Blume, G., 2011a. Colloidal carrier system with penetration properties for encapsulating lipophilic active agents and oils for topical use. EP 2 658 610.

Blume, G., 2011b. Novel support system for the transport of active substances into the skin. EP 2 (552), 413.

Blume, G., 2015. Colloidal carrier system with penetration properties for encapsulating lipophilic active agents and oils for topical use. WO002012089184A3.

Burlando, B., Parodi, A., Volante, A., Bassi, A.M., 2008. Comparison of the irritation potentials of Boswellia serrata gum resin and of acetyl-11-keto-β-boswellic acid by in vitro cytotoxicity tests on human skin-derived cell lines. Toxicol. Lett. 177 (2), 144–149.

Chantereau, G., Sharma, M., Abednejad, A., Neves, B.M., Sèbe, G., Coma, V., Freire, M.G., Freire, C.S.R., Silvestre, A.J.D., 2019. Design of nonsteroidal anti-inflammatory drug-based ionic liquids with improved water solubility and drug delivery. ACS Sustain. Chem. Eng. 7, 14126–14134.

Chevalier, Y., Bolzinger, M.-A., 2019. Micelles and Nanoemulsions. In: Cornier, J., Keck, C.M., Van de Voorde, M. (Eds.), Nanocosmetics: from ideas to products. Springer International Publishing, Cham, pp. 47–72.

Czaja, W., Krystynowicz, A., Kawecki, M., Wysota, K., Sakiel, S., Wróblewski, P., Glik, J., Nowak, M., Bielecki, S., 2007. Biomedical applications of microbial cellulose in burn wound recovery. In: Cellulose: Molecular and Structural Biology. Springer, pp. 307–321.

DIN EN ISO 17516:2013-08. Cosmetic-Microbiology-Microbiological limits (ISO/DIS 17516:2013), 2013.

European Pharmacopoeia 9.7, 5.1.1. Methods of preparation of sterile products-Steam

sterilization, 2019.
Food and Drug Administration (FDA), Cosmetic Labeling Guide, 2014.
Ganzera, M., Khan, I.A., 2001. A reversed phase high performance liquid chromatography method for the analysis of boswellic acids in Boswellia serrata. Planta Med. 67, 778–780.
Ganzera, M., Stöggl, W.M., Bonn, G.K., Khan, I.A., Stuppner, H., 2003. Capillary electrochromatography of boswellic acids in Boswellia serrata Roxb. J. Sep. Sci. 26, 1383–1388.
Gisela, H., Henrik, B., Aase, B., Ulf, N., Paul, G., Bo, R., 2006. In vivo biocompatibility of bacterial cellulose. J. Biomed. Mater. Res. Part A 76A, 431–438.
Goel, A., Ahmad, F.J., Singh, R.M., Singh, G.N., 2010. 3-Acetyl-11-keto-beta-boswellic acid loaded-polymeric nanomicelles for topical anti-inflammatory and anti-arthritic activity. J. Pharm. Pharmacol. 62, 273–278.
Gonzalez, A.C.D.O., Costa, T.F., Andrade, Z.D.A., Medrado, A.R.A.P., 2016. Wound healing-A literature review. Anais brasileiros de dermatologia 91, 614–620.
Gupta, A., Keddie, D.J., Kannappan, V., Gibson, H., Khalil, I.R., Kowalczuk, M., Martin, C., Shuai, X., Radecka, I., 2019. Production and characterisation of bacterial cellulose hydrogels loaded with curcumin encapsulated in cyclodextrins as wound dressings. Eur. Polym. J. 118, 437–450.
Guy, R.H., Hadgraft, J., 1989. Selection of drug candidates for transdermal drug delivery. Transdermal Drug Deliv. 59–81.
Hamburger, V., Hamilton, H.L., 1951. A series of normal stages in the development of the chick embryo. J. Morphol. 88, 49–92.
ICCVAM, 2010. Interagency Coordinating Committee on the Validation of Alternative Methods, Test Method Evaluation Report: Current Validation Status of In Vitro Test Methods Proposed for Identifying. Eye Injury Hazard Potential of Chemicals and Products.
Jeong, B., Bae, Y.H., Lee, D.S., Kim, S.W., 1997. Biodegradable block-copolymers as injectable drug delivery systems. Nature 388, 860–862.
Karlina, M.V., Pozharitskaya, O.N., Kosman, V.M., Ivanova, S.A., 2007. Bioavailability of boswellic acids: in vitro/in vivo correlation. Pharm. Chem. J. 41, 569–572.
Khalil, H., Cullen, M., Chambers, H., Carroll, M., Walker, J., 2015. Elements affecting wound healing time: An evidence based analysis. Wound Repair Regener. 23, 550–556.
Klang, V., Schwarz, J.C., Lenobel, B., Nadj, M., Auböck, J., Wolzt, M., Valenta, C., 2012. In vitro vs. in vivo tape stripping: Validation of the porcine ear model and penetration assessment of novel sucrose stearate emulsions. Eur. J. Pharm. Biopharm. 80, 604–614.
Kralisch, D., Hessler, N., Klemm, D., Erdmann, R., Schmidt, W., 2010. White biotechnology for cellulose manufacturing–the HoLiR concept. Biotechnol. Bioeng. 105, 740–747.
Luepke, N.P., 1985. Hen's egg chorioallantoic membrane test for irritation potential. Food Chem. Toxicol. 23, 287–291.
Marquele-Oliveira, F., da Silva Barud, H., Torres, E.C., Machado, R.T.A., Caetano, G.F., Leite, M.N., Frade, M.A.C., Ribeiro, S.J.L., Berretta, A.A., 2019. Development, characterization and pre-clinical trials of an innovative wound healing dressing based on propolis (EPP-AF®)-containing self-microemulsifying formulation incorporated in biocellulose membranes. Int. J. Biol. Macromol. 136, 570–578.
Mehta, M., 2014. Nanotechnologies for boswellic acid. Am. J. Drug Discov. Dev. 4, 1–11.
Miller, D.A., Keen, J.M., Brough, C., Ellenberger, D.J., Cisneros, M., Williams III, R.O., McGinity, J.W., 2016. Bioavailability enhancement of a BCS IV compound via an amorphous combination product containing ritonavir. J. Pharm. Pharmacol. 68, 678–691.
Moritz, S., Wiegand, C., Wesarg, F., Hessler, N., Muller, F.A., Kralisch, D., Hipler, U.C., Fischer, D., 2014. Active wound dressings based on bacterial nanocellulose as drug delivery system for octenidine. Int. J. Pharm. 471, 45–55.
Muangman, P., Opasanon, S., Suwanchot, S., Thangthed, O., 2011. Efficiency of microbial cellulose dressing in partial-thickness burn wounds. J. Am. Coll. Certified Wound Specialists 3, 16–19.
Müller, A., Ni, Z., Hessler, N., Wesarg, F., Müller, F.A., Kralisch, D., Fischer, D., 2013. The biopolymer bacterial nanocellulose as drug delivery system: Investigation of drug loading and release using the model protein albumin. J. Pharm. Sci. 102, 579–592.
Numata, Y., Mazzarino, L., Borsali, R., 2015a. A slow-release system of bacterial cellulose gel and nanoparticles for hydrophobic active ingredients. Int. J. Pharm. 486, 217–225.
Numata, Y., Sakata, T., Furukawa, H., Tajima, K., 2015b. Bacterial cellulose gels with high mechanical strength. Mater. Sci. Eng., C 47, 57–62.
Olsson, M., Jarbrink, K., Divakar, U., Bajpai, R., Upton, Z., Schmidtchen, A., Car, J., 2019. The humanistic and economic burden of chronic wounds: A systematic review. Wound Repair Regener. 27, 114–125.
Organisation for Economic Cooperation and Development (OECD), 2010. Guidelines for the Testing of Chemicals, Test No. 439: In Vitro Skin Irritation.
Pengzong, Z., Yuanmin, L., Xiaoming, X., Shang, D., Wei, X., Zhigang, L., Dongzhou, D., Wenjing, Y., Jianbiao, Y., Yang, X., Xia, L., 2019. Wound healing potential of the standardized extract of Boswellia serrata on experimental diabetic foot ulcer via inhibition of inflammatory, angiogenetic and apoptotic markers. Planta Med. 85, 657–669.
Poeckel, D., Werz, O., 2006. Boswellic acids: Biological actions and molecular targets. Curr. Med. Chem. 13, 3359–3369.
Portela, R., Leal, C.R., Almeida, P.L., Sobral, R.G., 2019. Bacterial cellulose: a versatile biopolymer for wound dressing applications. Microb. Biotechnol. 12, 586–610.
Pötzinger, Y., Kralisch, D., Fischer, D., 2017. Bacterial nanocellulose: the future of controlled drug delivery? Ther. Deliv. 8, 753–761.
Pötzinger, Y., Rahnfeld, L., Kralisch, D., Fischer, D., 2019. Immobilization of plasmids in bacterial nanocellulose as gene activated matrix. Carbohydr. Polym. 209, 62–73.
Powers, J.G., Higham, C., Broussard, K., Phillips, T.J., 2016. Wound healing and treating wounds: Chronic wound care and management. J. Am. Acad. Dermatol. 74, 607–625.
Pozharitskaya, O.N., Ivanova, S.A., Shikov, A.N., Makarov, V.G., 2006. Separation and quantification of terpenoids of Boswellia serrata Roxb. extract by planar chromatography techniques (TLC and AMD). J. Sep. Sci. 29, 2245–2250.
Rådmark, O., Werz, O., Steinhilber, D., Samuelsson, B., 2015. 5-Lipoxygenase, a key enzyme for leukotriene biosynthesis in health and disease. Biochimica et Biophysica Acta (BBA) - Molecular and Cell Biology of. Lipids 1851, 331–339.
Ravi, M., Paramesh, V., Kaviya, S.R., Anuradha, E., Solomon, F.D.P., 2015. 3D cell culture systems: advantages and applications. J. Cell. Physiol. 230, 16–26.
Ritger, P.L., Peppas, N.A., 1987. A simple equation for description of solute release II. Fickian and anomalous release from swellable devices. J. Control. Release 5, 37–42.
Rutala, W.A., Weber, D.J., 2013. Disinfection and sterilization: An overview. Am. J. Infect. Control 41, S2–S5.
Saghazadeh, S., Rinoldi, C., Schot, M., Kashaf, S.S., Sharifi, F., Jalilian, E., Nuutila, K., Giatsidis, G., Mostafalu, P., Derakhshandeh, H., 2018. Drug delivery systems and materials for wound healing applications. Adv. Drug Deliv. Rev. 127, 138–166.
Shah, S.A., Rathod, I.S., Suhagia, B.N., Pandya, S.S., Parmar, V.K., 2008. A simple high-performance liquid chromatographic method for the estimation of boswellic acids from the market formulations containing Boswellia serrata extract. J. Chromatogr. Sci. 46, 735–738.
Shaker, D.S., Ishak, R.A.H., Ghoneim, A., Elhuoni, M.A., 2019. Nanoemulsion: A review on mechanisms for the transdermal delivery of hydrophobic and hydrophilic drugs. Sci. Pharm. 87, 17.
Sharma, A., Gupta, N.K., Dixit, V.K., 2010. Complexation with phosphatidyl choline as a strategy for absorption enhancement of boswellic acid. Drug Delivery 17, 587–595.
Sharma, S., Thawani, V., Hingorani, L., Shrivastava, M., Bhate, V.R., Khiyani, R., 2004. Pharmacokinetic study of 11-keto β-boswellic acid. Phytomedicine 11, 255–260.
Shi, F., Zhao, J.H., Liu, Y., Wang, Z., Zhang, Y.T., Feng, N.P., 2012. Preparation and characterization of solid lipid nanoparticles loaded with frankincense and myrrh oil. Int. J. Nanomed. 7, 2033–2043.
Silva, H.D., Cerqueira, M.Â., Vicente, A.A., 2012. Nanoemulsions for food applications: Development and characterization. Food Bioprocess Technol. 5, 854–867.
Singh, S., Khajuria, A., Taneja, S.C., Johri, R.K., Singh, J., Qazi, G.N., 2008. Boswellic acids: A leukotriene inhibitor also effective through topical application in inflammatory disorders. Phytomedicine 15, 400–407.
Singh, Y., Meher, J.G., Raval, K., Khan, F.A., Chaurasia, M., Jain, N.K., Chourasia, M.K., 2017. Nanoemulsion: Concepts, development and applications in drug delivery. J. Control. Release 252, 28–49.
Skarke, C., Kuczka, K., Tausch, L., Werz, O., Rossmanith, T., Barrett, J.S., Harder, S., Holtmeier, W., Schwarz, J.A., 2012. Increased bioavailability of 11-keto-beta-boswellic acid following single oral dose frankincense extract administration after a standardized meal in healthy male volunteers: modeling and simulation considerations for evaluating drug exposures. J. Clin. Pharmacol. 52, 1592–1600.
Surma-Ślusarska, B., Presler, S., Danielewicz, D., 2008. Characteristics of bacterial cellulose obtained from Acetobacter xylinum culture for application in papermaking. Fibres Text. East. Eur 16, 108–111.
Trovatti, E., Freire, C.S., Pinto, P.C., Almeida, I.F., Costa, P., Silvestre, A.J., Neto, C.P., Rosado, C., 2012. Bacterial cellulose membranes applied in topical and transdermal delivery of lidocaine hydrochloride and ibuprofen: in vitro diffusion studies. Int. J. Pharm. 435, 83–87.
Tsai, Y.H., Yang, Y.N., Ho, Y.C., Tsai, M.L., Mi, F.L., 2018. Drug release and antioxidant/antibacterial activities of silymarin-zein nanoparticle/bacterial cellulose nanofiber composite films. Carbohydr. Polym. 180, 286–296.
Udhardt, U., Hesse, S., Klemm, D., 2005. Analytical investigations of bacterial cellulose. Macromol. Sympos. 223, 201–212.
White, R., Cutting, K.F., 2006. Modern exudate management: a review of wound treatments. World Wide Wounds 1.
Wiegand, C., Hipler, U.C., 2009. Evaluation of biocompatibility and cytotoxicity using keratinocyte and fibroblast cultures. Skin Pharmacol. Physiol. 22, 74–82.
Wiegand, C., Moritz, S., Hessler, N., Kralisch, D., Wesarg, F., Müller, F.A., Fischer, D., Hipler, U.-C., 2015. Antimicrobial functionalization of bacterial nanocellulose by loading with polihexanide and povidone-iodine. J. Mater. Sci. - Mater. Med. 26, 245.
Yano, S., Maeda, H., Nakajima, M., Hagiwara, T., Sawaguchi, T., 2008. Preparation and mechanical properties of bacterial cellulose nanocomposites loaded with silica nanoparticles. Cellulose 15, 111–120.
Ye, S., Jiang, L., Wu, J., Su, C., Huang, C., Liu, X., Shao, W., 2018. Flexible amoxicillin-grafted bacterial cellulose sponges for wound dressing: in vitro and in vivo evaluation. ACS Appl. Mater. Interfaces 10, 5862–5870.

Supplementary information for the publication 2

Development and characterization of bacterial nanocellulose loaded with *Boswellia serrata* extract containing nanoemulsions as natural dressing for skin diseases

Berit Karl[a], Yaser Alkhatib[a], Uwe Beekmann[a], Tom Bellmann[a], Gabriele Blume[b], Frank Steiniger[c], Jana Thamm[a], Oliver Werz[d,f], Dana Kralisch[a,f], Dagmar Fischer[a,f]

a Pharmaceutical Technology and Biopharmacy, Friedrich Schiller University Jena, Lessingstraße 8, 07743 Jena, Germany; berit.karl@uni-jena.de, yaser.alkhatib@uni-jena.de, uwe.beekmann@uni-jena.de, tom.bellmann@uni-jena.de, jana.thamm@uni-jena.de, dana.kralisch@uni-jena.de, dagmar.fischer@uni-jena.de

b Sopharcos Dr. Gabriele Blume, Im Schloss 7, Steinau an der Straße, Germany; info@sopharcos.de

c Electron Microscopy Center, University Hospital Jena, Friedrich Schiller University Jena, Ziegelmuehlenweg 1, 07743 Jena, Germany; frank.steiniger@med.uni-jena.de

d Pharmaceutical and Medicinal Chemistry, Philosophenweg 14, 07743 Jena, Germany; oliver.werz@uni-jena.de

f Jena Center for Soft Matter (JCSM), Friedrich Schiller University Jena, Philosophenweg 7, 07743 Jena, Germany; dana.kralisch@uni-jena.de, dagmar.fischer@uni-jena.de

corresponding author:

dagmar.fischer@uni-jena.de, phone: (0049)-3641-9-49901, fax: (0049)-3641-9-49902

Appendix. Supporting information

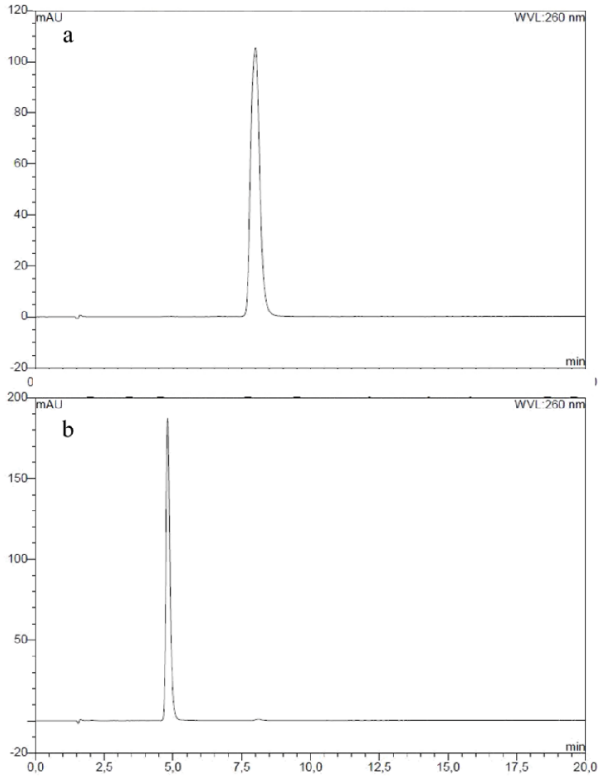

Fig. A.1

HPLC chromatograms showing peaks of AKBA (a) and KBA (b) measured at a wavelength of 260 nm

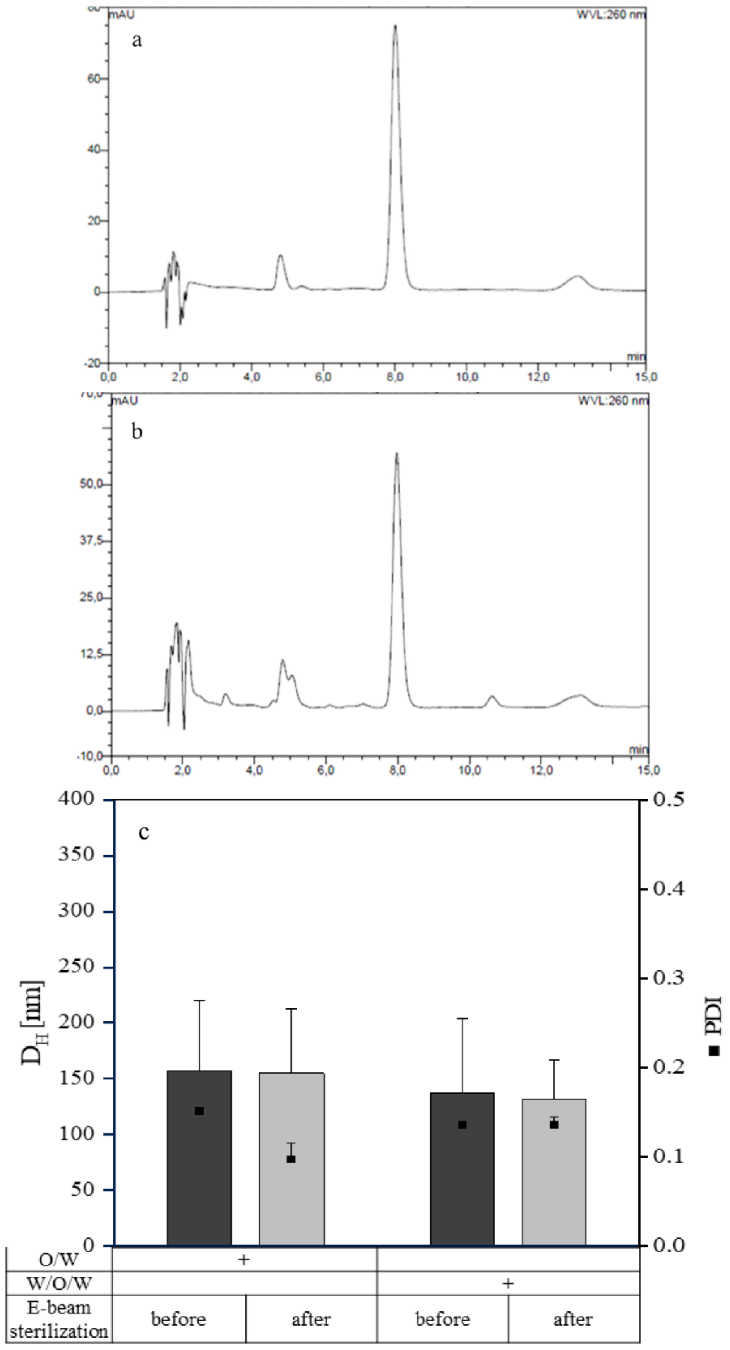

Fig. A.2

HPLC chromatograms of BSE before (a) and after autoclaving (b) at 121 °C and 2 bar for 15 min. D_H and PDI of nanoemulsions before and after e-beam sterilization measured by laser light scattering (mean ± SD; n=3) (c).

	Structural formula	Molecular formula	Molar mass [g/mol]	Log P	LOD [µg/mL]	LOQ [µg/mL]
AKBA	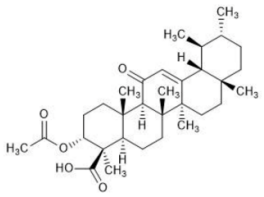	$C_{32}H_{48}O_5$	512.7	8 [a]	0.02	0.08
KBA	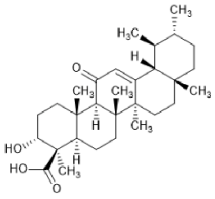	$C_{30}H_{46}O_4$	470.7	7 [a]	0.07	0.11

[a] according to (Karlina et al., 2007)

Table A.1

Comparison of AKBA and KBA regarding their chemical characteristics, log P values as well as LOD and LOQ determined by HPLC.

		D_H [nm]	PDI	ZP [mV]	pH	Visc. [mPa*s]	AKBA [mg/mL]	KBA [mg/mL]
Nanoemulsions	O/W	148.5 ± 1.3	0.11 ± 0.00	-72 ± 1	---	---		
	W/O/W	113.0 ± 0.7	0.11 ± 0.00	-80 ± 5	---	---		
Nanoemulsions with BSE	O/W	149.4 ± 1.6	0.09 ± 0.02	-72 ± 2	5.68	6.67 ± 0.17	3.87 ± 0.06	0.43 ± 0.06
	W/O/W	116.9 ± 2.3	0.14 ± 0.01	-78 ± 2	5.56	3.92 ± 0.17	3.66 ± 0.03	0.40 ± 0.01

Table A.2

Comparison of physicochemical characteristics of O/W and W/O/W nanoemulsions with and without BSE. D_H, PDI, ZP, pH value, viscosity, and amount of AKBA and KBA were investigated.

4.3. Publication 3

Controlled extended octenidine release from a bacterial nanocellulose/Poloxamer hybrid system

Y. Alkhatib, M. Dewaldt, S. Moritz, R. Nitzsche, D. Kralisch, D. Fischer

European Journal of Pharmaceutics and Biopharmaceutics, 2017, 112, p. 164-176

DOI 10.1016/j.ejpb.2016.11.025

European Journal of Pharmaceutics and Biopharmaceutics 112 (2017) 164–176

Contents lists available at ScienceDirect

European Journal of Pharmaceutics and Biopharmaceutics

journal homepage: www.elsevier.com/locate/ejpb

Research paper

Controlled extended octenidine release from a bacterial nanocellulose/Poloxamer hybrid system

Y. Alkhatib [a], M. Dewaldt [a], S. Moritz [a], R. Nitzsche [b], D. Kralisch [a,c], D. Fischer [a,c,*]

[a] Department of Pharmaceutical Technology, Friedrich-Schiller-University Jena, Otto-Schott-Straße 41, 07745 Jena, Germany
[b] Malvern Instruments GmbH, Rigipsstraße 19, 71083 Herrenberg, Germany
[c] Jena Center for Soft Matter (JCSM), Friedrich-Schiller-University Jena, Philosophenweg 7, 07743 Jena, Germany

ARTICLE INFO

Article history:
Received 25 July 2016
Revised 18 November 2016
Accepted in revised form 21 November 2016
Available online 24 November 2016

Keywords:
Bacterial nanocellulose
Poloxamer
Hydropolymer
Octenidine
Wound dressing

ABSTRACT

Although bacterial nanocellulose (BNC) has been widely investigated in the last 10 years as drug delivery system, up to now no long-term controlled release of drugs could be realized. Therefore, the aim of the present work was the development of a BNC-based drug delivery system that provides prolonged retention time for the antiseptic octenidine up to one week with improved mechanical and antimicrobial properties as well as a high biocompatibility. BNC was modified by incorporation of differently concentrated Poloxamers 338 and 407 as micelles and gels that were extensively investigated regarding size, surface charge, and dynamic viscosity. Depending on type and concentration of the Poloxamer, a retarded octenidine release up to one week could be accomplished. Additionally, superior material properties such as high compression stability and water binding could be achieved. The antimicrobial activity of octenidine against *Staphylococcus aureus* and *Pseudomonas aeruginosa* was not changed by the use of Poloxamers. Excellent biocompatibility of the Poloxamer loaded BNC could be demonstrated after local administration in a shell-less hen's egg model. In conclusion, a long-term delivery system consisting of BNC and Poloxamer could be developed for octenidine as a ready-to-use system e.g. for long-term dermal wound treatment.

1. Introduction

The unique natural hydropolymer bacterial nanocellulose (BNC) is an innovative bio-fabricated material, produced during fermentation by strains of the obligatory aerobic, Gram-negative bacteria *Komagataeibacter xylinus* in static culture [1]. Although the chemical formula is identical to plant cellulose, the most important difference is the diameter of the cellulose fibers that typically lies in the range of 20–100 nm. From the technological point of view, BNC is produced as an inherently stable three-dimensional hydropolymer consisting of about 1% cellulose and up to 99% water. The fiber diameter, the degree of polymerization and the network structure are responsible for the outstanding material properties such as high mechanical and thermal stability as well as softness [1,2].

The interest in BNC as drug delivery system dramatically increased during the last 10 years, as the nano-sized 3D-network of BNC is expected to hold a large amount of drug molecules due to its large surface area [3]. Active agents like small molecules [4–6], peptides [7] and proteins [8] as well as micro- and nanoparticles [9,10] including nanocrystals, precipitates or gels were integrated into the BNC network to accomplish a controlled drug release. Different drug loading strategies and functionalization methods were employed to combine material properties of BNC with the beneficial effects of drugs. Basically, *in situ* and *post* synthesis loading techniques can be distinguished where the active component is incorporated in the BNC nanofiber network during assembly or into the finally formed material after synthesis and purification, respectively [6,11,12]. The suitability of a method for a certain application depends on the physicochemical characteristics of the drug like molar mass and solubility, drug stability during each process step, modification of the BNC, and the intended drug release profile.

Typically, drugs were incorporated by sorption techniques under submerse conditions over several hours or days [8]. However, as drug loading is accomplished by diffusional or swelling controlled processes, the release often also follows these physical

* Corresponding author at: Department of Pharmaceutical Technology, Friedrich-Schiller-University, Otto-Schott-Straße 41, 07745 Jena, Germany.
E-mail addresses: yaser.alkhatib@uni-jena.de (Y. Alkhatib), marie.neumann@gmx.de (M. Dewaldt), sebastian.moritz@uni-jena.de (S. Moritz), rolf.nitzsche@malvern.com (R. Nitzsche), dana.kralisch@uni-jena.de (D. Kralisch), dagmar.fischer@uni-jena.de (D. Fischer).

http://dx.doi.org/10.1016/j.ejpb.2016.11.025
0939-6411/

transport processes. Therefore, in many studies the drug release was found to be characterized by a biphasic profile consisting of a fast burst release within the first 2–10 h followed by a slow release phase up to 24 h [4,5]. The incorporation of nano- and microparticles to extent the release phase did also not exceed a release phase of 24–72 h [9]. However, for several pharmaceutical applications long-term release rates are required. As an example, for the application of BNC as active wound dressing less frequent changes could reduce pain and prevent tissue trauma. For the use of BNC as implant, bone or cartilage replacement an extended release of antibiotics or growth factors to treat infection or to attract the growing cells over several days after surgery, respectively, seems to be favorable.

Poloxamers are presented by the Food and Drug Administration guide as an inactive ingredient for many different preparations such as parenteral, oral, topical and ophthalmic formulations [13]. They are highly attractive due to their biocompatibility and low toxicity [13]. They have been introduced to pharmaceutical applications as amphiphilic surfactants composed of polyethylene oxide (PEO)/polypropylene oxide (PPO) arranged in a triblock structure as PEOx-PPOy-PEOx [13,14] that form micelles with a core of hydrophobic PPO blocks and a shell of strongly hydrophilic PEO in an aqueous environment. Depending on polymer concentration and temperature, micellar structures or coherent gels can be formed. Although local applications have been widely described, for a sustained local delivery Poloxamers were found to be critical. The rapid erosion in the physiological environment by dilution drops the concentration below the critical micellar or gelation concentration followed by a fast release of drugs [13,14].

Previously, we reported BNC as a drug delivery system for the antiseptic octenidine intended for the local treatment of acute wounds which requires a fast, short-term drug release within several hours. This could be realized by the incorporation of octenidine into the BNC network without any additional excipients. In contrast, in the present study a long-term release drug delivery system should be developed by the combination of the advantages of two materials, BNC and Poloxamers. As model drug octenidine has been selected again as it has been widely described before for the administration by BNC with well-known drug release kinetics and mechanisms. Loading techniques for drug and Poloxamers in BNC were developed to accomplish controllable release profiles up to one week. These hybrid systems were intensively characterized regarding their physicochemical and biological characteristics *in vitro* and *in vivo*.

2. Materials and methods

2.1. Preparation and characterization of BNC fleeces

The biosynthesis of bacterial nanocellulose was accomplished by static cultivation of *Komagataeibacter xylinus* DSM 14666 (culture collection of the Friedrich-Schiller-University Jena, deposited at the DSMZ, German Collection of Microorganisms and Cell Cultures, Braunschweig, Germany) in Hestrin-Schramm medium at 28 °C in 24-well plates (Greiner-Bio-one, Frickenhausen, Germany) as described before [8]. BNC fleeces were rinsed with deionized water, boiled in 0.1 N aqueous sodium hydroxide solution (NaOH, Carl Roth, Karlsruhe, Germany) for 30 min and washed again in water until a neutral pH was reached. Finally, they were sterilized by autoclaving (121 °C, 20 min, 2 bar) before storage at 4 °C. All BNC fleeces were characterized by examination of their different dimensions (diameter, thickness, volume, and weight) as described before [8]. Surface area and volume were calculated according to the geometrical formulas of a circular cylinder or a cuboid [8].

2.2. Preparation of octenidine and Poloxamer loaded BNC

Octenidine was purchased from Schuelke & Mayr (Norderstedt, Germany) as a stock solution containing 0.5% octenidine. The Kolliphor® F108 (Poloxamer 338) and F127 (Poloxamer 407) were obtained as a kind gift from BASF SE (Ludwigshafen, Germany). For the preparation of loading solutions the Poloxamers were dissolved in the octenidine stock solution under constant stirring (IKA® Werke, Staufen, Germany) at 4 °C in a temperature-controlled refrigerator for 24 h to ensure complete dissolution. Octenidine stock solutions containing equal amounts of water instead of the Poloxamers were used as controls. Poloxamers were used in two different concentrations representing values above the critical micelle concentration (so called CMC samples) and the critical gelation concentration (named as CGC samples) according to Table 1. For loading of BNC with octenidine and octenidine/Poloxamer dispersion, BNC fleeces were incubated in 10.0 mL loading solution under submersed conditions for 48 h on an orbital shaker (KS 4000 ic control, IKA®-Werke) at 70 rpm. For CMC samples, the fleeces were treated at room temperature using dispersions that were warmed-up after dissolution at 4 °C to 21 °C. In contrast, the CGC samples were loaded at 4 °C and heated to room temperature after the loading process. The amount of loaded antiseptic was calculated from the difference of the octenidine concentration before loading and the octenidine concentration of the loading solution after 48 h.

2.3. Quantification of octenidine

The quantification of octenidine was performed by ultraviolet and visible (UV/Vis) spectrophotometric measurements in 0.1 M phosphate buffered solution (PBS) pH 7.4 (Carl Roth) at 281 nm using the Beckman DU 640 spectrophotometer (Beckmann Instruments Inc., Fullerton, CA, USA). Detailed descriptions can be found at [4]. All experiments were run in triplicate and repeated once.

2.4. Laser light scattering experiments

The hydrodynamic diameter and the polydispersity indices of the undiluted octenidine/Poloxamer dispersions (CMC samples) were measured using the Zetasizer Nano ZS (Malvern Instruments, Herrenberg, Germany; Software: Zetasizer v7.2) in a minimal volume cuvette ZEN 0040 (BRAND, Wertheim, Germany) equipped with a 4 mW He-Ne laser (633 nm) at a scattering angle of 173° at 20 °C. Results were shown as the mean Z-average of six runs. The measurements of the zeta potential were performed in a Zetasizer cuvette DTS1060 (Malvern instruments) by measuring the electrophoretic mobility at 20 °C. The results were calculated with the Malvern software 7.2 and shown as the mean ± SD of three independent measurements.

2.5. Determination of CMC and CGC

To determine the CMC of the Poloxamers, a UV/Vis spectroscopic method was performed. A mixture of iodine/iodide was used as a stock solution containing 6.4×10^{-4} and 2.0×10^{-3} -mol/L, respectively. Poloxamer concentrations in the range of 0.01–5% were tested. Samples (4 mL) of each Poloxamer concentration were mixed with 1 mL of the stock solution [15]. The mixture was stored under light exclusion for 12 h [16]. Afterwards, the absorbance measurements were carried out at 366 nm using the Beckman DU 640 spectrophotometer. The Poloxamer concentration which showed a sharp decrease in absorption was defined as the CMC value according to [15]. To determine the sol-gel transition temperature of the Poloxamers, the tube inverting method was employed [17,18]. Two mL Poloxamer solution were added

Table 1
Physicochemical characteristics of the Poloxamers and the CMC and CGC samples.

Type	PEO	PPO	Molar mass (g/mol)	CMC (%)	CGC (%)	Micelle size (nm)	Micelle zeta potential (mV)	Tsol/gel (°C)[a]
Pol. 338 (Water)	141	44	14,600	10	22	6.11	0.66 ± 0.23	26.3
Pol. 338 (Octenidine)	141	44	14,600	10	22	9.81	1.78 ± 0.44	18.4
Pol. 407 (Water)	101	56	12,600	5	18.5	9.42	−0.78 ± 1.09	24.5
Pol. 407 (Octenidine)	101	56	12,600	5	18.5	10.62	4.25 ± 1.38	16.3

[a] Determined by rheological measurements.

to a 15 mL tube (Greiner Bio-one). Different Poloxamer concentrations were selected (Poloxamer 338: 20%, 22%, and 25%, Poloxamer 407: 15%, 18.5%, and 20%) and incubated in a temperature-controllable water bath at 4 °C. The temperature of the water bath was raised 1 °C/5 min, and tubes were inverted. The gelation temperature was considered as the temperature where the liquid did not flow for 30 s. Experiments were performed in triplicate.

2.6. Rheological studies

Rheological measurements were carried out by a strain-controlled Bohlin CVO rheometer (Malvern Instruments Ltd., Worcestershire, UK). The rheometer was equipped with a cone/-plate configuration having a radius of 40 mm and a cone angel of 4 degrees as well as a parallel-plate fixture with a radius of 40 mm and a gap size of 0.15 mm. The test samples were equilibrated to 4 °C and approximately 2 mL were applied to the tempered sample holder. The dynamic viscosity was measured at a heating rate of 1 °C/min over a temperature range of 4–35 °C. The dynamic viscosity was calculated as a function of time from the measured shear stress at a constant shear rate of 1000/s every 25 seconds automatically by the Bohlin Rotational Software.

2.7. In vitro octenidine and Poloxamer release

Release studies of octenidine loaded BNC with and without Poloxamers were performed in 0.1 M PBS buffer, pH 7.4 at 32 °C using a vertical diffusion cell (Franz cell, SES-Analysensysteme, Bechenheim, Germany) with a receiver compartment volume of 12 mL and an effective area for diffusion of 1.77 cm^2. The receiver compartment was magnetically stirred and thermostated to 32 °C by a water jacket. Loaded BNC was placed in the donor compartment and after 0, 0.5, 1, 2, 3, 4, 5, 6, 8, 24, 30, 48, 72, 96, 120, 144, 168 and 192 h aliquots (0.5 mL) of the receiver compartment were withdrawn and replaced by fresh and preheated (32 °C) 0.1 M PBS (pH 7.4). The amount of released octenidine was quantified using the UV/Vis spectrophotometric measurement as described above. A semi-empirical equation proposed by Ritger and Peppas (Power Law)

$$M_t/M_\infty = kt^n \quad (1)$$

was used to analyze the octenidine release mechanism [19], where M_t and M_∞ represent the cumulative amounts of released drug at time t as well as at infinite time. Furthermore, M_∞ describes the octenidine amount of BNC fleeces after 48 h loading and k relates to the geometrical and structural properties of the delivery system. The logarithmic percentage release between 5–60% was plotted against the corresponding logarithmic time log (t) and the diffusional exponent n (slope of the resulting linear regression) was used to characterize the release mechanism. Release studies were carried out in triplicate and repeated once.

For the quantification of the Poloxamer release [20] a solution of cobalt thiocyanate was prepared by dissolving 10 g ammonium thiocyanate (Merck, Darmstadt, Germany) and 1.5 g of cobalt (II) nitrate (Carl Roth) in 50 mL water. Two milliliter Poloxamer sample and 1 mL cobalt thiocyanate solution were added to 2 mL ethyl acetate (Bernd Kraft, Duisburg, Germany). After mixing, the mixture was immediately centrifuged (Centrifuge 5904 R, Eppendorf, Hamburg, Germany) at 4500 g for 3 min. The upper ethyl acetate phase was removed. Two mL ethyl acetate were added to rinse the pellet and centrifuged again. This step was repeated several times until the ethyl acetate solution was colorless. Four milliliter acetone (Merck) were added to the pellet for dissolution by vigorous shaking. All colorimetric measurements were done using the multimode microplate reader Spark® 10 M (Tecan, Maennedorf, Switzerland) at 624 nm. Staining of fleeces was performed accordingly to demonstrate the homogeneity of Poloxamer loading.

2.8. Mechanical properties

The pressure stability of loaded and unloaded BNC was analyzed for mechanical characterization of native BNC (negative control) and octenidine loaded BNC with and without Poloxamers. A test weight of 400 g was applied on the BNC samples perpendicular for 10 min at 32 °C. Diameter, height and weight of the BNC samples were determined before and after loading as described in Section 2.1 as well as after the compression. The compressive strain (ε) of the BNC was calculated by

$$\Delta h/h_0 * 100\% \quad (2)$$

where Δh represents the change of the height during compression and h_0 [mm] the original height of the BNC samples.

2.9. Water binding characteristics

To determine the effect of octenidine and Poloxamers on the water absorption value (WAV) [21], native and octenidine loaded BNC fleeces with and without Poloxamers were cut into quarters and maintained for 2 h in the loading medium to re-swell. BNC pieces were air-dried at 50 °C until a constant weight was reached. The sample weight was determined before and after drying and the WAV was calculated based on the following equation:

$$WAV = Wi/Wd * 100 \quad (3)$$

where Wd represents the sample weight in the process of dry state and Wi the initial weight before drying. For determination of the water retention value (WRV) [22], BNC fleeces were cut into two halfs, and incubated for 2 h in the loading medium to re-swell. Afterwards, BNC samples were centrifuged in an Eppendorf MiniSpin® (Eppendorf, Hamburg, Germany) for 15 min at 1073 g. BNC pieces were air-dried at 50 °C to a constant weight and weighted before and after drying. The WRV was calculated based on the following equation:

$$WRV = (Wi - Wd/Wd) * 100 \quad (4)$$

where Wd represents the sample weight in the dry state and Wi the weight of the wet centrifuged sample. All experiments were performed with four BNC fleeces.

2.10. Ex ovo shell less hen's egg test

The biocompatibility of BNC loaded with and without Poloxamers was tested *in vivo* using a shell-less hen's egg model (HET-CAV, hen's egg test-chick area vasculosa) [23]. Fertilized eggs from a local supplier were incubated at 37 °C and at 80% relative humidity. After 72 h, the eggs were transferred into a Petri dish containing Ringer's solution pH 7.0. Only eggs with an intact yolk sac membrane, well-developed blood vessels and constant heart beat (0.5 Hz) (Hamburger and Hamilton stage 14–17), were selected for the experiments [24]. After one hour incubation, BNC samples ($n = 5$) were directly applied locally on the chick area vasculosa. BNC loaded only with Ringer's solution pH 7.0 was utilized as negative control, 1% (m/v) SDS solution (sodium dodecyl sulfate, Carl Roth) was used as positive control. After 1, 2, 4 and 8 h eggs were evaluated under a stereomicroscope for hemorrhage, vascular lysis, thrombosis and embryo lethality.

2.11. Preparation of extracts for biological studies

Octenidine loaded BNC fleeces with and without Poloxamers were extracted according to DIN EN ISO 10,993-12. Briefly, physiological saline solution (Merck, Darmstadt, Germany) was used as extraction medium, where 1 g of the loaded BNC was incubated in 50 mL of 0.9% NaCl for 24 h under shaking (KS 4000 ic control). Further extraction steps were carried out as described before [25].

2.12. Agar diffusion test

To evaluate the antimicrobial activity of octenidine loaded BNC with and without Poloxamers agar diffusion tests were employed. For these tests, a bacterial stock solution of *Staphylococcus aureus* (*S. aureus*, DSM 1104) as Gram-positive and *Pseudomonas aeruginosa* (*P. aeruginosa*, DSM 1117) as Gram-negative model bacteria were used. The agar diffusion tests were performed according to the standards of Clinical and Laboratory Standards Institute (CLSI) disk diffusion test VET01-A4 [26]. The antimicrobial activity was evaluated by the formation of an inhibition zone around the loaded BNC sample. Initially, 5 µL bacterial stock solution were inoculated in 50 mL sterile Caso-bouillon (Carl Roth) and incubated at 35 °C and 100 rpm for 24 h. Afterwards, the microbial inoculum was diluted with physiologic saline until the turbidity of the suspension was equal to that of 0.5 McFarland (~108 CFU/mL). The bacterial suspension was further diluted 10-fold with physiologic saline, and 100 µL were pipetted on a Mueller-Hinton 2 agar plate (prepared from Mueller-Hinton agar 2, Sigma-Aldrich, Munich, Germany). With a sterilized Drigalski spatula the inoculum was evenly spread over the complete agar surface. After incubation for 5 min at room temperature, BNC samples loaded with octenidine, octenidine/Poloxamer, and Poloxamer only were placed directly onto the surface of a bacteria-containing agar plate. BNC loaded with purified water was used as reference. Additionally, pure filter paper disks with a diameter of 6 mm (MACHEREY-NAGEL, Dueren, Germany) were used as negative control and filter disks treated with the antibiotics for *S. aureus* (30 µg kanamycin sulfate, Carl Roth) and *P. aeruginosa* (10 µg gentamicin sulfate, AppliChem, Darmstadt, Germany) were used as positive controls. Afterwards, the agar plates were placed in an incubator (Thermo Electron, Erlangen, Germany) for 24 h at 35 °C. After incubation, photographs were taken and the diameter of the inhibition zone surrounding the BNC samples was measured in triplicate. All experiments were performed five times.

2.13. Antimicrobial tests

To investigate the antimicrobial activity of octenidine and octenidine/Poloxamer loaded BNC, *S. aureus* was grown to the late log phase after an overnight culture in Trypticase soy yeast medium (Carl Roth). Afterwards, 25 mL of the cultures were concentrated by centrifugation at 10,000 *g* for 15 min (Avanti 30, Beckman Coulter, Krefeld, Germany). The pellet was suspended in 2 mL 0.9% NaCl solution (Merck) after removing the supernatant. The first half of the suspension was treated for 1 h with 70% isopropyl alcohol (Carl Roth) to obtain 100% dead cells, the second half was suspended in 0.9% NaCl solution (20 mL) to obtain living cells. Subsequently, both bacterial cell suspensions were centrifuged again. The supernatant was removed and the pellet was resuspended in 0.9% NaCl solution. Washing procedure was repeated twice. Afterwards, cells were suspended in 10 mL 0.9% NaCl followed by adjusting the optical density at 670 nm (OD_{670}) to 0.6 (4×10^7 cells/mL) using the UV/Vis spectrophotometer (BioPhotometer, Eppendorf). Viable and dead bacterial suspensions were mixed in different ratios (0:1, 1:9, 1:1, 9:1 and 1:0). Afterwards, the LIVE/DEAD® BacLight™ bacteria viability kit (L7012, Molecular Probes, Life Technologies Co., Japan) was applied according to the manufacturer's instructions. The fluorescence was measured using the Fluostar OPTIMA plate reader (BMG Labtech, Ortenberg, Germany). The excitation/emission wavelengths were 485/530 nm (green) for SYTO 9 and 485/630 nm (red) for propidium iodide. The percentage of viable cells was obtained by comparing the ratio of green/red fluorescence with the standard viability cells. Instead of treating the bacterial suspension with isopropyl alcohol extracts of loaded BNC were used and the same incubation and preparation procedure applied. All experiments were performed in triplicate.

2.14. Data and statistical analysis

An ANOVA one way analysis of variance was applied to the data to evaluate statistically significant differences (p-values < 0.05, Microsoft Excel®). The inflection points on the curve of the apparent viscosity was calculated using a sigmoid Boltzmann fit: $y = A2 + (A1A2)/(1 + \exp((x - x_0)/dx))$; A1: lower limit, A2: upper limit, x_0: center (inflection point, dx: width, OriginLab 9.1.).

3. Results and discussion

3.1. Preparation of BNC fleeces

Under static cultivation *K. xylinus* formed disk-shaped, mat like hydropolymer pellicles with diameters of about 1.61 ± 0.01 cm that accumulated at the interface between air and culture medium. The resulting fleeces were characterized by a thickness of 0.47 ± 0.04 cm, a weight of 0.93 ± 0.07 g, a calculated volume of 0.96 ± 0.08 cm^3 and a calculated surface area of 6.45 ± 0.22 cm^2. Only samples with macroscopically homogeneous morphology and intact shape and structure were selected for the following experiments. Electron microscopy (data not shown) revealed the typical architecture of triple-layered fleeces with a dense top layer, a nanofibrillar pore and tunnel system in the middle and the residues of the prepolymer at the bottom as shown in previous publications [12]. Extensive characterization of the material properties was reported before [4,21].

3.2. Preparation and physicochemical characterization of the octenidine/Poloxamer formulations

Two different types of Poloxamers 338 and 407 were selected since both have the ability to transform from a sol to a gel through micellation and gelation depending on polymer concentration and temperature. Although they have comparable molar masses, the size of the lipophilic part (PPO) increased from Poloxamer 338 to 407 from 44 to 56 g/mol resulting in a more lipophilic character of Poloxamer 407 (Table 1). As a first step, the formation of Poloxamer micelles and gels as well as the influence of octenidine were investigated to determine the conditions for an optimized preparation protocol. The so called "cold method" was used as it favors several advantages like easy handling, less solvent loss, limitation of possible drug alterations, and avoidance of thixotropic effects compared to methods applying high temperatures [13,27]. The Poloxamers were mixed with the octenidine in aqueous medium at 4 °C and stirred until a homogeneous solution was obtained that contained the copolymers in solution as unimers.

The self-aggregation of the unimers to micelles was initiated by the increase of the temperature to 21 °C. The critical micelle concentrations (CMC) of both Poloxamers to accomplish the formation of spherical structures under the chosen conditions were determined by the measurement of the changes of the absorption spectra of an iodine/iodide solution, caused by the Poloxamer assembly [15]. Testing a broad range of different copolymer concentrations from 0.01% to 5%, spectral changes could be observed for Poloxamer 338 and 407 already at concentrations of 0.4% and 0.3%, respectively, under the chosen conditions with a slightly higher CMC for Poloxamer 338 than for Poloxamer 407 due to the larger content of PEO and the higher molar mass [28]. In the presence of octenidine, the I_2/I^- mixture interacted chemically with the antiseptic and formed a colored complex that interfered with the UV/Vis measurement. Nevertheless, the formation of micelles could still be confirmed and the colocalization of octenidine and both Poloxamers visualized using thin layer chromatography. By increasing the amount of added Poloxamers, the covered distance of octenidine on the TLC plate and therefore the retardation factor (R_f) decreased in comparison to octenidine solution without Poloxamer (data not shown). Taken these results together with recommendations of the literature and the Poloxamer supplier [29,30], for the following experiments the concentrations of the so called "CMC samples" were adjusted to 10% and 5% for Poloxamer 338 and 407, respectively, to guarantee complete and stable micelle formation.

These micellar dispersions were macroscopically homogeneous, colorless and free of particulate matter. The hydrodynamic diameters of the optimized Poloxamer micelles were characterized by photon correlation spectroscopy and revealed nanoscaled dimensions in the range of 6–11 nm with and without octenidine (Table 1). As reported for other drug loaded Poloxamer micelles in the literature [31], measurements of the zeta potentials revealed values nearly zero suggesting a non-charged surface with and without octenidine (Table 1). Therefore, it was suggested that the charges of the octenidine were completely masked by incorporation of the drug into the micellar structures [32].

The phase transition temperature (Tsol/gel) was determined by the tube-inverting method using different polymer concentrations that were selected according to the literature [33]. The higher the amount of the copolymer, the faster was the formation of the gel and the lower the transition temperature (Fig. 1). An increase of the Poloxamer 338 concentration from 20% to 25% decreased the Tsol/gel from 34 °C to 25 °C. For Poloxamer 407 Tsol/gel was reduced from 33 °C to 21 °C by an increase of the amount of polymer from 15 to 20%. As reported by Alexandridis et al. [28], copolymers with larger hydrophobic PPO domains formed micelles even

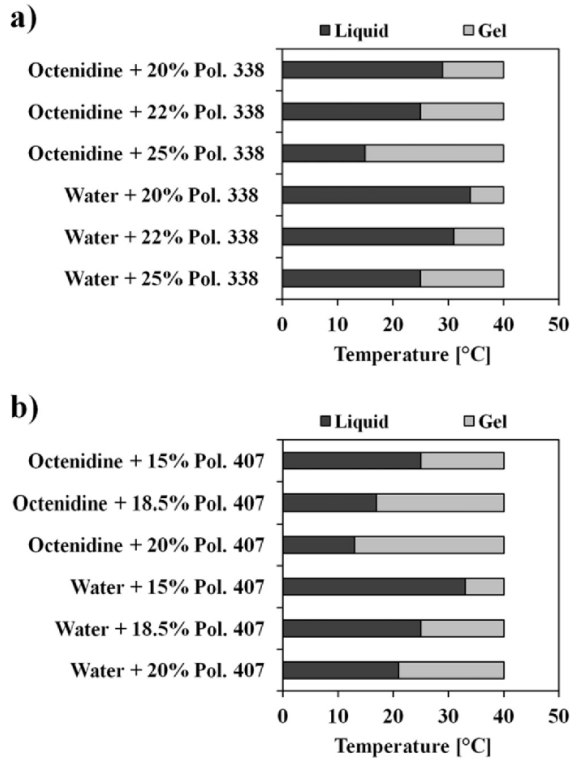

Fig. 1. Gelation temperatures of (a) Poloxamer 338 and (b) 407 in water compared to octenidine solution (0.5%) depending on the Poloxamer concentration.

at lower concentrations. The incorporation of the commercial octenidine solution decreased the phase transition temperature by 6–8% (Fig. 1) for both copolymers. This effect was suggested to be related to the presence of glycerol [27,34] as additive in the commercial octenidine solution [35], pronouncing the dehydration of the EO group, favoring the formation of micelles, increasing the micelle association number, and decreasing the gelation temperature. For the following experiments, 22% Poloxamer 338 and 18.5% Poloxamer 407 were selected for gel formation as they formed reproducibly stable and easy to handle gels for BNC loading at room temperature that represent storage conditions.

Comparable rankings were obtained by rheological measurements using a cone/plate geometry rheometer. The Tsol/gel was defined as the inflection point (calculated using OriginLab 9.1) on the curve of the apparent viscosity as a function of temperature (Table 1, Fig. 2) [36]. At 18–19 °C and 17–18 °C for Poloxamers 338 and 407, respectively, the formation of the gels started with an increase in viscosity. After incorporation of commercial octenidine solution in Poloxamers, the beginning of the gelation process and the Tsol/gel were shifted to lower temperatures (Fig. 2). As already discussed above the reason for this behavior seemed to be the added glycerol of the octenidine solution but not the octenidine itself (data not shown). These data (Table 1) confirmed for the selected Poloxamer concentrations (CGC samples) the gel formation at room temperature as well as at skin temperature of 32 °C.

3.3. Incorporation of octenidine/Poloxamer formulations in BNC

Fig. 3a gives a schematic overview of the preparation techniques for the BNC loading. For the loading of the 24-well BNC

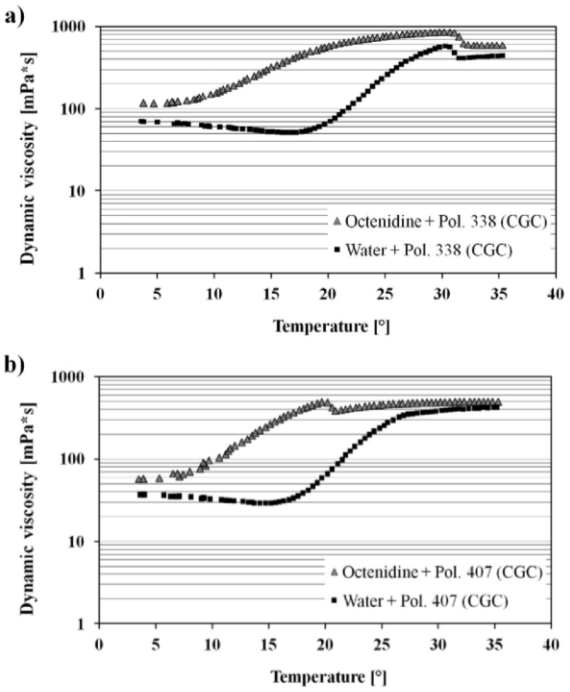

Fig. 2. Dynamic viscosity of water and octenidine solutions containing 22% Poloxamer 338 (a, CGC) and 18.5% Poloxamer 407 (b, CGC) in a temperature range between 4 and 35 °C applying a heating rate of 1 °C/min.

fleeces with octenidine micelles (CMC samples), a *post*-modification technique was selected using a submerse immersion process of the native fleeces in octenidine/Poloxamer dispersions at 21 °C as a well-established, easy to perform, mild conditioned technique [4,6]. Octenidine/Poloxamer dilutions were prepared at 4 °C and warmed up to 21 °C to form micelles before the addition of the BNC hydropolymer fleeces. Under gentle shaking (70 rpm) on a horizontal shaker the BNC was incubated for 48 h before removal for further experiments. In contrast, the incorporation of the octenidine containing Poloxamer gels into the BNC (CGC samples) was accomplished at 4 °C. BNC fleeces were placed in octenidine/Poloxamer solutions at 4 °C and incubated for 48 h under shaking to favor the homogeneous uptake of the liquid phase into the network of the BNC. After increase of the temperature to 21 °C, gelation appeared by forming *in situ* a Poloxamer network within the BNC pores.

The incorporation of liquid phases into BNC was suggested to be related to diffusion and capillary forces due to the large hydrophilic surface area of the network [37]. All loaded samples were homogeneous without macroscopically visible aggregates on the surface or any other visual changes (Fig. 3b). The staining of the loaded fleeces using a cobalt thiocyanate solution to form blue-colored complexes with Poloxamers confirmed the homogeneous distribution of the Poloxamers in the BNC (data not shown). The octenidine content of the loaded BNC fleeces was spectrophotometrically determined. To exclude any influence of the Poloxamers on the quantification of octenidine, its UV/Vis spectra were measured from 200–800 nm for mixtures of the antiseptic and the copolymer in varying concentrations as used in the following experiments. The absorption profiles of octenidine were not changed by the addition of the Poloxamers (data not shown). A comparison of the loading capacity expressed as percentage loading, revealed for all loaded BNC fleeces comparable values of about 8–9% (Fig. 3b) with the lowest drug load for the Poloxamer 338 (CGC) samples. The obtained loading performance was in accordance to results presented earlier when using the same loading technique [8,38]. A partial dewatering before loading seems to be a particularly effective method to further increase the drug uptake. Therefore, for future experiments the drug loading might additionally be improved by a partial or total dewatering of the BNC before loading. Hot or cold pressing and squeezing [4,8,11,39] are typically applied to controllably adjust the water content and were reported to increase the drug uptake by an overlay of diffusion and a spongy re-swelling process [4]. Completely dried BNC produced by freeze drying or critical point drying demonstrated the highest drug loading capacity, but suffered in some cases from structural changes [40,41].

3.4. Controlled release studies and physicochemical characterization of the loaded BNC

The release of the octenidine from the differently loaded BNC fleeces was quantified using a Franz cell diffusion system at skin temperature of 32 °C up to 192 h in PBS pH 7.4. The cumulative drug release was quantified by UV/Vis measurement in dependency of the release time as shown in Fig. 4a. The release profiles were found to be dependent on the type and the concentration of the copolymer. The cumulative release of free octenidine revealed a biphasic profile with an initial burst (48.7 ± 1.2%) within the first 8 h reaching a plateau and equilibrium conditions after 48 h with a total release of 80.5 ± 1.5%. The addition of 10% Poloxamer 338 (CMC) or 5% Poloxamer 407 (CMC) induced the formation of octenidine loaded micelles that demonstrated also a biphasic release profile but retarded the drug release by approx. 50% at 8 h compared to free octenidine. Also the time until equilibrium conditions were reached was increased to 96–120 h. Whereas the incorporation of Poloxamer 338 (CGC) as gel did not change the octenidine release profile compared to the CMC samples, the increase of the Poloxamer 407 (CGC) concentration to 18.5% retarded the drug release with a lower burst and a more continuous profile over up to 196 h (Fig. 4a insert). Although as described above, the viscosity of Poloxamer 338 (CGC) dispersions at the loading temperature and the gelation temperature were higher than for Poloxamer 407, both types of fleeces were homogeneously loaded as shown by the cobalt thiocyanate staining. However, in drug loading studies (Fig. 3b) for the Poloxamer 338 (CGC) samples a slightly lower uptake of octenidine could be determined. During release due to the higher hydrophilicity of Poloxamer 338 compared to Poloxamer 407, a faster dilution of the copolymer was induced leading to a disintegration of the gel structure and the formation of micelles which exhibited a octenidine release profile comparable to the Poloxamer 338 CMC samples. Furthermore, due to the lower loading of drug/Poloxamer 338 solution more diffusional space was available for diffusional processes during release.

This correlated well with the release profiles of the Poloxamers determined by the formation of blue-colored complexes with cobalt thiocyanate (Fig. 4b). The CMC samples demonstrated a faster Poloxamer release compared to the CGC samples with a significantly reduced release for the Poloxamer 407 (CGC) samples as also observed in the octenidine release determinations. Based on mathematical calculations, for the CMC samples mainly unimers could be found in the release medium, whereas for the CGC samples after 2–4 h the Poloxamer concentrations exceeded the CMC values and gave the chance for the formation of micelles in the release medium. However, whether the Poloxamers were released in form of unimers or micelles needs further investigation.

To the best of our knowledge this is the first time that a drug release could be sustained over up to 8 days by a BNC based carrier.

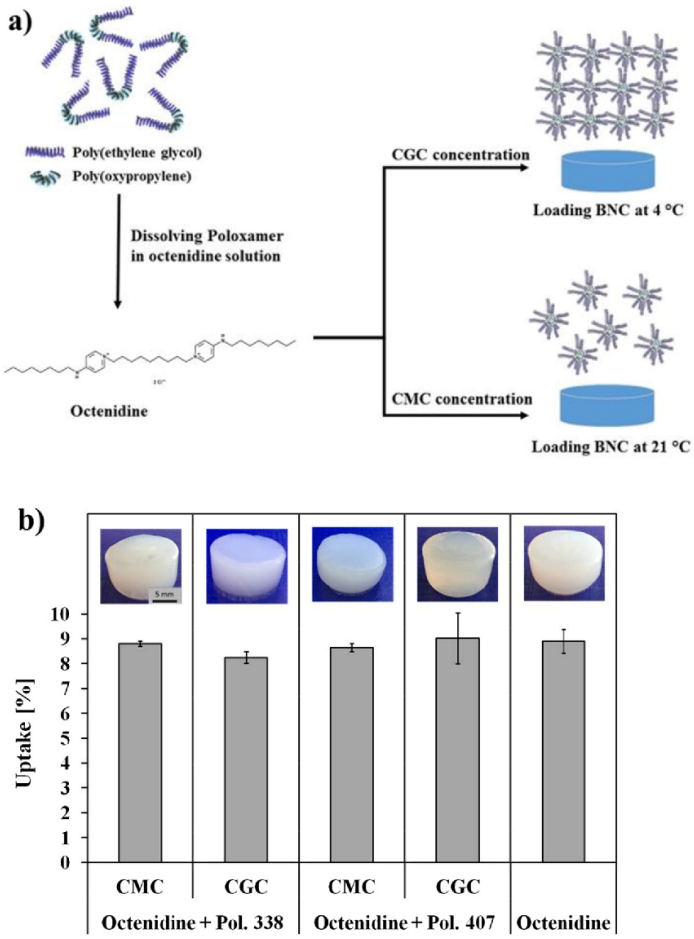

Fig. 3. (a) Schematic overview of the loading of BNC with Poloxamers forming CMC and CGC samples. (b) Photographs of octenidine and octenidine/Poloxamer loaded CMC and CGC BNC samples and percentage uptake of octenidine (mean ± SD, $n = 3$) after incubation of fleeces for 48 h.

Poloxamer gels were suggested to consist of large populations of micelles and aqueous channels in which incorporated drugs may be released by diffusional processes through the gel matrix [27,42]. In addition, Poloxamer gel dissolution was shown to play a role [43]. The decrease of the rate of release with increase of Poloxamer concentration could be attributed to the increase in the number of micelles accompanied by a decrease of aqueous channels [44,45] and correlated to a tortuosity in the channels and a slower rate of diffusion through aqueous channels and dissolution [43]. In previous experiments the BNC network was also shown to be responsible for a retarded migration of octenidine through the hydropolymer channel network [4,46]. To receive more insight into the release mechanism, the Ritger-Peppas model was applied to mathematically describe the cumulative release curves [19]. Taking a non-biodegradable material and a cylindric geometric dimension of the BNC into consideration, linear equations with regression coefficients (r^2) of 0.990–0.999 were calculated that demonstrated the applicability of the model (Table 2). All samples exhibited comparable diffusional exponents n (0.46–0.52) that were characteristic for a Fickian diffusion overlayed by swelling controlled (anomalous, non-Fickian transport) mechanisms ($0.45 < n < 0.89$ for cylinders and slabs). Conclusively, comparable transport mechanisms for octenidine can be assumed for the different formulations. As the characteristics of the BNC network did not change in all preparations, the different release rates could be attributed to the changes of viscosity of the Poloxamer gels that may control the velocity of drug diffusion and release. Diffusional processes seemed to dominate over dissolution controlled drug release [46].

To determine the impact of the Poloxamer incorporation on the favorable mechanical and water binding properties of the BNC and to maintain integrity during use, mechanical stability as well as the water absorption and retention were investigated in comparison to unloaded and octenidine loaded BNC. For compression stability tests CGC samples were submitted to a mass force of 400 g at 32 °C, and height and weight of the fleeces were measured before and after the treatment. Compressibility was expressed as the percentage reduction of both parameters (Fig. 5). The strongest deformation could be observed for the native and the octenidine loaded BNC, with a reduction of weight and height by about 65% and 48–55%, respectively. The samples formed flat disks coming along with a squeezing out of moisture that correlated with the loss of weight. BNC typically shows mechanical anisotropy with a high tensile modulus along the fiber layer direction, but a low compressive modulus perpendicular to the stratified direction [47]. In contrast, the octenidine/Poloxamer loaded CGC samples demonstrated a

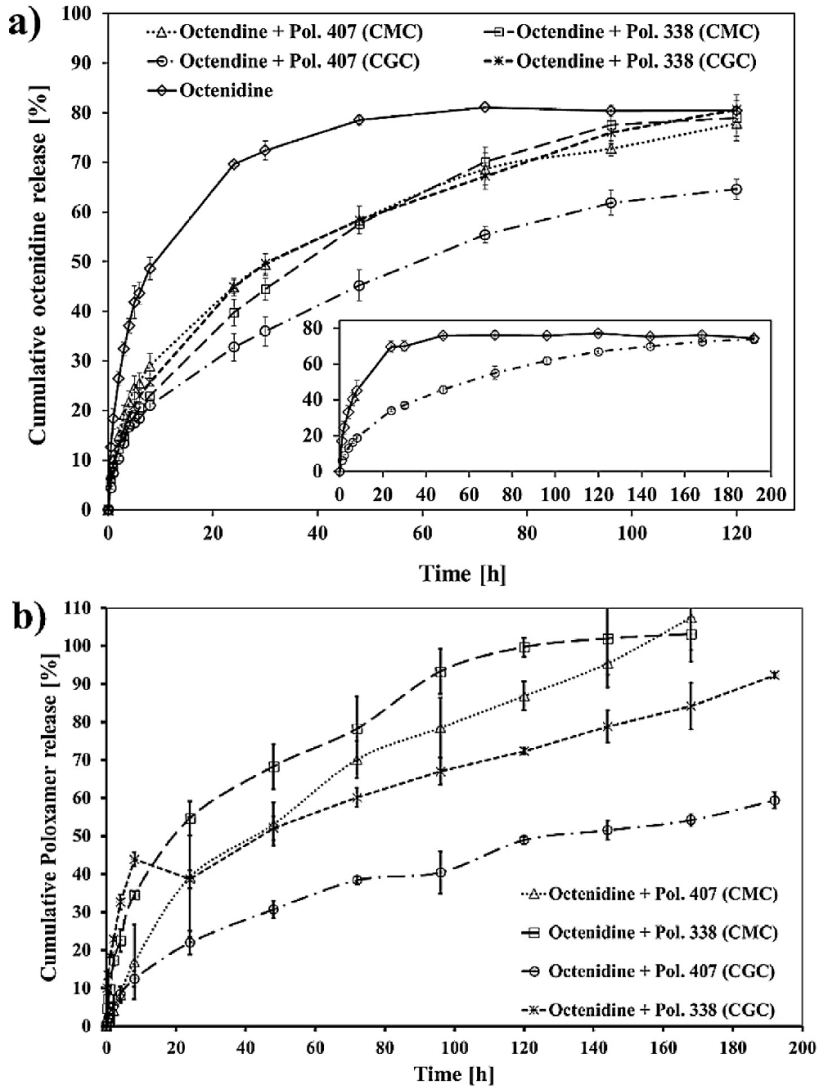

Fig. 4. Cumulative release profiles (mean of 3 BNC fleeces ± SD) at 32 °C of octenidine and octenidine/Poloxamer loaded CMC and CGC BNC measured using a Franz diffusion cell. Samples were taken at specified time points and the amount of (a) octenidine and (b) Poloxamers was quantified.

higher form stability with significantly lower reduction of height and weight by about 18–28% and 12–18% for Poloxamer 407 and 338, respectively. The *in situ* formation of the Poloxamer gel network inside the 3D-BNC network led to a substantial improvement of the mechanical stability and a reduced water release.

Table 2
Sample dependent diffusional exponents (n) and regression coefficients obtained from linear equations after modeling of cumulative octenidine release data according to the Ritger-Peppas equation.

Sample	Linear equation	Diffusion exponent n	Linear regression R^2
Octenidine	y = 0.52x + 1.22	0.52	0.994
Octenidine + 10% Pol. 338	y = 0.48x + 0.94	0.48	0.999
Octenidine + 5% Pol. 407	y = 0.46x + 1.03	0.46	0.990
Octenidine + 22% Pol. 338	y = 0.50x + 0.96	0.50	0.998
Octenidine + 18.5% Pol. 407	y = 0.47x + 0.87	0.47	0.990

Comparable effects were reported by several groups after integration of gelatine, poly(acrylamide), alginates, and polysaccharide gels into BNC [47,48].

For determination of the water absorption value (WAV) and the water retention value (WRV) all samples were incubated in a loading medium for 2 h. Afterwards, samples were either directly air dried up to a constant weight (WAV) or centrifuged before complete drying (WRV) (Fig. 6). The WAV was calculated as the percentage ratio between the dry and the wet weight of the BNC and represents the amount of water which was included in the BNC network structure. Native BNC showed a high WAV with almost 7300% whereas the WAV was reduced to 4500% as reason of the integration of octenidine into the BNC fleece. A further decrease to 1000–1500% and 440–740% (Fig. 6) was obtained for the Poloxamer CMC and CGC samples, respectively. The incorporation of octenidine and octenidine/Poloxamers influences the WAV and WRV, accordingly. It is generally described in the literature

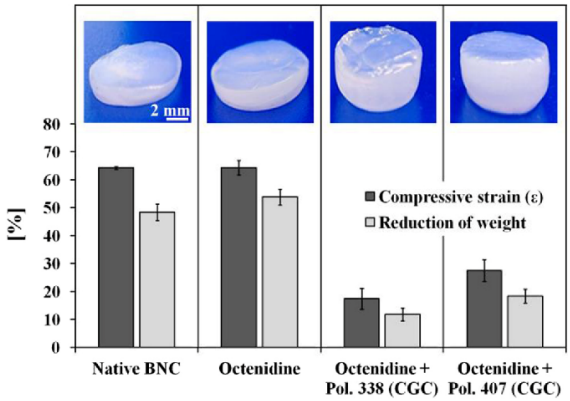

Fig. 5. Reduction of weight and compressive strain (ε) of native BNC compared to fleeces after loading for 48 h with octenidine solution or octenidine/Poloxamer 338 and 407 in concentrations above the critical gel concentration. Samples were burden in perpendicular direction for 10 min at 32 °C using a test weight of 400 g. Results are expressed as mean of 5 BNC fleeces ± SD and as photographs of BNC after compression.

that the impregnation of a secondary component into the BNC fiber network results in a filling of the pores and the formation of a more compact structure with denser fibril disposition (due to effects on the hydrogen bridge bonds), and therefore in a reduced pore volume and surface area. This fiber reorganization reduces the available space and amount of trapping sites for penetrating water molecules [49]. The water of the native BNC was replaced by the additives which remained in the BNC also after drying and resulted in a decrease of the WAV with increasing concentration of the additives. This is in line with reports in the literature [50] where BNC composites showed a lower WAV in comparison to native fleeces.

The WRV represents the behavior of BNC under the influence of mechanical pressure, which was simulated by centrifugation (Fig. 6). Native and octenidine loaded BNC exhibited a comparable WRV of approx. 1150% which is in accordance to data presented in the literature [21]. Similar to the WAV results also the WRV decreased with increasing Poloxamer concentration and Poloxamer 338 CMC and CGC samples showed higher values than the corresponding sample types of Poloxamer 407.

Conclusively, the lower compressibility of the hybrid systems improved the applicability of BNC as bioactive wound dressings without losing the excellent adhesion behavior of the dressing following the limp contours and even irregular skin surfaces. The reduction of the WAV may compromise the balance between liquid absorption and donation typical for a native BNC wound dressing. Therefore, further tests have to be performed in order to find the optimum between moisture donation effects, absorption capacity, pressure stability and drug release behavior in dependency from a specific application in wound management (e.g. treatment of acute, chronic, dry or exuding wounds) and phase of wound healing.

3.5. Biocompatibility testing of Poloxamer/BNC in a shell-less hen's egg test (HET-CAV)

To simulate the *in vivo* application as wound dressings more closely, BNC fleeces with and without Poloxamers were tested in an *ex ovo* hen's egg model regarding their biocompatibility in local administrations (Fig. 7a). Fertilized eggs are widely used for the toxicological testing of the irritative potential of drugs, chemicals and cosmetics with the advantage that they do not represent an animal model and do not require ethical permission [51,52]. In 2006 the US Food and Drug Administration (FDA) gave the permission to use the classical HET-CAM (hen's egg test on chorion allantois membrane) as an alternative preclinical test method for products to treat acute and chronic ulcers and wounds [53]. In the present *ex ovo* test, after 72 h pre-incubation egg content was transferred into a Petri dish and the test items were applied directly to the chick area vasculosa to determine their irritation potential by visual inspection regarding vascular lysis, thrombotic events, hemorrhage, and stop of the embryonal heart beat over 1, 2, 4 and 8 h. The adverse events were selected according to the recommendations of ICCVAM for the HET-CAM [51]. Only Poloxamer loaded BNC without octenidine was tested to exclude any cross-reaction with the effects of the antiseptic octenidine as observed in preliminary experiments (data not shown). Correspondingly, Marquardt et al. [54] reported a severe CAM irritation already after short-term applications of 1% octenidine.

Fig. 7b shows an overview of the adverse events caused by the different Poloxamer/BNC formulations in comparison to the controls up to 8 h. The local administration of the negative control (Ringer's solution pH 7.0) did not show any changes over up to 8 h. Acceptable concurrent negative control ranges based on historical data ranged between 0–1/10 eggs. In contrast, for the positive control hemorrhages and vascular lysis followed by the death of 20% of the embryos could be observed. Native BNC was found to be highly compatible with negligible hemorrhage in only 1/5 eggs after 8 h representing baseline conditions. All Poloxamer loaded BNC CMC samples gave comparable results with no (Poloxamer

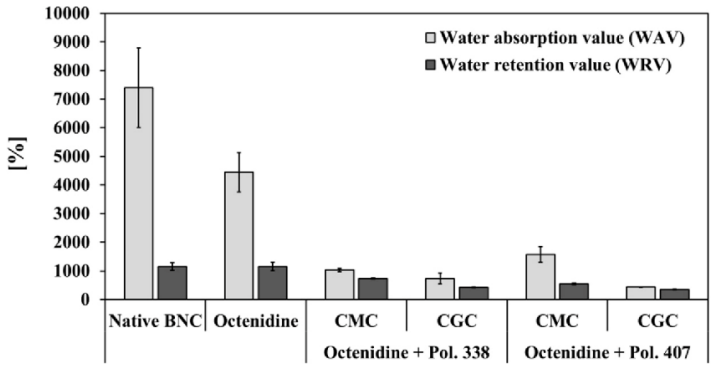

Fig. 6. Water absorption (WAV) and water retention values (WRV) of native BNC in comparison to octenidine loaded BNC fleeces with and without Poloxamers 338 and 407 (mean ± SD, $n = 4$). The concentration of Poloxamers was either above the critical micelle or critical gel concentration.

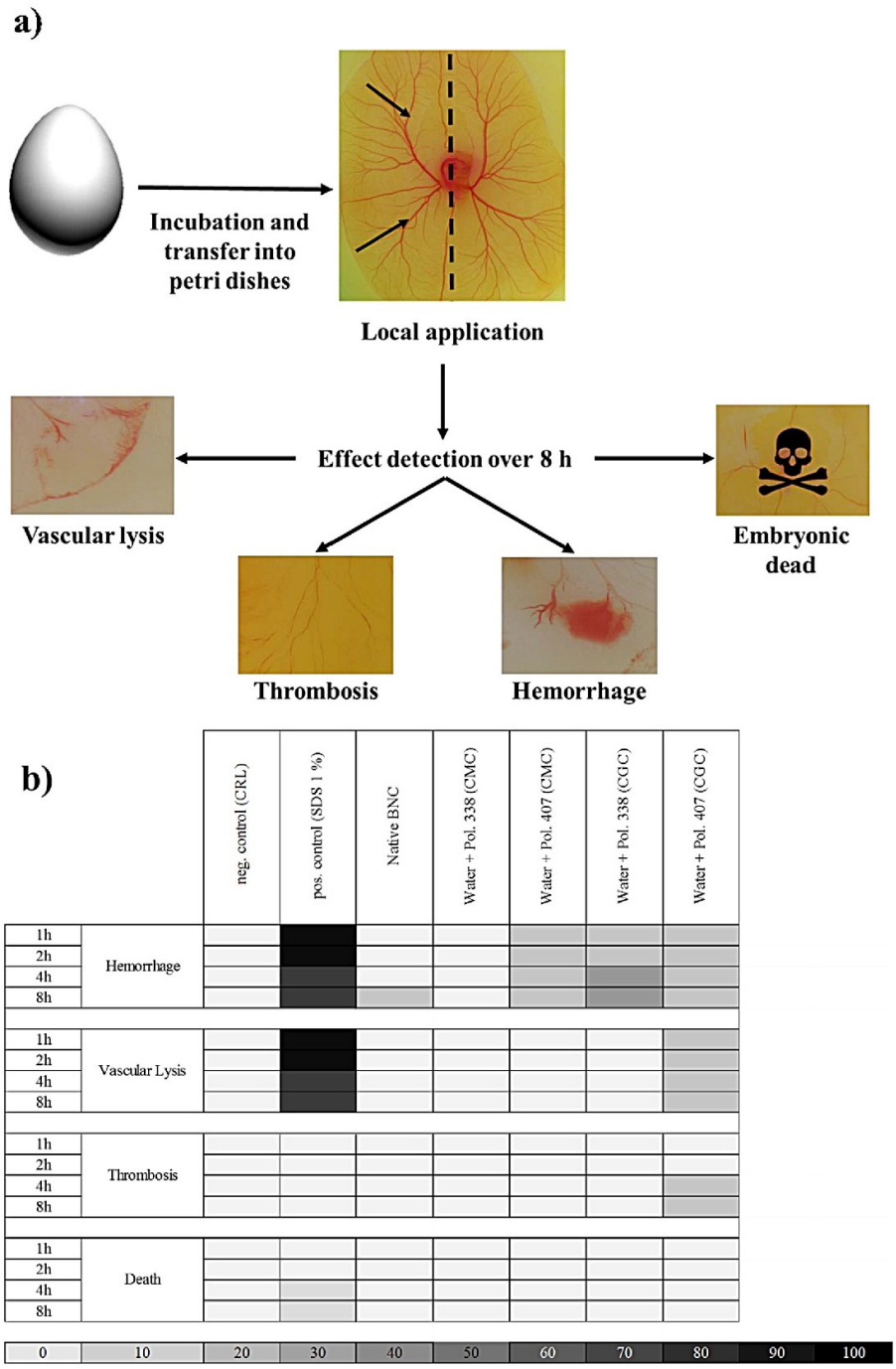

Fig. 7. Determination of the biocompatibility of the BNC fleeces using an *ex ovo* hen's egg model. (a) Schematic presentation of the experimental setup. Native BNC and BNC loaded with Poloxamers 338 and 407 were applied locally to the CAV and toxic effects were detected up to 8 h. (b) Clustergram showing the time-dependent toxic effects of locally applied BNC loaded with water, Poloxamer 338 and Poloxamer 407 (both as CMC and CGC samples). Each locally applied sample was presented in a column. The number of the affected eggs is represented proportionally by the intensity of the color. All experiments were run with n = 5 and repeated once.

338) or only one (Poloxamer 407) egg demonstrating hemorrhage. For the CGC samples supplemented with higher Poloxamer concentrations slight effects could be detected. Whereas Poloxamer 407 (CGC) induced only in one egg hemorrhage, vascular lysis and thrombosis, the Poloxamer 338 loaded BNC displayed in 1–2 eggs hemorrhages. Conclusively, a high tissue compatibility could be confirmed for the combination of BNC and Poloxamers by these experiments. BNC alone can be generally considered as

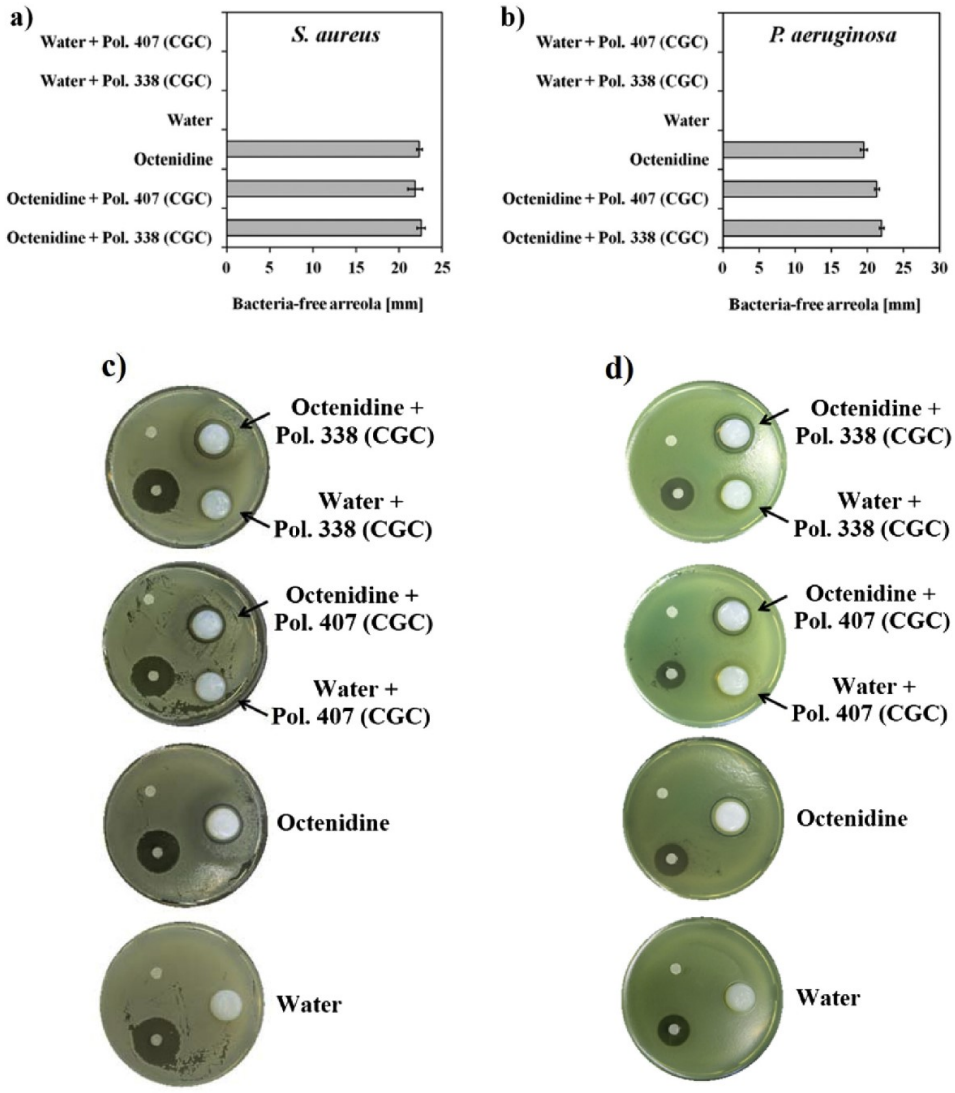

Fig. 8. Determination of the antibacterial activity of BNC fleeces using an agar diffusion test against *S. aureus* (a and c) and *P. aeruginosa* (b and d) after loading of BNC with water, octenidine, and water or octenidine containing Poloxamers 338 and 407 in concentrations above the critical gel concentration. Results are presented as the diameter of the bacteria-free arreola (a and b, mean ± SD, $n = 5$) and as photographs of the agar plates after incubation for 24 h at 35 °C. Pure filter paper disks and filter disks treated with kanamycin sulfate (*S. aureus*) or gentamicin sulfate (*P. aeruginosa*) were used as negative (left, top) and positive (left, bottom) controls, respectively.

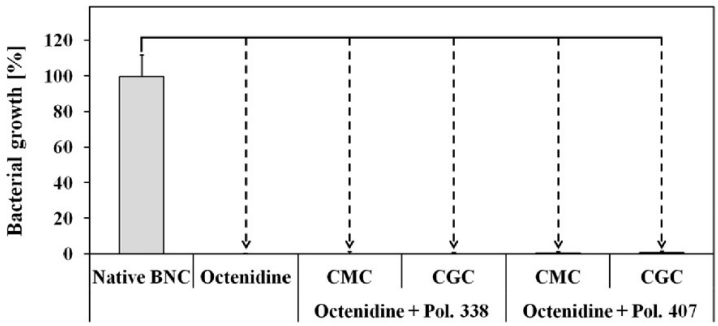

Fig. 9. Determination of the antibacterial activity against *S. aureus* of extracts of octenidine loaded BNC with and without addition of the Poloxamers 338 and 407 in concentrations above the critical micelle or critical gel concentration using a LIVE/DEAD® BacLight™ bacteria viability assay. Results (mean of 3 fleeces ± SD) are expressed as reduction of bacterial growth compared to extracts of native BNC.

broadly biocompatible invoking only moderate (if any) foreign body response *in vitro* and *in vivo* [55] Comparable compatibility during skin application has been confirmed in many clinical trials [56].

3.6. Antimicrobial activity of loaded BNC fleeces

The antibacterial activity of the loaded BNC samples was investigated *in vitro* by the agarose inhibition zone test and the LIVE/DEAD® BacLight™ bacterial viability assay to distinguish and quantify viable and dead bacteria. *Staphylococcus aureus* and *Pseudomonas aeruginosa* were selected as Gram-negative and Gram-positive bacterial model strains with the highest occurrence in acute and chronic wound infections [57].

Agar diffusion tests were carried out according to the Clinical and Laboratory Standards Institute. The antimicrobial activity was qualitatively evaluated by the formation of an inhibition zone around the loaded BNC samples after 24 h at 35 °C. The results of the agar diffusion tests are shown in Fig. 8. Pure BNC and BNC loaded with Poloxamers behaved similar as the negative control with absence of an inhibition zone, i.e. no antimicrobial effect *per se* as described previously [12]. The positive controls confirmed the validity of the assays and exposed inhibition zones with diameters of about 24 mm and 17 mm for kanamycin sulfate (*S. aureus*) and gentamycin sulfate (*P. aeruginosa*), respectively, that were within the limits of the CLSI guideline. Octenidine as well as octenidine/Poloxamer 338 and 407 loaded BNC samples showed comparable zones with no growth of bacteria in the range of 22–23 mm for *S. aureus* and 20–22 mm for *P. aeruginosa* (Fig. 8). As the CGC samples exhibited the slowest drug release especially for Poloxamer 407, only these sample types were used as a worst case scenario within this test. Repeating the tests over 8 days resulted in comparable data with an increase of the bacteria-free arreola for *S. aureus* and *P. aeruginosa* compared to 24 h (data not shown) demonstrating that the drug release systems were still antimicrobially active. Taking the results together, they confirmed that octenidine is released from the Poloxamer loaded BNC without loss of its antimicrobial activity.

To strengthen the relevance of the outcome, a quantitative test, the two-color fluorescent BacLight™ kit was additionally used to selectively stain viable and dead cells of *S. aureus*. It contains the two nucleic acid dyes SYTO 9, a green fluorescent dye that penetrates all cell membranes, and propidium iodide (PI), a red-fluorescent dye that transfers only damaged cell membranes and intercalates into DNA [58]. Integrated fluorescence emission intensities of suspensions of various proportions of living and isopropyl alcohol killed bacteria were measured and the green/red fluorescent ratios calculated for each proportion of live/dead bacteria. In preliminary experiments, for all samples an interaction of octenidine and/or the Poloxamers with the measurements could be excluded using serial dilutions of all components (data not shown). Fig. 9 shows the relative viability of the bacterial suspension after treatment with extracts of the different BNC samples formulated under optimized conditions. As a negative growth control, bacteria treated only with 0.9% NaCl were used to determine the maximum growth values that were set to 100%. Octenidine loaded BNC as well as all CMC and CGC BNC samples with Poloxamers 338 and 407 reduced the viability of the bacteria to values less than 1% demonstrating the release of octenidine and the antimicrobial activity of the drug after release.

4. Conclusion

In the last 10 years, many attempts have been made to realize the long-term delivery of drugs from BNC as carrier system. In the present study, an 8 day release of the antiseptic octenidine could be obtained by incorporation of Poloxamers into the three-dimensional BNC network. Release kinetics could be controlled by the type and the concentration of the selected Poloxamer. Additionally, the *in situ* formation of the Poloxamer gels in the BNC influenced the water binding characteristics and improved the mechanical stability which might be advantageous for compressed dressings. From the view of wound management in clinics, treatment costs can be reduced and patient compliance improved due to less frequent wound dressing changes. In the process of further development, e.g. storage stability, *in vivo* studies as well as a scale-up with different fleece dimensions will follow. In further experiments, other types of Poloxamers and combinations thereof or e.g. combinations with chitosan, poly(acrylic acid) or cyclodextrin will be taken into consideration [59–61]. Furthermore, different media will be tested as it is known that Poloxamer gelation and viscosity is highly dependent on the surrounding medium [62]. Further excipients such as Brij gave comparable effects as Poloxamers and are actually under investigation in more detail.

Acknowledgements

The authors would like to thank Ramona Brabetz and Elena Pfaff for their excellent technical assistance. We gratefully acknowledge the FAZIT Foundation, Gemeinnützige Verlagsgesellschaft mbH (S. M.) for financial support.

References

[1] D. Klemm, D. Schumann, F. Kramer, N. Heßler, M. Hornung, H.-P. Schmauder, S. Marsch, Nanocelluloses as innovative polymers in research and application, in: D. Klemm (Ed.), Polysaccharides II, Springer, Berlin, Heidelberg, Germany, 2006, pp. 49–96.
[2] D. Klemm, B. Heublein, H.P. Fink, A. Bohn, Cellulose: fascinating biopolymer and sustainable raw material, Angew. Chem. 44 (2005) 3358–3393.
[3] A.F. Jozala, L.C. de Lencastre-Novaes, A.M. Lopes, V. de Carvalho Santos-Ebinuma, P.G. Mazzola, A. Pessoa-Jr, D. Grotto, M. Gerenutti, M.V. Chaud, Bacterial nanocellulose production and application: a 10-year overview, Appl. Microbiol. Biotechnol. 100 (2016) 2063–2072.
[4] S. Moritz, C. Wiegand, F. Wesarg, N. Hessler, F.A. Müller, D. Kralisch, U.-C. Hipler, D. Fischer, Active wound dressings based on bacterial nanocellulose as drug delivery system for octenidine, Int. J. Pharm. 471 (2014) 45–55.
[5] E. Trovatti, C.S.R. Freire, P.C. Pinto, I.F. Almeida, P. Costa, A.J.D. Silvestre, C.P. Neto, C. Rosado, Bacterial cellulose membranes applied in topical and transdermal delivery of lidocaine hydrochloride and ibuprofen: *in vitro* diffusion studies, Int. J. Pharm. 435 (2012) 83–87.
[6] C. Wiegand, S. Moritz, N. Hessler, D. Kralisch, F. Wesarg, F.A. Müller, D. Fischer, U.-C. Hipler, Antimicrobial functionalization of bacterial nanocellulose by loading with polihexanide and povidone-iodine, J. Mater. Sci. - Mater. Med. 26 (2015) 1–14.
[7] F.K. Andrade, N. Alexandre, I. Amorim, F. Gartner, A.C. Maurício, A.L. Luís, M. Gama, Studies on the biocompatibility of bacterial cellulose, J. Bioactive Compat. Pol. 28 (2013) 97–112.
[8] A. Müller, Z. Ni, N. Hessler, F. Wesarg, F.A. Müller, D. Kralisch, D. Fischer, The biopolymer bacterial nanocellulose as drug delivery system: investigation of drug loading and release using the model protein albumin, J. Pharm. Sci. 102 (2013) 579–592.
[9] Y. Numata, L. Mazzarino, R. Borsali, A slow-release system of bacterial cellulose gel and nanoparticles for hydrophobic active ingredients, Int. J. Pharm. 486 (2015) 217–225.
[10] P. Pourali, B. Yahyaei, H. Ajoudanifar, R. Taheri, H. Alavi, A. Hoseini, Impregnation of the bacterial cellulose membrane with biologically produced silver nanoparticles, Curr. Microbiol. 69 (2014) 785–793.
[11] E. Trovatti, N.H. Silva, I.F. Duarte, C.F. Rosado, I.F. Almeida, P. Costa, C.S. Freire, A.J. Silvestre, C.P. Neto, Biocellulose membranes as supports for dermal release of lidocaine, Biomacromolecules 12 (2011) 4162–4168.
[12] S. Berndt, F. Wesarg, C. Wiegand, D. Kralisch, F. Müller, Antimicrobial porous hybrids consisting of bacterial nanocellulose and silver nanoparticles, Cellulose 20 (2013) 771–783.
[13] G. Dumortier, J. Grossiord, F. Agnely, J. Chaumeil, A review of Poloxamer 407 pharmaceutical and pharmacological characteristics, Pharm. Res. 23 (2006) 2709–2728.
[14] A.V. Kabanov, E.V. Batrakova, V.Y. Alakhov, Pluronic® block copolymers as novel polymer therapeutics for drug and gene delivery, J. Control. Release 82 (2002) 189–212.

[15] J.R. Lopes, W. Loh, Investigation of self-assembly and micelle polarity for a wide range of ethylene oxide–propylene oxide–ethylene oxide block copolymers in water, Langmuir 14 (1998) 750–756.
[16] V. Saxena, M.D. Hussain, Poloxamer 407/TPGS mixed micelles for delivery of gambogic acid to breast and multidrug-resistant cancer, Int. J. Nanomed. 7 (2012) 713–721.
[17] Q.F. Dang, J.Q. Yan, J.J. Li, X.J. Cheng, C.S. Liu, X.G. Chen, Controlled gelation temperature, pore diameter and degradation of a highly porous chitosan-based hydrogel, Carbohydr. Polym. 83 (2011) 171–178.
[18] J.C. Gilbert, J.L. Richardson, M.C. Davies, K.J. Palin, J. Hadgraft, The effect of solutes and polymers on the gelation properties of Pluronic F-127 solutions for controlled drug delivery, J. Control. Release 5 (1987) 113–118.
[19] P.L. Ritger, N.A. Peppas, A simple equation for description of solute release II. Fickian and anomalous release from swellable devices, J. Control. Release 5 (1987) 37–42.
[20] Y. Mao, M.J. Thompson, Q. Wang, E.W. Tsai, Quantitation of Poloxamers in pharmaceutical formulations using size exclusion chromatography and colorimetric methods, J. Pharm. Biomed. Anal. 35 (2004) 1127–1142.
[21] D. Kralisch, N. Hessler, D. Klemm, R. Erdmann, W. Schmidt, White biotechnology for cellulose manufacturing – the HoLiR concept, Biotechnol. Bioeng. 105 (2010) 740–747.
[22] D. Klemm, B. Philipp, T. Heinze, U. Heinze, W. Wagenknecht, General considerations on structure and reactivity of cellulose: section 2.1–2.1.4, in: Comprehensive Cellulose Chemistry, Wiley Online Library, 2004, pp. 9–29.
[23] R. Müller, O. Stranik, F. Schlenk, S. Werner, D. Malsch, D. Fischer, W. Fritzsche, Optical detection of nanoparticle agglomeration in a living system under the influence of a magnetic field, J. Magn. Magn. Mater. 380 (2015) 61–65.
[24] V. Hamburger, H.L. Hamilton, A series of normal stages in the development of the chick embryo, J. Morphol. 88 (1951) 49–92.
[25] C. Wiegand, M. Abel, P. Ruth, U.-C. Hipler, HaCaT keratinocytes in co-culture with *Staphylococcus aureus* can be protected from bacterial damage by polihexanide, Wound Repair Regen. 17 (2009) 730–738.
[26] CLSI VET01-A4, Performance Standards for Antimicrobial Disk and Dilution Susceptibility Tests for Bacteria Isolated From Animals, Approved standard - fourth ed., Clinical and Laboratory Standards Institute, 2013.
[27] E. Ricci, L. Lunardi, D. Nanclares, J. Marchetti, Sustained release of lidocaine from Poloxamer 407 gels, Int. J. Pharm. 288 (2005) 235–244.
[28] P. Alexandridis, J.F. Holzwarth, T.A. Hatton, Micellization of poly(ethylene oxide)-poly(propylene oxide)-poly(ethylene oxide) triblock copolymers in aqueous solutions: thermodynamics of copolymer association, Macromolecules 27 (1994) 2414–2425.
[29] A.Von der Höh, C. Abels, U. Knie, Gel for Treating Wounds, EP 1982696 B1, 2010.
[30] Z. Sezgin, N. Yuksel, T. Baykara, Preparation and characterization of polymeric micelles for solubilization of poorly soluble anticancer drugs, Eur. J. Pharm. Biopharm. 64 (2006) 261–268.
[31] P.K. Sharma, S.R. Bhatia, Effect of anti-inflammatories on Pluronic F127: micellar assembly, gelation and partitioning, Int. J. Pharm. 278 (2004) 361–377.
[32] A. Kelarakis, E.P. Giannelis, Nafion as cosurfactant: solubilization of nafion in water in the presence of Pluronics, Langmuir 27 (2011) 554–560.
[33] C. Ju, J. Sun, P. Zi, X. Jin, C. Zhang, Thermosensitive micelles-hydrogel hybrid system based on Poloxamer 407 for localized delivery of paclitaxel, J. Pharm. Sci. 102 (2013) 2707–2717.
[34] R. Ivanova, P. Alexandridis, B. Lindman, Interaction of Poloxamer block copolymers with cosolvents and surfactants, Colloids Surf. A 183–185 (2001) 41–53.
[35] P. Alexandridis, L. Yang, SANS investigation of polyether block copolymer micelle structure in mixed solvents of water and formamide, ethanol or glycerol, Macromolecules 33 (2000) 5574–5587.
[36] C.W. Cho, S.C. Shin, I.J. Oh, Thermorheologic properties of aqueous solutions and gels of Poloxamer 407, Drug Dev. Ind. Pharm. 23 (1997) 1227–1232.
[37] D.G. White, R.M. Brown Jr, Prospects for the commercialization of the biosynthesis of microbial cellulose, Cellulose and Wood-Chemistry and Technology, vol. 573, Wiley, New York, 1989, pp. 573–590.
[38] A. Müller, F. Wesarg, N. Hessler, F.A. Müller, D. Kralisch, D. Fischer, Loading of bacterial nanocellulose hydrogels with proteins using a high-speed technique, Carbohydr. Polym. 106 (2014) 410–413.
[39] R.-D. Pavaloiu, A. Stoica, M. Stroescu, T. Dobre, Controlled release of amoxicillin from bacterial cellulose membranes, Open Chem. 12 (2014) 962–967.
[40] Z. Cai, J. Kim, Preparation and characterization of novel bacterial cellulose/gelatin scaffold for tissue regeneration using bacterial cellulose hydrogel, J. Nanotechnol. Eng. Med. 1 (2010), 021002/021001-021002/021006.
[41] E. Haimer, M. Wendland, K. Schlufter, K. Frankenfeld, P. Miethe, A. Potthast, T. Rosenau, F. Liebner, Loading of bacterial cellulose aerogels with bioactive compounds by antisolvent precipitation with supercritical carbon dioxide, Macromole. Symp. 294 (2010) 64–74.
[42] B.C. Anderson, N.K. Pandit, S.K. Mallapragada, Understanding drug release from poly(ethylene oxide)-b-poly(propylene oxide)-b-poly(ethylene oxide) gels, J. Control. Release 70 (2001) 157–167.
[43] F. Nasir, Z. Iqbal, J.A. Khan, A. Khan, F. Khuda, L. Ahmad, A. Khan, A. Khan, A. Dayoo, Roohullah, Development and evaluation of diclofenac sodium thermorevesible subcutaneous drug delivery system, Int. J. Pharm. 439 (2012) 120–126.
[44] J.C. Gilbert, J. Hadgraft, A. Bye, L.G. Brookes, Drug release from Pluronic F-127 gels, Int. J. Pharm. 32 (1986) 223–228.
[45] L. Zhang, D.L. Parsons, C. Navarre, U.B. Kompella, Development and *in vitro* evaluation of sustained release Poloxamer 407 (P407) gel formulations of ceftiofur, J. Control. Release 85 (2002) 73–81.
[46] E. Ricci, M. Bentley, M. Farah, R. Bretas, J. Marchetti, Rheological characterization of Poloxamer 407 lidocaine hydrochloride gels, Eur. J. Pharm. Sci. 17 (2002) 161–167.
[47] A. Nakayama, A. Kakugo, J.P. Gong, Y. Osada, M. Takai, T. Erata, S. Kawano, High mechanical strength double-network hydrogel with bacterial cellulose, Adv. Funct. Mater. 14 (2004) 1124–1128.
[48] Y. Hagiwara, A. Putra, A. Kakugo, H. Furukawa, J.P. Gong, Ligament-like tough double-network hydrogel based on bacterial cellulose, Cellulose 17 (2010) 93–101.
[49] I. Sulaeva, U. Henniges, T. Rosenau, A. Potthast, Bacterial cellulose as a material for wound treatment: Properties and modifications. A review, Biotechnol. Adv. (2015).
[50] F. Kramer, D. Klemm, D. Schumann, N. Hessler, F. Wesarg, W. Fried, D. Stadermann, Nanocellulose polymer composites as innovative pool for (bio)material development, Macromol. Symp. 244 (2006) 136–148.
[51] ICCVAM Test Method Evaluation Report: Appendix G-ICCVAM Recommended HET-CAM Test Method Protocol, 2006.
[52] A. Vargas, M. Zeisser-Labouebe, N. Lange, R. Gurny, F. Delie, The chick embryo and its chorioallantoic membrane (CAM) for the *in vivo* evaluation of drug delivery systems, Adv. Drug Deliv. Rev. 59 (2007) 1162–1176.
[53] Guidance for Industry: Chronic Cutaneous Ulcer and Burn Wounds – Developing Products for Treatment, U.S. Department of Health and Human Services – Food and Drug Administration, 2006.
[54] C. Marquardt, E. Matuschek, E. Bölke, P.A. Gerber, M. Peiper, J.V. Seydlitz-Kurzbach, B.A. Buhren, M. van Griensven, W. Budach, M. Hassan, G. Kukova, R. Mota, D. Höfer, K. Orth, W. Fleischmann, Evaluation of the tissue toxicity of antiseptics by the hen's egg test on the chorioallantoic membrane (HET-CAM), Eur. J. Med. Res. 15 (2010) 204–209.
[55] B. Jeong, Y.H. Bae, D.S. Lee, S.W. Kim, Biodegradable block-copolymers as injectable drug delivery systems, Nature 388 (1997) 860–862.
[56] S. Napavichayanun, R. Yamdech, P. Aramwit, The safety and efficacy of bacterial nanocellulose wound dressing incorporating sericin and polyhexamethylene biguanide: *in vitro*, *in vivo* and clinical studies, Arch. Dermatol. Res. 308 (2016) 123–132.
[57] P.G. Bowler, B.I. Duerden, D.G. Armstrong, Wound microbiology and associated approaches to wound management, Clin. Microbiol. Rev. 14 (2001) 244–269.
[58] S. Stocks, Mechanism and use of the commercially available viability stain, BacLight, Cytometry Part A 61 (2004) 189–195.
[59] D.S. Jones, M.L. Bruschi, O. de Freitas, M.P.D. Gremião, E.H.G. Lara, G.P. Andrews, Rheological, mechanical and mucoadhesive properties of thermoresponsive, bioadhesive binary mixtures composed of Poloxamer 407 and carbopol 974P designed as platforms for implantable drug delivery systems for use in the oral cavity, Int. J. Pharm. 372 (2009) 49–58.
[60] T. Gratieri, G.M. Gelfuso, E.M. Rocha, V.H. Sarmento, O. de Freitas, R.F.V. Lopez, A Poloxamer/chitosan in situ forming gel with prolonged retention time for ocular delivery, Eur. J. Pharm. Biopharm. 75 (2010) 186–193.
[61] G. Bonacucina, M. Spina, M. Misici-Falzi, M. Cespi, S. Pucciarelli, M. Angeletti, G.F. Palmieri, Effect of hydroxypropyl β-cyclodextrin on the self-assembling and thermogelation properties of Poloxamer 407, Eur. J. Pharm. Sci. 32 (2007) 115–122.
[62] K. Edsman, J. Carlfors, R. Petersson, Rheological evaluation of Poloxamer as an *in situ* gel for ophthalmic use, Eur. J. Pharm. Sci. 6 (1998) 105–112.

5. Discussion

The natural biopolymer bacterial nanocellulose is intensively investigated and developed as a novel biomaterial for a variety of applications in life science. The biomedical field's interest in BNC has grown over the previous decades due to the unique 3D-nanostructure, enormous surface area, and its outstanding biocompatibility. BNC has been used utilized in scaffolds (280, 281) and tissue engineering (282, 283), wound dressings (5, 87, 163), drug delivery systems (110, 133, 284), cosmetics (80), and various other applications (70). BNC is also used as a drug delivery system by incorporating small molecules (149, 173, 177) and macromolecular substances (54, 152, 178). However, a clear trend is observed with more than 80% of the active pharmaceutical ingredients (API) used in combination with BNC targeting to act as a drug delivery system, being hydrophilic with a log P value of 4 or below (110). Due to the hydrophilic character of BNC and the high water content of more than 90%, loading of lipophilic drugs is considered challenging with the need for further development. This is reflected in the limited number of publications describing lipophilic molecules being loaded into BNC without chemical modifications (110). On the other hand, several concepts have been described in the literature to overcome the hydrophilicity of BNC, such as modification of drug solubility using different approaches (148, 195, 207, 209) or the chemical modification of BNC (86, 184). However, those modification approaches are restricted due to either the limited number of compatible drugs or the changes the impose upon the unique properties of BNC (97, 184, 211).

Although a higher number of lipophilic drugs have been developed in preclinical research (203), combining and the using them with BNC is limited due to the high hydrophilicity of the BNC. The presented work focused on the investigation of BNC as a drug delivery system for the controlled release of lipophilic drugs targeting dermal applications. The utilized strategy is considered as an alternative method to the previously mentioned modification aspects. Preferentially, *post*-loading

techniques were selected since they are less stressful for drugs and additives and are easy to perform (54, 133, 147). Additionally, the reproducibility was higher than for *in situ* loading since the growth of cellulose producing bacteria can be negatively affected by drugs or additives leading to inhomogeneous BNC network and thus uncontrolled loading and release (148, 166).

In this work, BNC was biosynthesized by static cultivation of *K. xylinus* (DSM 14666) in Hestrin-Schramm medium at 28 °C in 24 well-plates (54, 97, 152). The choice of the cultivation type and the cellulose-producing bacteria was based on the facts that the BNC produced by *K. xylinus* is well-established and extensively characterized for use as a drug delivery system (97, 110). The produced BNC was characterized by high mechanical stability, high crystallinity, enormous surface area which facilitate the uptake of a large amount of drug (80, 107, 285). The biosynthesis of BNC under static cultivation conditions was shown to be a reproducible and robust process (23, 286), which yields a white gelatinous material at the air-medium interface. The BNC was purified by alkaline treatment followed by washings and an autoclaving step, promoting a loss of heat-sensitive compounds, such as chemicals and bacterial residues like bioactive compounds and lipopolysaccharides which is an important aspect regarding the biocompatibility of BNC (44, 83, 287).

The optimization of loading and release for lipophilic drugs was investigated with regard to several aspects: utilized carrier system, loading technique and efficiency, release behavior, physicochemical characteristics, and biocompatibility of the loaded BNC. Three drugs were chosen as representatives of small molecules lipophilic drugs with a log P values in the range of 7-10: Coenzyme Q10 (CoQ10), *Boswellia serrata*-extract, and octenidine. They are considered well-established compounds for dermal applications as antioxidant, anti-inflammation, and antiseptic agent, respectively (254, 268, 270). Several advantages could be obtained by the combination of BNC and these drugs for a local dermal application with tailor-made release

profiles. These strategies aimed to have a controllable release for acute and long-term applications which reduces the number of applied doses for a given treatment plan, the frequency of dosage, and reduce side effects of the drugs and increases patient compliance.

To incorporate the lipophilic drugs into the hydrophilic BNC matrix, five different nanostructured carrier systems were selected. The choice of the carrier systems was based on a major property; the carrier systems were characterized as a disperse multiphase system with an aqueous outer phase enabling compatibility with the hydrophilic BNC environment. The first two investigated systems were single O/W nanoemulsions and double W/O/W nanoemulsions. Both nanoemulsions were composed of natural components with saturated oils and can be considered tolerable and skin friendly, since the surfactants and co-surfactants ratio when compared to typical nanoemulsions formulations is 3-folds lower (288, 289). The third system was a micellar system represented by two micellar systems of two different Poloxamers (Poloxamer 338 and 407, separately). Poloxamer micelles were formed at concentration above the CMC of 10% and 5% for Poloxamer 338 and 407, respectively. The forth system was a Poloxamer gel system represented by two different gels consisted of the Poloxamers 338 and 407 at a concentration of 22% and 18.5%, respectively. The thixotropic Poloxamer gels were formed at higher concentrations and temperatures and have a similar composition to the Poloxamer micelles since the gel are consisting of a large population of micelles (244, 290). Finally, the fifth investigated carrier system were liposomes, as a reference drug delivery system, composed of 10% Lipoid S75®.

CoQ10 and boswellic acids were formulated with O/W and W/O/W nanoemulsions by the top-down high-pressure homogenization and octenidine Poloxamer micelles and gels were prepared by dissolving the Poloxamer into octenidine stock solution under constant stirring at 4 °C in a temperature-controlled refrigerator to obtain the micellar and gel systems. The obtained drug loaded carrier systems have been physiochemically characterized with regard to the hydrodynamic

size as summarized in Table 3. All obtained carrier systems were characterized with a hydrodynamic size in the nanoscale with neutral to negative zeta potential values except for the Poloxamer gels which have a macrostructure (291). The octenidine cationic charge was masked by Poloxamer micelles to reveal a non-charged surface by the zeta potential measurements (292). Additionally, O/W and WO/W nanoemulsions and liposomes formulations demonstrated a stability over 30 days in three different temperatures: 4 °C as a storage temperature, room temperature for handling, and 37 °C temperature as body temperature.

Table 3. An overview of the hydrodynamic size and zeta potential of the prepared drug loaded carrier systems

Carrier system	**Hydrodynamic size (nm)**	**Zeta potential (mV)**
Poloxamer 338 + octenidine	9.8	1.78
Poloxamer 407 + octenidine	10.6	4.25
Liposomes + CoQ10	98.0	−62
O/W nanoemulsion + CoQ10	114.5	−68
W/O/W nanoemulsion + CoQ10	94.1	−72
O/W nanoemulsion + boswellic acids	149	−72
W/O/W nanoemulsion + boswellic acids	113	−80

Moreover, the O/W and O/W/O nanoemulsions showed a dynamic viscosity measured at shear rate of 100/s and a temperature of 20 °C of 6.67 and 3.92 mPa*s, respectively. The octenidine loaded Poloxamer gels demonstrated a viscosity at 20 °C with 579.64 and 487.53 mPa*s for Poloxamer 338 and 407 gels, respectively. And a lower viscosity at 4 °C of 116.85 and 56.65 mPa*s for Poloxamer 338 and 407 gels, respectively. The obtained viscosity values could be

explained by the fact that Poloxamer gels are thermoreversible gels (246).

To summarize the results of the publications contributed in this work (293-295), several major aspects are going to be highlighted in the following sections such as the loading and release behavior, physiochemical properties presented by water binding capacity and mechanical stability, biocompatibility, bioactivity and penetration ability. The first aspect to be mentioned, is the loading efficiency. The incorporation of CoQ10 O/W and W/O/W nanoemulsions and liposomes formulations into the BNC 3D-nanofiber structure was performed by the submerse absorption technique over 48 hours on an orbital shaker (146, 166, 177). This process yielded a loading efficiency of CoQ10 into BNC of about 10%, which is related to the ratio between the BNC (1 mL) and the loading solution (10 mL). The obtained loading efficiency is comparable to the values reported in literature for hydrophilic molecules using the same loading technique at the same ratio (147, 152, 177). The formulation of CoQ10 with the O/W and W/O/W nanoemulsions and liposomes formulations followed by loading into BNC showed a homogenous drug distribution over the BNC network without recrystallization phenomena. This contrasts with the loading of CoQ10 after dissolving in 100% ethanol, which suffered from recrystallization that was noticed macroscopically. The obtained loading efficiency for CoQ10 could be obtained with other drugs, where *Boswellia serrata*-extract in combination with O/W and W/O/W nanoemulsions was loaded into BNC and showed comparable loading efficiencies. The obtained high loading efficiency by using O/W and W/O/W nanoemulsions was also shown by the use of other carrier systems as Poloxamers micellar and gel systems for the antiseptic octenidine. Although all investigated carrier systems have different physiochemical characteristics such as different structure, hydrodynamic size, and viscosity, a high loading efficiency of the three different drugs could be obtained. Thus, the key factor is the use of a suitable drug loaded carrier system when using the submerse loading technique.

Loading of the carrier system into the BNC nanostructure network is suggested to be related to a replacement process of the water inside the BNC. This process is promoted by diffusion and capillary forces of the carrier systems into the enormously large surface area of the hydrophilic network of BNC with a content of water up to 99% (296, 297). Furthermore, the flexibility and small hydrodynamic size of the chosen colloidal systems promoted integration into the BNC 3D-nanostructure network, which consists of randomly distributed cellulose nanofibers and interconnected pores with sizes up to 5 µm (45, 284).

All the previously discussed observations were studied with the widely used submerse absorption loading technique (146, 177, 298). Moreover, further *post*-modification loading techniques were investigated such as the non-specific adsorption (reswelling) of freeze-dried BNC with 750 µL of CoQ10 loaded carrier systems for 15 min (299) and injection of 125 µL of CoQ10 loaded carrier systems into BNC to form a core-shell system (54). Both loading techniques showed a fast and efficient loading of controlled amount of the lipophilic CoQ10 with 100% loading efficiency and no drug loss when compared to other loading techniques such as submerse absorption (177), boiling (148) or vortexing (147).

The impact of the incorporation of carrier systems on the properties of BNC was investigated during this work, with focus on water binding ability as well as mechanical and compression stability. These properties are important for the intended applications, such as dermal films (80) or wound dressing (53). In these applications, it is essential to have a material that is mechanically stable during handling and packaging, and which can absorb wound exudates while maintaining a moisturized wound environment, which facilitates a faster wound healing process (53). For wound management applications, it is recommended to create a balance between a moist wound environment (95) and a low volume of wound exudate, especially in chronic wounds since an excessive amount of exudate may result in separation of tissue layers and delay the healing process

(53, 300). Those properties are represented by the water binding capacity of BNC. In general, native BNC is characterized by a high water binding property as reported by Kralisch and colleagues (21). The incorporation of the carrier systems resulted in a decrease in water binding capacity in comparison to native BNC. However, this decrease is related to the fact that newly integrated carrier systems in the BNC structure would replace the trapped water in BNC and would fill the BNC pores (297, 301). The results for Poloxamer 407 based carrier systems (micellar and gel) demonstrated a good example of the correlation between the water binding capacity and the concentration of the new incorporated compound, where by increasing the concentration of Poloxamer from the micellar concentration to the gel concentration, the water binding capacity was decreased. However, the concentration of carrier systems was not the only factor which could impact the water binding capacity. The characterizations of the carrier systems demonstrated also and impact on the water binding capacity. Where the addition of the higher lipophilic nanoemulsions (O/W nanoemulsions) showed an elevated decrease of the water binding capacity in comparison to the hydrophilic nanoemulsions (W/O/W nanoemulsions) due to the higher lipophilicity of O/W nanoemulsions in comparison to W/O/W nanoemulsions. These findings were independent from the drug presence since similar behavior was observed for both drug loaded and empty carrier systems as well as when the drug was incorporated into the carrier system and the properties of the carrier system became more dominant (294). Several publications reported a change of the water binding capacity of native BNC depending on the type of the incorporated additives into BNC such as poly(ethylene glycol) and chitosan (97, 139, 302). Kingkaew and colleagues (302), investigated the effect of incorporating chitosan with different molecular weights of 141, 199, and 263 kDa. They reported a significant decrease of the water binding capacity by about 56 to 65% in comparison to native BNC.

Beside the water binding capacity, the mechanical stability of the of the newly developed BNC

with the carrier systems was investigated. The 3D-nanostructure of BNC was characterized by an exceptional mechanical stability, which is essential to ensuring the dimensional stability of BNC during packaging, unpacking, application on skin and fixation by a secondary dressing. Low mechanical stability could lead to the deformation of the BNC fleece or loss of the incorporated drug. However, typically native BNC shows a low compressive modulus perpendicular to the stratified direction but a mechanical anisotropy with a high tensile modulus along the fiber layer direction (303, 304). Nevertheless, the loading process and the loaded compound might have an impact on the BNC structure with either an increase or decrease on its mechanical stability (10, 149, 305, 306). This influence could be related to the interaction between the BNC fibers and the incorporated compound or to the high viscosity of the incorporated compound into BNC structure. For example, Urbina and colleagues introduced poly(lactic acid) into BNC which negatively impacted the mechanical stability of BNC (307). On the other hand, Almeida and colleagues (308) demonstrated an increase in the tensile strength from 271.9 MPa for the native BNC to 360.3 MPa for BNC samples incorporated with 1% of glycerin. In this work, BNC samples were tested by applying a weight of 400 g perpendicularly for 10 min and characterized regarding the change in weight and compressive strain (54). Although the integrated carrier system replaced the water in the BNC structure, the integration of liposome, nanoemulsions, and micelles did not show an impact on the mechanical stability of BNC. These findings were independent from the hydrophilic properties and the hydrodynamic size of the carrier systems. Furthermore, the combination of the BNC network and the higher viscos Poloxamer gels lead to a substantial improvement of the BNC compression stability, where the native BNC demonstrated a reduction of its weight by 65% the octenidine loaded Poloxamer gels showed only a reduction of about 18-28% and 12-18% of Poloxamer 407 and 338, respectively. The *in situ* gel formation of the Poloxamer gels inside the BNC network could be described as a secondary gel structure inside the BNC. Similar effects were

also reported in the literature for other compounds such as alginates, poly(acrylamide) and polysaccharide (113, 303). Additionally, the change of the loading technique demonstrated an impact on the compression stability. By comparing the compression stability values of samples loaded with the submerse loading technique *vs.* the re-swelling loading technique, a superior compression stability for the re-swelling samples was recorded. This could be related to the structural BNC changes during the freeze-drying process as discussed previously. Those results were correlated to the findings in the literature (285). Müller and colleagues (152) showed an increase of tensile strength for freeze-dried BNC samples loaded with albumin. Overall, the mechanical stability of BNC could be influenced by the loading technique along with the additives. This would give flexibility in the future for tailor-made BNC loaded with a lipophilic drug for dermal application.

Along with the previously mentioned aspects, the biocompatibility of native BNC and the effect of the added carrier system on its biocompatibility were investigated. Biocompatibility is essential for dermal application. This is to avoid irritative reactions and cytotoxicity for skin cells, allowing safe skin regeneration during the wound healing process (53). Native BNC was described as a material with an outstanding biocompatibility which has been proven in several *in vitro* and *in vivo* studies even after long-term of application as an implant (35, 54, 61, 309) and in dermal application (59, 82). However, the newly developed lipophilic drug delivery system must prove not only its quality and effectivity but also its biocompatibility according to paragraph § 1 of the German Medicinal Product Act (in German: Arzneimittelgesetz - AMG § 1). The biocompatibility of BNC with and without the carrier systems was investigated by the *ex ovo* hen's egg test at the chick area vasculosa (HET-CAV) (54, 295, 310, 311). This test model complies with the 3R concept of Russel and Burch (Replacement, Reduction, and Refinement) to avoid animal testing (312), where it allowed a reduction as well as refinement of animal testing (311). This test was considered closer

to the complex physiological situation more than the often-used *in vitro* cell culture experiments and can detect irritative reactions of the tested material and does not need authorization of the ethical council (313, 314). The Interagency Coordinating Committee on the Validation of Alternative Methods (ICCVAM) suggested HET-CAM (hen's egg test at the chorion allantois membrane) as an alternative for some animal experiment methods (Draize test: Rabbit eye irritation test) (313, 315, 316). Although HET-CAV and HET-CAM are comparable methods, the preparation complexity of using a partially opened egg by HET-CAM test was higher than by HET-CAV where the egg was transferred into petri dishes and direct local application was possible. In this work, BNC samples were applied locally directly on chick area vasculosa of 72 hours pre-incubated eggs after transferring the egg content into a Petri dich, and the adverse effects such as vascular lysis, aggregation, hemorrhage, and stop of heartbeat were visually inspected after 1, 2, 4, and 8 hours. Ringer's solution pH 7.0 or physiological saline were used as a negative control which did not show any irritation up to 8 hours. As a positive control a solution of 1% sodium dodecyl sulfate was used, which developed a hemorrhage with in the first 1-2 hours followed by vascular lysis and afterwards a stoppage in the heartbeat (311). Native BNC showed no irritations and could be considered a material with high biocompatibility and invokes no or only moderate responses *in vitro* and *in vivo*, which has been confirmed in several clinical trials for skin application (57, 317). Moreover, BNC loaded carrier systems showed a good biocompatibility with slight adverse effects, such as for the Poloxamer gel of 338 which showed a hemorrhage effect on 1-2 tested eggs and for the samples with Poloxamer 407 gel which showed only one egg with hemorrhage, vascular lysis and thrombosis. BNC samples loaded with O/W or W/O/W showed a stoppage of heartbeat in 1-2 eggs, which is still in the range of the historical control values of the laboratory. However, BNC samples loaded with octenidine were excluded from this test due to the preliminary experiments showing that the antiseptic octenidine causes sever irritation which was

also proven by Marquardt and colleagues (318) by CAM investigation at the concentration of 1% for short-term applications.

The next investigated aspect was the release behavior of the loaded drug which could be impacted by several factors. For example by the molecular weight of the drug, recently several small molecules were incorporated in to BNC such as: tetracycline (167), diclofenac (173), doxorubicin (181), and benzalkonium chloride (150), as well as large molecules such as peptide, protein and plasmids (54, 152, 198). However, several publications supported the theory, that by increasing the molecular weight, the release profile will be slower (54, 177). Moreover, a delay in the drug release could be observed for higher viscos drugs or additives due to the higher resistance for diffusion of the drug. Wiegand and colleagues (177) showed that the release of polihexanide was faster than povidone-iodine due to its higher molecular weight and about 7 times higher viscosity of povidone-iodine 10% aqueous solution in comparison to polihexanide solution. Other factors that could impact the release are, carrier system-cellulose interactions or drug-cellulose interactions. These interactions are possible due to the high number of free hydroxyl groups in the BNC structure. These hydrogen bonds could have an impact on the release as shown for lidocaine (185), berberine salts (148) and protein (152).

In this work the cumulative release behavior in respect to the carrier systems was investigated. All *in vitro* release studies were performed using vertical Franz diffusion cells with a single side contact aiming to simulate the later application on the skin and as recommended by the Organization for Economic Co-operation and Development (OECD) (319, 320). After a successful loading of the lipophilic drug into the BNC in a comparable loading amount with hydrophilic compounds, the release profile, and its dependency on the different carrier systems were investigated. The cumulative release amount of CoQ10 formulated into either the O/W or W/O/W nanoemulsions showed the biphasic typical release profiles of a drug from BNC over 48 hours

with a high release burst in the first 8-10 hours which is important to reach fast the therapeutic concentration. This was followed by a slower release rate till reaching equilibrium conditions. The type of carrier system showed an influence on the release rate, where W/O/W nanoemulsions demonstrated a slightly superior comparing to O/W nanoemulsions, due to their higher hydrophilic content, the affinity to the recipient medium and their hydrodynamic size (293, 294). Moreover, a higher release ratio was recorded for both O/W and W/O/W nanoemulsions samples when compared to the liposome samples within 48 hours. The CoQ10 formulated with liposome demonstrated an incomplete release of the drug. This finding could be explained by the inflexibility of liposomes preventing them from diffusing out of the BNC structure and a possible interaction between the hydrated polar headgroups of the phosphatidylcholine and the cellulose fibers in the BNC (321). The release mechanism was mainly suggested to be by diffusion overlayed by swelling, as shown for hydrophilic and macromolecular compounds (322, 323). Different aspects were reported in the literature for an incomplete release such as lack of flexibility of the carrier systems or low stability (200). Numata and colleagues (200) successfully incorporated retinol into BNC by formulating retinol in poly(ethylene oxide)-*b*-poly(caprolactone) polymer nanoparticles. The incomplete release of retinol in their study was explained to be the lack of flexibility of the used solid nanoparticle and the low stability of the nanoparticle, which led to the early release of retinol out of the nanoparticles in the BNC and the subsequent participation of retinol into the BNC structure (200).

Very few attempts were reported in the literature for a long-term application of the BNC as drug delivery system (6, 54, 324). In previous work, the release of octenidine from the BNC without any additives was obtained within 24 hours for acute wounds, which require a fast release of the antiseptic drug within few hours (146). Herein, the release profile of the antiseptic octenidine was modified by the incorporation of octenidine into the Poloxamer micelles or gels to obtain a long-

term active wound dressing which could be applied for longer periods, up to seven days. This can reduce the pain associated with changing wound dressings, prevent tissue trauma, and increase patient compliance (295). The incorporation of Poloxamers into BNC fiber network formed a secondary gel structure inside the BNC structure, which led to the reduction of water content in BNC and to the reduction of the size of channels and pores resulting in a compact structure (325). This resulted in a prolongation of the release of octenidine out from BNC. This is demonstrated by the addition of Poloxamer 338 in both micellar and gel concentration and Poloxamer 407 in the micellar concentration which prolonged the release up to three days. Moreover, by further increase of the Poloxamer 407 concentration to the gel concentration a prolongation of the release up to seven days was observed. The release of micellar systems is suggested to be dependent on diffusion out of the BNC structure into the release medium. However, the release of the gel systems is controlled by an additional step which is the dissolution of the gel matrix and its disintegration into singular buildings units (unimers), followed by diffusion outside of the BNC (290, 326-328). The hydrophilicity of the Poloxamer gels could also impact the release profile. Although both Poloxamers have the same molar mass and structure of PEOx-PPOy-PEOx, Poloxamer 338 contains less polypropylene oxide parts (44 g/mol) than Poloxamer 407 (56 g/mol) which gives Poloxamer 338 a less lipophilic character. Thus, resulting dissolution of the Poloxamer 338 gel is faster than Poloxamer 407 which could explain the differences between the two release profiles.

Other aspects to be considered are the properties of the loaded drug and its affinity to the release medium. The two components 3-*O*-acetyl-11-keto-β-boswellic acid (AKBA) and 11-keto-β-boswellic acid (KBA) are the most effective anti-inflammatory compounds out of the components of the *Boswellia serrata*-extract in the field of treating skin diseases (268). AKBA and KBA were incorporated into BNC by using the two previously described nanoemulsions. Although AKBA and KBA were incorporated into the BNC with the same carrier system, a difference in the

cumulative release profiles was observed. The more hydrophilicity compound KBA, with a log P value of 7, showed a faster release rate than the AKBA with a log P value of 8 (329) this difference could be due to the affinity to the release medium.

Furthermore, in this work, the effect of the loading technique on the release behavior was investigated. Beside the submerse absorption technique, the re-swelling and injection techniques were tested aiming to test the incorporation of CoQ10 as described previously. Although the carrier systems (liposome as well as the O/W and W/O/W nanoemulsions) showed similar behavior regarding the loading process and similar efficiency with respect the loading amount, a general trend was noticed regarding release behavior. The cumulative drug release per time of all carrier systems were reduced *per se* by around 30% in a comparison between samples loaded by re-swelling and samples loaded by submersed technique. This reduction is mainly related to the BNC preparation step, especially the lyophilization (151, 299), where a partial aggregation of the free cellulose strands in the BNC structure is noticed, and which causes a retardation in the diffusion of the drug (299). On the other hand, the injection technique formed a core-shell system. This system provided the lowest drug release rate among the other loading techniques. Those findings were correlated to published results for large molecules (54), where the release of the plasmids was prolonged more than 20 days due to the fact that the drug had longer diffusion pathway from the core of the BNC to the surface of the release medium (54). Overall, several factors could influence the release profile of a lipophilic drug from BNC such as the BNC type (native or freeze-dried) and loading method, carrier system properties, and drug characteristics.

Based on the pervious findings and the reported examples from the literature, the uptake of a drug into the BNC was based on diffusional and capillary processes (146, 147, 177). The other way around, the release of drugs from the BNC was also by the same processes (146, 173, 195). Hence, the release media before and after the release experiments were investigated by photon correlation

spectroscopy (PCS). These measurements revealed no change of the carrier system before and after release with regard to the hydrodynamic diameters and the polydispersity index, which indicated that the carrier systems were released from the BNC. These measurements were not performed for the Poloxamers micellar and the gel systems, due to a direct dilution of the systems with the release medium and the concentration of Poloxamers reaching a level under the critical micellar concentration. Based on those findings it could be concluded that the release profiles of a lipophilic drugs were driven by the swelling and diffusion of the carrier systems of BNC matrix. To support this theory, the release mechanism of the investigated lipophilic drugs was investigated. The semi-empirical Ritger-Peppas equation was applied to mathematically describe the different release profiles, which is well-established for hydrogel materials (323, 330). It was done by plotting the logarithmic release between 5 and 60% against the logarithmic time and determination of the linear regression and the diffusional exponents (*n*). Based on the *n* values for cylindrical sample morphology, the release mechanism could be described as Fickian diffusion ($n < 0.45$), anomalous diffusion ($0.45 < n < 0.89$), or as Case-II transport. In this work, all lipophilic drugs exhibited diffusional exponents in the range of 0.45 – 0.60 which indicated a release by Fickian diffusion overlayed by swelling controlled mechanisms, which is also called anomalous or non-Fickian transport. The initial burst is related to the high initial concentration gradient between the drug incorporated into the BNC and the release medium which will be reflected in the fast diffusion of the drug from the BNC contact surface into the medium. With time, the diffusion pathways increase, and a slower release could be recorded. Conclusively, the utilization of the carrier system facilitated the incorporation of lipophilic drugs into the BNC and demonstrated a comparable release mechanism with hydrophilic molecules such as berberine (148) polihexanide (177), ibuprofen (322), lidocaine (149) and doxycycline hyclate (132). From the perspective of dermal application, which is the intended final application form of the developed system, the biphasic

release profile is advantageous, where the initial release burst of a drug is a necessary to reach an effective therapeutic concentration, and the following prolonged release depending on the used carrier system and the intended application time, is maintaining the therapeutic concentration without reaching concentrations which could lead to adverse side effects.

Beside the loading and release behavior, the influence of the carrier systems and the loading into BNC on the activity of the lipophilic drugs was investigated by determining the antimicrobial activity of octenidine. Although native BNC has several advantages in the wound dressing field which shorten the healing period as shown in several clinical trials (331-333), native BNC did not show an antibacterial effect (178, 213). In this work, BNC was activated with the antiseptic drug octenidine to act as wound dressing. The antibacterial activity was investigated against two bacterial strains: *Staphylococcus aureus* as a model strain for Gram-negative and *Pseudomonas aeruginosa* as a model strain for Gram-positive. Those two strains have the highest occurrence in infected wounds (334, 335). The qualitative agar diffusion test was used in this study and has been performed according to the Clinical and Laboratory Standards Institute (336), which is also a well-established method to characterize the antibacterial activity of BNC (96, 193, 324). The investigation was performed by incubation of bacterial stock solution of Caso-bouillon medium for 24 hours at 35 °C and 100 rpm. Followed with two dilution steps with physiological saline, the first dilution was done to reach a turbidity of 0.5 McFarland (~108 CFU/mL). The resulting bacterial suspension was diluted again with physiological saline to a ratio of 1:10. Afterwards, 100 µL of the bacterial suspension was spread on a Mueller-Hinton 2 agar plate. Pure filter papers (6 mm) soaked in antibiotic solutions (30 µg/mL of kanamycin sulfate for *S. aureus* and 10 µg/mL of gentamycin sulfate for *P. aeruginosa*) were used as positive control and pure filter papers as negative control. BNC samples were applied directly on the agar plate and incubated for 24 hours. The antibacterial activity was evaluated based on the formation of an inhibition zone around the

applied samples. The validity of the tests was proven by showing no inhibition zone around the negative control and an inhibition zone of 17 mm and 24 mm for gentamycin sulfate and kanamycin sulfate, respectively. Moreover, similar behavior was observed for the negative controls, native BNC, and BNC samples loaded with Poloxamers at the micellar and gel concentrations which did not show an inhibition zone around the samples. This indicated that native BNC and Poloxamers at both concentrations did not have antimicrobial activity. This confirms data reported in the literature (178, 213, 337). Furthermore, the inhibition zone of pure octenidine was not impacted by loading into BNC with and without Poloxamers in both micellar and gel concentrations for the short-term applications (24 hours) and long-term applications (8 days). Those results were confirmed by a second quantitative method, the two color fluorescent Live/Dead® BacLight™ kit which was utilized to quantify the viable bacterial cells after incubation with the samples (338). The results confirmed the absence of the antibacterial activity for native BNC and showed a viability of *S. aureus* of below 1% for octenidine samples. These viability values were not impacted after the addition of octenidine into BNC with and without Poloxamers in different concentrations. These results were also correlated to the reported results in the literature, where the drug did not lose its activity by the loading into BNC such as benzalkonium chloride (175), curcumin (207), and polihexanide (177).

Another possible application for the newly developed BNC-based drug delivery system is for skin diseases. In this field of application, it is important that the drug can penetrate the stratum corneum of the skin. Only a few drugs have the capability to overcome this barrier without the need for penetration enhancers and those drugs are ideally of a molecular weight less than 500 Da and log P value ≤ 2 (217, 339). The drugs in this work have a higher log P values. CoQ10, KBA and AKBA have log P values of 10, 7, and 8, respectively (329, 340). These drugs were incorporated into the BNC by O/W and W/O/W nanoemulsions. The utilization of nanoemulsions enhances the

penetration of drugs into intact skin due to their small hydrodynamic size and flexibility, which has been proven in several studies (226, 341-344). The *ex vivo* skin penetration of the drugs was investigated by the tape stripping technique of a full-thickness porcine ear skin, a well-established method to simulate skin penetration behavior (345-347). Both O/W and W/O/W nanoemulsions without BNC showed a penetration enhancement effect and the drugs were detected in the different skin layers. However, W/O/W nanoemulsions showed a superior effect compared to O/W nanoemulsions, where higher drug amounts were detected in the middle and deeper layers by utilizing W/O/W nanoemulsions, but O/W nanoemulsions had a higher concentration on the surface layers. These findings could be related the higher viscosity and larger hydrodynamic size of the O/W nanoemulsions in comparison to W/O/W nanoemulsions. The high amount of the drugs detected on the surface layers of the skin by using O/W nanoemulsion comparing to W/O/W nanoemulsions could be correlated to the higher lipophilicity of O/W nanoemulsions which will lead to less penetration and the O/W nanoemulsions would be stuck on the upper layers of skin, where a balanced lipophilicity is required for transdermal penetration (217). These findings were correlated to the reported penetration studies in the literatures (348, 349). This differing behavior of the two nanoemulsions could provide the possibility for a drug delivery system targeting specific layer of the skin. Moreover, the incorporation of the drug loaded carrier system into BNC did not influence the amount of drug that penetrated into the deeper layers of the skin and reduced the accumulation of the drug in the upper layers of the skin and increased the amount in the middle layers for the drug incorporated into O/W nanoemulsions formulation. This effect could be related to the lipophilicity of the O/W nanoemulsions which form less hydrogen bonds with the BNC, as well as to the change of the concentration gradient caused by the use of BNC as a depot matrix, which has an effect on the transport of a drug into the skin (350). Moreover, the nanoemulsions incorporated into the BNC were able to deliver the lipophilic CoQ10 within the therapeutic range

(351, 352). Another penetration study was performed to simulate a long-term application and to evaluate the effect of removal of the drug from the skin by transportation mechanisms. Where nanoemulsions loaded BNC samples were applied on a new skin after 24 hours of application on a first skin. The results demonstrated less penetrated drug in the second skin, which also correlate to the in vitro release profiles, where BNC samples acted as a depot matrix and the liberation of the carrier systems from the BNC was the controlling step which is the highest in the first 8 hours followed by a slower release.

Within this presented work, the observed data showed a homogeneous incorporation of BNC with a lipophilic drug by utilizing different carrier systems. The newly obtained BNC-based system maintained the outstanding properties of native BNC such as biocompatibility and mechanical stability. The release profiles could be controlled by the loading technique, BNC type and the utilized carrier system. The loaded drug maintained its activity and the presence of the carrier system facilitated improved skin penetration behavior.

6. Summary and Outlook

Bacterial nanocellulose has been established for the use as a drug delivery system and wound dressing due to its exceptional properties, especially its enormous surface area. However, its use until now has been limited to hydrophilic drugs for the treatment of acute skin infections. Due to its high hydrophilicity, the incorporation of lipophilic drugs for treating both acute and chronic skin infections is a major challenge which has not been well addressed up to now. In the present thesis, the focus was on overcoming the BNC hydrophilicity by the approach of incorporation of drug loaded nanoscaled carrier systems, such as micelles, liposomes, and O/W and W/O/W nanoemulsions, as well as gels structure. This approach was investigated to facilitate the use of BNC as drug delivery system for the treatment of skin infections by several lipophilic drugs: the anti-inflammatory *Boswellia serrata* extract, the antioxidant coenzyme Q10, and the antiseptic octenidine.

To investigate the suitability of the chosen carrier systems for incorporation into the BNC, a physicochemical characterization was performed with regard to the hydrodynamic diameter and zeta potential. The drug loaded carrier systems demonstrated stability over 30 days at the three temperatures of 2-8 °C as a storage temperature, room temperature for handling, and 37 °C representing body temperature. They showed a hydrodynamic diameter <200 nm, a monodisperse size distribution, and neutral to negative zeta potentials. After biosynthesis of BNC, the loading of BNC fleeces with the drug loaded carrier systems using different *post*-modifications loading techniques was tested. Although the carrier systems have different hydrodynamic sizes and viscosities, the five carrier systems revealed a homogenous drug distribution within the BNC fleeces with a high loading efficiency which is comparable to hydrophilic drugs under the same loading conditions. Moreover, time-saving and customizable loading techniques were investigated

and revealed a rapid and efficient loading of the lipophilic drugs.

Contrary to other approaches of loading lipophilic drugs into BNC, the newly developed drug delivery systems demonstrated no changes to the BNC inner nanostructure as observed by SEM investigation. Only the BNC samples loaded by the reswelling loading technique demonstrated the typical densification of BNC fibers due to the freeze-drying process. In view of the BNC mechanical stability during handling, application, and packaging, the investigation of the mechanical stability of the carrier systems loaded BNC demonstrated no changes to the mechanical stability of the native BNC but an increase of the compressive strength by using the Poloxamer 338 and 407 gels or by using the reswelling loading technique. With respect to the ability of BNC to absorb wound exudates during the treatment of infected skin, the water binding capacity was investigated for the newly developed BNC-based drug delivery system. In general, it was found that the impregnation with the carrier systems caused a decrease in water binding ability. However, this effect was not driven by the presence of the drug itself, but it was caused by the replacement of water bounded to BNC with the carrier systems. This effect is dependent on the concentration of the carrier systems where this decrease of the water binding ability was more pronounced for the BNC samples loaded with Poloxamer 338 and 407 gels in comparison to the BNC loaded with the micellar concentrations. Moreover, the lipophilicity of the carrier system played a major role where BNC loaded with W/O/W nanoemulsions showed higher values of water binding ability comparing to BNC loaded with the higher lipophilic system O/W nanoemulsions. Since the water binding capacity is a key property for the wound dressing application to provide a balance between absorption and retention of wound exudate, an optimal balance should be further investigated.

In the view of treating skin infections, two types of release profiles are required. A fast to moderate release within 24-48 hours to treat acute infections and a long-term release up to one week for the treatment of chronic infections. Therefore, the release behavior of the BNC samples was

characterized using the Franz diffusion cells to simulate dermal application. The obtained release data revealed a time dependent biphasic release profile with high initial release followed by a slower release. Initially, the first rapid release of drug within the first 8 hours, which is important to reach the therapeutic concentration fast, depends on the loading technique and the designed system, where the amount of the released drug increased in the order: injection < reswelling < submerse loading technique. Moreover, the lipophilicity of the carrier systems impacts the release profile where W/O/W nanoemulsions showed a faster release than the same drug incorporated in O/W nanoemulsions. For the first time, a long-term application of up to seven days to treat chronic infections with a prolonged release of octenidine has been achieved by incorporating Poloxamer gels. Additionally, the mathematical modeling of the obtained release profiles by the Ritger-Peppas equation demonstrated that the release mechanism of the lipophilic drugs is a diffusion overlayed by swelling controlled release.

The biocompatibility of the newly developed drug delivery systems is crucial for dermal applications to avoid irritation. The biocompatibility of the BNC samples with and without the drug loaded carrier system was investigated by the local application on the chick area vasculosa of fertilized hen's eggs. The excellent biocompatibility of native BNC was not impacted by the incorporation of the different types of carrier systems. Additionally, the biological activity of the newly developed BNC-based drug delivery system for octenidine was investigated by agar diffusion test against both the Gram-positive *Staphylococcus aureus* and the Gram-negative *Pseudomonas aeruginosa* and was also confirmed by a quantitative method using the Live/Dead® BacLight™ kit. Moreover, the skin penetration enhancement effect of both O/W and W/O/W nanoemulsions was investigated to ensure the delivery of the drug to the infected skin. This investigation was performed by the tape stripping experiment of a full-thickness porcine ear skin after incubation with the carrier systems with and without BNC. This studies demonstrated the

ability of BNC to act as a depot matrix for the O/W and W/O/W nanoemulsions which were able to deliver the loaded lipophilic drugs into the skin.

As presented in this thesis, the combination of BNC with lipophilic drugs to act as drug delivery system was accomplished while preserving the unique properties of BNC. Both the type of the utilized carrier system and the loading technique in addition to the type of BNC could be identified as key factors for custom-designed and controlled release behavior of lipophilic drugs. An extended controlled drug release was shown for the first time for long-term applications of up to seven days thus closes the gap of utilizing the BNC as drug delivery system for long-term application, for example as a wound dressing. In addition, this work is a proof-of-concept for further studies using other types of carrier systems to incorporate different active ingredients. The knowledge gained from the *in vitro* investigation should be tested *in vivo*. Moreover, a transfer of lab-scale production to commercial scale production should be optimized for all production steps, including packaging.

7. Zusammenfassung

Bakterielle Nanocellulose wurde aufgrund ihrer außergewöhnlichen Eigenschaften, insbesondere der sehr großen inneren Oberfläche, für die Verwendung als Wirkstoffträgersystem und Wundauflage etabliert. Bis heute ist die Nutzung jedoch auf hydrophile Wirkstoffe für die Behandlung von akuten Hautinfektionen beschränkt. Aufgrund der hohen Hydrophilie von BNC ist der Einbau von lipophilen Wirkstoffen zur Behandlung von akuten und chronischen Hautinfektionen eine der größten Herausforderungen, die bisher nicht addressiert wurde. In der vorliegenden Arbeit lag der Schwerpunkt auf der Überwindung der BNC-Hydrophilie durch die Beladung mit wirkstoffbeladenen nanoskalierten Trägersystemen wie Mizellen, Liposomen und O/W und W/O/W Nanoemulsionen sowie Gelstrukturen. Dieser Ansatz wurde untersucht, um die Verwendung von BNC als Wirkstoffträgersystem zur Behandlung von Hautinfektionen durch verschiedene lipophile Wirkstoffe, wie entzündungshemmende *Boswellia serrata* Extrakte, das Antioxidans Coenzym Q10 und das Antiseptikum Octenidin, zu ermöglichen.

Um die Eignung der gewählten Trägersysteme für die Beladung von BNC zu untersuchen, wurde eine physikochemische Charakterisierung hinsichtlich des hydrodynamischen Durchmessers und des Zetapotentials durchgeführt. Die wirkstoffbeladenen Trägersysteme zeigten eine Stabilität über bis zu 30 Tagen bei den drei relevanten Temperaturen von 2-8 °C als Lagertemperatur, Raumtemperatur für die Handhabung und 37 °C als Körpertemperatur. Sie zeigten einen hydrodynamischen Durchmesser < 200 nm, eine monodisperse Größenverteilung und neutrale bis negative Zetapotentiale. Nach der Biosynthese von BNC wurde die Beladung von BNC-Vliesen mit den wirkstoffbeladenen Trägersystemen durch verschiedene post-synthetische Beladungstechniken untersucht. Obwohl die Trägersysteme hinsichtlich der hydrodynamischen Größe und der Viskosität unterschiedlich waren, zeigten die fünf Trägersysteme eine homogene

Wirkstoffverteilung innerhalb der BNC-Vliese mit einer hohen Beladungseffizienz, die mit hydrophilen Wirkstoffen unter den gleichen Beladungsbedingungen vergleichbar war. Darüber hinaus wurden zeitsparende und individuell anpassbare Beladungstechniken untersucht, die eine schnelle und effiziente Beladung der lipophilen Wirkstoffen möglich machten.

Im Gegensatz zu anderen Ansätzen zur Beladung von BNC mit lipophilen Wirkstoffen zeigten die neu entwickelten Wirkstoffträgersysteme keine Veränderungen der inneren Nanostruktur von BNC, wie durch SEM-Untersuchungen nachgewiesen wurde. Nur die BNC-Proben, die durch die Requellung beladen wurden, zeigten die typische Verdichtung der BNC-Fasern aufgrund des Gefriertrocknungsprozesses. Im Hinblick auf die Handhabung, Anwendung und Verpackung zeigte die Untersuchung der mit Trägersystemen beladenen BNC keine Veränderung hinsichtlich der mechanischen Stabilität der nativen BNC, sondern lediglich eine Erhöhung der Druckfestigkeit unter Verwendung des Poloxamers 338 und 407 Gele oder unter der Reswelling Beladungstechnik. Angesichts der Fähigkeit der BNC, Wundexsudate während der Behandlung infizierter Haut zu absorbieren, wurde die Wasserbindungsfähigkeit für das neu entwickelte auf BNC basierende Wirkstoffträgersystem untersucht. Im Allgemeinen wurde festgestellt, dass die Imprägnierung der Trägersysteme mit einer Abnahme der Wasserbindungsfähigkeit einherging. Dieser Effekt wurde jedoch nicht durch das Vorhandensein des Wirkstoffs selbst ausgelöst, sondern durch den Austausch von an BNC gebundenem Wasser durch die Trägersysteme, welcher von der Konzentration der Trägersysteme abhängt. Im Vergleich zu den mit mizellaren Konzentrationen von Poloxamer beladenen BNC ließ sich die Abnahme der Wasserbindungsfähigkeit besonders ausgeprägt bei den mit Poloxamer 338 und 407 Gelen beladenen BNC-Proben zeigen. Darüber hinaus spielte die Lipophilie des Trägersystems eine wichtige Rolle, denn die mit W/O/W Nanoemulsionen beladene BNC zeigte höhere Werte der Wasserbindungsfähigkeit im Vergleich zu BNC Proben, die mit den höheren lipophilen O/W Nanoemulsionen beladen waren. Da die

Wasserbindungskapazität eine Schlüsseleigenschaft für die Wundauflage ist, um ein Gleichgewicht zwischen Absorption und Retention von Wundexsudat herzustellen, sollte ein Gleichgewicht weiter optimiert werden.

Im Hinblick auf die Behandlung von Hautinfektionen sind zwei Arten von Freisetzungsprofilen erforderlich: eine schnelle bis moderate Freisetzung innerhalb von 24-48 Stunden zur Behandlung akuter Infektionen und eine verlängerte Freisetzung über bis zu einer Woche zur Behandlung von chronischen Infektionen. Daher wurde das Freisetzungsverhalten der BNC-Proben unter Verwendung von Franz-Diffusionszellen charakterisiert, um die dermale Anwendung zu simulieren. Die erhaltenen Freisetzungsdaten zeigten ein zeitabhängiges zweiphasiges Freisetzungsprofil mit anfänglich hoher Freisetzung, gefolgt von einer langsameren Freisetzung. Initial wurde eine erste schnelle Freisetzung des Wirkstoffs innerhalb der ersten 8 Stunden beobachtet, die zu einem schnellen Erreichen der therapeutischen Konzentration führte. Die initiale Freisetzung war abhängig von der verwendeten Beladungstechnik und die Menge des freigesetzten Wirkstoffs stieg in der folgenden Reihenfolge: Injektions- < Requellungs- < Sorptions-Beladungstechnik an. Darüber hinaus beeinflusst die Lipophilie der Trägersysteme das Freisetzungsprofil, wobei W/O/W-Nanoemulsionen eine schnellere Freisetzung zeigten als derselbe Wirkstoff, welcher in O/W-Nanoemulsionen formuliert war. Zum ersten Mal wurde durch die Beladung von Poloxamer-Gelen eine Langzeitanwendung von bis zu sieben Tagen zur Behandlung chronischer Infektionen mit einer verlängerten Freisetzung von Octenidin erreicht. Zusätzlich zeigte die mathematische Modellierung der erhaltenen Freisetzungsprofile durch die Ritger-Peppas-Gleichung, dass der Freisetzungsmechanismus der lipophilen Wirkstoffe eine Diffusion ist, die durch quellungskontrollierte Freisetzung überlagert wurde.

Die Biokompatibilität der neu entwickelten Wirkstoffträgersysteme ist für die dermale Anwendung entscheidend, um Irritationen zu vermeiden. Die Biokompatibilität der BNC-Proben

und des wirkstoffbeladenen Trägersystems wurde durch die lokale Applikation auf die „Chick Area Vasculosa“ befruchteter Hühnereier untersucht. Die ausgezeichnete Biokompatibilität von nativer BNC wurde durch die Beladung verschiedener Arten von Trägersystemen nicht beeinträchtigt. Zusätzlich wurde die biologische Aktivität des neu entwickelten BNC basierten Trägersystems für den Wirkstoff Octenidin durch einen Agardiffusionstest sowohl gegen den grampositiven *Staphylococcus aureus* als auch gegen den gramnegativen *Pseudomonas aeruginosa* untersucht und durch ein quantitatives Verfahren unter Verwendung des Live/Dead® BacLight™ kit bestätigt. Darüber hinaus wurde die Verbesserung der Hautpenetration sowohl von O/W als auch von W/O/W Nanoemulsionen untersucht, um die Abgabe des Wirkstoffs in die infizierte Haut sicherzustellen. Diese Untersuchung wurde durch die „Tape-Stripping“ einer Schweineohrhaut voller Dicke nach Inkubation mit den Trägersystemen mit und ohne BNC durchgeführt. Diese Studien zeigten die Fähigkeit der BNC als eine Depotmatrix für die O/W und W/O/W Nanoemulsionen zu fungieren, welche die lipophilen Wirkstoffe in die Haut einbringen kann.

In der vorliegenden Arbeit wurde die Kombination von BNC mit lipophilen Wirkstoffen als Wirkstoffträgersystem unter Beibehaltung der einzigartigen Eigenschaften von BNC erreicht. Sowohl der Typ des verwendeten Trägersystems als auch die Beladungstechnik neben der Art der BNC konnten als Schlüsselfaktoren für ein maßgeschneidertes und kontrolliertes Freisetzungsverhalten von lipophilen Wirkstoffen identifiziert werden. Zum ersten Mal konnte eine verlängerte, kontrollierte Wirkstofffreisetzung für die Langzeitanwendung bis zu sieben Tagen gezeigt werden und schließt damit die Lücke der Verwendung von BNC als Wirkstofftransportsystem für die Langzeitanwendung, beispielsweise als Wundauflage. Darüber hinaus ist diese Arbeit ein Proof-of-Concept für weitere Studien unter Verwendung anderer Arten von Trägersystemen zum Einschluss verschiedener Wirkstoffe. Ebenso sollten die aus der *in vitro*

Untersuchung gewonnenen Erkenntnisse *in vivo* getestet werden. Außerdem kann eine Übertragung der Produktion vom aktuellen Labormaßstab auf einen kommerziellen Maßstab einschließlich aller Produktionsschritte wie der Verpackung optimiert werden.

8. References

1. Coughlan MP. *Cellulose hydrolysis: The potential, the problems and relevant research at Galway*. Biochemical Society Transactions. 1985;*13*(2):405-6.
2. Pérez J, Muñoz-Dorado J, De La Rubia T, Martínez J. *Biodegradation and biological treatments of cellulose, hemicellulose and lignin: An overview*. International Microbiology. 2002;**5**(2):53-63.
3. Klemm D, Heublein B, Fink HP, Bohn A. *Cellulose: Fascinating biopolymer and sustainable raw material*. Angewandte Chemie. 2005;**44**(22):3358-3393.
4. Mathew AP, Chakraborty A, Oksman K, Sain M. *The structure and mechanical properties of cellulose nanocomposites prepared by twin screw extrusion.* Cellulose Nanocomposites, American Chemical Society. ACS Symposium Series. 2006;**9**(38):114-131.
5. Naomi R, Bt Hj Idrus R, Fauzi MB. *Plant- vs. bacterial-derived cellulose for wound healing: A review*. International Journal of Environmental Research and Public Health. 2020;**17**(18):6803-28.
6. Marquele-Oliveira F, da Silva Barud H, Torres EC, Machado RTA, Caetano GF, Leite MN, Frade MAC, Ribeiro SJL, Berretta AA. *Development, characterization and pre-clinical trials of an innovative wound healing dressing based on propolis (EPP-AF®)-containing self-microemulsifying formulation incorporated in biocellulose membranes*. International Journal of Biological Macromolecules. 2019;**136**:570-578.
7. Retegi A, Gabilondo N, Peña C, Zuluaga R, Castro C, Gañan P, de la Caba K, Mondragon I. *Bacterial cellulose films with controlled microstructure–mechanical property relationships*. Cellulose. 2010;**17**(3):661-669.
8. Lea SR, Płoska J. *Study on the Use of Microbial Cellulose as a Biocarrier for 1,3-Dihydroxy-2-Propanone and Its Potential Application in Industry*. Polymers. 2018;**10**(4) 438-448
9. White DG, Brown Jr RM. *Prospects for the commercialization of the biosynthesis of microbial cellulose.* Cellulose and wood-chemistry and technology Wiley, New York. 1989;**1**:573-591.
10. Czaja W, Krystynowicz A, Bielecki S, Brown RM. *Microbial cellulose-the natural power to heal wounds*. Biomaterials. 2005;**27**(2):145-151.
11. Voon WW, Rukayadi Y, Meor Hussin AS. *Isolation and identification of biocellulose-producing bacterial strains from Malaysian acidic fruits*. Letters in Applied Microbiology. 2016;**62**(5):428-433.
12. Sani A, Dahman Y. *Improvements in the production of bacterial synthesized biocellulose nanofibres using different culture methods*. Journal of Chemical Technology & Biotechnology. 2010;**85**(2):151-164.
13. Brown AJ. *XLIII.-On an acetic ferment which forms cellulose.* Journal of the Chemical Society, Transactions. 1886;**49**(0):432-439.
14. Shoda M, Sugano Y. *Recent advances in bacterial cellulose production*. Biotechnology and Bioprocess Engineering. 2005;**10**(1):1-8.

15. Sharma C, Bhardwaj NK. *Bacterial nanocellulose: Present status, biomedical applications and future perspectives*. Materials Science and Engineering: C. 2019;**104**:109963.
16. Yamada Y, Yukphan P, Lan Vu HT, Muramatsu Y, Ochaikul D, Tanasupawat S, Nakagawa Y. *Description of Komagataeibacter gen. nov., with proposals of new combinations (Acetobacteraceae)*. The Journal of General and Applied Microbiology. 2012;**58**(5):397-404.
17. Matsutani M, Ito K, Azuma Y, Ogino H, Shirai M, Yakushi T, Matsushita K. *Adaptive mutation related to cellulose producibility in Komagataeibacter medellinensis (Gluconacetobacter xylinus) NBRC 3288*. Applied Microbiology and Biotechnology. 2015;**99**(17):7229-7240.
18. Ross P, Mayer R, Benziman M. *Cellulose biosynthesis and function in bacteria*. Microbiology Reviews. 1991;**55**(1):35-58.
19. Saxena I, Brown R. *Biosynthesis of bacterial cellulose*. In: Gama M, Gatenholm P, Klemm D, editors. Bacterial NanoCellulose: A Sophisticated Multifunctional Material: Taylor and Francis (CRC Press); 2012: 1-18.
20. Hestrin S, Schramm M. *Synthesis of cellulose by Acetobacter xylinum. 2. Preparation of freeze-dried cells capable of polymerizing glucose to cellulose**. Biochemical Journal. 1954;**58**(2):345-52.
21. Kralisch D, Hessler N, Klemm D, Erdmann R, Schmidt W. *White biotechnology for cellulose manufacturing—The HoLiR concept.* Biotechnology and Bioengineering. 2010;**105**(4):740-7.
22. Eslahi N, Mahmoodi A, Mahmoudi N, Zandi N, Simchi *A. Processing and properties of nanofibrous bacterial cellulose-containing polymer composites: A review of recent advances for biomedical applications*. Polymer Reviews. 2020;**60**(1):144-70.
23. Wang J, Tavakoli J, Tang Y. *Bacterial cellulose production, properties and applications with different culture methods–A review.* Carbohydrate Polymers. 2019;**219**:63-76.
24. Brown RM, Jr., Montezinos D. *Cellulose microfibrils: Visualization of biosynthetic and orienting complexes in association with the plasma membrane*. Proceedings of the National Academy of Sciences of the United States of America. 1976;**73**(1):143-7.
25. Klemm D, Schumann D, Udhardt U, Marsch S. *Bacterial synthesized cellulose - artificial blood vessels for microsurgery.* Progress in Polymer Science. 2001;**26**(9):1561-603.
26. Ahmed J, Gultekinoglu M, Edirisinghe M. *Bacterial cellulose micro-nano fibres for wound healing applications*. Biotechnology Advances. 2020;**41**:107549.
27. Zaar K. *Visualization of pores (export sites) correlated with cellulose production in the envelope of the gram-negative bacterium Acetobacter xylinum.* Journal of Cell Biology. 1979;**80**(3):773-777.
28. Koizumi S, Yue Z, Tomita Y, Kondo T, Iwase H, Yamaguchi D, Hashimoto T. *Bacterium organizes hierarchical amorphous structure in microbial cellulose.* The European Physical Journal E. 2008;**26**(1):137-42.
29. Williams WS, Cannon RE. *Alternative environmental roles for cellulose produced by acetobacter xylinum*. Applied and Environmental Microbiology. 1989;**55**(10):2448-52.
30. Iguchi M, Yamanaka S, Budhiono A. *Bacterial cellulose - a masterpiece of nature's arts*. Journal of Materials Science. 2000;**35**(2):261-70.

31. Bernardo EB, Neilan BA, Couperwhite I. *Characterization, differentiation and identification of wild-type cellulose-synthesizing acetobacter strains involved in Nata de Coco production.* Systematic and Applied Microbiology. 1998;**21**(4):599-608.
32. Kralisch D, Hessler N. *Large-scale production of BNC: State and challenges.* In: Gama M, Gatenholm P, Klemm D, editors. Bacterial NanoCellulose: A Sophisticated Multifunctional Material: Taylor and Francis; 2012:1-18.
33. Gorgieva S, Trcek J. *Bacterial cellulose: Production, modification and perspectives in biomedical applications*. Nanomaterials 2019;**9**(10):1352.
34. Torres FG, Arroyo JJ, Troncoso OP. *Bacterial cellulose nanocomposites: an all-nano type of material*. Materials Science and Engineering: C. 2019;**98**:1277-1293.
35. Picheth GF, Pirich CL, Sierakowski MR, Woehl MA, Sakakibara CN, de Souza CF, Martin AA, da Silva R, Freitas RA. *Bacterial cellulose in biomedical applications: A review.* International Journal of Biological Macromolecules. 2017;**104**:97-106.
36. Gao M, Li J, Bao Z, Hu M, Nian R, Feng D, An D, Li X, Xian M, Zhang H. *A natural in situ fabrication method of functional bacterial cellulose using a microorganism*. Nature Communications. 2019;**10**(1):437.
37. Lustri WR, de Oliveira Barud HG, Barud H, Peres MF, Gutierrez J, Tercjak A, de Oliveira OB, Ribeiro SJ. *Microbial cellulose—biosynthesis mechanisms and medical applications. Cellulose-Fundamental* Aspects and Current Trends. 2015;**1**:133-57.
38. R. Rebelo A, Archer AJ, Chen X, Liu C, Yang G, Liu Y. *Dehydration of bacterial cellulose and the water content effects on its viscoelastic and electrochemical properties.* Science and Technology of advanced Materials. 2018;**19**(1):203-211.
39. Fink H-P, Purz HJ, Bohn A, Kunze J. *Investigation of the supramolecular structure of never dried bacterial cellulose.* Macromolecular Symposia. 1997;**120**(1):207-217.
40. Gu J, Catchmark JM. *Impact of hemicelluloses and pectin on sphere-like bacterial cellulose assembly*. Carbohydrate Polymers. 2012;**88**(2):547-57.
41. Park S, Baker JO, Himmel ME, Parilla PA, Johnson DK. *Cellulose crystallinity index: Measurement techniques and their impact on interpreting cellulase performance*. Biotechnology for Biofuels. 2010;**3**(1):10.
42. Yano H, Nakahara S. *Bio-composites produced from plant microfiber bundles with a nanometer unit web-like network.* Journal of Materials Science. 2004;**39**(5):1635-8.
43. Barud H, Ribeiro C, Crespi M, Martines M, Dexpert-Ghys J, Marques R, Messaddeq Y, Ribeiro SJ. *Thermal characterization of bacterial cellulose–phosphate composite membranes*. Journal of Thermal Analysis and Calorimetry. 2007;**87**(3):815-8.
44. Junka A, Fijałkowski K, Ząbek A, Mikołajewicz K, Chodaczek G, Szymczyk P, Smutnicka D, Zywicka A, Sedghizadeh PP, Dziadas M, Mlynarz P, Bartoszewicz M. *Correlation between type of alkali rinsing, cytotoxicity of bio-nanocellulose and presence of metabolites within cellulose membranes.* Carbohydrate Polymers. 2017;**157**:371-9.
45. Wesarg F, Schlott F, Grabow J, Kurland HD, Hessler N, Kralisch D, Muller F. *In situ synthesis of photocatalytically active hybrids consisting of bacterial nanocellulose and anatase nanoparticles*. Langmuir : The ACS Journal of Surfaces and Colloids. 2012;**28**(37):13518-25.

46. Jozala AF, de Lencastre-Novaes LC, Lopes AM, de Carvalho Santos-Ebinuma V, Mazzola PG, Pessoa-Jr A, Grotto D, Gerenutti M, Chaud MV. *Bacterial nanocellulose production and application: A 10-year overview.* Applied Microbiology and Biotechnology. 2016;**100**(5):2063-72.
47. Hutchens SA, León RV, O'Neill HM, Evans BR. *Statistical analysis of optimal culture conditions for Gluconacetobacter hansenii cellulose production*. Letters in Applied Microbiology. 2007;**44**(2):175-80.
48. Dobre T, Stoica A, Parvulescu OC, Stroescu M, Iavorschi G. *Factors influence on bacterial cellulose growth in static reactors*. Revista de Chimie. 2008;**59**(5):591-4.
49. Zeng X, Small DP, Wan W. *Statistical optimization of culture conditions for bacterial cellulose production by Acetobacter xylinum BPR 2001 from maple syrup*. Carbohydrate Polymers. 2011;**85**(3):506-13.
50. Liu M, Li S, Xie Y, Jia S, Hou Y, Zou Y, Zhong C. *Enhanced bacterial cellulose production by Gluconacetobacter xylinus via expression of Vitreoscilla hemoglobin and oxygen tension regulation.* Applied Microbiology and Biotechnology. 2018;**102**(3):1155-65.
51. Ryngajłło M, Jędrzejczak-Krzepkowska M, Kubiak K, Ludwicka K, Bielecki S. *Towards control of cellulose biosynthesis by Komagataeibacter using systems-level and strain engineering strategies: current progress and perspectives.* Applied Microbiology and Biotechnology. 2020;**104**(15):6565-85.
52. Hu W, Chen S, Yang J, Li Z, Wang H. *Functionalized bacterial cellulose derivatives and nanocomposites*. Carbohydrate Polymers. 2014;**101**:1043-60.
53. Sulaeva I, Henniges U, Rosenau T, Potthast A. *Bacterial cellulose as a material for wound treatment: properties and modifications. A review.* Biotechnology Advances. 2015;**33**(8):1547-1571.
54. Pötzinger Y, Rahnfeld L, Kralisch D, Fischer D. *Immobilization of plasmids in bacterial nanocellulose as gene activated matrix.* Carbohydrate Polymers. 2019;**209**:62-73.
55. Azarniya A, Tamjid E, Eslahi N, Simchi A. *Modification of bacterial cellulose/keratin nanofibrous mats by a tragacanth gum-conjugated hydrogel for wound healing*. International Journal of Biological Macromolecules. 2019;**134**:280-9.
56. Moreira S, Silva NB, Almeida-Lima J, Rocha HAO, Medeiros SRB, Alves Jr C, Gama FM. *BC nanofibres: in vitro study of genotoxicity and cell proliferation.* Toxicology Letters. 2009;**189**(3):235-41.
57. Napavichayanun S, Yamdech R, Aramwit P. *The safety and efficacy of bacterial nanocellulose wound dressing incorporating sericin and polyhexamethylene biguanide: in vitro, in vivo and clinical studies.* Archives of Dermatological Research. 2016;**308**(2):123-32.
58. Chen YM, Xi T, Zheng Y, Guo T, Hou J, Wan Y, Gao C. *In vitro cytotoxicity of bacterial cellulose scaffolds used for tissue-engineered bone*. Journal of Bioactive and Compatible Polymers. 2009;**24**(1):137-45.
59. Helenius G, Backdahl H, Bodin A, Nannmark U, Gatenholm P, Risberg B. *In vivo biocompatibility of bacterial cellulose.* Journal of Biomedical Materials Research Part A. 2006;**76**(2):431-8.

60. Miyamoto T, Takahashi Si, Ito H, Inagaki H, Noishiki Y. *Tissue biocompatibility of cellulose and its derivatives.* Journal of Biomedical Materials Research. 1989;**23**(1):125-33.
61. Pita PC, Pinto FC, Lira MM, Melo Fde A, Ferreira LM, Aguiar JL. *Biocompatibility of the bacterial cellulose hydrogel in subcutaneous tissue of rabbits*. Acta Cirúrgica Brasileira. 2015;**30**(4):296-300.
62. Wippermann J, Schumann D, Klemm D, Kosmehl H, Salehi-Gelani S, Wahlers T. *Preliminary results of small arterial substitute performed with a new cylindrical biomaterial composed of bacterial cellulose.* European Journal of Vascular and Endovascular Surgery. 2009;**37**(5):592-6.
63. ASTM F756-00, *Standard Practice for Assessment of Hemolytic Properties of Materials*, ASTM International, West Conshohocken, PA, 2000.
64. Andrade FK, Silva JP, Carvalho M, Castanheira EM, Soares R, Gama M. *Studies on the hemocompatibility of bacterial cellulose*. Journal of Biomedical Materials Research. 2011;**98**(4):554-66.
65. Schumann DA, Wippermann J, Klemm DO, Kramer F, Koth D, Kosmehl H, Wahlers T, Salehi-Gelani S. *Artificial vascular implants from bacterial cellulose: preliminary results of small arterial substitutes*. Cellulose. 2009;**16**(5):877-85.
66. Database D. *Global microbial and bacterial cellulose market 2020 by manufacturers, regions, type and application, forecast to 2025*. https://wwwdecisiondatabasescom/ip/17285-microbial-and-bacterial-cellulose-market-analysis-report, Accessed on the 2nd of January 2021. 2021.
67. Andriani D, Apriyana AY, Karina M. *The optimization of bacterial cellulose production and its applications: A review*. Cellulose. 2020;**27**(12):6747-66.
68. Chau C-F, Yang P, Yu C-M, Yen G-C. *Investigation on the lipid- and cholesterol-lowering abilities of biocellulose.* Journal of Agricultural and Food Chemistry. 2008;**56**(6):2291-5.
69. Mamlouk D, Gullo M. *Acetic acid bacteria: Physiology and carbon sources oxidation*. Indian Journal of Microbiology. 2013;**53**(4):377-84.
70. Lin D, Liu Z, Shen R, Chen S, Yang X. *Bacterial cellulose in food industry: Current research and future prospects.* International Journal of Biological Macromolecules. 2020;**158**:1007-19.
71. Jipa IM, Stoica-Guzun A, Stroescu M. *Controlled release of sorbic acid from bacterial cellulose based mono and multilayer antimicrobial films.* Food Science and Technology. 2012;**47**(2):400-6.
72. Shi Z, Zhang Y, Phillips GO, Yang G. *Utilization of bacterial cellulose in food. Food*. Hydrocolloids. 2014;**35**:539-45.
73. Huang X, Zhan X, Wen C, Xu F, Luo L. *Amino-functionalized magnetic bacterial cellulose/activated carbon composite for Pb2+ and methyl orange sorption from aqueous solution.* Journal of Materials Science & Technology. 2018;**34**(5):855-63.
74. Hu M-X, Niu H-M, Chen X-L, Zhan H-B. *Natural cellulose microfiltration membranes for oil/water nanoemulsions separation.* Colloids and Surfaces A: Physicochemical and Engineering Aspects. 2019;**564**:142-51.

75. Hioki N, Hori Y, Watanabe K, Morinaga Y, Yoshinaga F, Hibino Y, Ogura T. *Bacterial cellulose: as a new material for papermaking.* Japan Tappi Journal. 1995;**49**(4):718-23.
76. Basta AH, El-Saied H. *Performance of improved bacterial cellulose application in the production of functional paper.* Journal of Applied Microbiology. 2009;**107**(6):2098-107.
77. Konuklu Y, Erzin F, Akar HB, Turan AM. *Cellulose-based myristic acid composites for thermal energy storage applications.* Solar Energy Materials and Solar Cells. 2019;**193**:85-91.
78. Gadim TD, Loureiro FJ, Vilela C, Rosero-Navarro N, Silvestre AJ, Freire CS, Figueiredoa F. *Protonic conductivity and fuel cell tests of nanocomposite membranes based on bacterial cellulose.* Electrochimica Acta. 2017;**233**:52-61.
79. Mautner A, Lee K-Y, Tammelin T, Mathew AP, Nedoma AJ, Li K, Bismarck A. *Cellulose nanopapers as tight aqueous ultra-filtration membranes.* Reactive and Functional Polymers. 2015;**86**:209-14.
80. Bianchet RT, Vieira Cubas AL, Machado MM, Siegel Moecke EH. *Applicability of bacterial cellulose in cosmetics – bibliometric review.* Biotechnology Reports. 2020;**27**:502.
81. Hasan N, Biak DRA, Kamarudin S. *Application of bacterial cellulose (BC) in natural facial scrub*. International Journal on Advanced Science, Engineering and Information Technology. 2012;**2**(4):272-5.
82. Pacheco G, de Mello CV, Chiari-Andréo BG, Isaac VLB, Ribeiro SJL, Pecoraro É, Trovatti E. *Bacterial cellulose skin masks—properties and sensory tests.* Journal of Cosmetic Dermatology. 2018;**17**(5):840-7.
83. Fernandes IdAA, Pedro AC, Ribeiro VR, Bortolini DG, Ozaki MSC, Maciel GM, Haminiuk CWI. *Bacterial cellulose: From production optimization to new applications.* International Journal of Biological Macromolecules. 2020;**164**:2598-611.
84. Enzymes™ B. *Bio enzymes mask hydration, the 1st moisturizing biocellulose mask, inspored by healing techniques*. https://wwwtalikacom/skin-care/masks/masks/bio-enzymes-mask-hydrating/33html, Accessed on the 3nd of January 2021. 2021.
85. Leaders™ e. *Leaders Cosmetics, Skin soft masks.* http://leaderscosmeticseu/en/labotica-skin-soft, Accessed on the 3nd of January 2021. 2021.
86. Beekmann U, Zahel P, Karl B, Schmölz L, Börner F, Gerstmeier J, Werz O, Lorkowski S,Wiegand C,Fischer D, Kralisch D. *Modified bacterial cellulose dressings to treat inflammatory wounds*. Nanomaterials. 2020;**10**(12):2508.
87. Portela R, Leal CR, Almeida PL, Sobral RG. *Bacterial cellulose: A versatile biopolymer for wound dressing applications*. Microbial Biotechnology. 2019;**12**(4):586-610.
88. Wang W, Lu K-j, Yu C-h, Huang Q-l, Du Y-Z. *Nano-drug delivery systems in wound treatment and skin regeneration.* Journal of Nanobiotechnology. 2019;**17**(1):82.
89. Nuutila K, Eriksson E. *Moist wound healing with commonly available dressings*. Advances in Wound Care. 2020;10(12):685-698.
90. Obagi Z, Damiani G, Grada A, Falanga V. *Principles of wound dressings: A review*. Surgical Technology International. 2019;**35**:50-7.
91. Akita S. *Wound repair and regeneration: Mechanisms, signaling*. International Journal of Molecular Sciences. 2019;**20**(24):265.

92. Sarheed O, Ahmed A, Shouqair D, Boateng J. *Wound healing-new insights into ancient challenges*. In; Tech London, United Kingdom, Edited by Vlad Alexandrescu;2016.
93. Cardona AF, Wilson SE. *Skin and soft-tissue infections: a critical review and the role of telavancin in their treatment*. Clinical Infectious Diseases. 2015;**61**(2):69-78.
94. Negut I, Grumezescu V, Grumezescu AM. *Treatment strategies for infected wounds*. Molecules. 2018;**23**(9):2392.
95. Powers JG, Higham C, Broussard K, Phillips TJ. *Wound healing and treating wounds: Chronic wound care and management*. Journal of the American Academy of Dermatology. 2016;**74**(4):607-25.
96. Khalid A, Khan R, Ul-Islam M, Khan T, Wahid F. *Bacterial cellulose-zinc oxide nanocomposites as a novel dressing system for burn wounds.* Carbohydrate Polymers. 2017;**164**:214-21.
97. Beekmann U, Schmölz L, Lorkowski S, Werz O, Thamm J, Fischer D, Kralisch D. *Process control and scale-up of modified bacterial cellulose production for tailor-made anti-inflammatory drug delivery systems*. Carbohydrate Polymers. 2020;**236:**116062.
98. Boateng JS, Matthews KH, Stevens HNE, Eccleston GM. *Wound healing dressings and drug delivery systems: A review.* Journal of Pharmaceutical Sciences. 2008;**97**(8):2892-923.
99. Colenci R, Miot HA, Marques MEA, Schmitt JV, Basmaji P, Jacinto JdS, Abbade L. *Cellulose biomembrane versus collagenase dressing for the treatment of chronic venous ulcers: a randomized, controlled clinical trial*. European Journal of Dermatology. 2019;**29**(4):387-95.
100. Solway DR, Consalter M, Levinson DJ. *Microbial cellulose wound dressing in the treatment of skin tears in the frail elderly*. Wounds. 2010;**22**(1):17-9.
101. Solway DR, Clark WA, Levinson DJ. *A parallel open-label trial to evaluate microbial cellulose wound dressing in the treatment of diabetic foot ulcers*. International Wound Journal. 2011;**8**(1):69-73.
102. Fontana JD, De Souza AM, Fontana CK, Torriani IL, Moreschi JC, Gallotti BJ, De Souza SJ, Narcisco GP, Bichara JA, Farah LFX. *Acetobacter cellulose pellicle as a temporary skin substitute.* Applied Biochemistry and Biotechnology. 1990;**24**(1):253-64.
103. Frankel VH, Serafica GC, Damien CJ. *Development and testing of a novel biosynthesized XCell for treating chronic wounds*. Surgical Technology International. 2004;**12**:27-33.
104. Piatkowski A, Drummer N, Andriessen A, Ulrich D, Pallua N. *Randomized controlled single center study comparing a polyhexanide containing bio-cellulose dressing with silver sulfadiazine cream in partial-thickness dermal burns*. Burns. 2011;**37**(5):800-4.
105. Czaja W, Kawecki M, Krystynowicz A, Wysota K, Sakiel S, Wroblewski P, Glik J, Bielecki S. *Application of bacterial cellulose in treatment of second and third degree burns.* Abstracts of Papers, 227th ACS National Meeting, Anaheim, CA, United States, March 28-April 1, 2004.
106. Schmitz M, Eberlein T, Andriessen A. *Wound treatment costs comparing a bio-cellulose dressing with moist wound healing dressings and conventional dressings.* Wound Medicine. 2014;**6**:11-4.

107. Klemm D, Schumann D, Kramer F, Heßler N, Koth D, Sultanova B. *Nanocellulose materials - different cellulose, different functionality*. Macromolecular Symposia. 2009;**280**(1):60-71.
108. Klemm D, Schumann D, Kramer F, Heßler N, Hornung M, Schmauder H-P, Marsch S. *Nanocelluloses as innovative polymers in research and application*. In: Klemm D, editor. Polysaccharides II. Advances in Polymer Science. 205: Springer Berlin Heidelberg; 2006:49-96.
109. Mokhena TC, John MJ. *Cellulose nanomaterials: New generation materials for solving global issues.* Cellulose. 2020;**27**(3):1149-94.
110. Klemm D, Petzold-Welcke K, Kramer F, Richter T, Raddatz V, Fried W, Nietzsche S, Bellmann T, Fischer D. *Biotech nanocellulose: A review on progress in product design and today's state of technical and medical applications*. Carbohydrate Polymers. 2020;**254**:117313.
111. de Oliveira Barud HG, da Silva RR, da Silva Barud H, Tercjak A, Gutierrez J, Lustri WR, de Oliveira Junior OB, Ribeiro SJL. *A multipurpose natural and renewable polymer in medical applications: Bacterial cellulose*. Carbohydrate Polymers. 2016;**153**:406-20.
112. Lima FM, Pinto FC, Andrade-da-Costa BL, Silva JG, Campos Junior O, Aguiar JL. *Biocompatible bacterial cellulose membrane in dural defect repair of rat.* Journal of Materials Science Materials in Medicine. 2017;**28**(3):37.
113. Hagiwara Y, Putra A, Kakugo A, Furukawa H, Gong J. *Ligament-like tough double-network hydrogel based on bacterial cellulose.* Cellulose. 2010;**17**(1):93-101.
114. Goncalves S, Padrao J, Rodrigues IP, Silva JP, Sencadas V, Lanceros-Mendez S, Girão H, Dourado F, Rodrigues LR. *Bacterial cellulose as a support for the growth of retinal pigment epithelium*. Biomacromolecules. 2015;**16**(4):1341-51.
115. Dutton JJ. *Coralline hydroxyapatite as an ocular implant*. Ophthalmology. 1991;**98**(3):370-7.
116. Wang J, Gao C, Zhang Y, Wan Y. *Preparation and in vitro characterization of BC/PVA hydrogel composite for its potential use as artificial cornea biomaterial*. Materials Science and Engineering: C. 2010;**30**(1):214-8.
117. Svensson A, Nicklasson E, Harrah T, Panilaitis B, Kaplan DL, Brittberg M, Gatenholm P. *Bacterial cellulose as a potential scaffold for tissue engineering of cartilage.* Biomaterials. 2005;**26**(4):419-31.
118. Ahrem H, Pretzel D, Endres M, Conrad D, Courseau J, Müller H, Jaeger R, Kaps C, Klemm D, Kinne R. *Laser-structured bacterial nanocellulose hydrogels support ingrowth and differentiation of chondrocytes and show potential as cartilage implants*. Acta Biomaterialia. 2014;**10**(3):1341-53.
119. Silveira FC, Pinto FC, Caldas Neto Sda S, Leal Mde C, Cesário J, Aguiar JL. *Treatment of tympanic membrane perforation using bacterial cellulose: A randomized controlled trial*. Brazilian Journal of Otorhinolaryngology. 2016;**82**(2):203-8.
120. Favi P, Benson R, Neilsen N, Ehinger C, Dhar M. *Novel biodegradable microporous bacterial cellulose scaffolds engineered for bone and cartilage regeneration.* Federation of American Societies for Experimental Biology; 2013;**27**(6):805.

121. Hu Y, Zhu Y, Zhou X, Ruan C, Pan H, Catchmark JM. *Bioabsorbable cellulose composites prepared by an improved mineral-binding process for bone defect repair*. Journal of Materials Chemistry B. 2016;**4**(7):1235-46.
122. Favi PM, Ospina SP, Kachole M, Gao M, Atehortua L, Webster TJ. *Preparation and characterization of biodegradable nano hydroxyapatite–bacterial cellulose composites with well-defined honeycomb pore arrays for bone tissue engineering applications.* Cellulose. 2016;**23**(2):1263-82.
123. Zaborowska M, Bodin A, Bäckdahl H, Popp J, Goldstein A, Gatenholm P. *Microporous bacterial cellulose as a potential scaffold for bone regeneration.* Acta Biomaterialia. 2010;**6**(7):2540-7.
124. Fink H, Hong J, Drotz K, Risberg B, Sanchez J, Sellborn A. *An in vitro study of blood compatibility of vascular grafts made of bacterial cellulose in comparison with conventionally-used graft materials.* Journal of Biomedical Materials Research Part A. 2011;**97**(1):52-8.
125. Wacker M, Kießwetter V, Slottosch I, Awad G, Paunel-Görgülü A, Varghese S, Klopfleisch M, Kupitz D, Klemm D, Nietzsche S, Petzold-Welcke K, Kramer F, Wippermann J, Veluswamy P, Scherner M. *In vitro hemo- and cytocompatibility of bacterial nanocelluose small diameter vascular grafts: Impact of fabrication and surface characteristics.* PloS one. 2020;**15**(6):e0235168.
126. Li Y, Jiang K, Feng J, Liu J, Huang R, Chen Z, Yang Y, Dai Z, Chen Y, Wang N, Zhang W, Zheng W, Yang G, Jiang X. *Construction of small-diameter vascular graft by shape-memory and self-rolling bacterial cellulose membrane*. Advanced Healthcare Materials. 2017; **6**(11):1601343.
127. Putra A, Kakugo A, Furukawa H, Gong JP, Osada Y. *Tubular bacterial cellulose gel with oriented fibrils on the curved surface*. Polymer. 2008;**49**(7):1885-91.
128. Tang J, Bao L, Li X, Chen L, Hong FF. *Potential of PVA-doped bacterial nano-cellulose tubular composites for artificial blood vessels*. Journal of Materials Chemistry B. 2015;**3**(43):8537-47.
129. Petersen N, Gatenholm P. *Bacterial cellulose-based materials and medical devices: current state and perspectives.* Applied Microbiology and Biotechnology. 2011;**91**(5):1277-86.
130. Hu Y, Catchmark JM. *Integration of cellulases into bacterial cellulose: Toward bioabsorbable cellulose composites.* Journal of Biomedical Materials Research Part B, Applied Biomaterials. 2011;**97**(1):114-23.
131. Coseri S, Biliuta G, Simionescu BC, Stana-Kleinschek K, Ribitsch V, Harabagiu V. *Oxidized cellulose—Survey of the most recent achievements.* Carbohydrate Polymers. 2013;**93**(1):207-15.
132. Weyell P, Beekmann U, Küpper C, Dederichs M, Thamm J, Fischer D, Kralisch D. *Tailor-made material characteristics of bacterial cellulose for drug delivery applications in dentistry*. Carbohydrate Polymers. 2019;**207**:1-10.
133. Potzinger Y, Kralisch D, Fischer D. *Bacterial nanocellulose: the future of controlled drug delivery?*. Therapeutic Delivery. 2017;**8**(9):753-61.
134. Stumpf TR, Yang X, Zhang J, Cao X. *In situ and ex situ modifications of bacterial cellulose for applications in tissue engineering.* Materials Science and Engineering: C. 2018;**82:**372-83.

135. Shah N, Ul-Islam M, Khattak WA, Park JK. *Overview of bacterial cellulose composites: A multipurpose advanced material*. Carbohydrate Polymers. 2013;**98**(2):1585-98.
136. Shao W, Liu H, Wu J, Wang S, Liu X, Huang M, Xu P. *Preparation, antibacterial activity and pH-responsive release behavior of silver sulfadiazine loaded bacterial cellulose for wound dressing applications*. Journal of the Taiwan Institute of Chemical Engineers. 2016;**63**:404-10.
137. Martin C, Low WL, Gupta A, Amin MC, Radecka I, Britland ST, Raj P, Kenward K. *Strategies for antimicrobial drug delivery to biofilm*. Current pharmaceutical design. 2015;**21**(1):43-66.
138. de Lima Fontes M, Meneguin AB, Tercjak A, Gutierrez J, Cury BSF, dos Santos AM, Ribeiro SJL, Baruda HS. *Effect of in situ modification of bacterial cellulose with carboxymethylcellulose on its nano/microstructure and methotrexate release properties*. Carbohydrate Polymers. 2018;**179**:126-34.
139. Heßler N, Klemm D. *Alteration of bacterial nanocellulose structure by in situ modification using polyethylene glycol and carbohydrate additives.* Cellulose. 2009;**16**(5):899-910.
140. Abdelraof M, Hasanin MS, Farag MM, Ahmed HY. *Green synthesis of bacterial cellulose/bioactive glass nanocomposites: Effect of glass nanoparticles on cellulose yield, biocompatibility and antimicrobial activity.* International Journal of Biological Macromolecules. 2019;**138**:975-85.
141. Ray D, Sain S. *In situ processing of cellulose nanocomposites.* Composites Part A: Applied Science and Manufacturing. 2016;**83**:19-37.
142. Sukhtezari S, Almasi H, Pirsa S, Zandi M, Pirouzifard M. *Development of bacterial cellulose based slow-release active films by incorporation of Scrophularia striata Boiss. extract*. Carbohydrate Polymers. 2017;**156**:340-50.
143. Wichai S, Chuysinuan P, Chaiarwut S, Ekabutr P, Supaphol P. *Development of bacterial cellulose/alginate/chitosan composites incorporating copper (II) sulfate as an antibacterial wound dressing.* Journal of Drug Delivery Science and Technology. 2019;**51**:662-71.
144. Cazón P, Velázquez G, Vázquez M. *Characterization of bacterial cellulose films combined with chitosan and polyvinyl alcohol: Evaluation of mechanical and barrier properties*. Carbohydrate Polymers. 2019;**216**:72-85.
145. Shao W, Liu H, Liu X, Sun H, Wang S, Zhang R. *pH-responsive release behavior and anti-bacterial activity of bacterial cellulose-silver nanocomposites.* International Journal of Biological Macromolecules. 2015;**76**(0):209-17.
146. Moritz S, Wiegand C, Wesarg F, Hessler N, Müller FA, Kralisch D, Hipler U, Fischer D. *Active wound dressings based on bacterial nanocellulose as drug delivery system for octenidine.* International Journal of Pharmaceutics. 2014;**471**(1–2):45-55.
147. Müller A, Wesarg F, Hessler N, Müller FA, Kralisch D, Fischer D. *Loading of bacterial nanocellulose hydrogels with proteins using a high-speed technique*. Carbohydrate Polymers. 2014;**106**:410-3.
148. Huang L, Chen X, Nguyen TX, Tang H, Zhang L, Yang G. *Nano-cellulose 3D-networks as controlled-release drug carriers.* Journal of Materials Chemistry B. 2013;**1**(23):2976-84.

149. Trovatti E, Freire CS, Pinto PC, Almeida IF, Costa P, Silvestre AJ, Neto CP,Rosado C. *Bacterial cellulose membranes applied in topical and transdermal delivery of lidocaine hydrochloride and ibuprofen: in vitro diffusion studies.* International Journal of Pharmaceutics. 2012;**435**(1):83-7.
150. Mohite BV, Suryawanshi RK, Patil SV. *Study on the drug loading and release potential of bacterial cellulose.* Cellulose Chemistry and Technology. 2016;**50**(2):219-23.
151. Clasen C, Sultanova B, Wilhelms T, Heisig P, Kulicke W-M. *Effects of different drying processes on the material properties of bacterial dellulose membranes.* Macromolecular Symposia. 2006;**244**(1):48-58.
152. Muller A, Ni Z, Hessler N, Wesarg F, Muller FA, Kralisch D, Fischer D. *The biopolymer bacterial nanocellulose as drug delivery system: investigation of drug loading and release using the model protein albumin.* Journal of Pharmaceutical Sciences. 2013;**102**(2):579-92.
153. GmbH LR. *Suprasorb® X + PHMB antimikrobieller hydroBalance-wundverband*. https://wwwlohmann-rauschercom/de-de/produkte/niedergelassener-bereich/wundversorgung/moderne-wundversorgung/suprasorb-x-phmb/, Accessed on the 3nd of January 2021. 2021.
154. Pötzinger Y, Rabel M, Ahrem H, Thamm J, Klemm D, Fischer D. *Polyelectrolyte layer assembly of bacterial nanocellulose whiskers with plasmid DNA as biocompatible non-viral gene delivery system*. Cellulose. 2018;**25:**1939–1960.
155. Xiao L, Poudel AJ, Huang L, Wang Y, Abdalla AME, Yang G. *Nanocellulose hyperfine network achieves sustained release of berberine hydrochloride solubilized with β-cyclodextrin for potential anti-infection oral administration*. International Journal of Biological Macromolecules. 2020;**153**:633-40.
156. Amin MCIM, Abadi AG, Ahmad N, Katas H, Jamal JA. *Bacterial cellulose film coating as drug delivery system: Physicochemical, thermal and drug release properties.* Sains Malaysiana. 2012;**41**(5):561-8.
157. Hsiao HL, Lin SB, Chen LC, Chen HH. *Hurdle effect of antimicrobial activity achieved by time differential releasing of nisin and chitosan hydrolysates from bacterial cellulose.* Journal of Food Science. 2016;**81**(5):1184-91.
158. Nguyen VT, Gidley MJ, Dykes GA. *Potential of a nisin-containing bacterial cellulose film to inhibit Listeria monocytogenes on processed meats*. Food Microbiology. 2008;**25**(3):471-8.
159. Stroescu M, Stoica-Guzun A, Jipa IM. *Vanillin release from poly(vinyl alcohol)-bacterial cellulose mono and multilayer films.* Journal of Food Engineering. 2013;**114**(2):153-7.
160. Pavaloiu R-D, Stoica A, Stroescu M, Dobre T. *Controlled release of amoxicillin from bacterial cellulose membranes.* Open Chemistry. 2014;**12**(9):962-7.
161. Kaplan E, Ince T, Yorulmaz E, Yener F, Harputlu E, Laçin NT. *Controlled delivery of ampicillin and gentamycin from cellulose hydrogels and their antibacterial efficiency*. Journal of Biomaterials and Tissue Engineering. 2014;**4**(7):543-9.
162. Lazarini SC, de Aquino R, Amaral AC, Corbi FCA, Corbi PP, Barud HS, Lustri W. *Characterization of bilayer bacterial cellulose membranes with different fiber densities: a promising system for controlled release of the antibiotic ceftriaxone*. Cellulose. 2016;**23**(1):737-48.

163. Cacicedo ML, Pacheco G, Islan GA, Alvarez VA, Barud HS, Castro GR. *Chitosan-bacterial cellulose patch of ciprofloxacin for wound dressing: Preparation and characterization studies.* International Journal of Biological Macromolecules. 2020;**147**:1136-45.
164. Liyaskina E, Revin V, Paramonova E, Nazarkina M, Pestov N, Revina N, Kolesnikova S. *Nanomaterials from bacterial cellulose for antimicrobial wound dressing*. Journal of Physics: Conference Series. 2017;**784**:012034.
165. Rouabhia M, Asselin J, Tazi N, Messaddeq Y, Levinson D, Zhang Z. *Production of biocompatible and antimicrobial bacterial cellulose polymers functionalized by RGDC grafting groups and gentamicin*. ACS Applied Materials & Interfaces. 2014;**6**(3):1439-46.
166. Shao W, Liu H, Wang S, Wu J, Huang M, Min H, Liu X. *Controlled release and antibacterial activity of tetracycline hydrochloride-loaded bacterial cellulose composite membranes*. Carbohydrate Polymers. 2016;**145**:114-20.
167. Stoica-Guzun A, Stroescu M, Tache F, Zaharescu T, Grosu E. *Effect of electron beam irradiation on bacterial cellulose membranes used as transdermal drug delivery systems*. Nuclear Instruments & Methods in Physics Research, Section B: Beam Interactions with Materials and Atoms. 2007;**265**(1):434-8.
168. Wan Y, Gao C, Han M, Liang H, Ren K, Wang Y, Luo H. *Preparation and characterization of bacterial cellulose/heparin hybrid nanofiber for potential vascular tissue engineering scaffolds*. Polymers for Advanced Technologies. 2011;**22**(12):2643-8.
169. Silva N, Mota JP, Almeida TS, Carvalho JPF, Silvestre AJD, Vilela C, Rosado C, Freire C. *Topical drug delivery systems based on bacterial nanocellulose: Accelerated stability testing.* International Journal of Molecular Sciences. 2020;**21**(4):1262.
170. Shi X, Zheng Y, Wang G, Lin Q, Fan J. *pH- and electro-response characteristics of bacterial cellulose nanofiber/sodium alginate hybrid hydrogels for dual controlled drug delivery*. RSC Advances. 2014;**4**(87):47056-65.
171. Pavaloiu R-D, Stoica-Guzun A, Stroescu M, Jinga SI, Dobre T. *Composite films of poly(vinyl alcohol)–chitosan–bacterial cellulose for drug controlled release.* International Journal of Biological Macromolecules. 2014;**68**(0):117-24.
172. Saïdi L, Vilela C, Oliveira H, Silvestre AJD, Freire CSR. *Poly(N-methacryloyl glycine)/nanocellulose composites as pH-sensitive systems for controlled release of diclofenac.* Carbohydrate Polymers. 2017;**169**:357-65.
173. Silva NHCS, Rodrigues AF, Almeida IF, Costa PC, Rosado C, Neto CP, Silvestre AJD, Freire CSR. *Bacterial cellulose membranes as transdermal delivery systems for diclofenac: In vitro dissolution and permeation studies*. Carbohydrate Polymers. 2014;106:264-9.
174. Valo H, Arola S, Laaksonen P, Torkkeli M, Peltonen L, Linder MB, Serimaa R, Kuga S, Hirvonen J, Laaksonen T. *Drug release from nanoparticles embedded in four different nanofibrillar cellulose aerogels*. European Journal of Pharmaceutical Sciences. 2013;**50**(1):69-77.
175. Wei B, Yang G, Hong F. *Preparation and evaluation of a kind of bacterial cellulose dry films with antibacterial properties*. Carbohydrate Polymers. 2011;**84**(1):533-8.

176. Eberlein T, Haemmerle G, Signer M, Gruber Moesenbacher U, Traber J, Mittlboeck M, Strohal MBR. *Comparison of PHMB-containing dressing and silver dressings in patients with critically colonised or locally infected wounds.* Journal of Wound Care. 2012;**21**(1):12, 4-6, 8-20.
177. Wiegand C, Moritz S, Hessler N, Kralisch D, Wesarg F, Muller FA, Fischer D, Hipler U. *Antimicrobial functionalization of bacterial nanocellulose by loading with polihexanide and povidone-iodine*. Journal of Materials Science: Materials in Medicine. 2015;**26**(10):245.
178. de Mattos IB, Nischwitz SP, Tuca A-C, Groeber-Becker F, Funk M, Birngruber T, Mautner S, Kamolz L, Holzer J. *Delivery of antiseptic solutions by a bacterial cellulose wound dressing: Uptake, release and antibacterial efficacy of octenidine and povidone-iodine.* Burns. 2020;**46**(4):918-27.
179. Luan J, Wu J, Zheng Y, Song W, Wang G, Guo J, Ding X. *Impregnation of silver sulfadiazine into bacterial cellulose for antimicrobial and biocompatible wound dressing.* Biomedical Materials. 2012;**7**(6):065006.
180. Bodhibukkana C, Srichana T, Kaewnopparat S, Tangthong N, Bouking P, Martin GP, Suedee R. *Composite membrane of bacterially-derived cellulose and molecularly imprinted polymer for use as a transdermal enantioselective controlled-release system of racemic propranolol.* Journal of Controlled Release. 2006;**113**(1):43-56.
181. Cacicedo ML, Cesca K, Bosio VE, Porto LM, Castro GR. *Self-assembly of carrageenin–CaCO3 hybrid microparticles on bacterial cellulose films for doxorubicin sustained delivery*. Journal of Applied Biomedicine. 2015;**13**(3):239-48.
182. L. Cacicedo M, E. León I, S. Gonzalez J, M. Porto L, A. Alvarez V, Castro GR. *Modified bacterial cellulose scaffolds for localized doxorubicin release in human colorectal HT-29 cells*. Colloids and Surfaces B: Biointerfaces. 2016;**140**:421-9.
183. Wu S-C, Wu S-M, Su F-M. *Novel process for immobilizing an enzyme on a bacterial cellulose membrane through repeated absorption.* Journal of Chemical Technology & Biotechnology. 2017;**92**(1):109-14.
184. Badshah M, Ullah H, Khan AR, Khan S, Park JK, Khan T. *Surface modification and evaluation of bacterial cellulose for drug delivery*. International Journal of Biological Macromolecules. 2018;**113**:526-33.
185. Trovatti E, Silva NH, Duarte IF, Rosado CF, Almeida IF, Costa P, Freire C, Silvestre AJD, Neto CB. *Biocellulose membranes as supports for dermal release of lidocaine*. Biomacromolecules. 2011;**12**(11):4162-8.
186. Almasi H, Jafarzadeh P, Mehryar L. *Fabrication of novel nanohybrids by impregnation of CuO nanoparticles into bacterial cellulose and chitosan nanofibers: Characterization, antimicrobial and release properties*. Carbohydrate Polymers. 2018;**186**:273-81.
187. Wu CN, Fuh SC, Lin SP, Lin YY, Chen HY, Liu JM, Cheng K. *TEMPO-oxidized bacterial cellulose pellicle with silver nanoparticles for wound dressing*. Biomacromolecules. 2018;**19**(2):544-54.
188. deBoer TR, Chakraborty I, Mascharak PK. *Design and construction of a silver(I)-loaded cellulose-based wound dressing: trackable and sustained release of silver for controlled*

therapeutic delivery to wound sites. Journal of Materials Science Materials in Medicine. 2015;**26**(10):243.

189. Wu J, Zheng Y, Wen X, Lin Q, Chen X, Wu Z. *Silver nanoparticle/bacterial cellulose gel membranes for antibacterial wound dressing: investigation in vitro and in vivo.* Biomedical Materials. 2014;**9**(3):035005.

190. Pourali P, Yahyaei B, Ajoudanifar H, Taheri R, Alavi H, Hoseini A. *Impregnation of the bacterial cellulose membrane with biologically produced silver nanoparticles*. Current Microbiology. 2014;**69**(6):785-93.

191. Berndt S, Wesarg F, Wiegand C, Kralisch D, Müller F. *Antimicrobial porous hybrids consisting of bacterial nanocellulose and silver nanoparticles.* Cellulose. 2013;**20**(2):771-83.

192. Malmir S, Karbalaei A, Pourmadadi M, Hamedi J, Yazdian F, Navaee M. *Antibacterial properties of a bacterial cellulose CQD-TiO2 nanocomposite.* Carbohydrate Polymers. 2020;**234**:115835.

193. Khalid A, Ullah H, Ul-Islam M, Khan R, Khan S, Ahmad F, Khan T, Wahid F. *Bacterial cellulose–TiO2 nanocomposites promote healing and tissue regeneration in burn mice model.* RSC Advances. 2017;**7**(75):47662-8.

194. Barud HdS, de Araújo Júnior AM, Saska S, Mestieri LB, Campos JADB, de Freitas RM, Ferreira NU, Nascimento AP, Miguel FG, de Oliveira Lima Leite Vaz MM, Barizon EA, Marquele-Oliveira F, Gaspar AMM, Ribeiro SJL, Berretta AA. *Antimicrobial brazilian propolis (EPP-AF) containing biocellulose membranes as promising biomaterial for skin wound healing.* Evidence-Based Complementary and Alternative Medicine. 2013;**2013**:703024.

195. Silva NCS, Drumond I, Almeida I, Costa P, Rosado C, Neto C, Freire CSR, Silvestre AJD. *Topical caffeine delivery using biocellulose membranes: A potential innovative system for cellulite treatment.* Cellulose. 2014;**21**(1):665-74.

196. Ahmad N, Amin MC, Mahali SM, Ismail I, Chuang VT. *Biocompatible and mucoadhesive bacterial cellulose-g-poly(acrylic acid) hydrogels for oral protein delivery.* Molecular Pharmaceutics. 2014;**11**(11):4130-42.

197. Molina de Olyveira G, Maria Manzine Costa L, Basmaji P. *Physically modified bacterial cellulose as alternative routes for transdermal drug delivery.* Journal of Biomaterials and Tissue Engineering. 2013;**3**(2):227-32.

198. Sampaio LM, Padrao J, Faria J, Silva JP, Silva CJ, Dourado F, Zille A. *Laccase immobilization on bacterial nanocellulose membranes: Antimicrobial, kinetic and stability properties*. Carbohydrate Polymers. 2016;**145**:1-12.

199. Aramwit P, Bang N. *The characteristics of bacterial nanocellulose gel releasing silk sericin for facial treatment*. BMC biotechnology. 2014;**14**:104.

200. Numata Y, Mazzarino L, Borsali R. *A slow-release system of bacterial cellulose gel and nanoparticles for hydrophobic active ingredients.* International Journal of Pharmaceutics. 2015;**486**(1–2):217-25.

201. Chantereau G, Sharma M, Abednejad A, Vilela C, Costa E, Veiga M, Antunes F, Pintado MM, Sèbe G, Coma V, Freire M.G, Freire CSR, Silvestre AJD. *Bacterial nanocellulose*

membranes loaded with vitamin B-based ionic liquids for dermal care applications. Journal of Molecular Liquids. 2020;**302**:112547.
202. Tarcsay Á, Keserű GM. *Contributions of molecular properties to drug promiscuity*. Journal of Medicinal Chemistry. 2013;**56**(5):1789-95.
203. Lobo S. *Is there enough focus on lipophilicity in drug discovery?* Expert Opinion on Drug Discovery. 2020;**15**(3):261-3.
204. Hu W, Chen S, Xu Q, Wang H. *Solvent-free acetylation of bacterial cellulose under moderate conditions*. Carbohydrate Polymers. 2011;**83**(4):1575-81.
205. Ávila Ramírez JA, Gómez Hoyos C, Arroyo S, Cerrutti P, Foresti ML. *Acetylation of bacterial cellulose catalyzed by citric acid: Use of reaction conditions for tailoring the esterification extent*. Carbohydrate Polymers. 2016;**153**:686-95.
206. Lee K-Y, Quero F, Blaker JJ, Hill CAS, Eichhorn SJ, Bismarck A. *Surface only modification of bacterial cellulose nanofibres with organic acids*. Cellulose. 2011;**18**(3):595-605.
207. Gupta A, Keddie DJ, Kannappan V, Gibson H, Khalil IR, Kowalczuk M, Martin C, Shuai X, Radeck I. *Production and characterisation of bacterial cellulose hydrogels loaded with curcumin encapsulated in cyclodextrins as wound dressings*. European Polymer Journal. 2019;**118**:437-50.
208. Szente L, Fenyvesi É. *Cyclodextrin-lipid complexes: Cavity size matters.* Structural Chemistry. 2017;**28**(2):479-92.
209. Chantereau G, Sharma M, Abednejad A, Neves BM, Sèbe G, Coma V, Freire MG, Freire CSR, Silvestre AJD. *Design of nonsteroidal anti-inflammatory drug-based ionic liquids with improved water solubility and drug delivery.* ACS Sustainable Chemistry & Engineering. 2019;**7**(16):14126-34.
210. Radek KA, Matthies AM, Burns AL, Heinrich SA, Kovacs EJ, Dipietro LA. *Acute ethanol exposure impairs angiogenesis and the proliferative phase of wound healing.* American Journal of Physiology Heart and Circulatory Physiology. 2005;**289**(3):1084-90.
211. Shah DK, Khandavilli S, Panchagnula R. *Alteration of skin hydration and its barrier function by vehicle and permeation enhancers: a study using TGA, FTIR, TEWL and drug permeation as markers.* Methods and Findings in Experimental and Clinical Pharmacology. 2008;**30**(7):499-512.
212. Numata Y, Muromoto K, Furukawa H, Gong JP, Tajima K, Munekata M. *Nonvolatile and shape-memorized bacterial cellulose gels swollen by poly(ethylene glycol).* Polymer Journal. 2009;**41**(7):524-5.
213. Tsai Y-H, Yang Y-N, Ho Y-C, Tsai M-L, Mi F-L. *Drug release and antioxidant/antibacterial activities of silymarin-zein nanoparticle/bacterial cellulose nanofiber composite films.* Carbohydrate Polymers. 2018;**180**:286-96.
214. Santos P, Watkinson AC, Hadgraft J, Lane ME. *Application of microemulsions in dermal and transdermal drug delivery*. Skin Pharmacology and Physiology. 2008;**21**(5):246-59.
215. Pastore MN, Kalia YN, Horstmann M, Roberts MS. *Transdermal patches: History, development and pharmacology.* British Journal of Pharmacology. 2015;**172**(9):2179-209.

216. Bos JD, Meinardi MM. *The 500 Dalton rule for the skin penetration of chemical compounds and drugs.* Experimental Dermatology. 2000;**9**(3):165-9.
217. Guy RH, Hadgraft J. *Selection of drug candidates for transdermal drug delivery*. Transdermal Drug Delivery New York: Marcel Dekker. 1989:59-81.
218. Hao Y, Li W, Zhou X, Yang F, Qian Z. *Microneedles-based transdermal drug delivery systems: A review.* Journal of Biomedical Nanotechnology. 2017;**13**(12):1581-97.
219. Yoon J, Park D, Son T, Seo J, Nelson JS, Jung B. *A physical method to enhance transdermal delivery of a tissue optical clearing agent: combination of microneedling and sonophoresis*. Lasers in Surgery and Medicine. 2010;**42**(5):412-7.
220. Benson HAE, McIldowie M, Prow T. *Magnetophoresis: Skin penetration enhancement by a magnetic field*. In: Dragicevic N, I. Maibach H, editors. Percutaneous Penetration Enhancers Physical Methods in Penetration Enhancement. Berlin, Heidelberg: Springer Berlin Heidelberg; 2017:195-206.
221. Dragicevic N, Maibach HI. *Percutaneous penetration enhancers chemical methods in penetration enhancement*: Nanocarriers: Springer; 2016.
222. Mathur V, Satrawala Y, Rajput MS. *Physical and chemical penetration enhancers in transdermal drug delivery system*. Asian Journal of Pharmaceutics. 2014;**4**(3).
223. Chen S, Hanning S, Falconer J, Locke M, Wen J. *Recent advances in non-ionic surfactant vesicles (niosomes): Fabrication, characterization, pharmaceutical and cosmetic applications*. European Journal of Pharmaceutics and Biopharmaceutics. 2019;**144**:18-39.
224. Cheng YC, Li TS, Su HL, Lee PC, Wang HD. *Transdermal delivery systems of natural products applied to skin therapy and care*. Molecules. 2020;25(21):5051.
225. Crommelin DJA, van Hoogevest P, Storm G. *The role of liposomes in clinical nanomedicine development. What now? Now what?*. Journal of Controlled Release. 2020;**318**:256-63.
226. Chen B-H, Stephen Inbaraj B. *Nanoemulsion and nanoliposome based strategies for improving anthocyanin stability and bioavailability*. Nutrients. 2019;**11**(5):1052.
227. Chacko IA, Ghate VM, Dsouza L, Lewis SA. *Lipid vesicles: A versatile drug delivery platform for dermal and transdermal applications.* Colloids and Surfaces B: Biointerfaces. 2020;**195**:111262.
228. Bangham AD, Standish MM, Watkins JC. *Diffusion of univalent ions across the lamellae of swollen phospholipids*. Journal of Molecular Biology. 1965;**13**(1):238-27.
229. Akbarzadeh A, Rezaei-Sadabady R, Davaran S, Joo SW, Zarghami N, Hanifehpour Y, Samiei M, Kouhi M, Nejati-Koshki K. *Liposome: Classification, preparation, and applications.* Nanoscale Research Letters. 2013;**8**(1):102.
230. Pierre MB, Dos Santos Miranda Costa I. *Liposomal systems as drug delivery vehicles for dermal and transdermal applications.* Archives of Dermatological Research. 2011;**303**(9):607-21.
231. Mezei M, Gulasekharam V. *Liposomes--a selective drug delivery system for the topical route of administration. Lotion dosage form.* Life sciences. 1980;**26**(18):1473-7.
232. Touitou E, Junginger HE, Weiner ND, Nagai T, Mezei M. *Liposomes as carriers for topical and transdermal delivery.* Journal of Pharmaceutical Sciences. 1994;**83**(9):1189-203.

233. Barenholz Y. *Doxil®--the first FDA-approved nano-drug: Lessons learned*. Journal of Controlled Release. 2012;**160**(2):117-34.
234. Bulbake U, Doppalapudi S, Kommineni N, Khan W. *Liposomal formulations in clinical use: An updated review*. Pharmaceutics. 2017;**9**(2):12.
235. Sood S, Jain K, Gowthamarajan K. *Optimization of curcumin nanoemulsion for intranasal delivery using design of experiment and its toxicity assessment.* Colloids and Surfaces B: Biointerfaces. 2014;**113**:330-7.
236. Rai VK, Mishra N, Yadav KS, Yadav NP. *Nanoemulsion as pharmaceutical carrier for dermal and transdermal drug delivery: Formulation development, stability issues, basic considerations and applications.* Journal of Controlled Release. 2018;**270**:203-25.
237. Aboofazeli R. *Nanometric-scaled emulsions (nanoemulsions).* Iranian Journal of Pharmaceutical Research. 2010;**9**(4):325.
238. Singh Y, Meher JG, Raval K, Khan FA, Chaurasia M, Jain NK, Chourasia MK. *Nanoemulsion: concepts, development and applications in drug delivery*. Journal of Controlled Release. 2017;**252**:28-49.
239. Sigward E, Mignet N, Rat P, Dutot M, Muhamed S, Guigner JM, Scherman D, Brossard D, Crauste-Manciet S. *Formulation and cytotoxicity evaluation of new self-emulsifying multiple W/O/W nanoemulsions*. International Journal of Nanomedicine. 2013;**8**:611-25.
240. Shakeel F, Baboota S, Ahuja A, Ali J, Shafiq S. *Celecoxib nanoemulsion: Skin permeation mechanism and bioavailability assessment.* Journal of Drug Targeting. 2008;**16**(10):733-40.
241. Lovelyn C, Attama AA. *Current state of nanoemulsions in drug delivery.* Journal of Biomaterials and Nanobiotechnology. 2011;**2**(05):626.
242. Kabanov AV, Batrakova EV, Alakhov VY. *Pluronic® block copolymers as novel polymer therapeutics for drug and gene delivery.* Journal of Controlled Release. 2002;**82**(2–3):189-212.
243. Yapar EA, Inal O. *Poly(ethylene oxide)-Poly(propylene oxide)-based copolymers for transdermal drug delivery: An overview*. Tropical Journal of Pharmaceutical Research. 2012;**11**(5):855-66.
244. Zarrintaj P, Ramsey JD, Samadi A, Atoufi Z, Yazdi MK, Ganjali MR, Amirabad LM, Zangene E, Farokhi M, Formela K, Saeb MR, Mozafari M, Thomas S. *Poloxamer: A versatile tri-block copolymer for biomedical applications*. Acta Biomaterialia. 2020;**110**:37-67.
245. Ruel-Gariépy E, Leroux JC. *In situ-forming hydrogels - Review of temperature-sensitive systems*. European Journal of Pharmaceutics and Biopharmaceutics. 2004;**58**(2):409-26.
246. Russo E, Villa C. *Poloxamer hydrogels for biomedical applications*. Pharmaceutics. 2019;**11**(12):671.
247. Johnston TP, Palmer WK. *Mechanism of poloxamer 407-induced hypertriglyceridemia in the rat.* Biochemical Pharmacology. 1993;**46**(6):1037-42.
248. Zhao YZ, Jiang X, Xiao J, Lin Q, Yu WZ, Tian FR, Mao K, Yang W, Wong HL, Lu C. *Using NGF heparin-poloxamer thermosensitive hydrogels to enhance the nerve regeneration for spinal cord injury.* Acta Biomaterialia. 2016;**29**:71-80.

249. El-Aassar MR, El fawal GF, El-Deeb NM, Hassan HS, Mo X. *Electrospun polyvinyl alcohol/ pluronic F127 blended nanofibers containing titanium dioxide for antibacterial wound dressing.* Applied Biochemistry and Biotechnology. 2016;**178**(8):1488-502.
250. de Araújo DR, Oshiro A, da Silva DC, Akkari ACS, de Mello JC, Rodrigues T. *Poloxamers as drug-delivery systems: physicochemical, pharmaceutical, and toxicological aspects.* Nanotoxicology: Springer; 2014:281-98.
251. Hou Y, Song Y, Sun X, Jiang Y, He M, Li Y, Chen X, Zhang L. *Multifunctional composite hydrogel bolus with combined self-healing, antibacterial and adhesive functions for radiotherapy*. Journal of Materials Chemistry B. 2020;**8**(13):2627-35.
252. Brown MB, Martin GP, Jones SA, Akomeah FK. *Dermal and transdermal drug delivery systems: current and future prospects*. Drug Delivery. 2006;**13**(3):175-187.
253. Kassem AA, Abd El-Alim SH. *Vesicular nanocarriers: A potential platform for dermal and transdermal drug delivery.* In: Yata VK, Ranjan S, Dasgupta N, Lichtfouse E, editors. Nanopharmaceuticals: Principles and Applications Vol 2. Cham: Springer International Publishing; 2021:155-209.
254. Kumar S, Rao R, Kumar A, Mahant S, Nanda S. *Novel carriers for coenzyme Q10 delivery.* Current Drug Delivery. 2016;**13**(8):1184-1204.
255. Schniertshauer D, Müller S, Mayr T, Sonntag T, Gebhard D, Bergemann J. *Accelerated regeneration of ATP level after Irradiation in human skin fibroblasts by coenzyme Q10*. Photochemistry and Photobiology. 2016;**92**(3):488-94.
256. Crane FL. *Discovery of ubiquinone (coenzyme Q) and an overview of function*. Mitochondrion. 2007;**7**:2-7.
257. Cordero MD, Cano-García FJ, Alcocer-Gómez E, De Miguel M, Sánchez-Alcázar JA. *Oxidative stress correlates with headache symptoms in fibromyalgia: coenzyme Q_{10} effect on clinical improvement*. PloS one. 2012;**7**(4):35677.
258. Hoppe U, Bergemann J, Diembeck W, Ennen J, Gohla S, Harris I, Jacob J, Kielholz J, Mei W, Pollet D, Schachtschabel D, Sauermann G, Schreiner V, Stäb F, Steckel F. *Coenzyme Q10, a cutaneous antioxidant and energizer*. BioFactors. 1999;**9**(2-4):371-378.
259. Yue Y, Zhou H, Liu G, Li Y, Yan Z, Duan M. *The advantages of a novel CoQ10 delivery system in skin photo-protection*. International Journal of Pharmaceutics. 2010;**392**(1–2):57-63.
260. Kim J, Kim K, Sung GY. *Coenzyme Q10 efficacy test for human skin equivalents using a pumpless skin-on-a-chip system.* International Journal of Molecular Sciences. 2020;**21**(22):8475-8486
261. Korkm E, Gokce EH, Ozer O. *Development and evaluation of coenzyme Q10 loaded solid lipid nanoparticle hydrogel for enhanced dermal delivery*. Acta Pharmaceutica Sinica. B. 2013;**63**(4):517-29.
262. Basch E, Boon H, Heerema TD, Foppo I, Hashmi S, Hasskarl J, Sollars D, Ulbricht C. *Boswellia: An evidence-based systematic review by the natural standard research collaboration*. Journal of Herbal Pharmacotherapy. 2004;**4**(3):63-83.
263. Abdel-Tawab M, Werz O, Schubert-Zsilavecz M. *Boswellia serrata. Clinical* Pharmacokinetics. 2011;**50**(6):349-69.

264. Poeckel D, Werz O. *Boswellic acids: Biological actions and molecular targets*. Current Medicinal Chemistry. 2006;**13**(28):3359-3369.
265. Sengupta K, Kolla JN, Krishnaraju AV, Yalamanchili N, Rao CV, Golakoti T, Raychaudhuri S, Raychaudhuri SP. *Cellular and molecular mechanisms of anti-inflammatory effect of Aflapin: A novel Boswellia serrata extract*. Molecular and Cellular Biochemistry. 2011;**354**(1):189-97.
266. Sasaki F, Yokomizo T. *The leukotriene receptors as therapeutic targets of inflammatory diseases.* International Immunology. 2019;**31**(9):607-615.
267. Gilbert NC, Gerstmeier J, Schexnaydre EE, Börner F, Garscha U, Neau DB, Werz O, Newcomer M. *Structural and mechanistic insights into 5-lipoxygenase inhibition by natural products*. Nature Chemical Biology. 2020;**16**(7):783-90.
268. Pengzong Z, Yuanmin L, Xiaoming X, Shang D, Wei X, Zhigang L, et al. *Wound healing potential of the standardized extract of Boswellia serrata on experimental diabetic foot ulcer via inhibition of inflammatory, angiogenetic and apoptotic markers.* Planta Medica. 2019;**85**(8):657-669.
269. Mehta M, Satija S, Nanda A, Garg M. *Nanotechnologies for boswellic acids.* American Journal of Drug Discovery and Development. 2014;**4**(1):1-11.
270. Malanovic N, Ön A, Pabst G, Zellner A, Lohner K. *Octenidine: Novel insights into the detailed killing mechanism of Gram-negative bacteria at a cellular and molecular level.* International Journal of Antimicrobial Agents. 2020;**56**(5):106-146.
271. Hubner NO, Siebert J, Kramer A. *Octenidine dihydrochloride, a modern antiseptic for skin, mucous membranes and wounds*. Skin Pharmacology and Physiology. 2010;**23**(5):244-258.
272. Sedlock DM, Bailey DM. *Microbicidal activity of octenidine hydrochloride, a new alkanediylbis[pyridine] germicidal agent*. Antimicrobial Agents and Chemotherapy. 1985;**28**(6):786-790.
273. Hardy K, Sunnucks K, Gil H, Shabir S, Trampari E, Hawkey P, Webber M. *Increased usage of antiseptics is associated with reduced susceptibility in clinical isolates of Staphylococcus aureus*. mBio. 2018;**9**(3):894-904.
274. Bührer C, Bahr S, Siebert J, Wettstein R, Geffers C, Obladen M. *Use of 2% 2-phenoxyethanol and 0.1% octenidine as antiseptic in premature newborn infants of 23–26 weeks gestation.* Journal of Hospital Infection. 2002;**51**(4):305-7.
275. Chum JD, Lim DJZ, Sheriff SO, Pulikkotil SJ, Suresh A, Davamani F. *In vitro evaluation of octenidine as an antimicrobial agent against Staphylococcus epidermidis in disinfecting the root canal system*. Restorative Dentistry and Endodontics. 2019;**44**(1):8-16.
276. Slee AM, O'Connor JR. *In vitro antiplaque activity of octenidine dihydrochloride (WIN 41464-2) against preformed plaques of selected oral plaque-forming microorganisms*. Antimicrobial Agents and Chemotherapy. 1983;**23**(3):379-384.
277. Eisenbeiss W, Siemers F, Amtsberg G, Hinz P, Hartmann B, Kohlmann T, Ekkernkamp A, Albrecht U, Assadian O, Kramer A. *Prospective, double-blinded, randomised controlled trial assessing the effect of an Octenidine-based hydrogel on bacterial colonisation and epithelialization of skin graft wounds in burn patients*. International Journal of Burns and Trauma. 2012;**2**:71-79.

278. Tirali RE, Bodur H, Sipahi B, Sungurtekin E. *Evaluation of the antimicrobial activities of chlorhexidine gluconate, sodium hypochlorite and octenidine hydrochloride in vitro*. Australian Endodontic Journal 2013;**39**:15-28.
279. Jenull S, Hojdar K, Laggner H, Velimirov B, Zemann N, Huettinger M. *Cell growth and migration under octenidine-antiseptic treatment*. Journal of wound care. 2015;**24**(6):280-288.
280. Torgbo S, Sukyai P. *Bacterial cellulose-based scaffold materials for bone tissue engineering*. Applied Materials Today. 2018;**11**:34-49.
281. Roman M, Haring AP, Bertucio TJ. *The growing merits and dwindling limitations of bacterial cellulose-based tissue engineering scaffolds.* Current Opinion in Chemical Engineering. 2019;**24**:98-106.
282. Khan S, Ul-Islam M, Ikram M, Islam SU, Ullah MW, Israr M, Jang JH, Yoon S, Park JK. *Preparation and structural characterization of surface modified microporous bacterial cellulose scaffolds: A potential material for skin regeneration applications in vitro and in vivo*. International Journal of Biological Macromolecules. 2018;**117**:1200-1210.
283. Klemm D, Ahrem H, Kramer F, Fried W, Wippermann J, Kinne RW. *Bacterial nanocellulose hydrogels designed as bioartificial medical implants*. Bacterial NanoCellulose a Sophisticated Multifunctional Material; Gama, M, Gatenholm, P, Klemm, D, Eds. 2013:175-196.
284. Irene A-S, Uwe B, Anna L, Anna R, Dana K. *Opportunities of bacterial cellulose to treat epithelial tissues*. Current Drug Targets. 2019;**20**(8):808-22.
285. Zeng M, Laromaine A, Roig A. *Bacterial cellulose films: influence of bacterial strain and drying route on film properties.* Cellulose. 2014;**21**(6):4455-69.
286. Klemm D, Kramer F, Moritz S, Lindström T, Ankerfors M, Gray D, Dorris A. *Nanocelluloses: A new family of nature-based materials.* Angewandte Chemie International Edition. 2011;**50**(24):5438-5466.
287. Klemm D, Cranston ED, Fischer D, Gama M, Kedzior SA, Kralisch D, Kramer F, Kondo T, Lindström T, Nietzsche S,8Petzold-Welcke K, Rauchfuß F. *Nanocellulose as a natural source for groundbreaking applications in materials science: Today's state*. Materials Today. 2018;**21**(7):720-748.
288. Abd E, Benson HAE, Roberts MS, Grice JE. *Minoxidil skin delivery from nanoemulsion formulations containing eucalyptol or oleic acid: enhanced diffusivity and follicular targeting*. Pharmaceutics. 2018;**10**(1):19.
289. Blume G. *Colloidal carrier system with penetration properties for encapsulating lipophilic active agents and oils for topical use*. WO002012089184A3; 2015.
290. Anderson BC, Pandit NK, Mallapragada SK. *Understanding drug release from poly(ethylene oxide)-b-poly(propylene oxide)-b-poly(ethylene oxide) gels*. Journal of Controlled Release. 2001;**70(**1–2):157-67.
291. Jiang J, Li C, Rafailovich MH, Sokolov JC. *Rheological and morphological characterization of triblock copolymer (PEO-PPO-PEO)-clay gel in aqueous solution*. MRS Online Proceedings Library. 2005;**898**(1):1-5.
292. Harke HP. Octenidine dihydrochloride, properties of a new antimicrobial agent. International Journal of Hygiene and Environmental Medicine. 1989;**188**:188-191.

293. Alkhatib Y, Blume G, Thamm J, Steiniger F, Kralisch D, Fischer D. *Overcoming the hydrophilicity of bacterial nanocellulose: Incorporation of the lipophilic coenzyme Q10 using lipid nanocarriers for dermal applications*. European Journal of Pharmaceutics and Biopharmaceutics. 2021;**158:**106-112.
294. Karl B, Alkhatib Y, Beekmann U, Bellmann T, Blume G, Steiniger F, Thamm J, Werz O, Kralisch D, Fischer D. *Development and characterization of bacterial nanocellulose loaded with Boswellia serrata extract containing nanoemulsions as natural dressing for skin diseases*. International Journal of Pharmaceutics. 2020;**587**:119635.
295. Alkhatib Y, Dewaldt M, Moritz S, Nitzsche R, Kralisch D, Fischer D. *Controlled extended octenidine release from a bacterial nanocellulose/Poloxamer hybrid system.* European Journal of Pharmaceutics and Biopharmaceutics. 2017;**112**:164-76.
296. Gelin K, Bodin A, Gatenholm P, Mihranyan A, Edwards K, Strømme M. *Characterization of water in bacterial cellulose using dielectric spectroscopy and electron microscopy*. Polymer. 2007;**48**(26):7623-31.
297. Ul-Islam M, Khan T, Park JK. *Water holding and release properties of bacterial cellulose obtained by in situ and ex situ modification*. Carbohydrate Polymers. 2012;**88**(2):596-603.
298. Yano S, Maeda H, Nakajima M, Hagiwara T, Sawaguchi T. *Preparation and mechanical properties of bacterial cellulose nanocomposites loaded with silica nanoparticles*. Cellulose. 2008;**15**(1):111-120.
299. Muller A, Zink M, Hessler N, Wesarg F, Muller FA, Kralisch D, Fischer D. *Bacterial nanocellulose with a shape-memory effect as potential drug delivery system*. Royal Society of Chemistry Advances. 2014;**4**(100):57173-84.
300. White R, Cutting K. *Modern exudate management: a review of wound treatments*. World Wide Wounds. 2006;**1**.
301. Wang J, Wan YZ, Luo HL, Gao C, Huang Y. *Immobilization of gelatin on bacterial cellulose nanofibers surface via crosslinking technique.* Materials Science and Engineering: C. 2012;**32**(3):536-41.
302. Kingkaew J, Kirdponpattara S, Sanchavanakit N, Pavasant P, Phisalaphong *M. Effect of molecular weight of chitosan on antimicrobial properties and tissue compatibility of chitosan-impregnated bacterial cellulose films*. Biotechnology and Bioprocess Engineering. 2014;**19**(3):534-544.
303. Nakayama A, Kakugo A, Gong JP, Osada Y, Takai M, Erata T, Kawano S. *High mechanical strength double-network hydrogel with bacterial cellulose*. Advanced Functional Materials. 2004;**14**(11):1124-1128.
304. Abeer MM, Mohd Amin MCI, Martin C. *A review of bacterial cellulose-based drug delivery systems: their biochemistry, current approaches and future prospects*. Journal of Pharmacy and Pharmacology. 2014;**66**(8):1047-1061.
305. Ul-Islam M, Khan T, Khattak WA, Park JK. *Bacterial cellulose-MMTs nanoreinforced composite films: novel wound dressing material with antibacterial properties.* Cellulose. 2013;**20**(2):589-596.

306. Numata Y, Sakata T, Furukawa H, Tajima K. *Bacterial cellulose gels with high mechanical strength*. Materials Science and Engineering: C. 2015;**47**:57-62.
307. Urbina L, Algar I, García-Astrain C, Gabilondo N, González A, Corcuera M, Eceiza A, Retegi A. Biodegradable composites with improved barrier properties and transparency from the impregnation of PLA to bacterial cellulose membranes. Journal of Applied Polymer Science. 2016;**133**(28):43669.
308. Almeida IF, Pereira T, Silva NHCS, Gomes FP, Silvestre AJD, Freire CSR, Lobo JMS, Costa PC. *Bacterial cellulose membranes as drug delivery systems: An in vivo skin compatibility study*. European Journal of Pharmaceutics and Biopharmaceutics. 2014;**86**(3):332-336.
309. Wiegand C, Abel M, Ruth P, Hipler U-C. *HaCaT keratinocytes in co-culture with Staphylococcus aureus can be protected from bacterial damage by polihexanide*. Wound Repair and Regeneration. 2009;**17**(5):730-8.
310. Schlenk F, Werner S, Rabel M, Jacobs F, Bergemann C, Clement JH, Fischer D. *Comprehensive analysis of the in vitro and ex ovo hemocompatibility of surface engineered iron oxide nanoparticles for biomedical applications*. Archives of Toxicology. 2017:**91**:3271–3286.
311. Warncke P, Fink S, Wiegand C, Hipler UC, Fischer D. *A shell-less hen's egg test as infection model to determine the biocompatibility and antimicrobial efficacy of drugs and drug formulations against Pseudomonas aeruginosa.* International Journal of Pharmaceutics. 2020;**585**:119557.
312. Russell WMS, Burch RL. *The principles of humane experimental technique*: Methuen; 1959.
313. Interagency Coordinating Committee on the Validation of Alternative Methods (ICCVAM), 2010. *ICCVAM test method evaluation report: Current validation status of in vitro test methods proposed for identifying eye injury hazard potential of chemicals and products* (Appendix B3, NIH Publication No. 10-7553).
314. Vargas A, Zeisser-Labouebe M, Lange N, Gurny R, Delie F. *The chick embryo and its chorioallantoic membrane (CAM) for the in vivo evaluation of drug delivery systems*. Advanced Drug Delivery Reviews. 2007;**59**(11):1162-1176.
315. Luepke NP, Kemper FH. *The HET-CAM test: An alternative to the draize eye test*. Food and Chemical Toxicology. 1986;**24**(6-7):495-496.
316. Luepke NP. *Hen's egg chorioallantoic membrane test for irritation potential*. Food and Chemical Toxicology. 1985;**23**(2):287-291.
317. Helenius G, Bäckdahl H, Bodin A, Nannmark U, Gatenholm P, Risberg B. *In vivo biocompatibility of bacterial cellulose.* Journal of Biomedical Materials Research Part A. 2006;**76**(2):431-8.
318. Marquardt C, Matuschek C, Bölke E, Gerber P, Peiper M, Seydlitz-Kurzbach Jv, Buhren B A, van Griensven M, Budach W, Hassan M, Kukova G, Mota R, Höfer D, Orth K, Fleischmann W. *Evaluation of the tissue toxicity of antiseptics by the hen's egg test on the chorioallantoic membrane (HETCAM)*. European Journal of Medical Research. 2010;**15**(5):204-209.
319. Bartosova L, Bajgar J. *Transdermal drug delivery in vitro using diffusion cells*. Current Medicinal Chemistry. 2012;**19**(27):4671-4677.

320. OECD (2004), *Test No. 428: Skin Absorption: In Vitro Method, OECD Guidelines for the Testing of Chemicals,* Section 4, OECD Publishing, Paris.
321. Gurtovenko AA, Mukhamadiarov EI, Kostritskii AY, Karttunen M. *Phospholipid–cellulose interactions: Insight from atomistic computer simulations for understanding the impact of cellulose-based materials on plasma membranes.* The Journal of Physical Chemistry B. 2018;**122**(43):9973-9981.
322. Luo H, Ao H, Li G, Li W, Xiong G, Zhu Y, Wan Y. *Bacterial cellulose/graphene oxide nanocomposite as a novel drug delivery system*. Current Applied Physics. 2017;**17**(2):249-254.
323. Ritger PL, Peppas NA. *A simple equation for description of solute release II. Fickian and anomalous release from swellable devices*. Journal of Controlled Release. 1987;**5**(1):37-42.
324. Inoue BS, Streit S, dos Santos Schneider AL, Meier MM. *Bioactive bacterial cellulose membrane with prolonged release of chlorhexidine for dental medical application*. International Journal of Biological Macromolecules. 2020;**148**:1098-1108.
325. Gilbert JC, Richardson JL, Davies MC, Palin KJ, Hadgraft J. *The effect of solutes and polymers on the gelation properties of pluronic F-127 solutions for controlled drug delivery*. Journal of Controlled Release. 1987;**5**(2):113-118.
326. Ricci E, Lunardi L, Nanclares D, Marchetti J. *Sustained release of lidocaine from Poloxamer 407 gels.* International Journal of Pharmaceutics. 2005;**288**(2):235-244.
327. Ricci E, Bentley M, Farah M, Bretas R, Marchetti J. *Rheological characterization of Poloxamer 407 lidocaine hydrochloride gels*. European Journal of Pharmaceutical Sciences. 2002;**17**(3):161-167.
328. Nasir F, Iqbal Z, Khan JA, Khan A, Khuda F, Ahmad L, Khan A, Khan A, Dayoo A, Roohullah. *Development and evaluation of diclofenac sodium thermorevesible subcutaneous drug delivery system*. International Journal of Pharmaceutics. 2012;**439**(1–2):120-126.
329. Karlina MV, Pozharitskaya ON, Kosman VM, Ivanova SA. *Bioavailability of boswellic acids: in vitro/in vivo correlation.* Pharmaceutical Chemistry Journal. 2007;**41**(11):569-572.
330. Ritger PL, Peppas NA. *A simple equation for description of solute release I. Fickian and non-fickian release from non-swellable devices in the form of slabs, spheres, cylinders or discs*. Journal of Controlled Release. 1987;**5**(1):23-36.
331. Li Y, Wang S, Huang R, Huang Z, Hu B, Zheng W, Yang G, Jiang X. *Evaluation of the effect of the structure of bacterial cellulose on full thickness skin wound repair on a microfluidic chip*. Biomacromolecules. 2015;**16**(3):780-789.
332. Loh EYX, Fauzi MB, Ng MH, Ng PY, Ng SF, Mohd Amin MCI. *Insight into delivery of dermal fibroblast by non-biodegradable bacterial nanocellulose composite hydrogel on wound healing*. International Journal of Biological Macromolecules. 2020;**159**:497-509.
333. Kwak MH, Kim JE, Go J, Koh EK, Song SH, Son HJ, Kim HS, Yun YH, Jung YJ, Hwang DY. *Bacterial cellulose membrane produced by Acetobacter sp. A10 for burn wound dressing applications*. Carbohydrate Polymers. 2015;**122**:387-98.
334. Serra R, Grande R, Butrico L, Rossi A, Settimio UF, Caroleo B, Amato B, Gallelli L, de Franciscis S. *Chronic wound infections: the role of Pseudomonas aeruginosa and Staphylococcus aureus*. Expert Review of Anti-Infective Therapy. 2015;**13**(5):605-613.

335. Cendra MdM, Blanco-Cabra N, Pedraz L, Torrents E. *Optimal environmental and culture conditions allow the in vitro coexistence of Pseudomonas aeruginosa and Staphylococcus aureus in stable biofilms*. Scientific Reports. 2019;**9**(1):162-184.
336. NCCLS M27-A2. *Reference method for broth dilution antifungal susceptibility testing of yeasts; approved standard-second edition*. Clinical and Laboratory Standards Institute 2002.
337. Maneerung T, Tokura S, Rujiravanit R. *Impregnation of silver nanoparticles into bacterial cellulose for antimicrobial wound dressing*. Carbohydrate Polymers. 2008;**72**(1):43-51.
338. Stocks S. *Mechanism and use of the commercially available viability stain, BacLight.* Cytometry Part A. 2004;**61**(2):189-195.
339. Naik A, Kalia YN, Guy RH. *Transdermal drug delivery: Overcoming the skin's barrier function*. Pharmaceutical Science & Technology Today. 2000;**3**(9):318-326.
340. Lucangioli S, Tripodi V. *The importance of the formulation in the effectiveness of coenzyme Q10 supplementation in mitochondrial disease therapy*. Der Pharmacia Sinica. 2012;**3**(4):406-407.
341. Pielenhofer J, Sohl J, Windbergs M, Langguth P, Radsak MP. *Current progress in particle-based systems for transdermal vaccine delivery*. Frontiers in Immunology. 2020;**11**:266-274.
342. Sonneville-Aubrun O, Simonnet JT, L'Alloret F. *Nanoemulsions: A new vehicle for skincare products.* Advances in Colloid and Interface Science. 2004;**108-109**:145-9.
343. Shaker DS, Ishak RA, Ghoneim A, Elhuoni MA. Nanoemulsion: *A review on mechanisms for the transdermal delivery of hydrophobic and hydrophilic drugs*. Scientia Pharmaceutica. 2019;**87**(3):17.
344. Schwarz JC, Klang V, Karall S, Mahrhauser D, Resch GP, Valenta C. *Optimisation of multiple W/O/W nanoemulsions for dermal delivery of aciclovir.* International Journal of Pharmaceutics. 2012;**435**(1):69-75.
345. Lademann J, Jacobi U, Surber C, Weigmann HJ, Fluhr JW. *The tape stripping procedure – evaluation of some critical parameters*. European Journal of Pharmaceutics and Biopharmaceutics. 2009;**72**(2):317-323.
346. Jacobi U, Kaiser M, Toll R, Mangelsdorf S, Audring H, Otberg N, Sterry W, Lademann J. *Porcine ear skin: an in vitro model for human skin.* Skin Research and Technology. 2007;**13**(1):19-24.
347. Klang V, Schwarz JC, Lenobel B, Nadj M, Auböck J, Wolzt M, Valenta, C. *In vitro vs. in vivo tape stripping: Validation of the porcine ear model and penetration assessment of novel sucrose stearate emulsions.* European Journal of Pharmaceutics and Biopharmaceutics. 2012;**80**(3):604-14.
348. Sah A, Mukherjee S, Wickett R. *An in vitro study of the effects of formulation variables and product structure on percutaneous absorption of lactic acid.* Journal of the Society of Cosmetic Chemists. 1998;**49**(4):257-73.
349. Ferreira L, Seiller M, Grossiord J, Marty J, Wepierre J. *Vehicle influence on in vitro release of glucose: w/o, w/o/w and o/w systems compared.* Journal of Controlled Release. 1995;**33**(3):349-356.

350. Alkilani AZ, McCrudden MT, Donnelly RF. *Transdermal drug delivery: Innovative pharmaceutical developments based on disruption of the barrier properties of the stratum corneum*. Pharmaceutics. 2015;**7**(4):438- 470.
351. Teeranachaideekul V, Souto EB, Junyaprasert VB, Müller RH. *Cetyl palmitate-based NLC for topical delivery of coenzyme Q10 – development, physicochemical characterization and in vitro release studies*. European Journal of Pharmaceutics and Biopharmaceutics. 2007;**67**(1):141- 148.
352. Zhou H, Yue Y, Liu G, Li Y, Zhang J, Yan Z, Duan M. *Characterisation and skin distribution of lecithin-based coenzyme Q10-loaded lipid nanocapsules.* Nanoscale Research Letters. 2010;**5**(10):1561- 1569.

Attachments

Publication list:

Peer-reviewed publications

H. Rothe, J. Rost, F. Kramer, Y. Alkhatib, K. Petzold-Welcke, D. Klemm, D. Fischer, K. Liefeith
Bacterial nanocellulose: Reinforcement of compressive strength using an adapted mobile matrix reservoir technology and suitable post-modification strategies
Accepted at Journal of the Biomechanical Behavior of Biomedical Materials

Y. Alkhatib, G. Blume, J. Thamm, F. Steiniger, D. Kralisch, D. Fischer
Overcoming the hydrophilicity of bacterial nanocellulose: Incorporation of the lipophilic coenzyme Q10 using lipid nanocarriers for dermal applications
European Journal of Pharmaceutics and Biopharmaceutics, 2021, 158, P. 106-112

B. Karl, Y. Alkhatib, U. Beekmann, T. Bellmann, G. Blume, F. Steiniger, J. Thamm, O. Werz, D. Kralisch, D. Fischer
Development and characterization of bacterial nanocellulose loaded with *Boswellia serrata* extract containing nanoemulsions as natural dressing for skin diseases
International Journal of Pharmaceutics, 2020, 587, Article 119635

Y. Alkhatib, M. Dewaldt, S. Moritz, R. Nitzsche, D. Kralisch, D. Fischer
Controlled extended octenidine release from a bacterial nanocellulose/Poloxamer hybrid system
European Journal of Pharmaceutics and Biopharmaceutics, 2017, 112, p. 164-176

Patent

D. Fischer, Y. Alkhatib, G. Blume
"Einbringen von schwer und/oder nicht wasserlöslichen Wirkstoffen mittels auf Lipiden basierenden Nanopartikeln/Vesikeln in ein hydrophiles aus Cellulose bestehendes dreidimensionales Netzwerk"
DE 102017000368A1, Patent ceased

Presentations

Y. Alkhatib, M. Dewaldt, S. Moritz, D. Kralisch, D. Fischer
Bacterial nanocellulose for sustained drug release in skin applications
German Society for Biomaterials (DGBM), Annual Meeting, 9th – 11th November 2017, Wurzburg, Germany

Alkhatib, Y., Blume, G., Fahr, A.
Niosomes as topical drug delivery system: preparation, characterization and skin penetration studies
23rd Mountain /Sea Liposome Workshop, 24th – 28th March 2014, Oberjoch, Germany

Abstracts and posters

B. Karl, Y. Alkhatib, U. Beekmann, G. Blume, S. Lorkowski, D. Kralisch, O. Werz, D. Fischer
A Toolbox of Pharmaceutical Strategies for the Controllable Skin Delivery of Boswellia Extracts using Bacterial Nanocellulose
4th International Symposium on Bacterial Nanocellulose (ISBNC), 3rd – 4th October, 2019, Porto, Portugal

B. Karl, Y. Alkhatib, U. Beekmann, G. Blume, S. Lorkowski, D. Kralisch, O. Werz, D. Fischer
The role of additives for bacterial nanocellulose to enhance the penetration of anti-inflammatory frankincense extract into skin
Controlled release society (CRS) Germany Local Chapter, 23rd Annual Meeting, 7th – 8th March 2019, Leipzig, Germany

B. Karl, Y. Alkhatib, U. Beekmann, G. Blume, D. Kralisch, O. Werz, S. Lorkowski, D. Fischer
Bacterial nanocellulose loaded with frankincense extract as natural wound dressing to treat local dermal inflammations
5th European Symposium & Exhibition on Biomaterials and Related Areas (BioMAT), 8th – 9th May 2019, Weimar, Germany

B. Karl, Y. Alkhatib, U. Beekmann, G. Blume, D. Kralisch, S. Lorkowski, O. Werz, D. Fischer
Bacterial nanocellulose containing frankincense extract as tailor-made anti-inflammatory wound dressing
German Society for Biomaterials (DGBM), Annual Meeting, 8th – 10th November 2018, Braunschweig, Germany

B. Karl, Y. Alkhatib, U. Beekmann, G. Blume, S. Lorkowski, D. Kralisch, O. Werz, D. Fischer
Bacterial nanocellulose loaded with lipophilic frankincense extract as tailor-made wound dressing to treat inflamed wounds
German pharmaceutical society (DPhG), Annual Meeting, 2nd – 5th October 2018, Hamburg, Germany

Y. Alkhatib, G. Blume, D. Kralisch, D. Fischer
Challenging the hydrophilicity of natural bacterial nanocellulose for dermal applications
Society for Dermopharmacy, 22nd Annual Meeting, 12th – 13th March 2018, Berlin, Germany

Y. Alkhatib, G. Blume, D. Kralisch, D. Fischer
Overcoming the hydrophilicity of bacterial nanocellulose for the transport of lipophilic drugs
German Society for Biomaterials (DGBM), Annual Meeting, 9th – 11th November 2017, Wurzburg, Germany

Y. Alkhatib, G. Blume, D. Kralisch, D. Fischer
Overcoming the hydrophilicity of natural bacterial nanocellulose
SEPAWA Congress 2017, 64th Annual Meeting, 18th – 20th October 2017, Berlin, Germany

Y. Alkhatib, G. Blume, D. Kralisch, D. Fischer
Challenging the hydrophilicity of bacterial nanocellulose
German pharmaceutical society (DPhG), Annual Meeting, 26th – 29th September.2017, Saarbrucken, Germany

Y. Alkhatib, G. Blume, D. Kralisch, D. Fischer
Innovative carrier systems to overcome bacterial nanocellulose hydrophilicity
Controlled release society (CRS) Germany local chapter, 21st annual meeting, 2nd – 3rd March 2017, Marburg, Germany

Y. Alkhatib, M. Dewaldt, S. Moritz, D. Kralisch, D. Fischer
A slow release system of bacterial nanocellulose for octenidine as wound dressing
German pharmaceutical society (DPhG), Annual Meeting, 23rd – 25th September 2015, Düsseldorf, Germany

Scientific awards:

Poster award: International Symposium on Bacterial Nanocellulose (ISBNC), 3rd – 4th October 2019, Porto, Portugal

Poster award: 5th European Symposium & Exhibition on Biomaterials and Related Areas (BioMAT), 8th – 9th May 2019, Weimar, Germany

Lesmüller Poster Award: Category of pharmaceutical technology, German pharmaceutical society (DPhG), Annual Meeting, 2nd – 5th October 2018, Hamburg, Germany

Phoenix Scientific Award: Category of pharmaceutical technology, for the publication "Controlled extended octenidine release from a bacterial nanocellulose/Poloxamer hybrid system" 25th October 2018, Frankfurt am Main

Hans Christian Korting Award: Young Talent Award for Dermopharmacy: German Dermopharmacy Society, Annual Meeting, 12th – 13th March 2018, Berlin

Lesmüller Poster Award: Category of pharmaceutical technology, German pharmaceutical society (DPhG), Annual Meeting, 23rd – 25th September 2015, Düsseldorf, Germany

Declaration

Herewith I, Yaser Alkhatib, born on 03.01.1990 in Anabek, Syria, declare that I am familiar with the valid doctoral examination regulations of the Faculty of Biological Sciences in the Friedrich-Schiller-University Jena. All chapters of this dissertation were produced by myself. I did neither use any text passages from third parties not their own previous final theses without citing them.
I would like to mention that Prof. Dr. Dagmar Fischer assisted me in selecting and analyzing materials, and especially be the linguistic correction.
I would like also to declare that I did not enlist the assistance of any "dissertation-counseling agent" and that I did not provide any direct or indirect financial benefits to any third party for work connected to my dissertation.
I would like also to confirm that this dissertation has not submitted as a final thesis for a state examination or other scientific examination. I confirm that neither this dissertation nor a similar dissertation or another scientific paper was submitted by me to any other institution of high education or to any other faculty.

Neu-Ulm, 10.03.2021 Yaser Alkhatib